SEISMIC MICROZONATION ATLAS OF GUWAHATI REGION

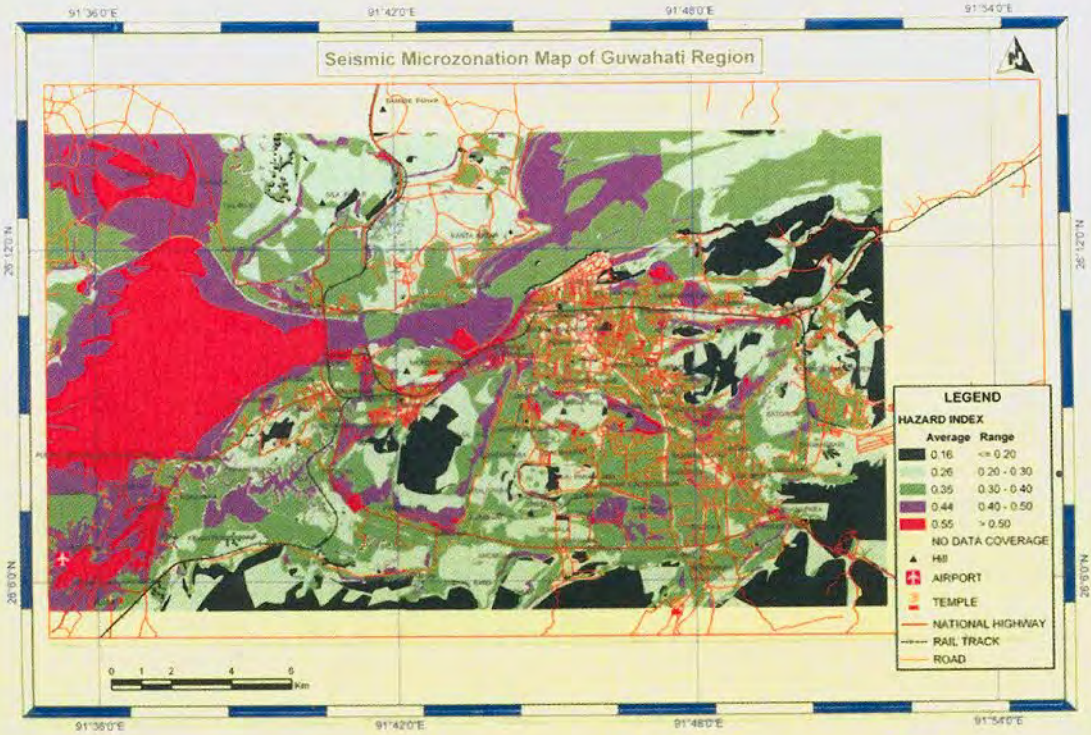

सत्यमेव जयते

Department of Science & Technology
Government of India
New Delhi - 110 016

2007

डा.टी.रामसामी
सचिव
DR. T. RAMASAMI
SECRETARY

भारत सरकार
विज्ञान और प्रौद्योगिकी मंत्रालय
विज्ञान और प्रौद्योगिकी विभाग
टेक्नोलॉजी भवन, नया महरौली रास्ता, नई दिल्ली-110 016
GOVERNMENT OF INDIA
MINISTRY OF SCIENCE & TECHNOLOGY
DEPARTMENT OF SCIENCE & TECHNOLOGY
Technology Bhavan, New Mehrauli Road, New Delhi-110 016

FOREWORD

Reliable assessment of earthquake hazard is of top priority for successful earthquake disaster mitigation in India with more than 55% of land area being seismically active. In spite of advances in knowledge, prediction of the occurrence of earthquake in terms of its size, time and location has been challenging. Efforts are being made to develop suitable mechanisms to minimize loss of life and property from such events through forewarning and advanced preparedness. The historical as well as recent records indicate that most casualties are caused by the collapse of buildings. Keeping this in view and the rapid rise of population as well as large scale infrastructural developments, Department of Science & Technology had initiated a major programme for microzonation of important cities in the country. A pilot study was first taken up for Jabalpur region, through a multi-disciplinary and multi-institutional programme. The microzonation and vulnerability maps for Jabalpur were prepared through integration of geological, seismological and geotechnical data and these efforts were further extended to Sikkim, Delhi, Bangalore and Ahmedabad.

Guwahati city falls in Seismic Zone V and supports a vibrant population base. In view of the importance of the region, a study on seismic hazard microzonation has been taken up in the scale of 1:25,000. The seismic hazard index map has been prepared through the integration of ground motion attributes with the geological, geotechnical, geomorphological and local site conditions.

"Seismic Microzonation Atlas of Guwahati Region", encapsulates the major multi-institutional collaborative endeavors of relevant organizations. I hope that the Atlas would prove useful to the planners. Design engineers, architects, developers and State authorities in preparing strategies for future constructions and retrofitting of existing structures in Guwahati urban centre.

(T. Ramasami)

Tel.:26510068, 26511439, Fax : 0091-11-26863847, 0091-11-26862418, E-mail : dstsec@alpha.nic.in

PREAMBLE

Natural disasters are the result of various complex geophysical characteristics plus the related societal circumstances that are subjected to a hazard. All these events are location specific in the sense that a hazard is aggravated by the geological, topographical and land cover of a hazard region. Natural hazards turn into disasters when human societies and built environment are affected by them. Five major earthquakes visited India in the past decade, culminating in the devastating Bhuj earthquake of 26 January 2001, which called attention to the hazards posed by buildings not designed to withstand major and obviously probable great earthquakes. A replication of the 1950 Assam earthquake, the largest intra-continental earthquake in recorded history along the more populous segments of the Himalaya would be devastating. The population of India has doubled since the last great Himalayan earthquake in 1950. Today, about 50 million people are at risk from great Himalayan earthquakes, many of them in towns and villages in the Gangetic plain and Brahmaputra valley. The northeastern region in India is recognized as being highly seismic hazard prone and two of the world's most severe earthquakes of June 1897 and August 1950 visited the region, which has affected Guwahati city. If we go by the periodicity of major earthquakes, a large earthquake may be expected in the region in the near future. Guwahati city being a state capital and densely populated in the high seismically active region of the country, needs a serious attention for disaster preparedness.

Urban seismic risk is rapidly increasing with population growth and the potential encroachment due to urban development into areas susceptible to earthquakes. The problem is even more severe for sprawling city like Guwahati, in the Northeast India, which is in Zone V of seismic zonation map of BIS (2002) and the gateway to seven northeastern states. The city of Guwahati is located in the Brahmaputra valley that serves as a divide between the tectonic regime of the Himalayan mobile belt in the north and the Meghalaya plateau in the south. The landscape is immature and is dominated by a drowned topography. The recent studies have revealed the presence of several active faults in the region having distinct seismological and morphotectonic signatures. The major earthquakes having considerable effect in Guwahati include that of 1897 Great Assam, 1918 Srimangal, 1930 Dhubri, 1950 Assam, 1988 Indo-Burma and 1997 south of Dauki fault.

The Department of Science and Technology, Government of India initiated the seismic microzonation of Guwahati city in a multi institutional mode in September 2002. The main organizations involved in this endeavor are the Geological Survey of India, IIT Kharagpur, IIT Guwahati, IIT Roorkee, Assam Engineering College, Jorhat Engineering College, DGM-Assam, CGWB, RRL-Jorhat, IMD, and AMTRON (Govt. of Assam). Microzonation is a process of dividing a seismically active region into sub regions such that any characteristic of interest may be considered to be reasonably same over the micro zones. This is similar to the macro level hazard evaluation but requires more rigorous inputs about the site specific geological, geophysical, geotechnical, seismotectonic, ground response to earthquake motions and their effects on the safety of the constructions, taking into consideration the design aspects of buildings, ground conditions which would enhance the earthquake effects like soil amplification, liquefaction of soils etc. Seismic microzonation is an effective mitigation method and it is an important guiding tool in land use planning and safe construction practices to avoid the losses from the future earthquakes. In the present context, the hazard mapping of Guwahati city poses huge challenge as it has complex tectonics around and varied topography such as deep alluvial, mountains, flow of mighty river Brahamputra through the city, water logged area, pond and lakes etc.

The work on geological, seismological and geotechnical zonation are substantially completed leading to various zonation maps. These are overlaid on each other on GIS platform - towards formation of a comprehensive hazard map. Final seismic hazard microzonation map is thus, prepared by assigning the weightage to the relevant thematic layers and overlaying them. The integration of all the relevant maps has been done at IIT Kharagpur.

It is hoped that the seismic microzonation demarcating various hazard zones will greatly benefit in the long run in mitigating earthquake disasters in this region and lead to safer living.

Brijesh K. Bansal
Director and In-charge (Seismology)
Department of Science and Technology
New Delhi

EXECUTIVE SUMMARY

On request and initiative of the Hon'ble Chief Minister of Assam, Sri Tarun Gogoi, the Department of Science & Technology, Government of India constituted a national level Expert Group vide DST Office Order No. DST/ Exp Group/Guwahati-microzonation/2002 dated August 19, 2002 (Annexure-I) to carry out the Seismic Microzonation of Guwahati Region. The Expert Group met for the first time at AMTRON in Guwahati on 12th and 13th of September, 2002 and thereby set the plan of action and the broad framework for the participating institutions. It was acknowledged that the Seismic Microzonation of Guwahati Region posed a challenge hitherto unattempted, when compared with the similar work being carried out by DST for the city of Jabalpur and New Delhi. In case of Guwahati, most of the data would have to be collected afresh, meaning it would require extensive ground survey, including geophysical, geomorphological, land use, land cover, ground noise response spectra, basement configurations and landslide hazard mapping, deployment of strong motion accelerographs, studies on Peak Ground Acceleration etc.

Accordingly, the Expert Group set out the tasks and priorities for the participating members and institutions. The Groups so far held eight sittings (two at AMTRON, two at IIT Guwahati & four at IIT Kharagpur Salt Lake City Campus, Kolkata), and has monitored the progress of work, held critical review of the outcome, and thus, ensured quality output at every stage.

IDENTIFICATION OF WORK COMPONENTS FOR THE FIRST PHASE

Having the foregoing information in the background the following items of work were identified and carried out as the first step towards seismic microzonation of Guwahati region mostly based on available data.

1. Preparation of Base map on 1:25,000 scale of Guwahati Region on a digital platform by AMTRON.
2. Compilation and synthesis of geological and geomorphological map of Guwahati region on the base of SOI toposheets on 1:25,000 scale by GSI.
3. Preparation of bed rock contour map of the area on 1:25,000 scale from the results of vertical electrical resistivity sounding

surveys carried out by GSI during 1986-87 and 1987-88, supplemented by similar data generated by GSI during 2002-03 field seasons. These data were compared and contrasted with similar set of data obtained by DGM from about 30 bore holes in the basin area. Finally a synthesized basement contour map was prepared by examining both the sets of data and superimposed the same on the geological map of the area.

4. Preparation of landslide hazard zonation map of the hilly tract of the area on 1:25,000 scale by GSI.

5. A seismotectonic map, prepared by GSI of the area of 200km radius around Guwahati based mostly on the data published by GSI in the Seismotectonic Atlas of India (2000).

6. Recent satellite imageries of the area studied by AMTRON to verify and update the change in landforms and land use pattern from that given in the SOI toposheets surveyed during 1986-87 to achieve an updated landuse map of the study area.

7. Instrumental site response studies by using ambient noise (Nakamura ratio technique) were carried out by GSI, IMD and RRL-J to determine the maximum site amplification factors and corresponding peak frequency covering almost the entire area at 141 sites.

8. 200 Borehole geotechnical studies by Assam Engineering College.

9. Compilation of results of macroseismic surveys of the past major earthquakes affecting Guwahati town by D.R. Nandy, Retd. Director, GSI.

10. All the data digitized and stored at AMTRON, Guwahati.

11. Map analysis (raster & vector) for Microzonation by IIT Kharagpur.

12. Empirical site response synthesis by IIT Kharagpur.

13. Estimation of scenario earthquake magnitude from the earthquake catalogue of 140 years by IIT Kharagpur.

14. Site amplification, classification, strong motion spectral acceleration analysis and synthesis by IIT Kharagpur, IIT Guwahati, Assam Engineering College, Geological Survey of India, IMD and RRL Jorhat.

15. Site classification map on GIS platform using shear wave velocity (V_S^{30}),

site response, predominant frequency and factor of safety by IIT Kharagpur.

16. Demography and Preliminary Seismic Population Risk Assessment by Jorhat Engineering College and IIT Kharagpur.
17. Integration of all the thematic layers and preparation of Seismic Microzonation map on GIS platform in the scale of 1:25,000 by IIT Kharagpur.
18. Integration of Seismic Microzonation and demographic distribution maps on GIS platform for the preparation of Preliminary Seismic Population Risk map in the scale of 1:25,000 by IIT Kharagpur.
19. Data repository, web based GIS and hosting on a special website by AMTRON.

Due to untiring effort of the Group and initiatives of DST in sorting out issues arising out of inter institutional coordination; the basic groundwork has been completed, collated and compiled for Guwahati Region. Finally following maps have been prepared and included in the Atlas

Map I	Satellite image of Guwahati Region
Map II	Landuse map of Guwahati Region
Map III	Geological & Geomorphological map of Guwahati Region
Map IV	Basement contour map of Guwahati Region
Map V	Basement zonation map of Guwahati Region
Map VI	Seismotectonic map of Guwahati Region covering 200km radius of Guwahati Area
Map VII	Landslide hazard zonation map of Guwahati Region
Map VIII	Bedrock Section Profile (1)
Map IX	Bedrock Section Profile (2)
Map X	Bedrock Section Profile (3)
Map XI	Road network map of Guwahati Region
Map XII	Borehole location map of Guwahati Region

Map XIII	Ambient noise survey location map (Predominant frequency observation sites)
Map XIV	Boreholes, Ambient noise survey and Strong motion station map
Map XV	Shear wave velocity(V_s^{30}) contour map of Guwahati Region
Map XVI	Shear wave velocity(V_s^{30}) zonation map of Guwahati Region
Map XVII	Factor of Safety contour map of Guwahati Region
Map XVIII	Factor of Safety zonation map of Guwahati Region
Map XIX	Bulk density contour map of Guwahati Region
Map XX	Predominant frequency contour map of Guwahati Region
Map XXI	Predominant frequency distribution map of Guwahati Region
Map XXII	Site response contour map of Guwahati Region
Map XXIII	Site response distribution map of Guwahati Region
Map XXIV	Site classification of Guwahati Region based on integration of V_s^{30}, predominant frequency, site response and factor of safety
Map XXV	Peak Ground Acceleration (PGA) map of Guwahati Region. PGA is estimated through Spectral Strong Motion Synthesis by Brune ω^2-circular Crack source model for an SEM of Mw 8.7 nucleating from the 1897 Great Shillong Earthquake of Mw 8.7
Map XXVI	Peak Ground Acceleration (PGA) map of Guwahati Region. PGA is estimated through Spectral Strong Motion Synthesis by Synthetic Green's Function Simulation for an SEM of Mw 8.7 nucleating from the 1897 Great Shillong Earthquake of Mw 8.7
Map XXVII	Seismic Microzonation map of Guwahati Region (PGA from Green's Function Simulation)

Map XXVIII	Seismic Microzonation map of Guwahati Region with PGA contours overlaid
Map XXIX	Demographic distribution map of Guwahati Region
Map XXX	Preliminary Seismic Population Risk map of Guwahati Region

This report gives indepth analysis of the data collated and compiled for the above mentioned themes. The data has been given in the Data volume, 27 Map Plates and 3 Section profiles.

The Site response was computed empirically at all 141 predominant frequency observation sites and as well as at five strong motion stations using waveform data. Site response contour map was drawn taking all the sites into consideration. This map matches very well with the surface geology and shear wave velocity map (V_s^{30}). Earthquake catalogue derived from ISC and USGS from 1866 - 2006 were used for computing the Scenario Earthquake Magnitude (SEM) for Guwahati region. It is to be noted that the historical earthquakes 1897 Shillong, 1918 Srimangal, and 1950 Assam constrained this catalogued estimation. Peak Ground Acceleration (PGA) is estimated through Spectral Strong Motion Synthesis by both Brune ω^2-circular Crack source model and impulsive source function using Empirical Green's Function Simulation for an SEM of Mw 8.7 nucleating from hypocenter of the 1897 Great Shillong Earthquake. PGA is contoured for the region with the SEM at the focus of the 1897 Shillong Earthquake to create a seismic hazard scenario in the region. It is found that PGA varies monotonically between 0.15g - 0.93g (1g = 1000gal) in the region. Through the overlaying and subsequent integration of Geology and Geomorphology (GG), Basement (B), Landslide Zones (L) and Seismological themes such as Shear Wave Velocity (V_s^{30}), Site Response (SR), Peak Ground Acceleration (PGA) and Predominant Frequency (PF) on GIS platform, the final seismic hazard Microzonation map is prepared.

Five zones are mapped where the average PSHI index is 0.55, 0.44, 0.35, 0.26 and 0.16. We termed these zones as very high, high, moderate, low and very low hazard regions. An integration of this microzonation vector layer with the demographic distribution of the urban center yielded a preliminary seismic population risk map of the region.

Prof. Sankar Kumar Nath
IIT Kharagpur

CONTENTS

CHAPTER 1

Introduction and Background Information

1.1 INTRODUCTION

The northeast India and its adjoining regions are characterized by high seismic activity. This region encompasses the northern part of the Assam-Arakan geological province and includes the eastern Himalayas, the Indo-Myanmar arc, the Mishmi Massif, the Shillong Plateau and adjoining parts, the Tripura folded belt, the Assam intermountain depression, and the northern part of the Bengal basin. The earlier seismicity studies of the region were mostly those of investigations of the major earthquakes originating from the region. One of the first scientific study could be associated with the classic work of Oldham (Oldham,1899) on the 1897 Great Assam Earthquake. Pioneering works on seismicity studies of the region also include that of Bullore, 1904; Pendse, 1948; Tandon, 1954, and Banerjee, 1957. Moreover several investigators have also studied the seismic phenomena in the region (Dutta, 1964; Dutta, 1967; Santo, 1969; Than, 1975; Tandon and Srivastava, 1975; Gyi, 1973; Verma *et al*., 1976; Khattri and Wyss, 1978). Dutta (1964) studied the annual frequency relationship. In another paper, Dutta (1967) introduced a further division of the region into four zones, which coincide with the main geotectonic units of the region comprising the eastern Himalayas, the Shillong Plateau, the Mishmi Massif and the Burmese arc. Later, Saikia *et al.* (1977) introduced another zone encompassing the Upper Assam depression, parts of the Surma Valley and the Tripura folded belt. Dutta and Saikia (1976) examined the factors responsible for structural instability of the fold resistant Assam wedge and the pattern of seismicity, and attributed the cause to the transformation force systems originating from the two adjoining arcuate systems - the Himalayan and the Indo-Myanmar. Santo (1969) related the seismicity to the interaction between India and the Asian continent during

the northward movement of the former. Furthermore, he attributed the seismicity of Myanmar (shallow and intermediate depths) to the lithospheric underthrusting beneath the Myanmar plate. Verma *et al.* (1976) examined a correlation between seismicity and gravity in the region. They attributed the high seismicity of the Shillong Plateau to its gradual rise and that of the Dauki fault system and south of it, as far as Dhaka, to a secondary effect resulting from the plate movements. Occurrence of high seismicity, intermediate depth loci and the strong negative anomaly in Myanmar were considered to be the result of lithospheric underthrusting beneath the Arakan-Yoma and the Burmese plains. Khattri and Wyss (1978) postulated the concept of the 'Assam Gap' between the epicentral regions of the last two earthquakes - the Great Assam Earthquake of 1897 and the Assam Earthquake of 1950. They considered the relatively quiet period since 1950 as a preparatory stage for a future great earthquake.

Though most part of the northeast India is prone to earthquakes, the intensity is quite different, ranging from 5 to 8 and above, in Richter scale. Earthquakes of low magnitude of less than 5 on Richter scale are scattered all over the region. However, most of the earthquakes having a magnitude of more than 5 have been observed in northern most part of Arunachal Pradesh, some part of lower Brahmaputra Valley, Central Manipur and West Tripura. Earthquakes ranging between 5 and 6 have been experienced mainly in northern rim of Assam, West Tripura, Southern Manipur and eastern rim of Mizoram. Most of the earthquakes, ranging from 6 to 7 magnitudes of Richter scale, were common in the Brahmaputra Valley, northern Manipur, eastern Nagaland, and east-central Mizoram. Maximum concentrations of severe earthquakes, ranging from 7 to 8 magnitudes, have been observed along eastern Arunachal Pradesh, Central and lower Brahmaputra Valley, and South Eastern Manipur. Earthquakes having highest magnitude of above 8.0 have been observed only in the eastern most part, beyond the borders of Arunachal Pradesh and east Khasi Hills.

The whole of northeast India falls in zone V of the seismic hazard zonation map (BIS, 2002) of India as shown in Figure 1.1, the highest vulnerable zone in the country. However, it has been observed during the recent past that earthquake shaking affects nearby areas differently. Severity of shaking is closely related to local site conditions.

The Guwahati city being located almost at the center of the region, acts as the gateway and transit point for communication and transportation for the seven sister states of northeastern region of India. Shifting of the capital of Assam from Shillong to Guwahati in 1972 has increased its importance manifold. People from all over Assam and from the neighboring states have been migrating to Guwahati for job, business and education. This has resulted in very fast and unplanned growth of the

Table 1.1 Major Earthquakes in the Northeast India

Place	**Year**	**Magnitude**
Cachar, Assam	January 10, 1869	Mw > 7.0
Shillong plateau	June 12, 1897	Mw 8.1 - 8.7
Sibsagar	August 31, 1906	Ms 7.0
Myanmar	December 12, 1908	Ms 7.5
Srimangal	July 08, 1918	Ms 7.6
SW Assam	September 9, 1923	Ms 7.1
Dhubri	July 2, 1930	Ms 7.1
Assam	January 27, 1931	Ms 7.6
Nagaland	1932	Ms 7.0
N-E Assam	October 23, 1943	Ms 7.2
Arunachal	July 07, 1947	Ms 7.5
Upper Assam	July 29, 1949	Ms 7.6
Upper Assam	August 15, 1950	Mw 8.6-8.7
Patkai Range, Arunachal	1950	Ms 7.0
Manipur-Myanmar border	1954	Ms 7.4
Indo-Myanmar border	August 06, 1988	Mw 7.2

city which, otherwise, geographically has very limited space in between the relatively steep sided granite hillocks as seen in Figure 1.2. In early 70s only a few multistoried buildings existed in the city except in the Downtown area. Most of the houses were kutchcha-pucca Assam type with corrugated (G.I.) sheet or thatched roofs. But during the recent past many tall buildings have come up which are juxtaposed to each other in the main commercial and business hubs and markets, perhaps due

to acute shortage of space. Many natural water bodies have been filled up for construction of houses making them more vulnerable to earthquake hazard. In some cases steep slope of the hillocks has been occupied making life and property vulnerable to landslides, especially during earthquake and heavy rains. During the heavy rains of 6-7 October, 2004, 17 people were killed by landslides right within the city from places like Dhiren Para, Jyotinagar, Chandmari, Jorabat, 9-mile and Lalganesh.

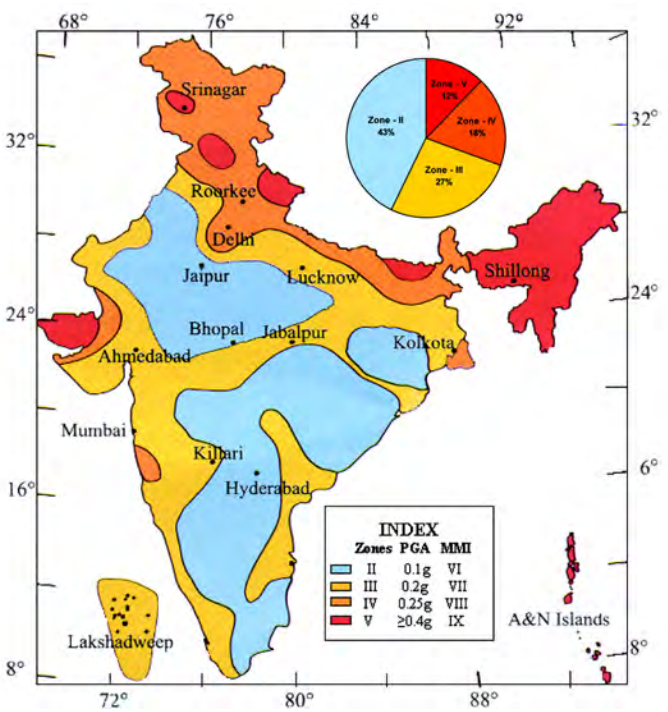

Figure 1.1 Seismic Zonation Map of India (BIS, 2002) with an inset showing the area occupied by different seismic hazard zones.

Table 1.2 Decadal Growth of Population of Guwahati City since 1901 to 2001 (Under Guwahati Municipal Corporation Area)

Year	Total Population	Decadal Growth (%)
1901	11,661	
1911	12,481	+7.03
1921	16,480	+32.04
1931	21,797	+32.26
1941	29,598	+35.79
1951	84,601	+185.83
1961	1,66,695	+97.04
1971	2,52,305	+51.36
1981	NO CENSUS	NO CENSUS
1991	5,84,342	+131.60
2001	8,09,895	+38.60

Source: *District Census Handbook (1991) Part XII-A & B, Census of India, Assam*

Keeping in view the importance of Guwahati city which is located in seismic hazard zone V, and on request of Sri Tarun Gogoi, Hon'ble Chief Minister of Assam in 2002, the Department of Science and Technology (DST), Government of India took the initiative for the preparation of Seismic Microzonation map of Guwahati Region of about 600 sq km bounded by latitudes $26^0$05' and $26^0$15', and longitudes $91^0$55' and $91^0$55'. The Government of Assam designated Assam Electronics Development Corporation Ltd. (AMTRON), a Govt. of Assam undertaking and Nodal IT agency of the state, to coordinate on behalf of the State Government with DST on matters concerning the Microzonation work of the city. An Expert Group was promptly constituted by DST for the preparation of comprehensive proposal on Microzonation of Guwahati region vide DST's Office Memorandum dated 19.08.2002. From the deliberation in the meetings the Expert Group identified different institutions viz. Geological Survey of India (GSI), India Meteorological Department (IMD), Survey of India (SOI), Regional Research Laboratory, Jorhat (RRL-J), IIT Kharagpur (IITKGP), IIT Guwahati (IITG), IIT Roorkee (IITR), Assam

Engineering College, Guwahati (AEC), Jorhat Engineering College, Jorhat (JEC), Guwahati University (GU), Central Ground Water Board (CGWB), Department of State Geology and Mining (DGM), and Assam Electronic Development Corporation (AMTRON) as resource organizations for the job. Later on, the Expert Group was designated as the Working Group vides DST's O.M. No. DST/Exp. Group/Guwahati Microzonation/2002 dated 25.09.2002.

Number of items of work relevant to the project was identified including collation of already available data and were assigned to different organizations. Of them, GSI took the major load of work. AMTRON acted as the nodal agency to compile, digitize and store all the multidisciplinary data sets supplied/generated by the participating organizations. Under the main project the DST sanctioned a few sub-projects to IITKGP, IITG, AEC, JEC and AMTRON.

1.2 REGIONAL SEISMICITY OF NORTHEAST INDIA

A regional seismicity map for northeast India (Nandy, 2001) and the adjoining region, covering the area between 88°E and 98°E longitudes and 20°N and 31°N latitudes is given in Figure 1.3. Most of the events falling in the tectonic domains of the eastern Himalaya, Mishmi block, Assam shelf, Meghalaya Plateau and Mikir Hills, Surma and Bengal basins have shallow focal depth i.e. <70km except for a few events in the N-W trending wedge shaped block lying between the Kopilli and Bomdila faults (Figures 1.3 and 1.4).The earthquake events in these tectonic domains occur in diffused pattern having post-collisional intracratonic characteristics. On the other hand, most of the earthquake events falling in the Indo-Myanmar (Burmese) tectonic domain have focal depths varying from 70-200km where seismicity is more intense and defines the westerly convex broadly N-S subduction zone of the Indian plate.

Seismicity in the Eastern Himalaya, Tethyan Himalaya and over the Yarlung Zangbo or Tsangpo suture zone is relatively sparse. Events mostly locate in-between the MBT and MCT and are more concentrated in the areas traversed by the transverse faults/lineaments running across the Himalayan trend. There is a narrow N-S cluster of events in the Yarlung-Zangbo suture zone area falling in the line of 90°E meridian, which are associated with the Yadong-Gulu garben. Most of the events are of shallow focus (0-40km depth) in these domains with a few having a depth range of 41 to

70km, and a very few having depth of focus varying from 71 to 150km and occur in the zone where E-W thrust sheets of the Himalaya take NE trend and are intersected by cross structures. Magnitudes of the earthquakes were from Mw 4.0 to Mw 5.9 except one event of 1947 having magnitude Mw=7.9 with its epicenter at 28°30´, 94°00´. So far no great earthquakes have been reported from these tectonic domains (Nandy, 2001).

The Mishmi block and the transverse mountain range are seismically more active than the adjoining Eastern Himalaya. This tectonic domain generated the 1950 Great Assam earthquake (Mw=8.7), perhaps due to strike-slip movement along the Po Chu fault. This tectonic domain is traversed by many NW-SE thrusts and faults (Nandy, 2001).

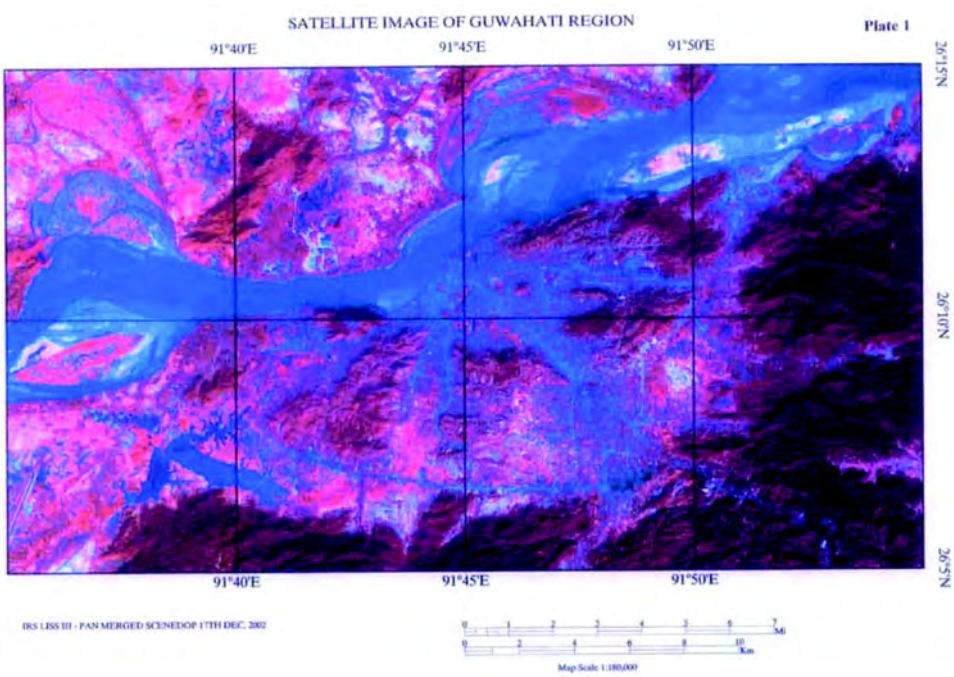

Figure 1.2 A Satellite image of Guwahati Region

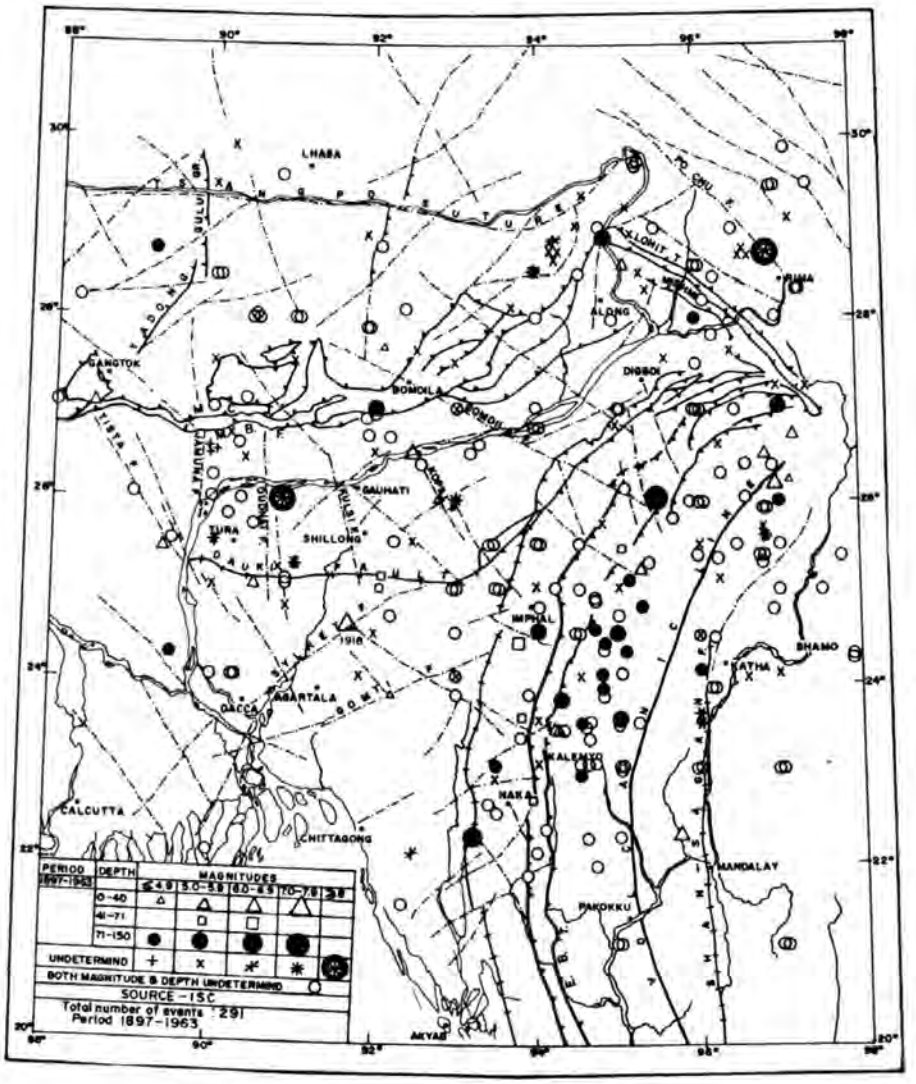

Figure 1.3 Seismicity map of Northeast India and adjoining region (after Nandy, 2001)

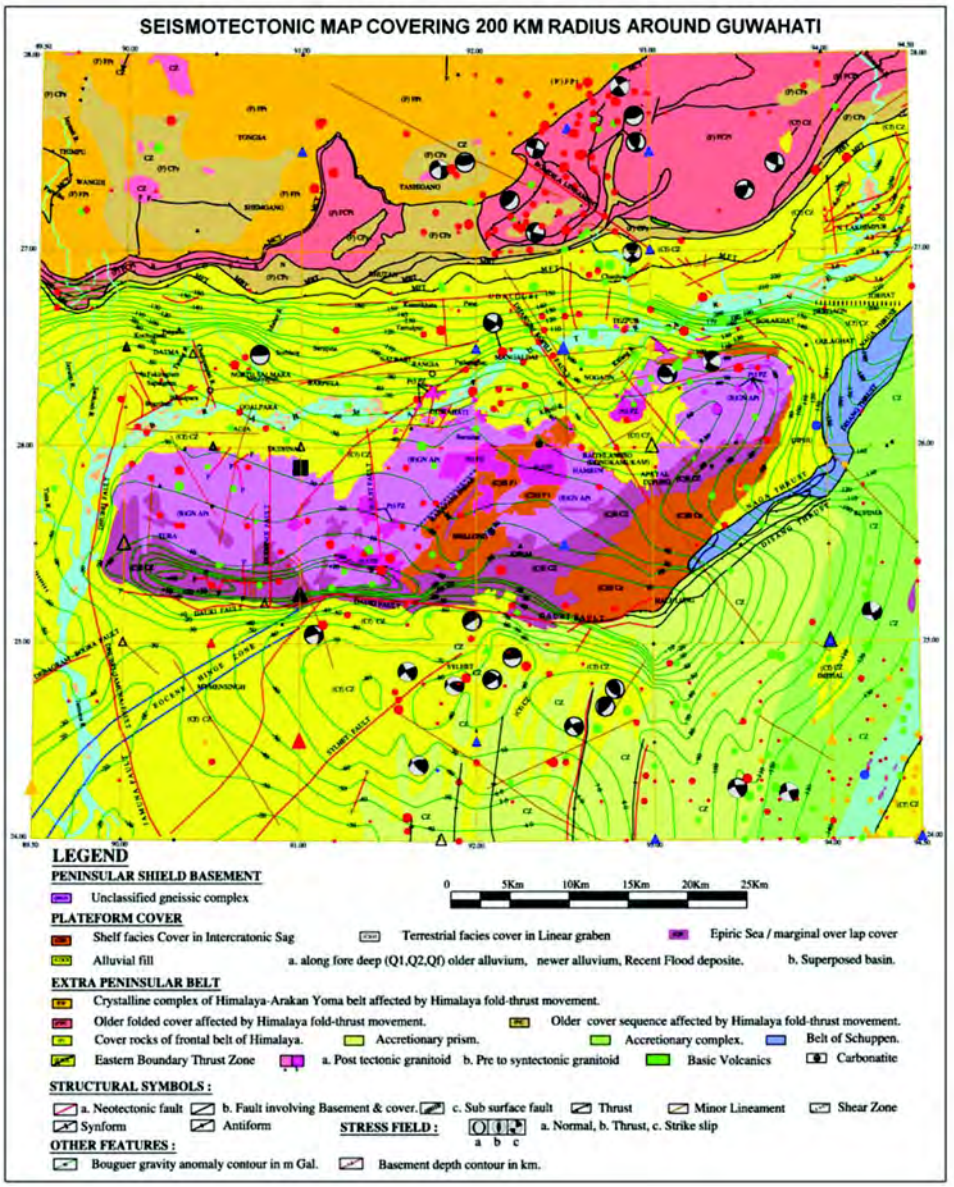

Figure 1.4 Seismotectonic map of Guwahati Region

As shown in Figure 1.3, there is a cluster of earthquake events in the Namcha Barwa area where the Tsangpo or Zangbo rivers take a hairpin bend to cut across the Himalaya. This cluster falls in the junction of the E-W Tethyan Himalayan domain and N-W Mishmi block and the transverse mountain range, which might be acting as the present day pivot or hinge for post-collisional anticlockwise rotation of the Indian plate. In this tectonic domain also most of earthquake events are of shallow depth (<40km) with a few events having focal depth up to 70km, occurring mostly along the Siang fracture zone. The zone of contact between the Mishmi block and the northernmost zone of Indo-Myanmar tectogene seems to be very much active seismically during the period under consideration (Figure 1.3).

1.3 EFFECTS OF PAST EARTHQUAKES IN THE AREA

Two great and three major earthquakes occurred around Guwahati during the period of last 137 years. They are

a) 1869-Cachar Earthquake, magnitude >7 and epicentral distance of about 60km;

b) 1897-Great Assam Earthquake, magnitude 8.7 and epicentral distance of about 60 km;

c) 1918-Srimangal Earthquake, magnitude 7.6 and epicentral distance of about 210km;

d) 1931-Dhubri Earthquake, magnitude 7.1 and epicentral distance of about 185km;

e) 1950-Great Earthquake of Assam, magnitude 8.7, epicentral distance of about 600km.

Of these the 1897 event had severe damaging effects in and around Guwahati city.

During 1869 earthquake severe shock was felt at Guwahati (Oldham, 1882). Almost all the brick buildings suffered damage. East and west wall of the jail developed horizontal cracks and were tilted; wicket damaged with slight cracks in the arches. One side of the roof of graveyard porch slipped down. The native infantry hospital

had developed bad cracks either due to faulty construction or settlement of the wall. The spire of the church got badly cracked. None of the native house in the bazaar area suffered any damage and no loss of life was reported.

During 1897-Great Assam Earthquake (Oldham, 1899) one of the gate pillars of Loki Rani's house fell to N60^{0}E, the other gate pillar was removed; a pair of gate pillars in the compound east of Telegraph Club was severely broken and overthrown; in the cemetery a marble cross was broken across the socket; the base of stone pillar of Robert Beecher monument had been projected to a distance of 84cm horizontally and 1.15m vertically; the clock of the telegraph office stopped at 5.15 pm, local time, the pendulum was broken up the shock; one of the 3m high pillars of the Deputy Commissioner's Bungalow had broken through 84cm from the ground and got twisted by 6 degrees, other pillar had broken at the same level but was not twisted, low compound wall had fallen; out of the 4 gate pillars made of masonry at two entrance of the old Dak Bungalow three were broken and twisted and the fourth one was only broken and fallen; the Commissioner's and Deputy Commissioner's offices were wrecked with the collapse of the walls; capping of the small gate pillar was shoot off to a distance of 1.30m from the center of the pillar; the obelisk of almost all the tombs in the old cemetery situated over alluvial ground south of the station had broken and fallen, one of them was twisted by 48^0, one recently built (1875) marble tomb was badly damaged whereas the new cemetery situated on the flanks of the low hill of gneissic rock east of the station, had suffered little or no damage; newly constructed brick building of the Railway Station was greatly damaged with fallen center gable and broken walls and diagonal cracks; E-W wall of the old temple at the streamer ghat had fallen completely.

The bridge made of three girders over a small stream near the western end of the bazaar along the G.T. Road had shortened by 45cm due to fissuring of the banks on both side of the river-abutment having been carried forward, one of the piers was tilted. Ground in the country surrounding Guwahati had suffered fissuring along the bank of the river and consequent subsidence of surface, and ejection of sands had filled up rivers and water bodies; Strand Road from Sukleswar ghat to Bhorolumukh furnished striking illustration of fissures which developed parallel to the river bank having 60cm to 120cm width. Near Chouki, 8km north of Guwahati, a small landslip

occurred from a hill on the roadside. Further north, near Chutiapara, a huge rock fell down the Kohra and Deodual hill.

During 1931 Dhubri Earthquake, both the Revenue and Judicial Record rooms were badly damaged. The walls of the buildings were separated at the corners and cracked from the post-plates through door and window lintels. The wall of the Jail was damaged for a length of 12m from the height of 1.5m to the top. The walls were cracked horizontally and moved out about 2.50cm. The Commissioner's Record room was damaged over two windows.

There was no appreciable damage at Guwahati during the 1819-Srimangal and 1950-Great Earthquake of Assam.

From the foregoing description it is evident that the alluvial tract of the city is more vulnerable to damage than the hilly tracts by earthquake shaking excepting the chance of land/rock slides; and alluvial tracts by the side of the river are highly vulnerable to liquefaction phenomenon.

1.4 SITE RESPONSE AND SEISMIC MICROZONATION

It is an established fact that ground shaking by earthquake and intensities of damage depend on the source and path of the earthquake, and on the local site conditions. It has also been long known that effects of local geology on ground shaking represent an important factor in earthquake risk evaluation. Site response parameters deciphered from geotechnical property of soil, geological setting and instrumental studies can give a good estimate of risk factor by removing both source and deep path effects assuming that these effects are same for records on bed rock and on the surface of nearby overlying soil cover (Parolai *et al.*, 2000).

In San Francisco, USA, local amplification over unconsolidated sediments have been shown to be responsible for intensity variations as large as two degrees (MM scale) during both 1906 San Francisco earthquake and more recent Loma Prieta event. In Mexico City there exists very soft lacustrine clay underneath the down town area of the city. These led to very large amplification, which caused the high death toll and large economic losses during the distant Guerrero Michoacan earthquake of 1985. Nearly all recent destructive earthquakes including the 26th

January, 2001 Gujarat earthquake have brought additional evidence of dramatic importance of site effects.

The local conditions affecting variations in seismic wave amplification are:

i. Topography,

ii. Geotechnical characteristics of surficial soil, and

iii. Depth of sedimentary basin and bed rock (basement) topography, basin edge conditions and lateral inhomogeneities, vertical/inclined layering of sediments etc.

Amplitude and shape of the seismic waves are modified by surficial soil through which they are transmitted in at least three ways:

(i) By causing reflected and refracted waves at velocity discontinuity (basin effect).

(ii) By causing incoming waves to scatter as it encounters inhomogeneities within the soil.

(iii) By causing wave to increase in amplitude in soil that are less tightly packed.

Basin effect generally influences long-period wave energy and cause amplified motion in high-rise building and multi-span bridges. Scattering alters the short-period wave energy that affects shorter structures. Impedance contrast affects the amplitude and phase of both short and long period wave. Detailed analysis of macroseismic data of past earthquakes, if available, with reference to topographic and geotechnical maps may lead to qualitative appraisal of most hazardous zone.

Beside considering the above factors for the purpose of seismic microzonation, in the absence of well spaced strong motion data, site condition may directly be obtained by direct measurement of shear wave velocity at each site by down hole instrumental probing up to 30m depth or indirectly through noise survey and microtremor measurement over the area. It has been observed that the ratio between Fourier spectra of horizontal and vertical components can be used to identify the resonance fundamental frequency of soft soil (Nakamura, 1989), but it fails for higher harmonics and that peak amplitude is somewhat different from amplification measured in the spectral ratio.

CHAPTER 2

Analysis of Seismicity in the Northeast India

2.1 INTRODUCTION

The northeast Indian region falls into the category of high seismic zone (BIS, 2002). There have been incidents of 20 large earthquakes (8.0>Mw>7.0), in addition to the two great earthquakes (Mw 8.7) - the Great Shillong Earthquake of 1897 and the Great Assam Earthquake of 1950 in the region since 1897 (Kayal *et al.*, 2006). The region as such, is placed in Zone V, the highest level of seismic hazard potential, according to the seismic zonation map of India (BIS, 2002). The Global Seismic Hazard Assessment Programme (GSHAP) also classifies the region in the zone of highest risk with Peak Ground Acceleration (PGA) values in the order of 0.35-0.4g (Bhatia *et al.*, 1999). Moreover, in the region, there is a higher level of man-made constructions and a significantly larger population than at the time of great earthquakes implicating more vulnerability to earthquake disasters.

We begin the present analysis by constructing an earthquake database from various data sources. The completeness and heterogeneity aspects of the catalogue are studied. An acceptable data catalogue in moment magnitude (Mw) is achieved by conversions and assumptions specific to types of magnitude scales. The spatial seismicity behavior due to the recent activities is studied with the evaluation of spatial distribution of b-values for the entire region. Subsequently the distributions along with seismotectonic setting of the region are employed for potential source zone classification. The analysis is then concluded with the estimation of the maximum earthquakes (m_{max}) constrained with the seismic moment release computed from data catalogue for each of the source zones.

2.2 EARTHQUAKE DATABASE (DATA 1: DATA VOLUME)

Data sources considered are USGS catalogue, ISC catalogue (ISC, 2006), IRIS catalogue, and ISET catalogue (Bapat *et al*., 1983). Data for the study pertains to a spatial scope of latitudes 21^{o}N to 31^{o}N and longitudes 87^{o}E to 99^{o}E that include an extra of 1^{o} on each side of the rectangular area as a buffer for the spatial windowing. Lower limit of magnitude 4.0 is taken since magnitude = 4.0 is considered well recorded. We look into the aspect of heterogeneity of the catalogue, which is due to different types of magnitude scales employed. However, magnitude scales: surface-wave magnitude (Ms), body-wave magnitude (Mb) and Local magnitude (M_L) are related to the largest amplitude that is recorded on a seismogram (Shearer, 1999). Ms and Mb are generally adopted and calibrated to agree with the M_L for the small events. Mb and M_L are found to be saturated for the large/great events such that Ms or moment magnitude (Mw) is used for the purpose. Mw and M_L are approximated as equal below 5.5. Mw and Ms are identical up to magnitude 7.5 (Chen and Scawthorn, 2003). So, Mw and Ms can be taken as equivalent within their measuring limits. We can convert Mb into Ms using the empirical relation constructed with record's entry of both type of magnitude scales.

A simple method is adopted in order to enrich the database yet avoid duplications. The data sources are compared with each year's record. The record of the particular year with the maximum number of earthquakes is selected to construct the data-base for the specific year. This is done for each year, till all the years are covered and the database is completed. Though events for the period from 1764 to 1897 are found in the ISET and USGS catalogues, there are large gaps in the recorded earthquake history prior to 1866. Therefore, the period accounted for the present study is from May 23, 1866 to May 15, 2006. The USGS catalogue refers to the merged NEIC database of PDE, India and significant earthquakes worldwide for the mentioned period and the study region. For the period prior to 1964, USGS provides an overall higher count. However ISET catalogue shows higher count for the years 1880 and 1956, and ISC catalogue has more events in the years 1914, 1931-35, 1938-39 and 1941. From 1964 onwards IRIS catalogue is found to have higher counts for most of the years. ISET catalogue has more events in the year 1964. Higher counts are found in the ISC catalogue for the years 1965, 1967-70, 1973-75 and 2004-06. Higher

number of events for the year 1976 is found with the USGS catalogue. After merger, the catalogue is scanned through to remove any trivial entries.

The database obtained contains a good number of entries in Mb. The entire catalogue histogram is given in Figure 2.1(a). To establish an empirical relation between Ms and Mb, a linear regression is performed using records with both magnitudes which are found in the ISC and IRIS catalogue as shown in the Figure 2.1(b). The relation obtained is

$$Ms = (0.89 \pm 0.049)\, Mb + (0.18 \pm 0.024) \quad \text{.....} \quad (2.1)$$

The linear regression is compared with that of Richter (1958) given below,

$$Ms = 1.59\, Mb - 3.97 \quad \text{.....} \quad (2.2)$$

The former relation gives an average weight to the higher and the lower magnitudes which is rational to the data. The Richter (1958) relation pulls down the lower magnitudes of Mb to further lower values and elevates the higher value of Mb to further higher value of Ms.

The magnitudes in Mb are converted to equivalent values in Ms using equation (2.1). We assume the magnitudes in M_L in the database to be equivalent to Mw since no M_L entry in the database exceeds 5.5. The types of magnitudes listed in the USGS catalogue and the ISET catalogue for the period prior to 1972. The indicated as equivalent to Ms. For the present analysis we assume that magnitudes are approximated to be equivalent to Mw within their measuring limits. Thus, we achieve an acceptable level of homogeneity in the type of magnitude scales in the catalogue (Data I). A seismotectonic map prepared with the database is shown in Figure 2.2.

Shallow earthquakes dominate the catalogue. Approximately 73% of the available earthquake depth information in the data catalogue indicates shallow earthquake (0-70km depth) scattered all over the region and the remaining is of intermediate depth (70-300km depth) mainly clustered in the Arakan Yoma Subduction Region. The relation between seismic energy, E_0, and scalar moment, M_0, adopting average

values of stress drop, ó = 50bars and rigidity, ì = 5x1011dyn/cm^2 for earthquakes in the crust and upper mantle is

$$\text{Log}_{10}\ E_o = \text{Log}\ M_o - 4.3 \quad \text{..... (2.3)}$$

where E_o is in ergs which is equivalent to dyne-cm (Stein and Wysession, 2003). However, seismic moment is often quoted in dyne-cm (1dyne-cm=10^{-7}Nm).

Also we have,

$$\text{Log}_{10}\ M_o = 1.5\ Mw + 16.1 \quad \text{..... (2.4)}$$

where M_o is in dyne-cm (Hanks and Kanamori, 1979) and it gives,

$$\text{Log}_{10}\ M_o = 1.5\ Mw + 9.1 \quad \text{..... (2.5)}$$

where M_o is in Nm.

It may be noted that there is a marked difference in the clustering of earthquakes as can be seen in the data for the period prior to 1964 and that of 1964 onwards. The difference may be due to the advent of the Worldwide Seismograph Station Network (WWSSN) in 1964. However spluttering of events from 1950 onwards is evident.

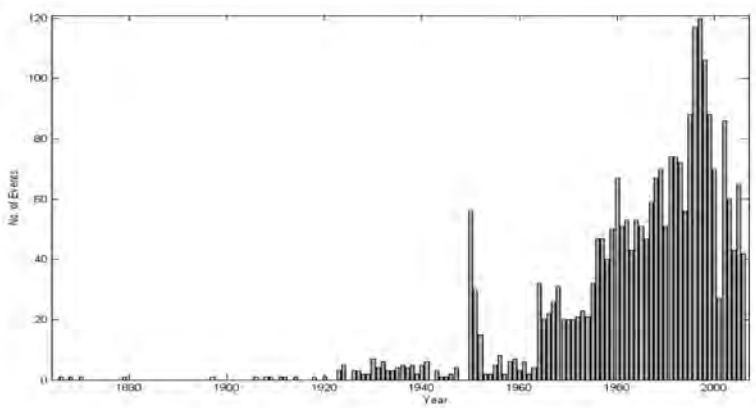

(a)

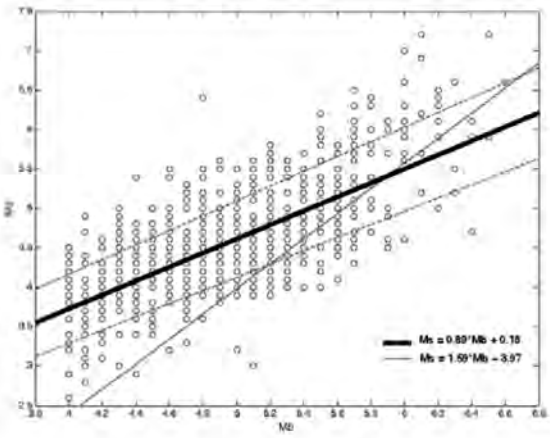

(b)

Figure 2.1 (a) The number of events per year in the merged catalogue from ISET, IRIS, ISC and USGS for the period May 23, 1866 - May 15, 2006, consisting only of events with M ³ 4 earthquakes. The difference in the clustering of earthquakes can be seen in the data for period prior to 1964 and that of 1964 onwards. A difference owed to the deployment of the World Wide Seismograph Station Network (WWSSN) in 1964. (b) Linear regression on Ms against Mb of the total 1201 records of events found with both of the magnitudes in the ISC and IRIS catalogues merged, which are most likely duplicated (obviously not determinant in this workout), yields an empirical relation Ms=(0.89 ± 0.049) Mb + (0.18 ± 0.024) as given by thick line. The dash lines represents upper and lower bounds with 95% confidence. The normal line plot of Richter (1958) Ms=1.59 Mb - 3.97 is given for comparison purpose.

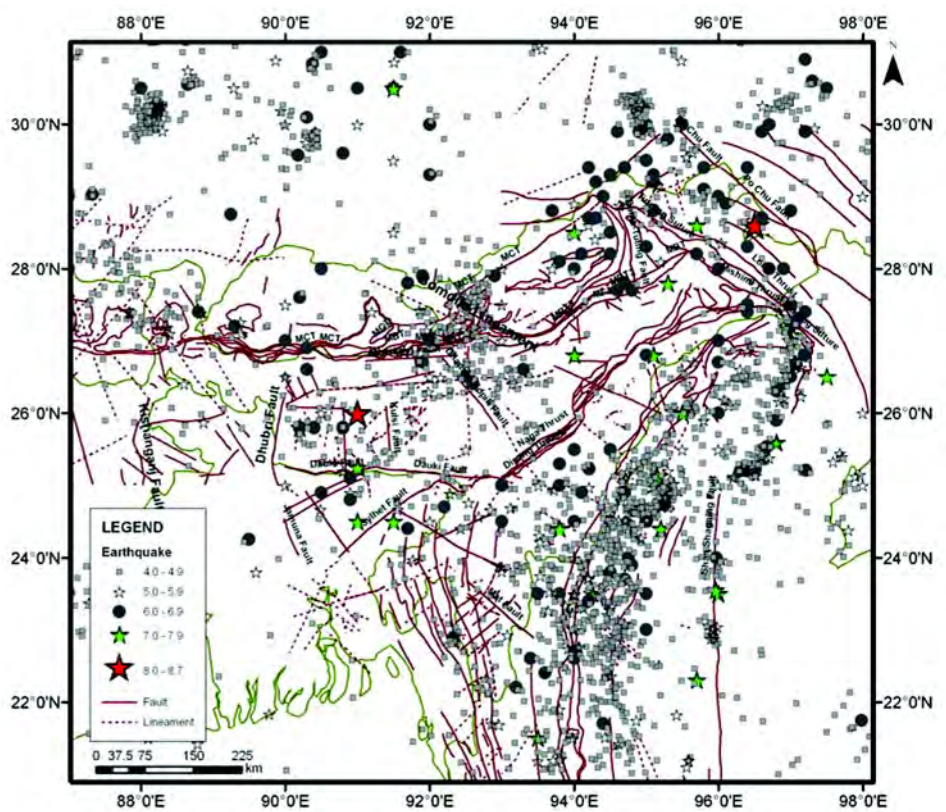

Figure 2.2 A seismotectonic map of Northeast India on GIS platform depicts the seismicity with Mw $\geq$ 4.0 from the earthquake catalogue (Modified after Seismotectonic Atlas of India and its Environs, GSI, 2000). The magnitude scales Mw, Ms and M_L are assume to be equivalent within their measuring limits.

2.3 SPATIAL b-VALUE DISTRIBUTION

Owing to the improvement of quality of recordings from 1964 onwards, a sub catalogue derived from the ISC catalogue for the period 1964-2006 is employed for the assessment of the b-value distribution. The detail of the analysis is discussed by Thingbaijam *et al.* (2007).

The scaling law for the earthquake recurrence is given by Gutenberg-Richter Frequency Magnitude Distribution (FMD) (Gutenberg and Richter, 1944). The relation employed is

$$\log_{10}(N) = a - bm \quad \text{..... (2.6)}$$

where N is the incremental or cumulative frequency of occurrence of the magnitude m in a given earthquake database.

The b-value is found to vary both spatially and temporally and is often employed as one parameter approach for earthquake studies (Gibowicz and Lasocki, 2001; Nuannin *et al.*, 2005). The different interpretations of b-value variations are discussed in (Mogi, 1962; Scholz, 1968; Schorlemmer *et al.*, 2005; Warren and Latham, 1970; Wyss, 1973; Wesnouski *et al.*, 1983). A low value implies that majority of earthquakes are of higher magnitude and a high value implies that the majority of earthquakes are of lower magnitude. The variations of b-values are seen to be inversely related to stress (Mogi, 1962; Schorlemmer *et al.*, 2005; Wesnouski *et al.*, 1983). Large material heterogeneities are reported with higher b-values (Scholz, 1968). High b-values are associated with aftershocks and low b-values with foreshocks (Suyehiro *et al.*, 1964; Nuannin *et al.*, 2005). The maximum likelihood method for the evaluation of b-values is widely accepted (Aki, 1965; Bender, 1983; Utsu, 1965). The b-value is estimated as

$$b = \frac{\log_{10}(e)}{\left[m_{Mean} - \left(m_t - \frac{\Delta m}{2}\right)\right]} \quad \text{..... (2.7)}$$

where m_{Mean} is the average magnitude, m_t is the threshold or the minimum magnitude and Δm is the magnitude bin size. The standard deviation, δb, of the b-value in equation (2.7) is estimated as

$$\delta b = 2.30 b^2 \sqrt{\sum_{i=1}^{N} (m_i - m_{Mean})^2 / N(N-1)} \quad \text{..... (2.8)}$$

where N is the total number of events in the sample (Shi and Bolt, 1982).

The temporal seismicity pattern involving the number of events indicates period of commencement of seismicity buildup from 1964 onwards. The period is also accounted for improvement in quality of records due to the advent of digital

instrumentation. Hence, the sub catalogue for the period 1964 - 2006 is preferred and used for the estimation of spatial distribution of the seismicity parameters.

We employ a sliding square spatial window of 2° by 2° which is moved by 0.5 degree each time from one corner of the study region to other end covering the whole area. The estimated value is obtained if the window encompassed 50 events or more and is assigned to the centroid of the window. The 50 events criterion is essential for a meaningful statistical analysis (Utsu, 1965). The size of the spatial window and the sliding distance is fixed on trial basis for an optimal. A fixed window size is preferred to a fixed number of events with varying window size, in order to have smooth dithering of low and high seismicity zones.

The estimated b-value ranges from 0.59 to 1.42. The variation of b-values is shown in Figure 2.3(a). An examination of the spatial distribution reveals relatively higher b-values on the eastern Himalayan area. The b-values are low in most of the central Eastern Boundary Thrust (EBT) encompassing the Arakan Yoma range with an increase towards both the south and the north. However eastern end of the Lohit thrust and southern most end of the EBT zone also have lower b-values. Southeast part of the map is observed to have low b-values. The standard deviations of the b-value, db, is found to vary from as low as 0.033 to as high as 0.165 and are depicted in Figure 2.3(b). Though comparative quite high b-values are observed in Dhansiri Kopili fault and Bomdila lineament zone and adjoining region, large standard deviations are also seen. High deviation is also marked on the northwest end of the Lohit thrust. However, across the EBT and the upper Himalayan zone, the standard deviations associated with the b-values are low to moderate.

2.4 SOURCE ZONE CLASSIFICATION

The source zone classification is done to accommodate the unknown subsurface complexities in the region (Chen and Scawthorn, 2003). The source zone classification in the present study is carried out by taking into account the historical earthquake distributions, seismotectonic regime and the spatial b-value distribution. Four great earthquakes, the Shillong Earthquake with Mw=8.7 during 1897, the eastern boundary earthquake Ms=8.2 during 1908, the Assam Earthquake with Mw=8.7 during 1950 and the earthquake in the upper Himalayan with Ms=8.0 during 1951 provide a

framework of classification. The tentative precincts are setup with the historical great earthquakes and thereafter, the seismotectonic settings are segregated into four zones according to indicative trends observed in the spatial distributions of b-value.

The trends indicate high values on the eastern Himalayan region. While low values are seen in the thrust zones especially in the central EBT dominated by intermediate depth earthquakes. However higher values are observed on the north and the south of the EBT zone. High values are again seen on the regions of Mishmi block and Po Chu fault. The Shillong plateau region has dominantly moderate values.

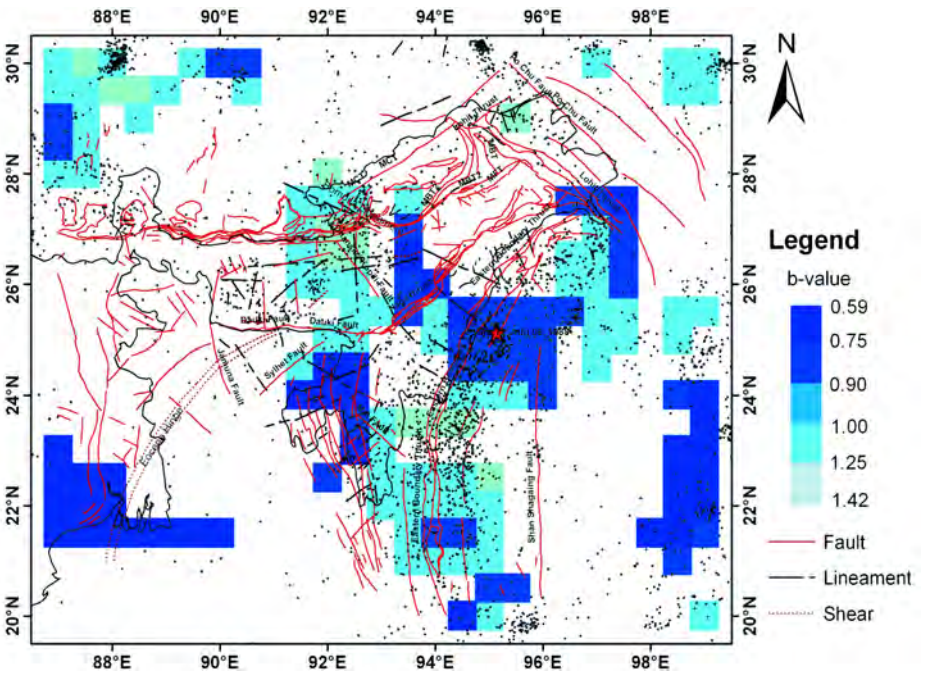

(a)

Figure 2.3 cont'd...

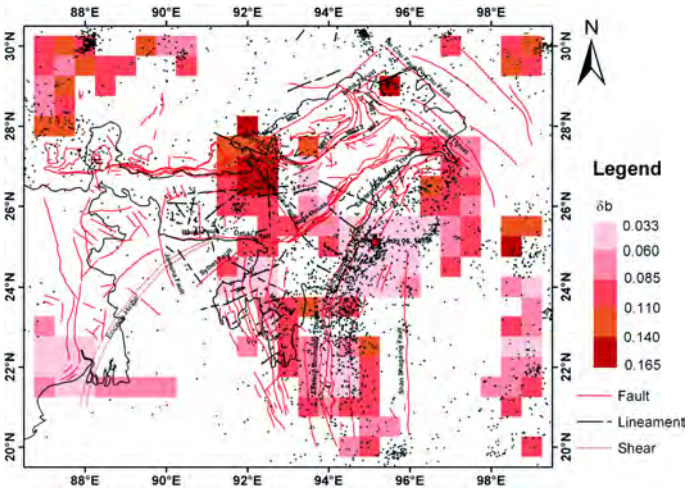

(b)

Figure 2.3 The spatial distributions over the backdrop of seismicity with Mw ³ 4.0 from the sub catalogue covering a period 1964-2006: (a) b-value, and (b) standard deviation of the b-value (db)

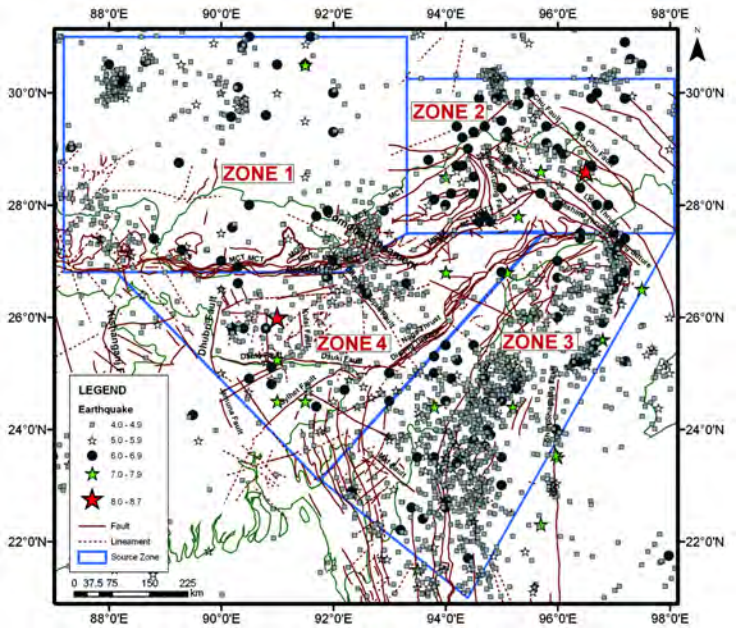

Figure 2.4 The classified source zones demarcated by the polygons on the seismotectonic map of Figure 2.2.

Finally the boundaries are demarcated with the consideration of tectonic regimes. Four source zones are classified as given in Figure 2.4. Zone 1 is Himalayan Source, Zone 2 is figured on Mishmi block. Zone 3 outlines the Indo Myanmar arc and Zone 4 encompasses the Bhramaputra basin, Kopili fault, Naga thrust, Shillong plateau and Duaki fault. Zone 1 is delineated in the coordinates 87°13.2'E, 31°N; 93°19.8'E, 31°N; 93°19.8'E, 27°30'N; 92°12'E, 26°48'N; and 87°13.2'E, 26°48'N. The coordinates demarcating Zone 2 are 93°19.8'E, 30°15' N; 98°06.6'E, 30°15'N; 98°06.6'E, 27°30'N; and 93°19.8'E, 27°30'N. Zone 3 is bound within 95°48'E, 27°30'N; 98°06.6'E, 27°3'N; 94°24'E, 21°N; and 91°48'E, 23°06'N and the coordinates of Zone 4 are 88°07.8'E, 26°48'N; 92°12'E, 26°4'2N; 93°19.8'E, 27°30'N; 95°48'E, 27°30'N; and 91°48'E, 23°06'N.

2.5 MAXIMUM EARTHQUAKES

We estimate the maximum earthquake in the region to establish the Scenario Earthquake Magnitude (SEM). Out of the four classified potential source zones (Figure 2.4) for the earthquake occurrence; zone 4 is potential source zone for earthquakes in the Guwahati region.

The approach for the estimation of the maximum earthquake, M_{max}, is similar to one employed for the Aegean area by Koravos *et al.*,(2003). With the idea that there is a bound on the maximum energy release, the predicted maximum earthquake magnitudes are generally constrained with finite seismic moment release or tectonic moment release or both. In the present analysis we employ the seismic moment release computed from the data catalogue. We looked into the four seismic zones separately and in addition, the whole region as singular source regime using five data catalogs, one for each zone and the main catalogue for the entire region. The data catalogs are extracted from the main data catalogue according to the coordinates defined by the source zones. It is noted that a potential source of uncertainty is the number of year gaps in the preceding years of the catalogue duration. The gaps are made less promiscuous by considering that there is neither significant number of events, nor events of significantly big magnitude during the gaps. The seismic moment release rate for each catalogue, is estimated by summing up the moment release for each earthquake in the data and dividing with the catalogue duration.

Main(1995) observed that the maximum effective or credible earthquake estimated with physical constraints from seismic moment rate are either dependent solely on the exponential tail of Frequency Magnitude Distribution (FMD) or by events near the maximum magnitudes as shown in Figure 2.5. Similarly we consider the moment releases only due to the higher magnitude earthquakes, since the higher magnitudes earthquakes are seen to play pivotal roles in the moment release. The completeness thresholds, m_c, gives the lower bound on the higher magnitudes and is estimated from the frequency magnitude distribution. The thresholds are then employed for the determination of annual number of events and annual seismic moment release for each zone.

The results for all four source zone are shown in Table 2.1. The source zone 4 encompassing Shillong plateau which is the potential source of earthquake hazard to the Guwahati region, is associated with M_{max} of M_w 9.1 ± 0.14 implicating the historical maximum of M_w 8.7 as a more realistic choice for the SEM.

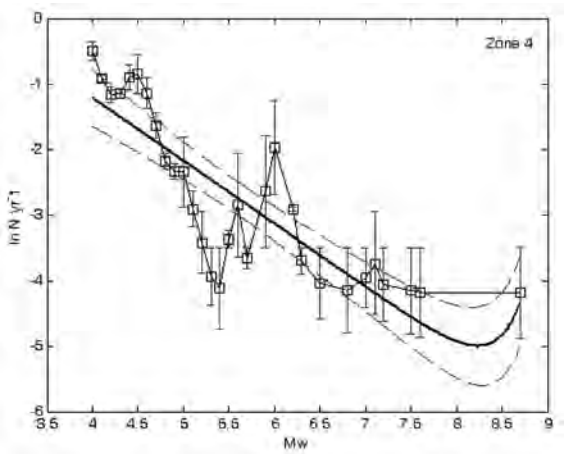

Figure 2.5 Incremental frequency magnitude distribution plots for Source Zone 4. The thick lines in the plot indicate the best fit line. The dashed lines illustrate the 95 per cent intervals on this fit. The error bars given for each magnitude are estimated as F/ÖN where F is the frequency and N is the number of observations used to compute F (Koravos *et al.*, 2003).

Table 2.1: The estimated maximum earthquake is compared with historical maximum earthquake. The completeness thresholds m_c estimated from the frequency magnitude distribution which conforms to of the fitting model at the lower magnitude bound are also listed. The thresholds are employed for the determination of annual number of events and annual seismic moment release for each source zone. # indicates the entire region.

Zone	m_c	Historical m_{max}	Estimated m_{max} (Mw)
1	6.6	8.00 Ms	8.33 ± 0.05
2	6.7	8.70 Mw	9.01 ± 0.05
3	6.1	8.20 Ms	8.48 ± 0.09
4	6.3	8.70 Mw	9.10 ± 0.14
#	7.0	8.70 Mw	8.83 ± 0.04

Maximum estimated earthquake in the region is Mw 9.24.

CHAPTER 3

Site Response Analysis from Geotechnical and Strong Ground Motion Data

3.1 INTRODUCTION

It has long been known that each soil type responds differently when subjected to ground motion from earthquakes. Usually the younger softer soil amplifies the ground motion relative to older more competent soils or bedrock. The potentially severe consequences of this phenomenon were recently demonstrated in the damage patterns of the 1985 Michoacan, Mexico earthquake (Singh *et al.*, 1988), the 1988 Armenian earthquake (Borcherdt *et al.*, 1989), the 1989 Loma Prieta earthquake (Hough *et al.*, 1990; Borcherdt and Glassmoyer, 1992) and the Northridge earthquake in Los Angeles, California (EERI, 1994). Numerous other studies have also demonstrated the ability of surface geologic conditions to alter seismic motions (Borcherdt, 1970; King and Tucker, 1984; Aki, 1988; Field *et al.*, 1992).

There are many factors that influence the way a site will respond to earthquake ground motion (Aki, 1988; Aki and Irikura, 1991; Bard, 1995). These include: (i) the source location, (ii) the prevalence of energy focused or scattered from lateral heterogeneity, and (iii) the degree to which sediments behave nonlinearly, which causes the response to depend on the level of input motion. However, the site effects in the assessment of seismic hazard follow a simple approach wherein, for the potential sources of earthquake ground motion in a region the unique behavior of one site in relation to others is calculated.

After the occurrence of large destructive earthquakes during the last 20 years, such as the Mexico 1985 (Bard and Chávez-García, 1993), the Armenia 1988 (Borcherdt *et al.*, 1989), the Loma Prieta 1989 (Hough *et al.*, 1990), the Northridge 1994 (EERI, 1994), and the Kobe 1995 (EERI, 1995), both the seismologists and earthquake engineers have focused their attention on the importance of local site response on seismic ground motion. The observed unequal distribution of damage from these earthquakes prompted a series of studies on scenarios and parameters concerning local geological conditions responsible for the differentiation of the seismic ground motion. Indeed, many factors affect the seismic motion near the recording site: seismic–wave velocities and geometry of the stratigraphy (the thickness and position of the discontinuities of the geological formations), topography (Boore, 1972, 1973; Bard, 1995), and intensity of excitation (weak or strong) that can induce nonlinear phenomena in correlation with local geology (Aki, 1993; Field *et al.*, 1997).

The term ‘site effect’ means different things to different audiences. We take the term to represent local ground response, basin effects, and the influence of surface topography. The definition of surface topography is obvious. ‘Local ground response’ refers to the influence of relatively shallow geologic formations on (nearly) vertically propagating body waves. These effects are ideally modeled using the full soil profile, but for deep alluvial basins the modeling domain generally does not extend beyond depths of 100-200m.

Site effects play a very important role in characterizing seismic ground motions because they may strongly amplify (or de-amplify) seismic motions at the last moment just before reaching the surface of the ground or the basement of man-made structures.

The greatest challenge in estimating site response from earthquake data is removing the source and path effects. Borcherdt (1970) introduced a simple procedure to divide the spectrum observed at the site in question by the same observed at a nearby reference site, preferably on competent bedrock. The resulting spectral ratio constitutes an estimate of the site response if the reference site has a negligible site response. Andrews (1986) introduced a generalized inverse technique to compute site response by solving data of a number of recorded events for all source/path effects and site effects simultaneously. These techniques for computing site response

depend on the availability of an adequate reference site (on competent bedrock) with negligible site response. Since such a site may not always be available, it is desirable to develop alternative methods that do not depend on a reference site. Boatwright *et al.* (1991b) suggested a generalized inversion scheme where shearwave spectra are represented with a parameterized source- and path-effect model and a frequency-dependent site response term for each station. Another non-reference-site-dependent technique involves dividing the horizontal-component shear wave spectra at each site by the vertical-component spectrum observed at that site (Lermo and Chávez-García, 1993). This method analogous to the so-called receiver function technique (Langston, 1979) used to study the upper mantle and crust from tele-seismic records, assumes that the local site conditions are relatively transparent to the motion that appears on the vertical component. Nakamura (1989) introduced another technique for analyzing the ambient seismic noise. He hypothesized that site response could be estimated by dividing horizontal-component noise spectra by vertical-component noise spectra. Several studies have since shown that Nakamura's procedure can be successful in identifying the fundamental resonant frequency of sedimentary deposits (Omachi *et al.*, 1991; Lermo and Chávez-García, 1992; Field and Jacob, 1993; Field *et al.*, 1995).

The receiver function analysis exploits the fact that tele-seismic P-waves that are incident upon the crustal section below a station produce P to S conversions at crustal boundaries as well as multiple reverberations in the shallow layers. By deconvolving the vertical-component signal from the horizontal-components, the obscuring effects of source function and instrument response can be removed, leaving a signal composed of primarily S-wave conversions below the station. The deconvolved horizontal component called receiver function trace is a best representative of the site response as the local site conditions are relatively transparent to the motion that appears on the vertical component.

3.2 THEORETICAL CONSIDERATIONS OF SITE RESPONSE

To evaluate site response several techniques have been utilized and compared in recent studies (Field and Jacob, 1995). Two of the proposed methods - the standard spectral ratio (SSR) (Borcherdt, 1970) and the receiver function technique (HVSR)

(Langston, 1979; Lermo and Chávez-García, 1993; Nath *et al.*, 2000, 2002a, 2002b) are based on a spectral ratio scheme. In both these techniques, the source and path contributions are removed from the seismic recordings by means of a deconvolution operation using a function free of site effects.

An alternative method to calculate site response is the generalized inversion technique (GINV) (Andrews, 1986; Castro *et al.*, 1990; Boatwright *et al.*, 1991b; Hartzell, 1992) that is also considered for our study to compute site response by solving data of a number of recorded events for all source/path effects and site effects simultaneously.

The seismograms of the selected events were first corrected for the system response. Next the S-wave packets recorded by the seismographs were windowed with a window width containing the maximum amplitude. The window length was selected following the results of Seekins *et al.* (1996). A Hanning taper is applied to the time windowed data and then butterworth bandpass filtered before the amplitude spectra were computed.

Let the S-wave spectral amplitude and that of the background noise be $O(r_{ij}, f_k)$ and $B(r_{ij}, f_k)$ respectively at the hypocentral distance r_{ij}. Then the signal amplitude spectrum at the frequency f_k can be expressed as,

$$A\left(r_{ij}, f_k\right) = O\left(r_{ij}, f_k\right) - B\left(r_{ij}, f_k\right) \quad \text{..... (3.1)}$$

The corrected spectra are smoothed in order to reduce the data variance using a five-point smoothing window and a spline interpolator at 0.1Hz interval.

Suppose a network has recorded i events by j stations. The amplitude spectrum of the i^{th} event recorded at the j^{th} station for the k^{th} frequency, $A(r_{ij}, f_k)$ can be written in the frequency domain as a product of a source term $SO_i(f_k)$, a propagation path term $P(r_{ij}, f_k)$, and a site effect term $SI_j(f_k)$ (Lermo and Chávez-García, 1993; Nath *et al.*, 2002a, 2002b):

$$A\left(r_{ij}, f_k\right) = SI_j\left(f_k\right) \cdot P\left(r_{ij}, f_k\right) \cdot SO_i\left(f_k\right) \quad \text{.....(3.2)}$$

3.2.1 Different Techniques for Site Response Estimation

3.2.1.1 Site Amplification Factor by Horizontal-to-Vertical-Spectral Ratio (HVSR) or Receiver Function Technique

The receiver function $HVSR_{ij}(f_k)$ can be computed at each j site for the i^{th} event at the central frequency f_k from the root mean square average of the amplitude spectra as,

$$HVSR_{ij}(f_k) = \frac{\frac{1}{\sqrt{2}}\sqrt{absH_{ij}(f_k)\Big|^2_{NS} + absH_{ij}(f_k)\Big|^2_{EW}}}{absV_{ij}(f_k)} \quad \ldots\ldots\ldots\ldots\ldots\ldots \quad (3.3)$$

where,

$H_{ij}(f_k)|_{NS}$: Fourier spectra of the NS component,

$H_{ij}(f_k)|_{EW}$: Fourier spectra of the EW component and

$V_{ij}(f_k)$: Fourier spectra of the vertical component.

Finally, the event average receiver function $HVSR_{ij_j}^{ave}(f_k)$ (Field and Jacob, 1995) is computed at each j site for the k^{th} frequency to consider the contribution of all the seismic events recorded at that station.

3.2.1.2 Site Response Estimation using Geotechnical Parameters

Site response can be calculated from geotechnical data as follows:

$$Amp(f) = \sqrt{\frac{\rho\beta}{\rho_s(f)\beta_s(f)}\exp(-\pi k_o f)} \quad \ldots\ldots\ldots\ldots\ldots\ldots \quad (3.4)$$

where b and r are the shearwave velocity and density of the crust beneath the site. The effective velocity $b_s(f)$, effective density $r_s(f)$, and site damping factor K_o are calculated from the expressions given by Boore (2003).

In this study two hundred boreholes were used for the site response calculation. All the geotechnical parameters as well as estimated site response at 141 noise survey locations is given in Table 3.1.

3.3 SITE RESPONSE STUDY IN THE GUWAHATI REGION USING STRONG MOTION DATA

The tectonic setting of the Himalaya and its relation with the seismicity of the region has drawn world attention from earth scientists. The Guwahati region, which is a part of the northeast India, is placed in Zone V (PGA > 0.4g), the highest region of the seismic zonation map of India (BIS, 2002, Figure 1.1). Northeast India lies at the junction of the Himalayan Arc to the north and the Burmese Arc to the east. The high seismicity in the region is attributed to the collision tectonics between the Indian plate and the Eurasian plate to the north and Indo-Myanmar range to the east. Global Positioning System (GPS) measurements show that India and southern Tibet converge at 20±3mm/year (Bilham *et al.,* 2001). Bilham *et al.* (2001) divided the Himalaya into 10 imaginary sections, each around 220km in length. At the observed convergence rate of 20mm/year, at least 6 of these 10 regions have an accumulated slip potential of 4m. This is equivalent to the slip believed to be associated with the 1934 Nepal-Bihar earthquake that killed 10,700 people. Site amplification is one of the important factors which contribute strongly to the hazard. Strong motion data is record of short period ground motion which strongly accumulate the soil effect due to which amplification takes place. Amplification of shear-wave at free surface is easily estimated from strong motion data by deconvolving the vertical component of accelerogram from radial and transverse component.

3.3.1 Waveform Data Source for Site Response Study in the Guwahati Region

A semi-permanent five-station strong motion array (which is being upgraded to twelve stations) in Guwahati urban area established by Indian Institute of Technology (IIT) Guwahati, India has been operative in the terrain. Five Kinemetrics ETNA have been installed at AEC, AMTRON, Cotton College Guwahati, IIT Guwahati and Irrigation department site (Figure 4.1). A trigger level is set at 0.005% of the full-scale (2g), except for the sites with high ambient noise where it was kept at higher value. The dynamic range of the systems is 108dB at 200 samples/sec with 18-bit resolution. The present analysis is based on 6 earthquakes of magnitude ranging from 3.1 to 5.7, which are recorded with good signal-to-noise ratio (signal-to-background noise ratio ^{3} 3).

3.3.2 Strong Motion Data Processing

The uncorrected acceleration time series, $x(n)$, recorded by a given station were corrected for the instrument response and baseline following the standard algorithm as outlined in the software package of Kinemetrics inc. The onset of S-wave arrival time (t_0) was estimated in $x(n)$ Then, $x(n)$ was bandpass filtered between 0.1 and 30.0Hz. From the filtered dataset b(n), a time window of 5.0s duration, starting from t_0 and containing the maximum of S-wave arrival was selected for all the analysis undertaken in this study.

3.3.3 Analysis of Strong Motion Data

3.3.3.1 Path effect

Q_S is determined and its dependence on frequency is established in the form of a power law through regression analysis of the direct S-wave data recorded by strong motion station as shown in Figure 3.1. The equation thus established with negligible uncertainty in the constant and the exponential terms is as follows:

$$Q_s = (134.15 \pm 29.92)\, f^{(0.52 \pm 0.09)} \quad \text{.....} \quad (3.5)$$

The Q_S obtained in the present study represents the overall attenuation of the seismic wave energy, which includes the direct S-wave, early coda, and possibly L_g phase of the recorded data from events with focal depths more than 10km, except for a few shallow foci earthquakes. Since in our case there is no deeper event with a focal depth beyond 35km, we restrict our observations to only one seismic wave energy attenuation relation with a trade off between the source and the attenuation factors built in the convolution model.

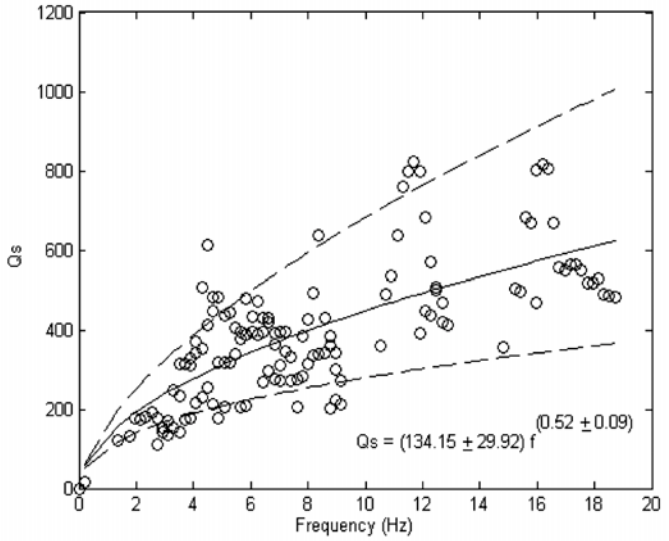

Figure 3.1 The plots of Q_S verses frequency. The dashed lines represent the zone of scatter of the data points with respect to the power law relation between Q_S and frequency with ± one standard deviation in the constant and the exponent

3.3.3.2 Site Response Analysis from Waveform data

Station site amplification has been computed from 2 strong motion events with signal-to-background noise ratio greater than 3. The site response has been calculated by using HVSR technique for all the events at each site for different source azimuths. Figure 3.2 (d) and (e) represents the site response due to events recorded at 302.34°N and 335.17°N azimuth at the station .

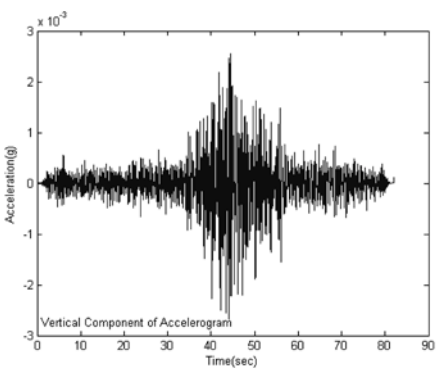

(a)

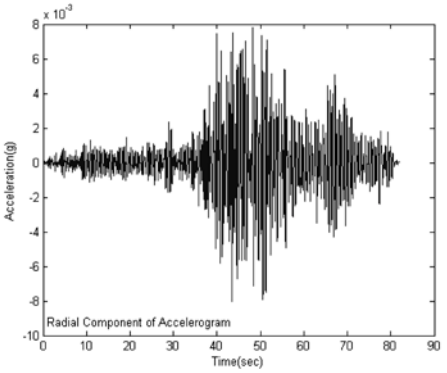

(b)

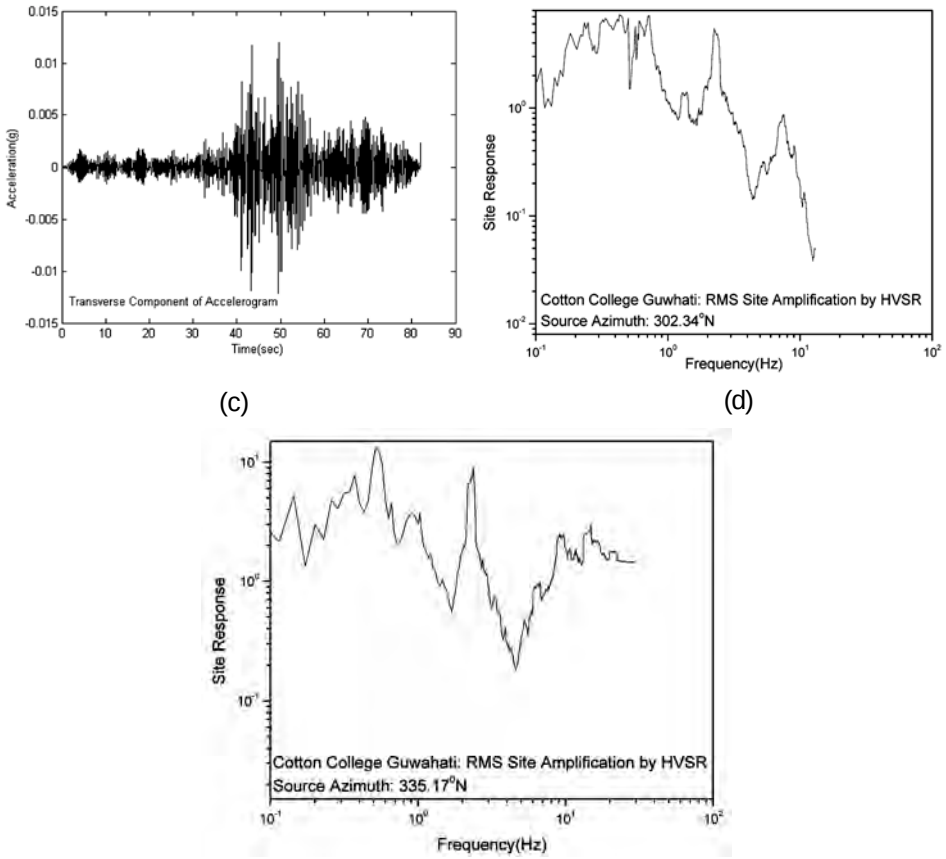

Figure 3.2 (a) Radial component, (b) Transverse component, (c) Vertical component of accelerogram recorded at an azimuth 335.17°N, (d) RMS site response by HVSR for source azimuth 302.34°N and (e) RMS site response by HVSR for source azimuth 335.17°N

3.3.3.3 Estimation of Site Amplification using WESHAKE 91

The US Army Waterways Experiment Station (WES) has been using the computer program SHAKE to calculate site response for level-ground soil sites for more than 15 years, including use on a number of USACE projects. WES has continually made adaptations to SHAKE as the use for each new project required. The original version for use on a personal computer was obtained from the University of California at Berkeley (UCB) around 1985. This program at WES is now called WESHAKE91

to reflect the numerous changes that have been made to keep pace with state-of-the-art technology, to provide for needs of USACE users, and to provide a user-friendly interface. These adaptations facilitate transfer technology to, and wide-spread use among USACE personnel.

A site response analysis, sometimes referred to as a soil amplification analysis, involves the determination of components of ground motion for design or seismic evaluation. Typically, as in this study, that determination is made for a “free-field” response at the ground surface of an ideal soil deposit (horizontal layers extending to infinity) to a spatially-uniform motion applied at the base. The motions at these three points, as well as any other point in the vertical profile, are unique. Design earthquakes are frequently specified as corresponding to a rock outcrop. Mathematical expressions (transfer functions) are then used to find the equivalent motion for the base rock and then the seismic waves are propagated through the soil column to determine the free-field motion.

The determination of site-specific earthquake response of soil deposits generally involves four basic steps: a) Selection of earthquake motions, usually corresponding to rock outcrop, b) Idealization of stratigraphy and selection of material properties, c) Calculation and evaluation of site response, and d) step of a site-specific earthquake response analysis.

SHAKE was developed to calculate the horizontal response caused by an earthquake at any depth of a soil profile. The approach and algorithms incorporated in the program are simple, straight forward and adequate for the purpose intended. The simplicity associated with SHAKE is attributed to some basic assumptions regarding the cyclic behavior of materials and geometry of the problem. The basic assumptions used in the formulation are: a) The soil layers are horizontal and extend to infinity, b) The ground surface is level, c) Each soil layer is completely defined by the shear modulus and damping as a function of strain, the thickness, and unit weight, d) The non-linear cyclic material behavior is adequately represented by the linear visco-elastic (Voigt) constitutive model and implemented with the equivalent-linear method, and e) The incident earthquake motions are spatially-uniform, horizontally-polarized shear waves, and propagate vertically. In general, assumptions (a), (b), and (c) used to derive this model would seem to significantly limit the applicability of this method. However,

past studies have shown that reasonable results are obtained for a much broader spectrum of in situ conditions. The equivalent-linear constitutive model, assumption (d), is described later in this section. The last assumption (e) narrows the focus to a simple class of problems, but, is a common assumption for this type of problem. It is important to realize that the formulation of SHAKE for wave propagation is based on a total stress analysis. The materials are considered to be continua and pore water pressures are non-existent. The calculation of shear modulus using values of K2 does involve the determination of mean effective stress using the depth of the water table and the unit weight of water.

Figure 3.3 represents the comparison of site response obtained by WESHAKE91 and strong motion data at AEC. The former provides lower values however both the computations represent the maximum amplification at same frequency.

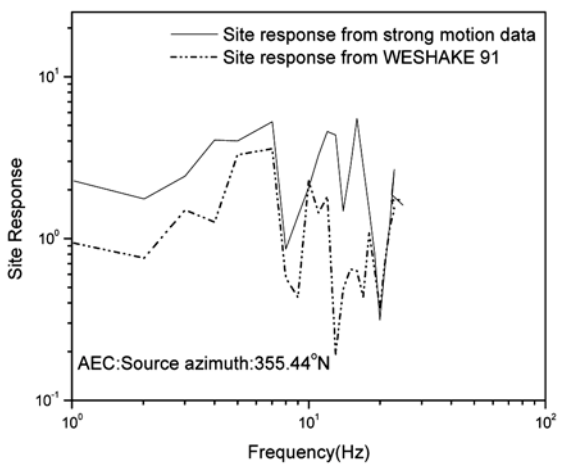

Figure 3.3 Comparison of site response estimated from strong motion data and WESHAKE91 at AEC for an earthquake recorded at an azimuth 355.44°N

3.4 ESTIMATION OF PREDOMINANT FREQUENCY FROM AMBIENT NOISE SURVEY USING H/V OR NAKAMURA RATIO

It is widely recognized that local geological conditions have pronounced impact on ground motion at a given site. Each soil type responds differently, when subjected to the ground motions, imposed due to earthquake loading. Usually the younger softer soil amplifies ground motion relative to older, more competent soils or bedrock. Local amplification of the ground is often controlled by the soft surface layer, which leads to the trapping of the seismic energy, due to the impedance contrast between the soft surface soils and the underlying bedrock. Moreover, the relatively simple onset of vertical resonances can be transformed into a complex pattern of resonances, strongly dependent on the characteristics of the lithological attributes, geometry and topography *(*Aki,1993; Bard, 1994; Faccioli, 1991,1995; Chavez-Garcia *et al.*, 1996).

Resonance frequency of each soil type also differs depending upon the physical property, and depth to bedrock. Quantification of this amplification of ground motion and determination of natural resonance frequency is the main objective of site response study. This frequency dependent amplification forms an important factor for seismic hazard analysis and microzonation studies. The site response parameters are also used to distinguish regions where seismic hazard is high due to amplification from the surface geology and match of natural frequency of the soil with the construction. The mapping of the soil behavior before a seismic wave-field propagates also provides an overview of the possible damage to individual structure or a set of buildings.

The total area of the Guwahati city is about 600 sq km lying between longitude 91^0 30¢91^0 50¢E and latitude 26^0 05¢ 26^0 12¢N, covering almost the entire urban part of the city. The Guwahati city is covered with recent alluvium with some Archean hillocks at places. The area falls in the Lower Assam valley bounded by the Eastern Himalaya to the north and Shillong Plateau to the south. The Lower Assam valley consists of crystalline rocks that are covered by gently dipping Tertiary and younger sediments. The sediment thickness varies from ten to few hundred meters in the study area.

Several methods for soil characterization are described in literature and used for site response study of several cities (Bard, 1997, 2000; Kudo, 1995). Broadly these methods can be categorized as follows:

i) Numerical,

ii) Empirical, and

iii) Experimental.

The influence of local geological structure on the spectral characteristics of ambient noise of relatively distant sources has long been recognized. Experimental Methods based on noise or earthquake data has been found to be most economical and less time consuming. Nakamura type study based on microtremor was found to be suitable in Indian context and has been used in several previous Microzonation studies of Indian cities such as for Jabalpur and Delhi.

This method considers that spectral amplification of a surface layer could be obtained by evaluating the horizontal to vertical spectral ratio of the microtremors recorded at the site. The main challenge to determine site amplification characteristics from microtremors is to remove source and path effect. Nakamura (1989, 1996) proposed an approximate procedure for removing source effects from microtremor records based on a modification of the conventional transfer function of the site. The following hypothesis are adopted:

(i) The horizontal tremor may be considered, to certain accuracy, to be amplified through multi-reflection of the S-wave while the vertical tremor is amplified through multi-reflection of P-wave.

(ii) The effect of Rayleigh waves remarkably appears in the vertical tremor.

Comparison with other techniques by different investigators, it shows that Nakamura technique is very simple for obtaining the fundamental resonant frequency, but fails for higher harmonics and that peak amplitude is somewhat different from amplification measured on spectral ratios. However, this Nakamura version of the microtremor method has already proved to be one of the most inexpensive and convenient

techniques to reliably estimate fundamental frequencies of soft deposits. It certainly deserves more work so as to elucidate the factors influencing peak amplitudes.

3.4.1 Methodology Adopted

Use of microtremors appears to be very convenient because of its cost and time effective nature. The studies when conducted in conjunction with other complementary techniques, such as shear wave velocity measurements (Aki's technique), receiver-function type technique based on weak motion data and especially in reference site dependent mode, would be an effective tool for site characterization ascertaining peak/resonance frequency and amplification.

Hence, the site response studies at Guwahati were conducted resorting to Nakamura type studies based on microtremor data and geological attributes. 141 sites **(Annexure II)** were selected for response studies to characterize the ground condition defining their response parameters.

3.4.2 Field work/Data Acquisition

Microtremor measurements were performed in the urban area of Guwahati city by deploying several digital seismic recorders with short period velocity sensors. One station approximately per square km is considered; observations were taken at 141 recording stations covering the total area of approximately 600 sq. km, of almost the entire urban part of Guwahati city (longitude 91°30¢91°50¢E and latitude 26°05¢ 26°12¢N) as shown in Figure 3.4. The exact location of the stations was determined by the built-in GPS system with a precision of 0.0001 degree. The instruments were installed for a period ranging from one hour to maximum 48 hours**.** The studies were conducted jointly by India Meteorological Department, New Delhi, and Geological survey of India, Kolkata and Regional Research Laboratory, Jorhat between February-May 2003.

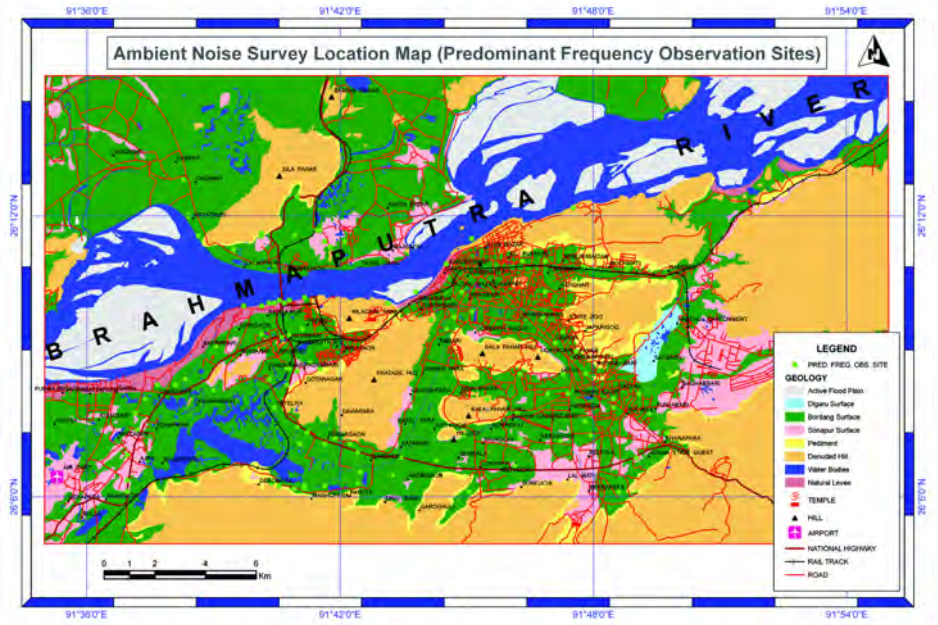

Figure 3.4 Ambient noise survey location map

3.4.3 Nakamura Type Studies

The response studies were conducted in long term array and rapid modes for ascertaining response parameters for different ground conditions. The data acquisition was made following the recommendations of Bard (2000) and Mucciarelli (1998) using velocity sensor of natural period 1sec.

To avoid errors due to day and night variations in noise pattern at Guwahati, enough data of about 24 hours to several days have been collected at each representative site covering day, night and local variation and each hour data is used for spectrum analysis. At most of the stations arrangements have been made to ensure perfect coupling between sensor and the natural soil of the site.

3.4.4 Data Processing

3.4.4.1 Selection of Data

For processing of acquired data, the following steps have been adopted

a) Continuous waveform data collected for several days have been divided in one hour waveform data files and thus 80 to 100 waveform data files have been created for each representative site.

b) Continuous waveform data collected for one hour have been divided in 8 to 10min waveform data files and thus about 6 to 8 waveform data files have been created for each representative site.

c) For the data collected in trigger mode for 24 to 48 hours, each waveform file created through trigger algorithm has been examined and approximately 80 to 100 waveform data files have been created for each site.

d) It is seen that H/V ratio, gets affected by “heavy” traffic; similarly, walking near the sensor create spurious transients. To avoid spurious inconsistent data, a portion of uniform wave train has been selected for the analysis. Each waveform data file generated has been plotted and a portion of smooth common wave train of about 120 seconds has been separated from these and new waveform data file has been created for selected portion of data.

e) Appropriate data portion of each file then has been used for spectrum analysis as per the criteria of time window length selection described below.

3.4.4.2 Selection of Time Window Length

In such a study, selection of time window for spectral analysis is an important aspect. The application of the spectral ratio technique to micro tremor records present a basic problem; it is very difficult to identify a common wave train for a longer duration for the station involved, particularly in urban areas due to the movement of heavy transport, adjacent to the observational sites, which cannot be avoided.

Generally accepted rule of thumb in site response studies is that the window length should have at least 10 cycles for the lowest frequency analyzed (Bard, 1997). The frequency of interest can be ascertained on the basis of frequency of structures in the area of interest, which can be determined using the relationship between the height of the building and its fundamental period of vibration T=Number of storey/10. In the Jabalpur area frequency of built environment ranging from 0.33 sec (3Hz) to 0.16sec (6Hz), therefore, about 30 sec time window length is found to be appropriate.

3.4.4.3 Computation of Spectra

For computation of Fourier transform spectra of individual component and relative spectra of horizontal versus vertical components, SPEC program tagged with SEISAN incorporating minor modifications to appropriate the programme with the data set has been used. SEISAN is an earthquake analysis software developed by Jens Havskov and Lars Ottemoller, Institute of Solid Earth Physics, University of Bergen, Norway (Havskov and Ottemoller, 2000).

3.4.4.4 Computation of Resultant Spectra from SPEC Program

The SPEC program computes H/V of individual component. Then, root mean square is calculated for all the individual plots to get the final H/V ratio. To avoid spurious peak links with sharp troughs on spectrum and for clear identification of Peak frequency, spectra need to be appropriately smoothened. In the present study, smoothing has been performed 300 times.

3.5 ESTIMATION OF PREDOMINANT FREQUENCY FROM EMPIRICAL RELATION

Following the Ibs-von Seht and Wohlenberg (1999) relationship which is given by equation (3.6), predominant frequency is empirically derived from the basement depth (Table 3.1). Good match has been observed between predominant frequencies derived from empirical relation and those estimated from ambient noise survey.

$$m = 96\left(f^{-1.388} \right) \quad \text{.....(3.6)}$$

'm' is the basement depth in metre and 'f' in Hz is the predominant frequency of the site under consideration.

3.6 REMARKS

Due to highly variable geological features of the Guwahati urban agglomeration, the peak resonance frequency showed high variation from site to site. The frequency for most part of the urban area lies between 0.5Hz to 5.0Hz. However, there are isolated sites, where peak frequency is more than 5 Hz and lies between 5 to 10Hz. Figure 3.5 illustrates the corresponding peak frequency contour map. It shows that Geological domain of Active Flood plain and Levee have the peak frequency >0.5Hz, Digaru Surface have peak frequency between 0.5-0.8Hz, Bordang Surface have peak frequency between 0.8-2.0Hz; Sonapur Surface between 2.0–4.0Hz; Rocky areas of Pediment have peak frequency between 4-6Hz and Denuded Hill have peak frequency greater than 6.0Hz.

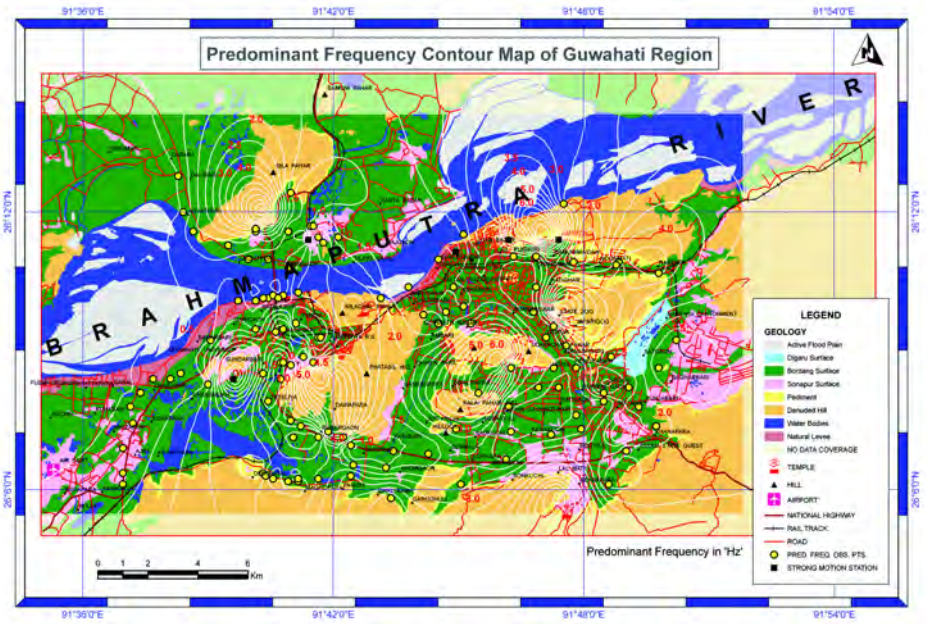

Figure 3.5 Peak Frequency contour map of Guwahati Region

3.7 SITE RESPONSE ANALYSIS FROM GEOTECHNICAL DATA

Most important parameter for site response study is the shear wave velocity of each site, determination of which is very expensive and time consuming. Some empirical relations between SPT-N values and S-wave velocity have been established that can be used to obtain ideas about the expected shear wave velocity of the surfacial soft soil. Fumal and Tinslay (1985), after measuring N-values and corresponding shear wave velocities of Holocene-Pleistocene sediments of the Los Angeles region in California, USA, have developed three separate correlations between N-values and shear wave velocities for three textural group of sediments, viz. clay and silty clay, silt loam and sandy clay, and gravelly sand respectively. The three correlations are as follows:

$$Vs = 5.3N + 134 \text{ for clay and silty clay} \quad \ldots\ldots (3.7)$$

$$Vs = 4.3N + 218 \text{ for silt loam and sandy clay} \quad \ldots\ldots (3.8)$$

$$Vs = 5.1N + 152 \text{ for sand and gravelly sand} \quad \ldots\ldots (3.9)$$

Tonouchi, *et al.* (1983) has given another empirical relation between N-values and S-wave velocities as under –

$$Vs = 97 * N^{0.314} \quad \ldots\ldots (3.10)$$

A fifth relation has been given by Kayabali (1996) as

$$Vs = 3.75N + 175 \quad \ldots\ldots (3.11)$$

SPT data of 200 borehole sites (Figure 3.6) were collected having depth range varying from 6m to 30m. Majority of locations of these sites fall in the Downtown area and along a zone on either side of the G-S road. Depth-wise N-value data have been tabulated for each site; then each N-value has been converted in to S-wave velocity from the Equations 3.10 and 3.7. The values thus obtained for each layer were averaged to arrive at average V_s^{30} according to the individual relations as stated. Ultimately the S-wave velocities obtained through each relationship were again averaged to arrive at expected V_s^{30} at the site. Details of geotechnical/lithological parameter used in these analyses have been given in the Annexure: Annexure III for Location, Depth of Ground

Water Table, and Date of drilling and Litho-Log of each SPT borehole; Annexure IV for Physical and Shear Parameters of sediment as obtained from boreholes; Annexure V for Shear wave velocity data at different depth; Annexure VI for Shear wave velocity (V_s^{30}) at each borehole; Annexure VII for Soil density at different depth and Annexure VIII for Factor of safety.

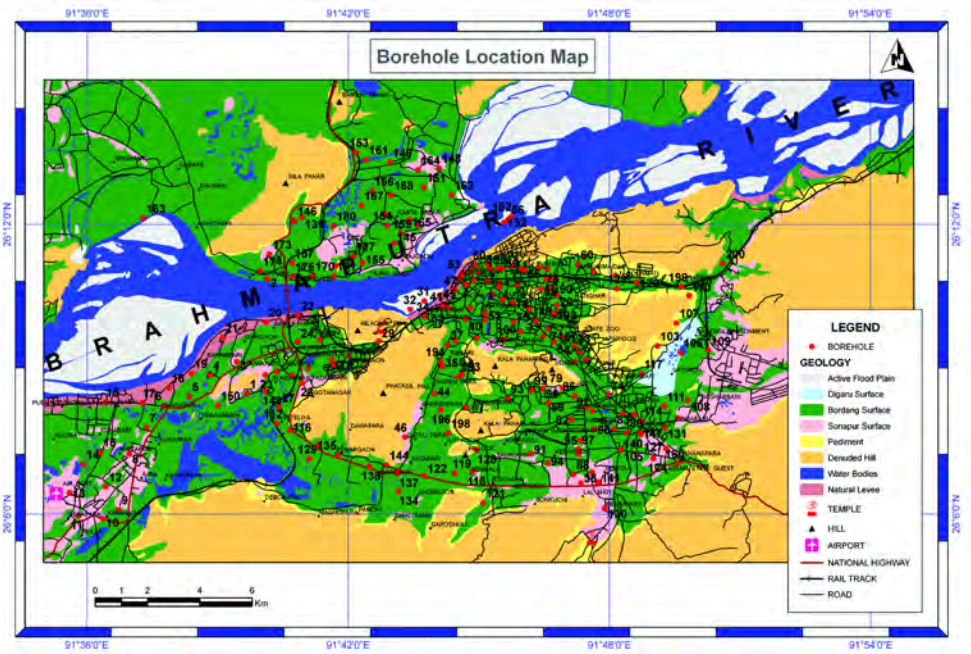

Figure 3.6 Borehole location map of Guwahati Region

The values of shear wave velocity (V_s^{30}), thus obtained, vary from 200m/s to 360m/s. High shear wave velocities have been found at a few spots along the G-S road, northern portion of the Cantonment area and over the rocky ground by the side of Brahmaputra River in the Ujan Bazar area. While plotting on the base map the shear wave velocity data have been grouped into 4 classes viz. 200-240, 240-280, 280-320 and >320 meter per second. The first group indicates soft soil and the rest indicate stiff soil as per the classification of UBC, 1977.

Contour map of bulk density and effective shear wave velocity (V_s^{30}) calculated from Boore's (2003) relation is shown in Figures 3.7 and 3.8. Site response for Guwahati region was calculated at 131 predominant frequency observation sites out of 141. Rest of the observations were taken on hillocks where borehole information was not available. Site response calculated from Equation (3.4), along with geotechnical parameters used in site amplification is given in Table 3.1. Table 3.2 represents a comparison between the site response calculated from HVSR (strong motion data) and empirical method at predominant frequencies. Value obtained by both the method depicts good match. We have used the empirical site response at borehole locations for our analysis to avoid extrapolation in the contouring because boreholes are well distributed in the region. Figure 3.9 represents site response contour map of Guwahati region.

Table 3.1: Site Response and Geotechnical Parameters in Guwahati Region at 141 Noise Survey Locations

Sl. No.	Lat (°N)	Long (°E)	Predominant frequency estimated by noise survey (Hz)	Predominant frequency estimated by empirical relation (Hz)	Effective Shear Wave Velocity V_s^{30} (m/sec)	Effective Density (gm/cc)	Q-factor	Damping Factor (K_0*10^{-4})	Site Response
1	26.142	91.693	8.4	———-	On Hill (Rock)	———-	———-	———-	No amplification
2	26.169	91.669	0.2	0.73	253.81	1.9806	78.70	15.0	4.63
3	26.171	91.674	0.7	0.73	257.73	1.8861	141.81	8.21	4.71
4	26.170	91.676	0.7	0.73	264.55	2.0635	141.81	8.00	4.44
5	26.172	91.680	0.4	0.73	263.71	2.0045	109.01	10.4	4.52
6	26.171	91.686	2.3	0.97	216.45	1.7645	248.04	5.59	5.31
7	26.169	91.719	2.3	0.97	232.56	1.8636	248.04	3.12	4.99
8	26.106	91.616	0.7	0.57	260.42	1.8915	141.81	8.12	4.68
9	26.199	91.672	7.5	———	On Hill (Rock)	———-	———-	———-	No amplification
10	26.193	91.669	2.0	———	245.10	1.9415	232.27	5.27	4.76
11	26.169	91.672	0.7	0.97	222.22	1.9205	141.81	9.52	5.03
12	26.158	91.669	1.2	1.14	261.78	1.9360	182.69	6.27	4.61
13	26.155	91.694	1.2	1.14	233.92	1.7560	182.69	5.62	5.12
14	26.157	91.677	3.4	1.6	245.00	2.1000	298.06	4.11	4.57
15	26.160	91.685	1	———	274.73	1.6350	167.69	6.51	4.90
16	26.155	91.695	0.8	1.14	210.53	1.7793	150.99	9.44	5.36
17	26.140	91.628	0.9	1.14	299.40	2.0321	159.59	6.28	4.21

Sl. No.	Lat (°N)	Long (°E)	Predominant frequency estimated by noise survey (Hz)	Predominant frequency estimated by empirical relation (Hz)	Effective Shear Wave Velocity V_s^{30} (m/sec)	Effective Density (gm/cc)	Q-factor	Damping Factor (K_0*10^{-4})	Site Response
18	26.142	91.639	0.7	0.49	277.78	2.0682	141.81	7.62	4.33
19	26.154	91.651	0.8	0.69	295.86	1.8530	150.99	6.72	4.43
20	26.148	91.666	4.4	———	267.38	2.1200	336.46	3.33	4.35
21	26.138	91.650	0.9	1.60	299.40	2.0321	159.59	6.28	4.21
22	26.142	91.672	2.7	———	331.13	2.1200	267.45	3.39	3.92
23	26.146	91.679	0.5	0.91	261.78	2.0725	121.07	9.47	4.46
24	26.145	91.683	2	1.19	240.38	2.1075	232.27	5.37	4.61
25	26.148	91.688	4.7	1.19	257.73	2.0630	347.05	3.35	4.50
26	26.146	91.692	0.9	———	258.62	1.8960	159.59	4.36	4.69
27	26.130	91.619	0.6	0.49	280.90	1.8800	131.90	8.10	4.52
28	26.119	91.684	0.6	0.69	282.49	2.1160	131.90	8.05	4.25
29	26.140	91.679	0.3	———	270.27	1.8525	95.23	11.7	4.64
30	26.106	91.672	3	———	299.40	2.1415	281.03	3.57	4.10
31	26.135	91.623	0.5	0.53	280.99	1.9925	121.07	8.82	4.39
32	26.132	91.674	0.3	0.73	255.10	2.0980	95.23	12.3	4.49
33	26.125	91.683	2.5	2.31	241.55	1.8685	257.95	4.81	4.88
34	26.123	91.687	2	2.31	295.86	2.0258	232.27	4.37	4.24
35	26.124	91.620	0.6	0.53	207.97	1.9450	131.90	10.9	5.16
36	26.119	91.694	0.5	0.97	236.69	1.8500	121.07	8.38	4.96
37	26.121	91.698	5.3	1.60	287.36	1.5845	367.21	2.84	4.86
38	26.116	91.707	0.4	1.05	222.22	1.8836	109.01	12.4	5.08
39	26.115	91.616	0.7	0.53	250.00	1.1813	141.81	6.77	6.04
40	26.105	91.673	2.2	———	273.22	2.0520	242.91	4.52	4.38
41	26.104	91.676	0.9	———	261.78	2.1090	159.59	7.18	4.42
42	26.103	91.686	0.7	———	210.97	1.9295	141.81	10.0	5.15
43	26.104	91.694	2.1	2.63	287.36	2.0895	237.66	4.39	4.23
44	26.104	91.686	2.4	3.09	241.55	1.9060	253.05	4.91	4.83
45	26.105	91.707	3.2	2.63	253.81	2.1090	289.69	4.08	4.48
46	26.109	91.708	1	1.05	260.42	2.1356	167.69	6.87	4.40
47	26.119	91.704	5.3	2.31	240.38	1.9924	367.21	3.40	4.74
48	26.158	91.680	4.4	———	199.72	1.7010	336.46	4.42	5.59
49	26.102	91.616	0.8	0.59	273.22	2.1065	150.99	7.27	4.33
50	26.140	91.635	0.9	0.61	264.55	1.9561	159.59	5.68	4.56
51	26.171	91.722	1.1		227.27	1.9150	175.37	7.53	4.97
52	26.200	91.640	0.5	0.57	235.85	1.9595	121.07	10.5	4.83
53	26.188	91.658	1.3	0.65	212.77	1.7450	189.70	7.43	5.39

Sl. No.	Lat (°N)	Long (°E)	Predominant frequency estimated by noise survey (Hz)	Predominant frequency estimated by empirical relation (Hz)	Effective Shear Wave Velocity V_s^{30} (m/sec)	Effective Density (gm/cc)	Q-factor	Damping Factor (K_0*10^{-4})	Site Response
54	26.169	91.662	1.4	0.65	210.08	1.8755	196.42	7.27	5.23
55	26.103	91.682	2	3.09	240.38	2.1075	232.27	5.37	4.61
56	26.213	91.638	0.5	0.30	314.47	1.9668	121.07	7.88	4.18
57	26.146	91.680	0.9	0.91	227.27	1.8675	159.59	8.27	5.04
58	26.170	91.678	0.4	0.91	223.21	1.6059	109.01	12.3	5.48
59	26.193	91.644	1.4	0.76	210.08	1.8755	196.42	7.27	5.23
60	26.195	91.691	1.1	1.40	260.42	1.7595	175.37	6.57	4.85
61	26.195	91.692	0.9	1.40	201.34	1.9583	159.59	5.60	5.23
62	26.207	91.683	1.1	1.40	223.21	1.8071	175.37	7.66	5.17
63	26.193	91.682	0.8	———	216.45	1.8430	150.99	9.18	5.20
64	26.191	91.694	3.4	1.40	289.86	2.0607	298.06	3.47	4.24
65	26.191	91.702	1.4	1.40	277.78	1.8953	196.42	5.50	4.52
66	26.183	91.666	0.9	0.69	290.70	1.6190	159.59	6.47	4.79
67	26.194	91.669	5.3	———	250.00	2.0319	367.21	2.61	4.60
68	26.183	91.674	0.8	0.76	274.73	2.0745	150.99	7.23	4.35
69	26.189	91.696	3.2	0.76	252.53	1.9370	289.69	4.10	4.69
70	26.180	91.682	1.1	———	248.76	1.9225	175.37	6.88	4.75
71	26.190	91.692	3.4	———	On Hill (rock)	———	———	———	No amplification
72	26.108	91.721	0.9	0.69	259.07	2.1630	159.59	7.26	4.39
73	26.127	91.797	1.1	0.91	257.73	1.9780	175.37	6.64	4.60
74	26.173	91.730	1	0.91	360.14	1.8094	167.69	4.01	4.09
75	26.114	91.724	0.8	0.69	225.23	1.5730	150.99	8.82	5.52
76	26.184	91.781	1.9	1.88	216.45	1.7640	226.74	6.11	5.31
77	26.097	91.789	7.5	———	On Hill (rock)	———	———	———	No amplification
78	26.158	91.818	3.5		214.59	1.8635	302.15	4.63	5.18
79	26.166	91.752	1.2	0.91	261.78	1.8290	182.69	6.27	4.74
80	26.122	91.799	1.2	2.63	214.59	1.9035	182.69	7.65	5.13
81	26.120	91.787	0.9	1.14	234.74	1.8175	159.59	8.01	5.03
82	26.144	91.788	1.5	1.49	256.41	1.8874	202.89	5.77	4.72
83	26.160	91.755	2.3	2.63	232.22	1.9790	248.04	5.21	4.84
84	26.164	91.780	1.1	1.14	255.10	1.9565	175.37	6.71	4.65
85	26.184	91.772	1.9	1.49	259.07	1.9535	226.74	5.11	4.61
86	26.190	91.758	2.9		292.40	1.9594	276.59	3.71	4.33
87	26.163	91.790	8.2	———-	On Hill (rock)	———	———	———	No amplification

Sl. No.	Lat (°N)	Long (°E)	Predominant frequency estimated by noise survey (Hz)	Predominant frequency estimated by empirical relation (Hz)	Effective Shear Wave Velocity V_s^{30} (m/sec)	Effective Density (gm/cc)	Q-factor	Damping Factor (K_0*10^{-4})	Site Response
88	26.129	91.745	4.1	———	292.40	1.9578	325.47	3.15	4.33
89	26.130	91.721	1.8	———	260.42	2.1460	221.05	5.21	4.39
90	26.137	91.790	0.8	1.49	280.90	2.1295	150.99	7.07	4.25
91	26.183	91.742	1.2	1.19	261.78	1.9360	182.69	6.27	4.61
92	26.155	91.785	1.7	1.49	331.13	2.0065	215.19	4.21	4.03
93	26.172	91.796	5.3	———	On Hill (rock)	———	———	———	No amplification
94	26.185	91.752	1.1	———	263.16	1.9900	175.37	6.50	4.54
95	26.164	91.745	2.1	3.09	224.22	1.9895	237.66	5.63	4.91
96	26.097	91.723	4.4	3.09	201.61	1.7010	336.46	4.42	5.59
97	26.138	91.725	1.6	1.60	248.76	1.8906	209.14	5.77	4.79
98	26.173	91.781	1.4	1.19	210.08	1.8755	196.42	7.27	5.23
99	26.182	91.796	1.2	1.88	270.27	2.0300	182.69	6.08	4.43
100	26.137	91.782	1.5	1.40	251.57	1.9769	202.89	5.88	4.65
101	26.148	91.811	2.2	1.19	271.74	1.9105	242.91	4.54	4.55
102	26.152	91.793	2.4	1.40	271.74	2.0005	253.05	4.36	4.45
103	26.159	91.788	1.6	2.63	304.88	2.066	209.14	4.70	4.14
104	26.133	91.737	3.6	———	294.12	2.0375	306.17	3.33	4.24
105	26.199	91.778	7	———	On Hill (rock)	———	———	———	No amplification
106	26.190	91.784	9.5	———	On Hill (rock)	———	———	———	No amplification
107	26.123	91.829	2.4	1.10	268.82	1.8582	253.05	4.41	4.64
108	26.163	91.707	3.6	2.63	304.88	2.0660	209.14	4.70	4.14
109	26.118	91.815	4	———	On Hill (rock)	———	———	———	No amplification
110	26.144	91.771	3.4	———	264.90	1.8907	298.06	———	———
111	26.135	91.758	7.2	2.63	284.09	2.1160	424.09	2.49	4.23
112	26.160	91.742	0.6	1.14	270.27	1.9162	131.90	8.42	4.56
113	26.121	91.771	0.9	0.91	222.22	1.9525	159.59	7.03	4.37
114	26.146	91.768	8.2	2.63	On Hill (rock)	———	———	———	No amplification
115	26.147	91.752	4.8	———	265.96	1.9195	350.50	2.57	4.59
116	26.102	91.751	2.2	0.91	234.74	1.8980	242.91	5.26	4.91
117	26.113	91.738	0.9	1.40	267.38	2.1150	159.59	7.03	4.37
118	26.178	91.830	4.9	2.63	243.90	1.9205	353.92	3.48	4.79
119	26.203	91.792	2.4	———	255.10	2.0740	253.05	4.65	4.51
120	26.182	91.814	4.7	1.88	255.10	1.8165	347.05	3.39	4.82

Sl. No.	Lat (°N)	Long (°E)	Predominant frequency estimated by noise survey (Hz)	Predominant frequency estimated by empirical relation (Hz)	Effective Shear Wave Velocity V_s^{30} (m/sec)	Effective Density (gm/cc)	Q-factor	Damping Factor (K_0*10^{-4})	Site Response
121	26.190	91.801	0.9	———	270.27	1.9150	159.59	5.56	4.56
122	26.130	91.770	1.2	1.40	246.31	1.9615	182.69	6.67	4.72
123	26.191	91.767	1.6	———	233.92	1.7560	209.14	4.91	5.12
124	26.181	91.813	2.9	1.4	259.07	1.8665	276.59	4.19	4.72
125	26.130	91.822	2.1	3.09	219.78	1.7147	237.66	4.59	5.35
126	26.171	91.830	3.5	———	265.49	1.6054	302.15	2.24	5.03
127	26.137	91.818	3	1.19	259.07	1.8910	281.03	4.12	4.69
128	26.163	91.736	1	1.19	205.76	1.5720	167.69	8.69	5.77
129	26.102	91.810	1.1	3.09	263.16	2.0140	175.37	6.50	4.51
130	26.173	91.748	1.5	0.91	260.42	2.1005	202.89	5.68	4.44
131	26.122	91.749	3.1	2.63	277.78	1.9620	285.40	3.78	4.44
132	26.144	91.797	1	1.19	225.23	1.8567	167.69	7.94	5.08
133	26.111	91.769	1.1	1.14	250.00	1.7012	175.37	5.47	5.03
134	26.132	91.808	1.1	0.97	292.40	1.9035	175.37	5.85	4.40
135	26.154	91.837	1.1	0.91	257.73	1.8435	175.37	6.64	4.76
136	26.144	91.830	1.1	1.14	273.22	1.9915	175.37	6.26	4.45
137	26.135	91.808	4.2	———	304.88	2.0480	329.18	2.99	4.15
138	26.135	91.808	4.6	———	304.88	2.0480	329.18	2.99	4.15
139	26.114	91.817	1.6	1.32	282.49	1.8520	209.14	5.08	4.54
140	26.192	91.752	1.6	———	264.55	1.9700	209.14	5.42	4.55
141	26.178	91.758	2.2	———	284.09	1.9279	242.91	4.35	4.43

Table 3.2: Comparison of site response calculated from empirical relation and strong ground motion data

Station (Latitude, Longitude)	Predominant Frequency	Empirically Calculated Site Response	Site Response from strong ground motion data
AEC (26.14191^0 N, 91.66107^{o}E)	7.2	4.97	5.60
AMTRON (26.18573^0 N, 91.7861^{o}E)	6.2	5.12	4.38
Cotton College Guwahati (26.18586^0 N, 91.74524^{o}E)	0.8	4.41	3.98
IIT Guwahati (26.18748^0 N, 91.69056^{o}E)	0.6	6.63	6.73
Irrigation (26.184713^0 N, 91.77269^{o}E),	5.4	4.88	5.45

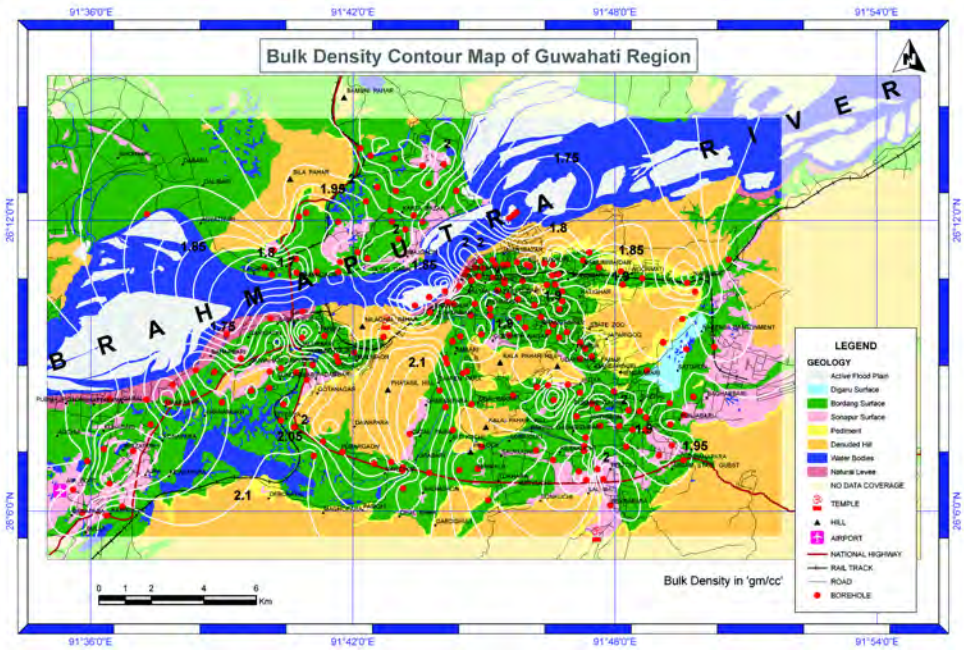

Figure 3.7 Bulk density contour map of Guwahati Region

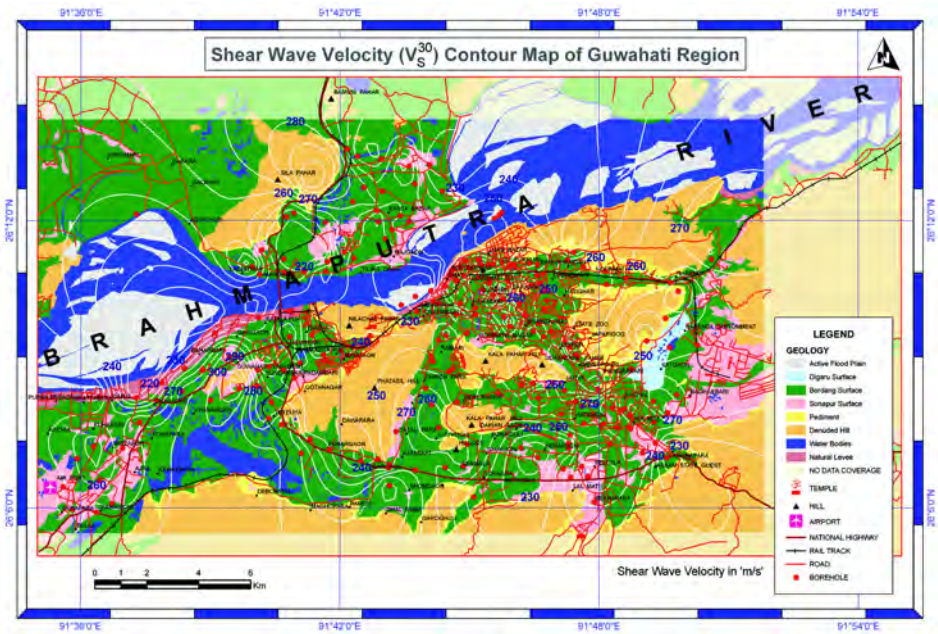

Figure 3.8 Shear wave velocity (V_s^{30}) contour map of Guwahati Region

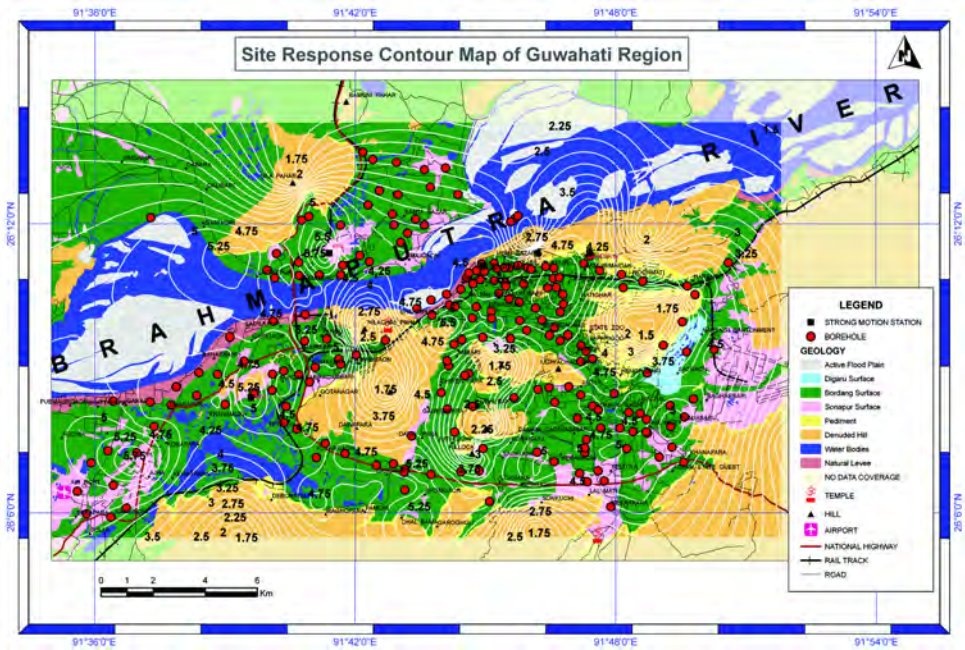

Figure 3.9 Site response contour map of Guwahati Region

3.8 SITE CLASSIFICATION OF GUWAHATI REGION

Site classification in Guwahati Region is done on the basis of shear wave velocity, site response, predominant frequency and factor of safety. These themes are integrated using multi criteria decision making method (Saaty, 1980). Figure 3.10 depicts the site classification of Guwahati Region. Range of effective shear wave velocity and predominant frequency are given in Table 3.3.

Table 3.3: Shear wave velocity and Predominant frequency of each site class

Site Class	Shear Wave Velocity (m/s)	Predominant Frequency (Hz)
IIIA	200-240	0.5-2.0
IIIB	240-280	2.0-4.0
IIIC	280-320	4.0-6.0
IIID	320-360	6.0-8.2

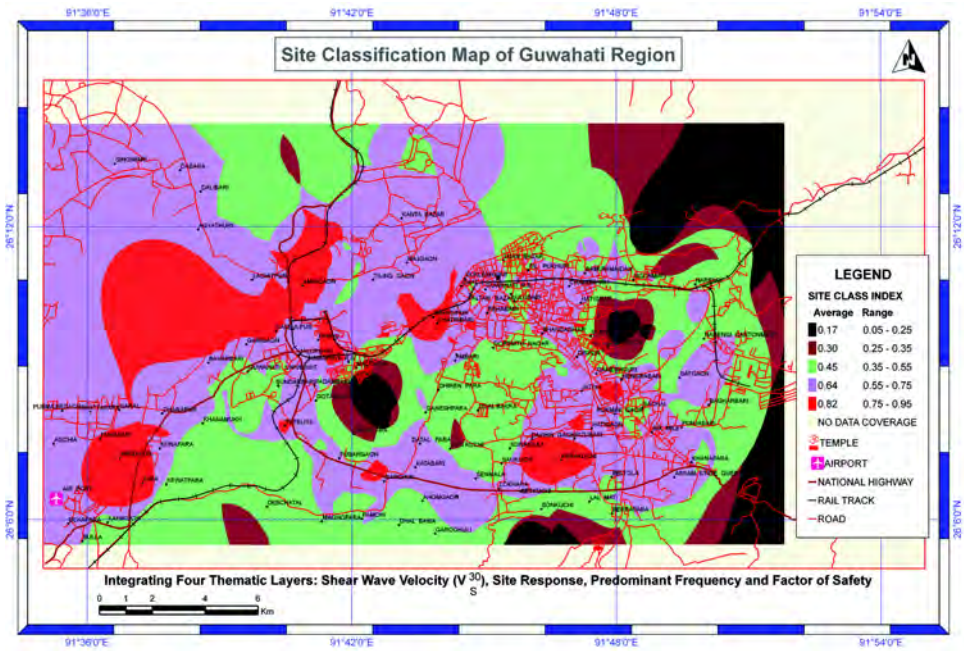

Figure 3.10 Site classification of Guwahati Region

CHAPTER 4

Strong Ground Motion Synthesis and Seismic Scenario in the Guwahati Region

4.1 INTRODUCTION

The introduction of performance based earthquake resistant design for buildings and other civil engineering structure has increased the need for simulating realistic ground motions. Combined with recent developments in software tools and structural modeling techniques for time domain transient nonlinear dynamic analysis, the use of simulated time histories of ground motion has gained major importance. Although the use of recorded ground motion under condition similar to the design earthquake is appealing, there may never be an adequate suite of such data in terms of tectonic structures, earthquake size, local geology, and near field conditions. The variability of ground acceleration traces depends on the source, propagation path, and site characteristics. A number of methods have been developed and are in use for the adjustment of selected recorded time histories to provide conformity to site condition (so-called accelerogram scaling) and other spectrum technique that aim to generate time histories of ground motion whose response spectra match the design response spectrum. There are several approaches to the modeling and simulation of strong ground motion taking into account the physics of source and propagation process. Each approach accommodates, to varying degrees, the seismic wave radiation from a fault rupture propagation through the crust, and modification by local site conditions. we perform the simulation and modeling of ground motion by two approaches, first by recorded strong motion data of two earthquakes considering omega $(\omega_k = 2\pi f_k)$ squared circular crack source model (Brune,1970) and second by generating synthetic seismogram using continuous wave number integration method (Wang and Herrmann, 1980).

4.2 SOURCE SPECTRA AND SIMULATION OF SPECTRAL ACCELERATION

In the previous chapter, it has been estimated that propagation path term $P(r_{ij},f_k)$, and site effect term $SI_j(f_k)$ follow the equation (3.2). Brune (1970) gives the source term as,

$$SO_j(f_k) = \frac{\left[R_{\theta\phi}F(2\pi f_k)^2\right]}{\sqrt{2}(4\pi\rho\beta^3)} \cdot \frac{M_{oi}}{1+\left(\frac{f_k}{f_{ci}}\right)\gamma_i} \quad \text{..... (4.1)}$$

where M_{oi}, f_{ci} and g_i control the Brune's source model (Brune, 1970). We initialize M_{oi} by computing the value of M_0 in dyne-cm for a given Mw using Kanamori's relation (Hanks and Kanamori, 1979),

$$Mw = \frac{2}{3}\log(M_0) - 10.73 \quad \text{..... (4.2)}$$

The initial values of f_{ci} and g_i are assumed to be 0.1Hz (Dutta *et al.*, 2003) and 2 (Hwang and Huo, 1997) respectively. Estimation of these values is carried out in an iterative fashion. Iteration continues until the difference between the observed and the simulated source spectra tends to approach a minimum value. This exercise was carried out for 2 events at five stations as well as for borehole locations those coming in azimuthal range of these events. The location of all the five stations and 200 boreholes are shown in Figure 4.1.The simulated moment rate spectra and the spectral acceleration have also been compared with those extracted from observed data at the respective stations. The site response, source spectra, moment rate spectra and the spectral acceleration at station IIT Guwahati (26.19° N, 91.69°E) are furnished in Figure 4.2.

At IIT Guwahati, the site response as given in Figure 4.2(a) has been computed for the event recorded in the azimuthal direction of 306.15°N. The observed and simulated source amplitude spectra in Figure 4.2(b) find good match, the same has been observed for moment rate spectra, $\dot{M}_{Oi}$ in Figure 4.2(c) and the spectral acceleration in Figure 4.2(d). A corner frequency 5.4Hz for this event of Mw 3.1 with a scalar moment of 2.5×10^{21}dyne-cm seems to have replicated the observed spectra to a great extent with the resulting stress drop of 1.8 bars.

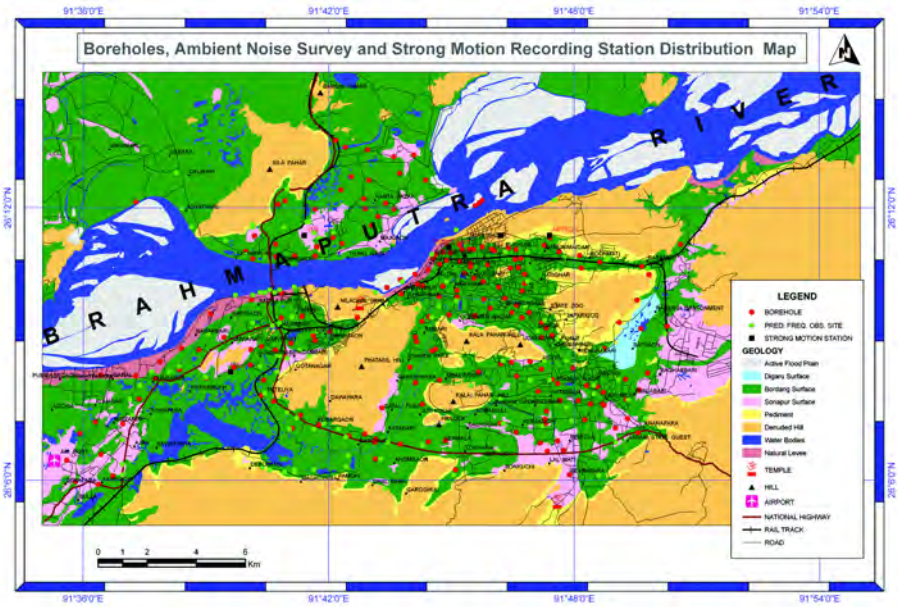

Figure 4.1 Borehole location, strong motion station and ambient noise survey sites in Guwahati Region

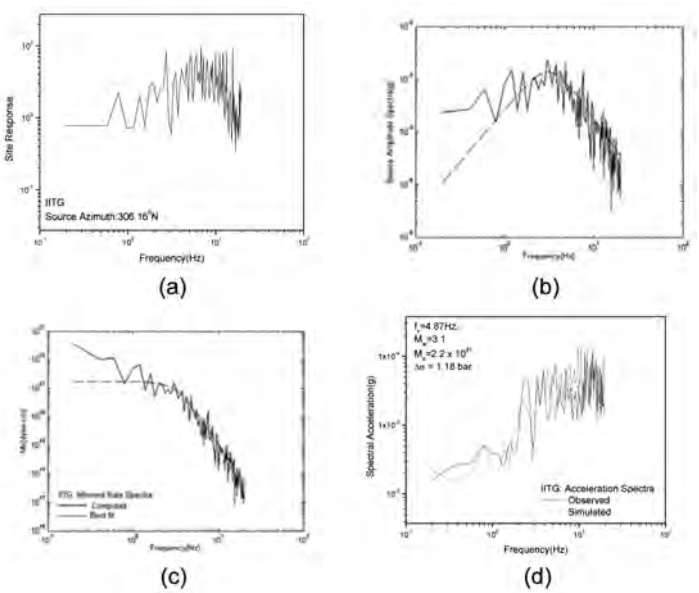

Figure 4.2 (a) Site Response for the source azimuth 306.15°N, (b) Observed and simulated source spectra, (c) Computed and best fit moment rate spectra, and (d) Observed and simulated spectral acceleration with source parameters at IIT Guwahati (26.19^0 N, 91.69^{o}E).

Table 4.1: List of source parameters: Moment Magnitude (Mw), Corner frequency (f_c), Scalar moment (M_0) and Stress Drop (Ds) determined for representative events in this study.

Sl. No.	Mw	f_c (Hz)	M_0 (dyne-cm)	Ds (bars)
1	3.1	2.20	2.5E+21	1.8
2	5.1	5.04	4.8E+22	0.30

The value of corner frequency f_{ci} can also be computed using the relation (Hwang and Huo, 1997),

$$f_{ci} = 4.9 * 10000 * \beta * \left(\frac{\Delta\sigma}{M_0}\right)^{\frac{1}{3}} \quad \text{.....} \quad (4.3)$$

Equation (4.2) given by Kanamori can be used to compute M_0 from M_L. To estimate the value of stress drop (Ds) we used the relation (Kanamori and Anderson, 1975),

$$\log(M_0) = \frac{3}{2}\log(S) + \log\left(\frac{16\Delta\sigma}{7\pi^{\frac{3}{2}}}\right) \quad \text{.....} \quad (4.4)$$

where S represents the surface area, that can further be calculated using the relation given by Bath and Duda (1964).

As already discussed we have appropriated a magnitude Mw 8.7 as SEM for the region. The same has been simulated in the present study. The historical Shillong Earthquake of Mw 8.7, 1897 has been the maximum magnitude event in the span from 1897 to 2006. As a first approximation, we consider the focus of the Shillong Earthquake to be an omega-squared circular-crack source model (Brune's Source) as the point source regime from where an SEM of 8.7 will germinate at a focal depth of 35 km. A hazard scenario in Guwahati region is thereby, established in terms of PGA using the convolution model for simulating the spectral acceleration at all the five stations as well as at 133 borehole locations. Site response was chosen for these boreholes on the basis of site class and azimuthal coverage of these recorded events.

The corresponding spectral acceleration computed at AMTRON along with the PGA values is presented in Figure 4.3. Figure 4.4 shows the site response and spectral acceleration at borehole location 1 (26.14167^{0}N, 91.66125^{o}E). Figure 4.5 represents PGA distribution map of Guwahati Region considering omega squared circular crack model. The highest PGA of 0.53g being observed at IIT Guwahati and 0.49g at AEC, diminishing towards the east where the value reached 0.26g at Cotton College Guwahati. This aspect is further analyzed through Green's function simulation and attenuation study from strong motion accelerometric data.

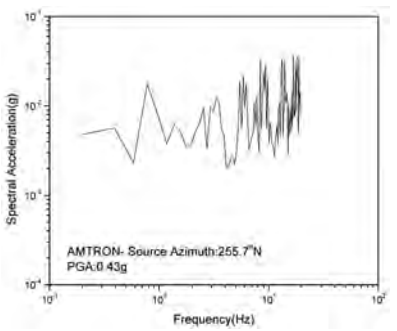

Figure 4.3 Simulated spectral acceleration for the Scenario Earthquake Magnitude (SEM) Mw 8.7 nucleating at the focus of 1897 Shillong earthquake at AMTRON

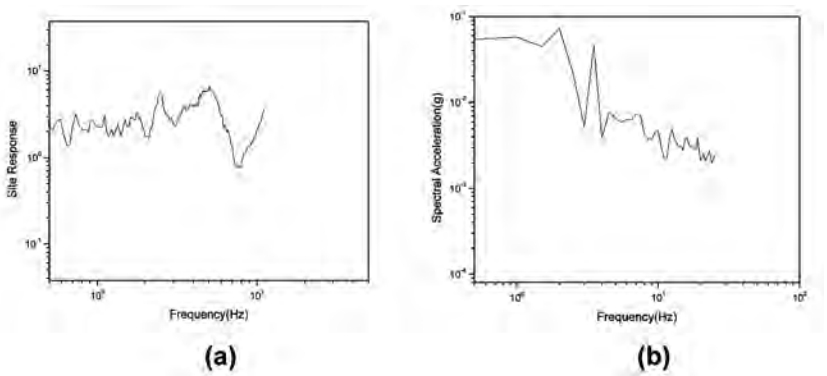

Figure 4.4 (a) Site response, (b) Spectral acceleration at the bore hole with the spatial coordinate 26.14167^{0}N, 91.66125^{o}E

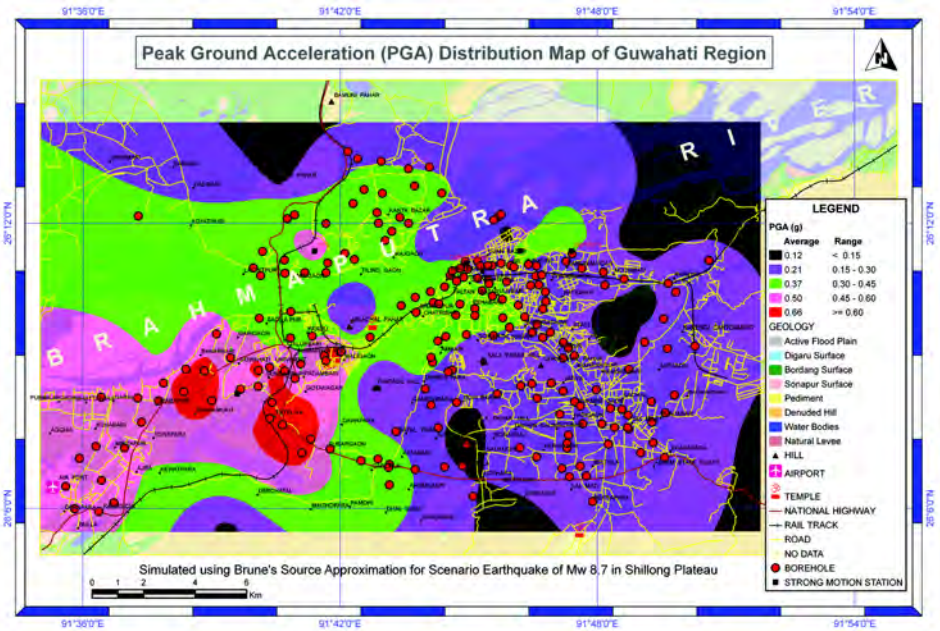

Figure 4.5 Spatial distribution of PGA in the Guwahati Region estimated from the Simulation of scenario earthquake of Mw 8.7 nucleating from 1897 Shillong earthquake

4.3 SYNTHESIS OF STRONG GROUND MOTION BY WAVE NUMBER INTEGRATION METHOD (GREEN'S FUNCTION APPROACH)

Wave number integration method or Green's function approach is useful if the range of possible fault rupture history is narrow enough to functionally constrain the predicted strong ground motion as is the case here. For the computation of synthetic accelerogram impulsive source has been used as a first approximation for the near-field effect. The wave number integration method of Herrmann and Mandal (1986) is then followed.

The generation of synthetic seismograms for point sources in simply layered structures has made rapid advances in the past decade. Two approaches, involving Laplace transform and Fourier transform techniques, are actively being pursued. The Laplace transform or Cagniard-de Hoop technique, usually referred to as the generalized ray method (Helmberger, 1968), constructs the solution by tracking the individual seismic arrivals ray by ray from the source to receiver. This method is valid at high frequencies

and works well at predicting particular phases, but is poorly suited to models with many layers and larger distances when a complete seismogram is desired. The other approach involves expressing the solutions in terms of a double integral transformation over wave number and frequency (Hudson, 1969). The complete solution rather than individual rays, is considered in such a full wave theory approach. This method can handle a larger number of plane layers, but requires considerable computational effort, especially at high frequencies.

Suppose that an earthquake can be represented by a double-couple without moment source model with the symbols 'n' for the vector normal to the fault and 'f' for the direction of force as used by Haskell (1963, 1964). The Fourier transformed vertical displacement generated by such a dislocation source can be written as

$$u_z(r,\phi,0,\omega) = ZSS\left[(f_1n_1 - f_2n_2)\cos 2\phi + (f_1n_2 + f_2n_1)\sin 2\phi\right]$$
$$+ZDS\left[(f_1n_3 + f_3n_1)\cos\phi + (f_2n_3 + f_3n_2)\sin\phi\right]$$
$$+ ZDD\left[f_3n_3\right] \quad \ldots\ldots\ldots\ldots\ldots\ldots\ldots\ldots\ldots\ldots\ldots\ldots\ldots\ldots\ldots\ldots \quad (4.5)$$

where *ZSS* is the Z-component displacement of a strike-slip type of source, *ZDS* is the Z-component displacement of a dip-slip type of source, and *ZDD* is the Z-component displacement of a 45° dip-slip type of source. Following the same procedure, the tangential and radial component of displacement can be written as

$$u_r(r,\phi,0,\omega) = RSS\left[(f_1n_1 - f_2n_2)\cos 2\phi + (f_1n_2 + f_2n_1)\sin 2\phi\right]$$
$$+RDS\left[(f_1n_3 + f_3n_1)\cos\phi + (f_2n_3 + f_3n_2)\sin\phi\right]$$
$$+ RDD\left[f_3n_3\right] \quad \ldots\ldots\ldots\ldots\ldots\ldots\ldots\ldots\ldots\ldots\ldots\ldots\ldots\ldots\ldots\ldots \quad (4.6)$$

$$u_\phi(r,\phi,0,\omega) = TSS\left[(f_1n_2 + f_2n_1)\cos 2\phi - (f_1n_1 - f_2n_2)\sin 2\phi\right]$$
$$+ TDS\left[(f_2n_3 + f_3n_2)\cos\phi - (f_1n_3 + f_3n_1)\sin\phi\right] \quad \ldots\ldots\ldots\ldots\ldots\ldots \quad (4.7)$$

ZDD, ZDS, ZSS, RSS, RDS, RDD, TSS and *TDS* are referred as Green's Functions. It is apparent, that these three components are necessary to represent the *P-SV* motion for any shear-dislocation source (Harkrider, 1976). *RSS* and *RDS* in equation (4.6) also include the near-field terms. These terms decrease faster than the others and therefore, are important only at short distances.

The values of $u_r(r,\phi,0,\omega)$, $u_z(r,\phi,0,\omega)$ and $u_\phi(r,\phi,0,\omega)$ are calculated at several discrete frequencies in the range of interest. The inverse Fourier transform of Equations (4.5), (4.6) and (4.7) on multiplication of $-w^2$ needs a convolution of the source spectra for the generation of acceleration time history of the vertical, radial and tangential components of ground motion as given below,

$$u_{r,z,\phi}(r,\phi,0,t) = \int_{-\infty}^{\infty} S(\omega) u_{r,z,\phi}(r,\phi,0,\omega) \exp(i\omega t) \frac{d\omega}{2\pi} \quad \text{.....} \quad (4.8)$$

where $S(\omega)$ is the Fourier spectra of the impulse source function as described by Herrmann (1979).

The S-wave part of the accelerogram is convolved with site response of each station to obtain the response on engineering bed rock.

4.3.1 Crustal Model

We have used the crustal model derived by inverting Rayleigh wave dispersion curve, (Mitra *et al.*, 2006). The model and dispersion curve, which has been taken for this study are shown in Figure 4.6(a-b). This model is derived by inverting Rayleigh wave dispersion curve. In each layer of the model the seismic energy attenuation due to both absorption by intrinsic anelasticity and scattering by heterogeneities is parameterized by the quality factor of S-wave Q_β and of P-wave Q_α. They are assumed to be frequency independent. Nath *et al.* (2005) has derived Q_β for Sikkim. The relation between the P-wave quality factor Q_α and the S-wave quality factor Q_β proposed in the literature (Anderson et al., 1965; Kijko and Mitchell, 1983) implicates $Q_\alpha = k\, Q_\beta$ with $1 \le k \le 2.5$. We have chosen k =2.5, so that in our study the effect of attenuation for a given Q_β can be considered to be minimal.

4.3.2 Simulation of Spectral Acceleration using Green's Function

The SEM as considered in the foregoing analysis is assigned with the focal mechanism of 1897 Great Shillong Earthquake for the synthesis of strong motion acceleration at all the borehole locations in the study region. Fault plane parameters that have been used for the Green's Function synthesis (after Bilham *et al.*, 2003) corresponds to a

slip of 16m on a fault plane striking ESE for 110km and dipping SSW at 57° beneath the northern edge of the plateau, slip on the plane extends from 9 to 45km beneath the surface, with a rake of 76°. The dip of the fault and the rake of the slip are constrained within 15° by the distribution of shear strains.

Our next step is to validate the PGA calculated by simulation using Brune's source with the PGA estimated by Synthetic Accelerogram Simulation. Hence the PGA is calculated using synthetic seismogram simulation at 200 borehole locations as well as at five strong motion instrument locations. Figure 4.7 shows the calculated Green's Function at borehole location 141 (26.11113°N, 91.79567°E). This computed synthetic accelerogram was band pass filtered between the frequency range 0.5Hz to 25Hz. Figure 4.8(a)-(e) show synthetic accelerogram convolved with site response and simulated spectral acceleration at borehole location 141(26.11113°N, 91.79567°E). Figures 4.9 and 4.10 represent Green's function and simulated spectral acceleration at IIT Guwahati station. Figure 4.11 represents spatial distribution of simulated PGA using Green's function simulation in Guwahati Region. A comparative plot of the PGA estimated by point source approximation w^2- circular crack source model, and by Wave Number Integration is presented in Figure 4.12 with a good 1:1 correspondence observed in the cross plot with $\pm$ 1 standard deviation bounds. However, in case of a homogeneous, elastic 2D or 3D horizontally stratified half space the wave fields radiated by an arbitrary internal point source may be described as a superposition of cylindrical waves (Green's function) characterized by horizontal wave numbers pertaining to different directions.

Response at any seismometer is the convolution of source, site and path terms. Path effect is the one which is dependent on the media in which the wave traverses. In Green's function simulation, superposition of impulsive layered earth responses are considered with the fault attitude and Haskel source approximation, thereby estimating realistic near - field effect having better accuracy at lower frequencies. The radiation pattern in case of Brune source approximation of w^2- circular crack source model does not incorporate layered earth responses rather a simplified reciprocal term for the path effect in an otherwise homogeneous half space for free-field modeling especially at higher frequencies. Therefore, simulation by Brune's source approximation provides over-estimated ground motions at seismic stations.

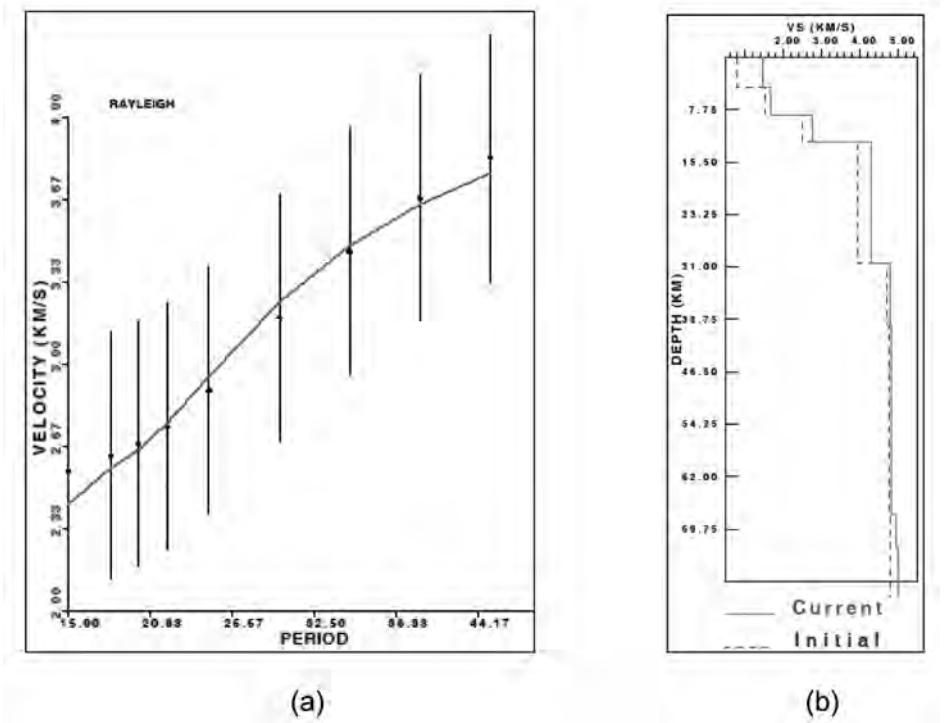

Figure 4.6 (a) Dispersion curve for the velocity model (after Mitra *et al.*, 2006), (b) Inverted shear wave crustal model used for continuous wave number integration

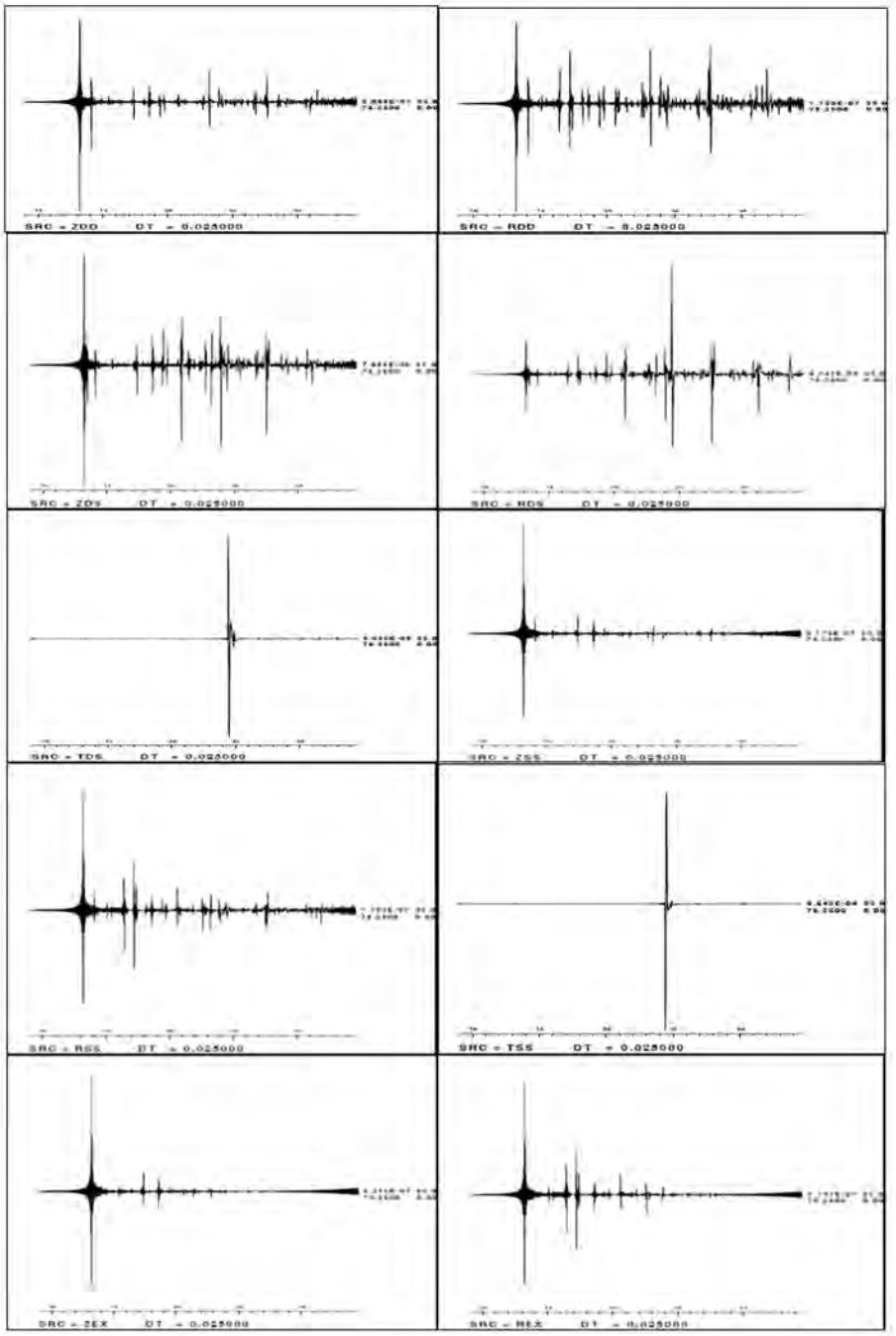

Figure 4.7 Green's functions at the bore hole no. 141(26.11113^{o}N, 91.76^{o}E)

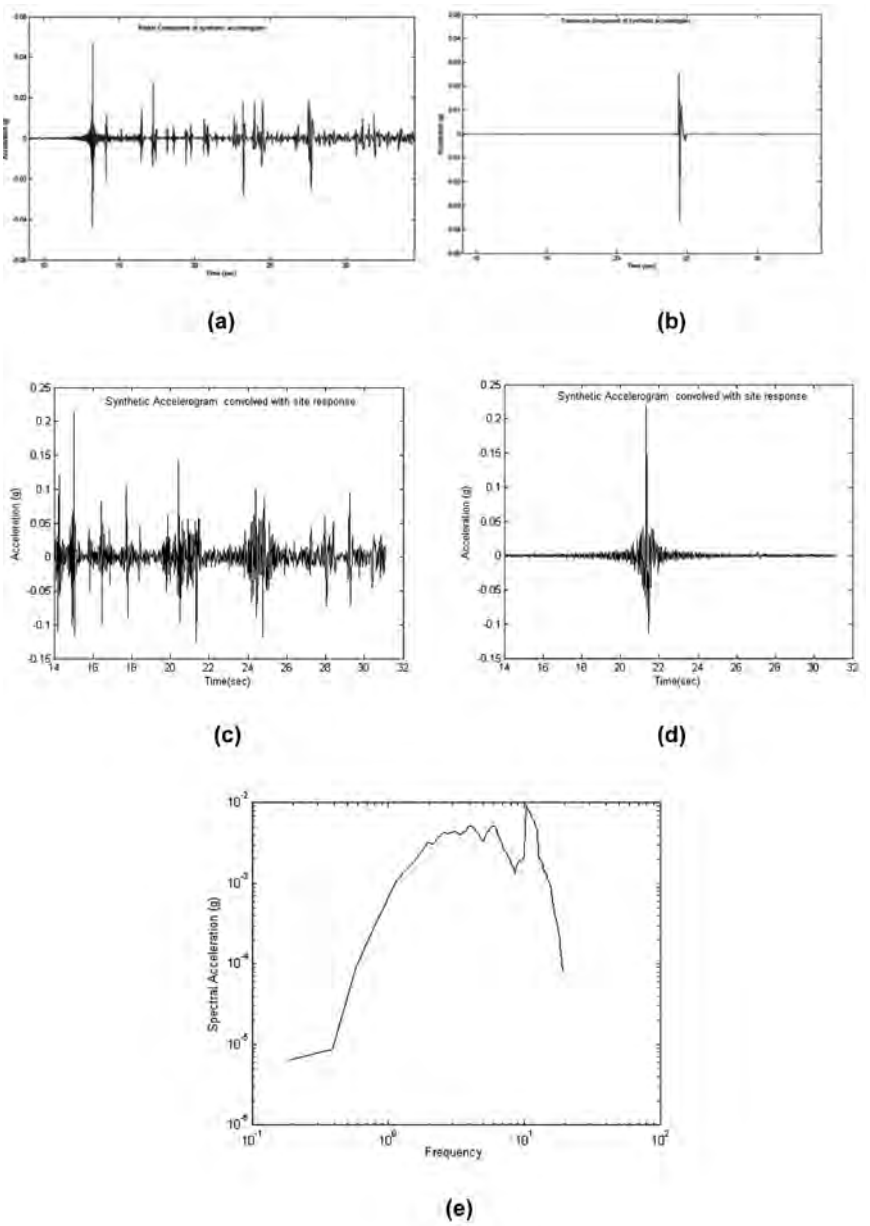

Figure 4.8 (a) Radial component of synthetic accelerogram, (b) Transverse component of synthetic accelerogram, (c) Radial component of synthetic accelerogram convolved with site response, (d) Transverse component of synthetic accelerogram convolved with site response, (e) Simulated spectral acceleration for Mw 8.7 at borehole no. 141(26.11113°N, 91.79567°E).

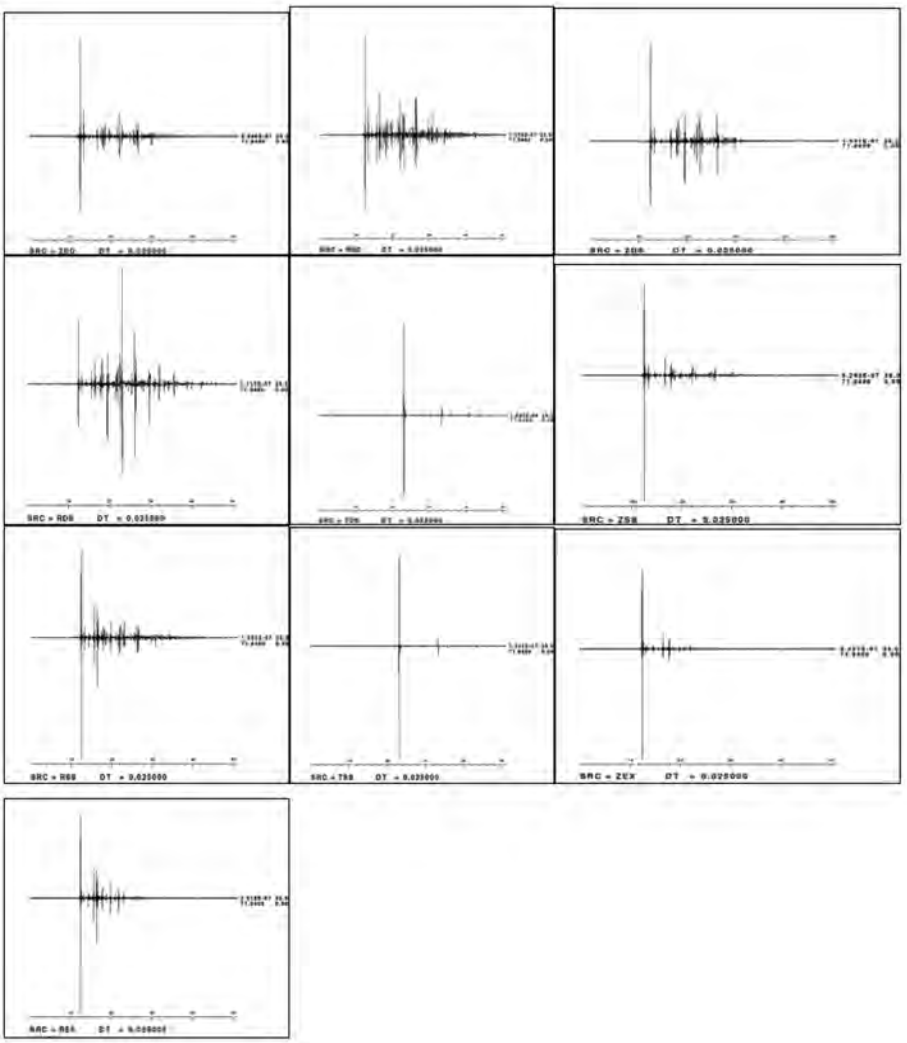

Fig 4.9 Green's functions at Guwahati station (26.18748˚N, 91.69056˚E)

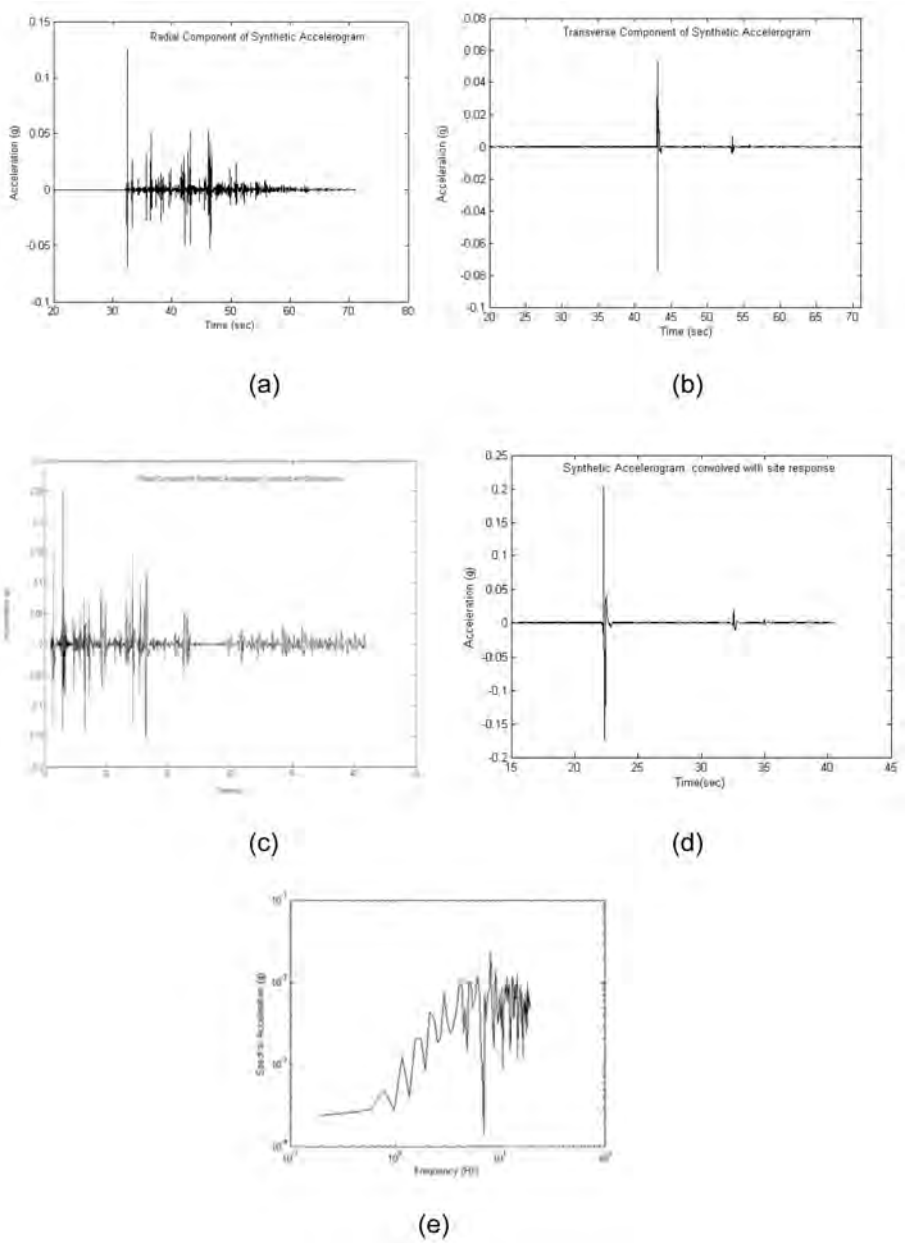

Figure 4.10 (a) Radial component of synthetic accelerogram, (b) Transverse component of synthetic accelerogram, (c) Radial component of synthetic accelerogram convolved with site response, (d) Transverse component of synthetic accelerogram convolved with site response, (e) Simulated spectral acceleration for Mw 8.7 at Guwahati station (26.18748^0 N, 91.69056^{o}E).

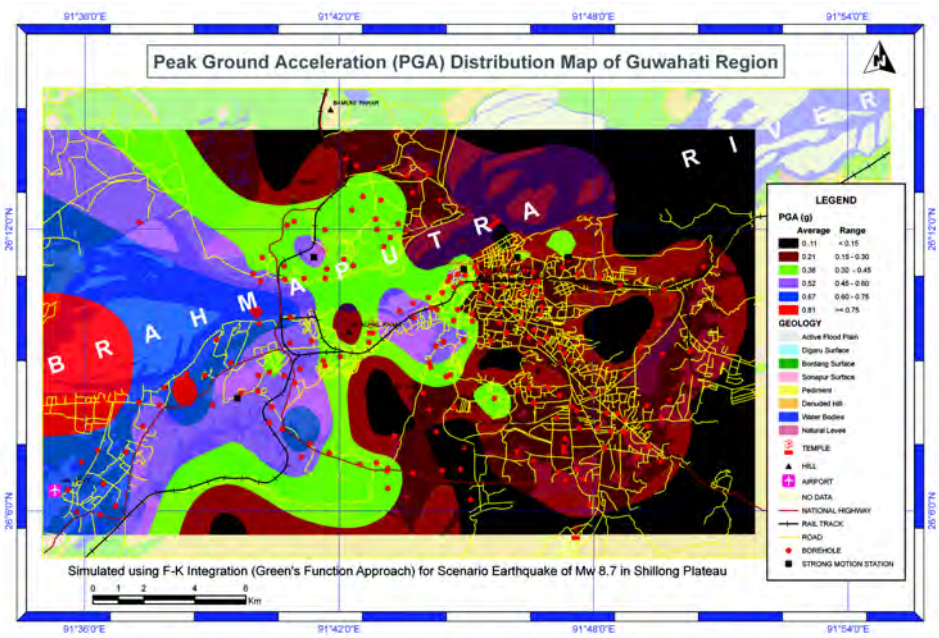

Figure 4.11 Spatial distribution of PGA in the Guwahati Region estimated through simulation of the scenario earthquake of Mw 8.7 by continuous Wave Number (F-K) integration method (Green's Function Approach)

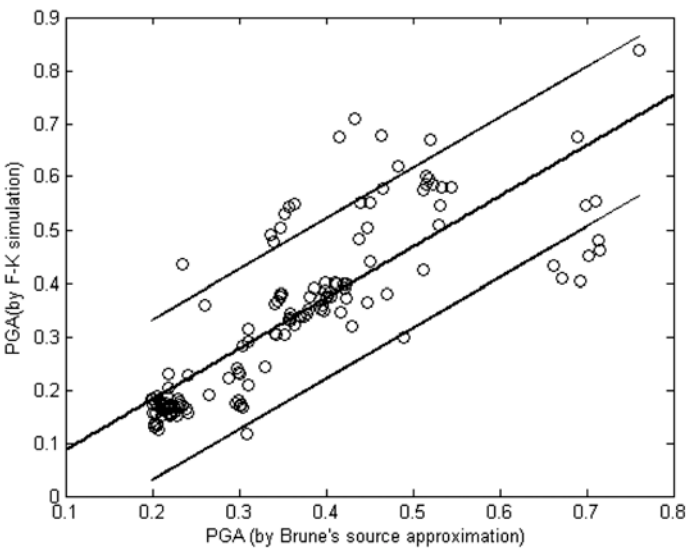

Figure 4.12 Scatter plot between PGA (by Brune source approximation) and PGA (by F-K Integration) depicting data clustering around the 45°, 1:1 correspondence line.

4.4 COMPUTATION OF RESPONSE SPECTRA FOR SINGLE DEGREE OF FREEDOM (SDOF)

A ground response analysis consists of studying the behavior of a soil deposit subjected to an acceleration time history applied to a layer of the profile. Ground response analyses are used to predict ground surface motions for the evaluation of amplification potential and for the development of design response spectrum. In the present study, ground response spectra have been computed using WESHAKE91 software (from the Waterways Experiment Station of US Navy) for the analysis of non-linear behavior of soil very often approximated by a 'linear-equivalent' method that uses an iterative procedure to adapt the soil parameters (i.e., rigidity and damping) to the actual strain it undergoes. The behavior of soil under irregular cyclic loading is modeled by using modulus reduction (G/Gmax) and damping (â) vs. strain curves, by calibrating with a standard database input. The degradation curves for sand and rock used for the present work are those proposed by Seed and Idriss (1970) and Schnabel (1973) respectively.

4.4.1 Input (Object) Motions

A strong motion accelerograph network is operating in the Guwahati region since 2004 and recorded ground motion for strong earthquake in locality has been used for site response analysis, study of moment rate spectra and spectral fall off. Eventually, it is to infer the shear wave quality factor (Q_s) response versus frequency and ground motion synthesis for a range of large earthquakes.

4.4.2 Ground Response Analysis

Synthesized acceleration time history for scenario earthquake of Mw 8.7 at each of the 200 borehole locations as well as five strong motion stations has been used as input ground motion at the bedrock level for simulation of response spectra through WESHAKE91. Both absolute as well as normalized response spectra at representative 12 borehole locations have been displayed in Figures 4.13 – 4.15 for site classes IIIA, IIIB and IIIC respectively. These response spectra will act as seismic design code in each of the site class.

Site Class IIIA

Borehole No # 01 (26.14167°N, 91.66125°E)

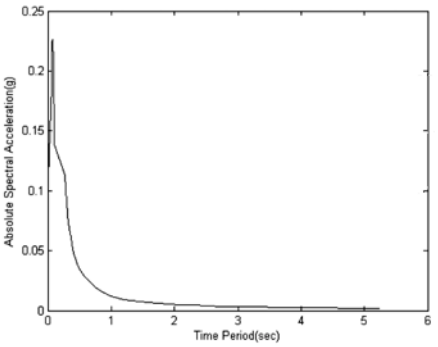

(a)

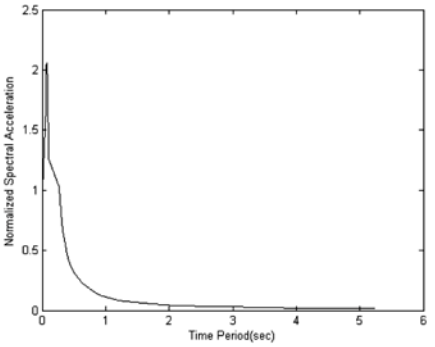

(b)

Borehole No # 13 (26.10744°N, 91.59333°E)

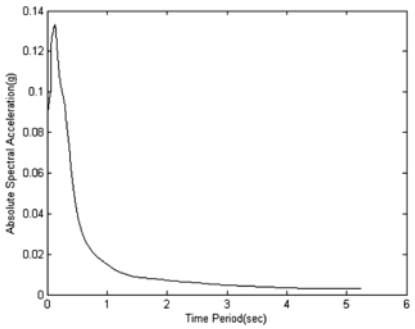

(a)

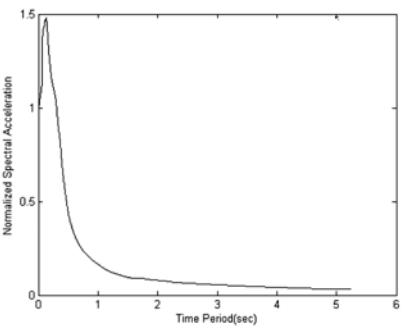

(b)

Figure 4.13 Contd.

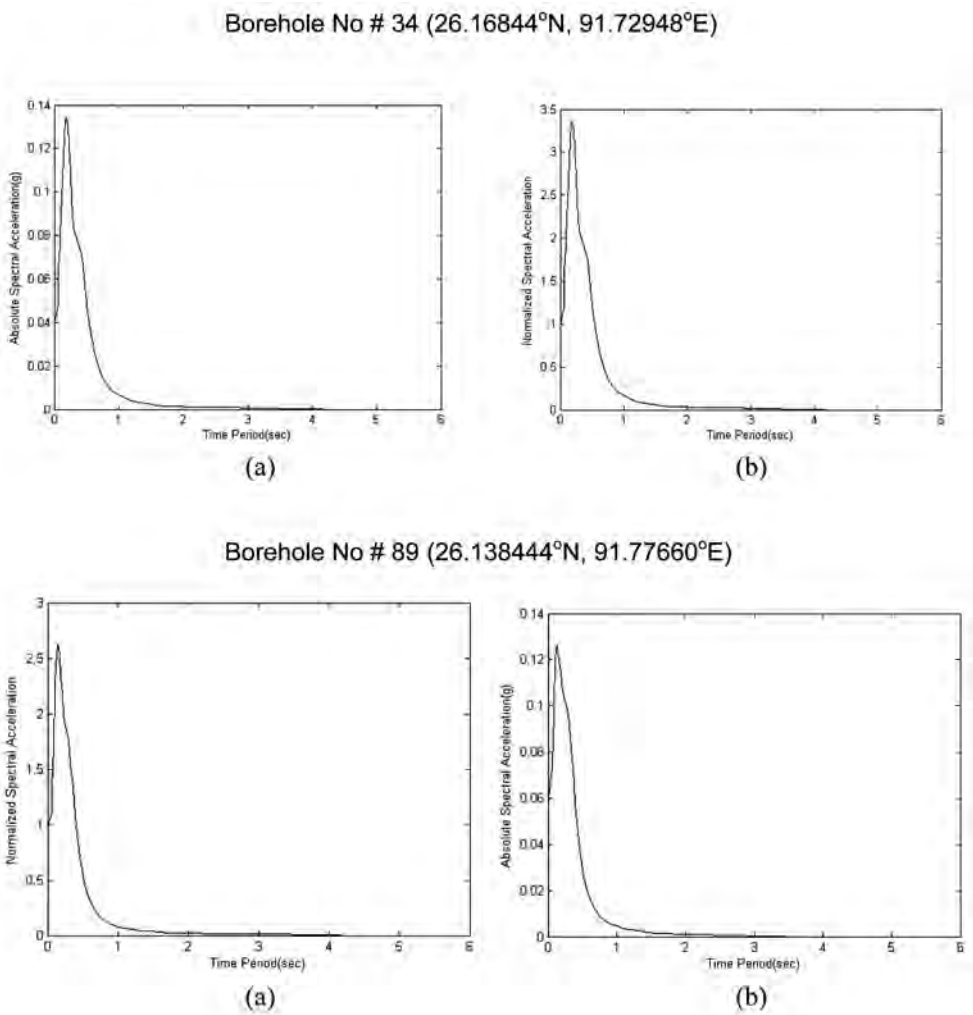

Figure 4.13 (a) Absolute and (b) Normalized spectral acceleration at site class IIIA

Site Class IIIB

Borehole No # 21(26.16420°N, 91.64974°E)

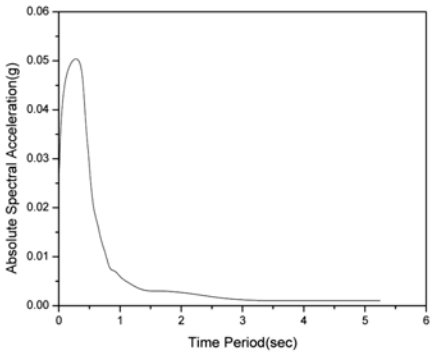

(a)

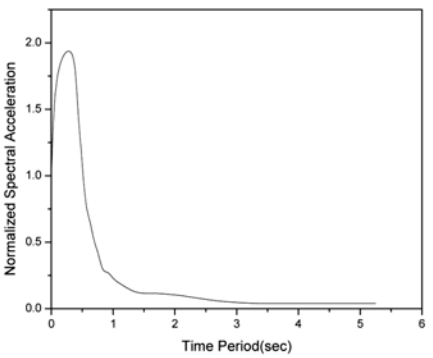

(b)

Borehole No # 53 (26.18457°N, 91.74117°E)

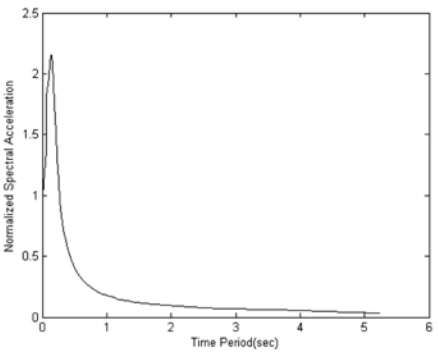

(a)

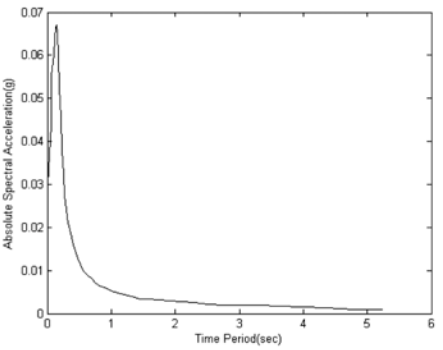

(b)

Figure 4.14 Contd.

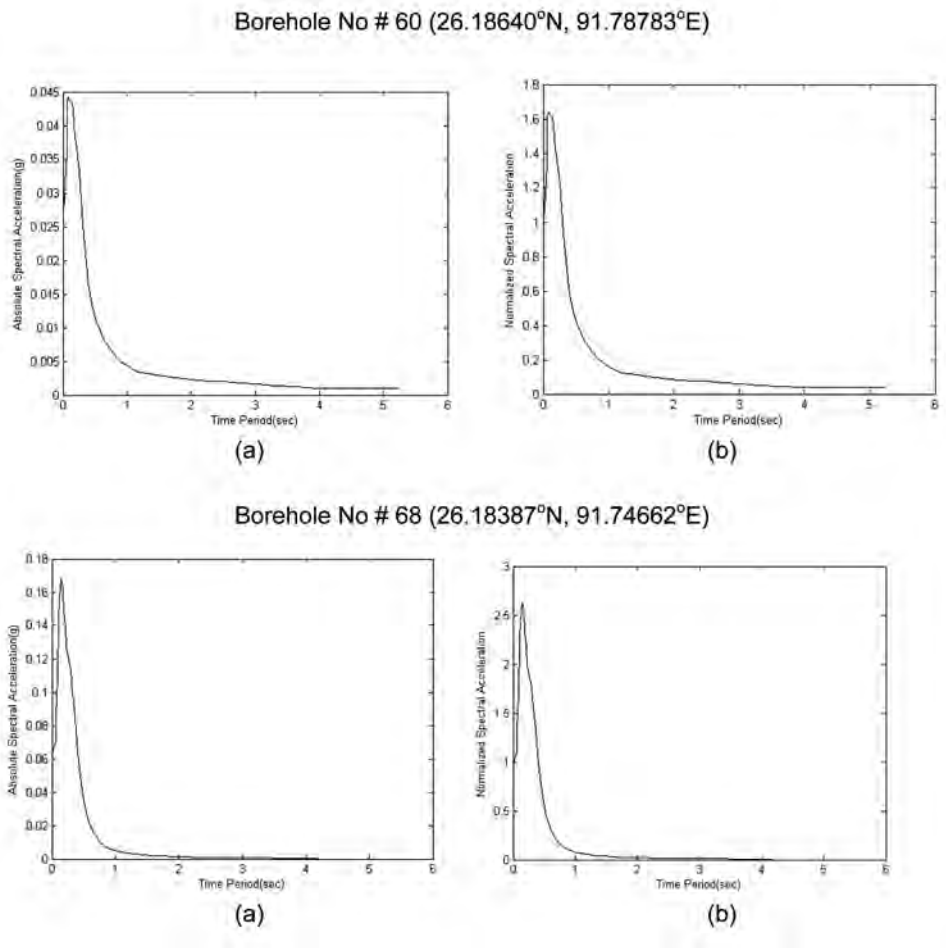

Figure 4.14 (a) Absolute and (b) Normalized spectral acceleration at site class IIIB

Site Class IIIC

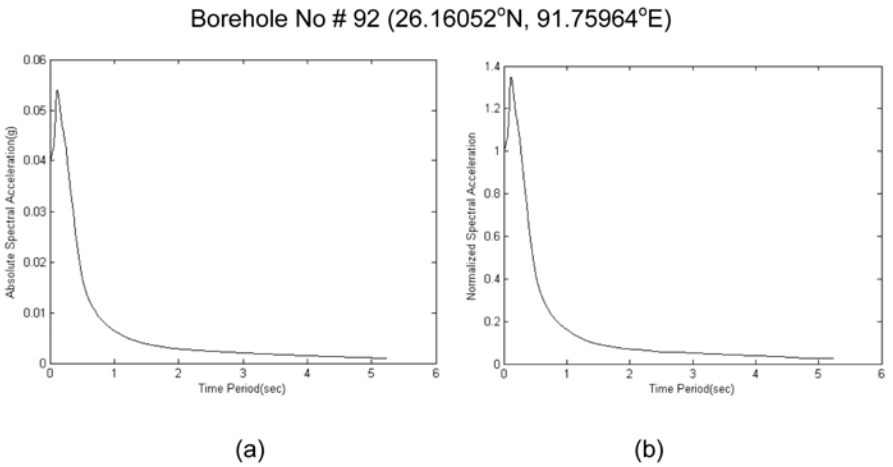

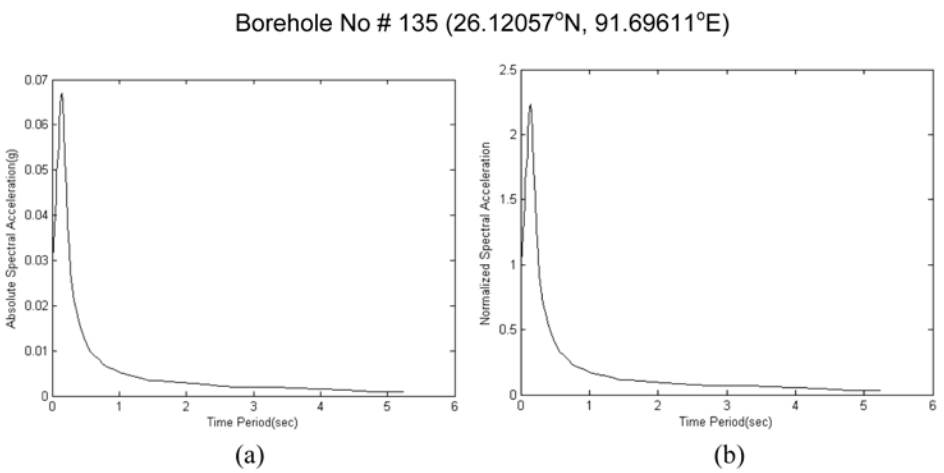

Figure 4.15 Contd.

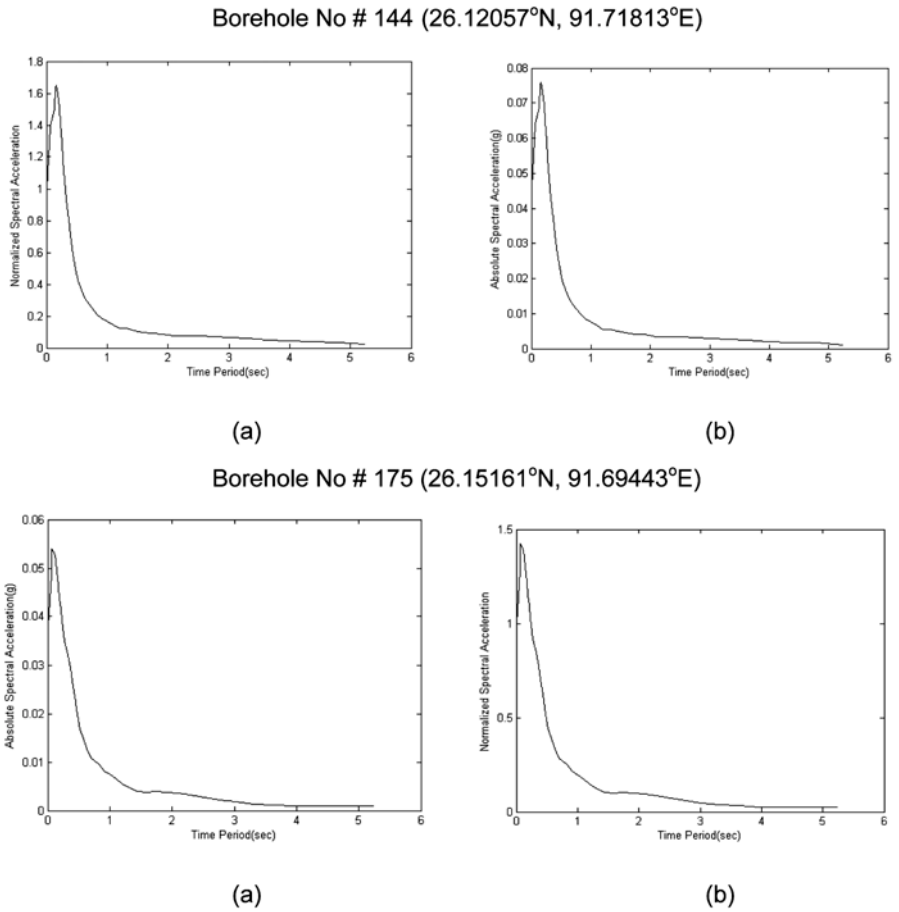

Figure 4.15: (a) Absolute and (b) Normalized spectral acceleration at site class IIIC

4.5 SITE SPECIFIC ATTENUATION RELATIONSHIPS IN THE GUWAHATI REGION

Nath *et al.* (2005) used a semi-empirical approach by selecting to minimize the difference between the observed and estimated values of ground motion and obtained the attenuation law for Sikkim Himalaya. A similar algorithm has been used to develop site specific attenuation relation in the Guwahati region.

We have already observed in our previous analysis that the spectral acceleration depends on site amplification, topography, source azimuth and the local site conditions and hence it became necessary to work out a site specific attenuation relation.

We started with the general form of equation given by Campbell's attenuation law (Campbell, 1997) for spectral acceleration as,

$$\ln\left(SA_{\hat{H}}\right) = \ln\left(A_{\hat{H}}\right) + c_1 + c_2 \tanh[c_3 (M - 4.7)] + (c_4 + c_5 M)r$$
$$+.5c_6 S_{SR} + c_7 \tanh(c_8 D)(1 - S_{HR}) + f_{SA}(D) + \varepsilon \quad \ldots\ldots\ldots\ldots\ldots\ldots\ldots\ldots \quad (4.9)$$

where $SA_{\hat{H}}$ is the horizontal spectral acceleration, $A_{\hat{H}}$ is the PGA, S_{SR} and S_{HR} are variables representing local site conditions for soft rock and hard rock respectively, D is the depth to the basement rock and f_{SA} is a function of D. We introduced a term for site amplification to take into account local site conditions. Our established second order attenuation relation, therefore, takes the following shape,

$$\ln (PGA) = \ln(SA) - a_1 - (a_2 + a_3 m)r - a_4 V_s^{30} - a_5 \ln(SR) \quad \ldots\ldots\ldots\ldots\ldots\ldots (4.10)$$

where SR is the site response and SA is the spectral acceleration at respective frequency for which the relation holds well and an additional term V_s^{30} corresponding to shear wave velocity of first 30 meter layer, was incorporated in attenuation relations. A set of spectral attenuation relations has been determined at different frequencies. These frequencies are selected on the basis of frequency ranges in different site class. Site Classification is done by integrating the layers of Shear Wave Velocity, Site Response, Predominant Frequency and Factor of Safety. Finally four zones were classified with frequency range 0.2Hz – 1.6Hz, 1.8Hz-3.0Hz, 3.25Hz-5.50Hz and 5.8Hz-8.2Hz. Accordingly these frequencies were selected for derivation of attenuation relation. Figure 4.16 shows the spline smoothened variation of different coefficient of the attenuation relationship as a function of frequency. In order to judge the authenticity of these attenuation relations, we attempted to simulate spectral acceleration using the Brune's source model and also by using the attenuation relation at all the five stations. The result at AMTRON is shown in Figure 4.17. It is to be noted that due to the paucity of data within the magnitude range 5.0 to 8.7, we simulated the spectral acceleration for this magnitude range. This relation, therefore, uses both the recorded and simulated events, with local site conditions incorporated in the simulation. Furthermore, we computed the PGA for the scenario earthquake

with SEM 8.7 .The median PGA is tabulated in Table 4.3 along with PGA values computed by the simulation as well as those estimated using various global relationships. The PGA estimated through simulation and spectral attenuation relations closely follow each other, both being consistent with the occurrence of a scenario earthquake of great magnitude in the Guwahati Region.

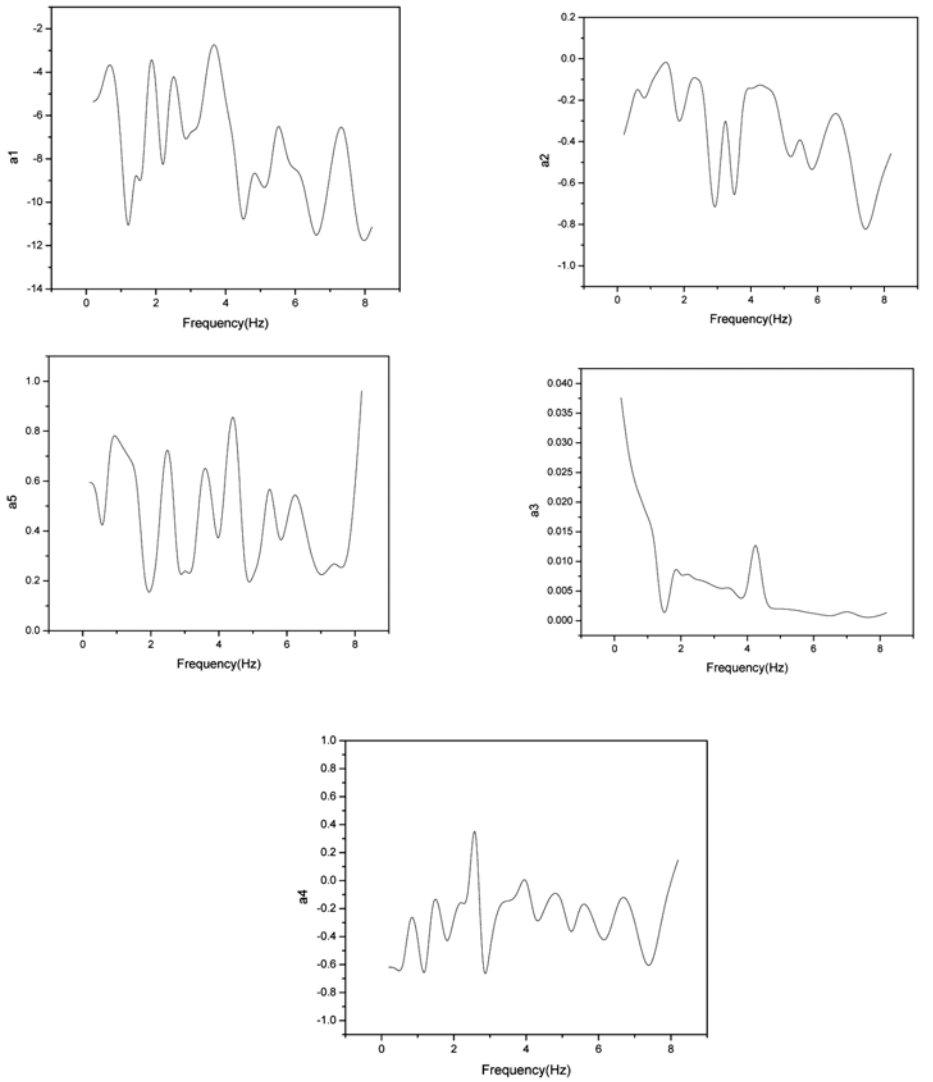

Figure 4.16 Spline smoothened variation of different coefficients with frequency in the spectral attenuation relations of the Guwahati Region

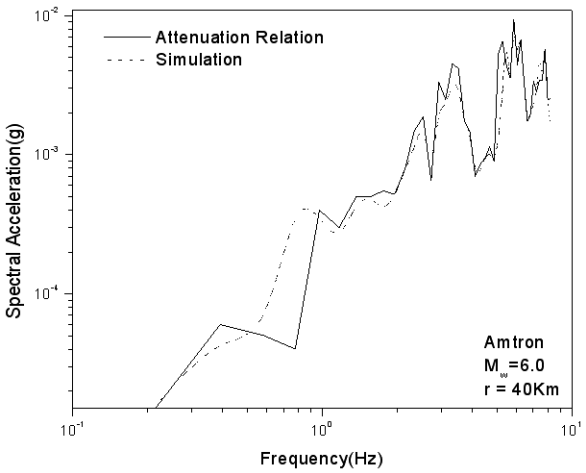

Figure 4.17 Comparative plots of simulated spectral acceleration for Mw 6.0 using the Brune's source model and by the spectral attenuation relation at AMTRON station

Table 4.3: Comparison of PGA values at all the stations computed by Campbell's Relation, Simulation of spectral acceleration, and the 2nd order local spectral attenuation laws derived in this study

Stations	**Campbell (1997)**	**Simulated**	**Our local relations of attenuation at different frequencies PGA(g)**			
			(1.4Hz)	**(5.6Hz)**	**(8.2Hz)**	**(Median)**
AEC	0.26	0.49	0.47	0.49	0.51	0.51
AMTRON	0.23	0.43	0.38	0.46	0.41	0.46
Cotton College Guwahati	0.21	0.26	0.23	0.21	0.26	0.26
IIT Guwahati	0.31	0.53	0.51	0.58	0.55	0.58
Irrigation	0.16	0.47	0.45	0.52	0.49	0.52

CHAPTER 5

GIS Based Thematic Mapping

5.1 INTRODUCTION

Geographic Information System (GIS) platform was adopted as a primary working tool in preparing the seismic hazard microzonation map for the Guwahati region. Multitasking functionality of GIS makes it ideally suited to seismic microzonation as it enables automation of data manipulation and information of maps. The complex spatial analysis associated with seismic microzonation necessitates GIS technology for the data dissemination and management. GIS stores spatial and aspatial data into two different databases. GIS links the two databases by maintaining one-to-one relationship between records of object location in the topological database and records of the object attribute in relational database by using end-user defined common identification index or code (Marble and Pequet, 1983; Korte, 1997; Hohl, 1998). GIS uses three types of data to represent a map or any geo-referenced data, namely, point type, line type, and area or polygon type. It can work with both the vector and the raster geographic models. The vector model is generally used for describing the discrete features, while the raster model does it for the continuous features (Burrough, 1986; Davis, 1996; Burrough and Mcdonnell, 1998).

The GIS framework allowed us to account for added levels of details and complexity. It is very important that the relevant data layers be consistent in their level of detail, in order to successfully combine them and cross analyze them in the pair-wise comparison process. A schematic process flow is shown in Figure 5.1. Prior to presenting the methodologies used to produce the integrated seismic hazard maps, a review of all the thematic coverage with their analytical detail is presented here.

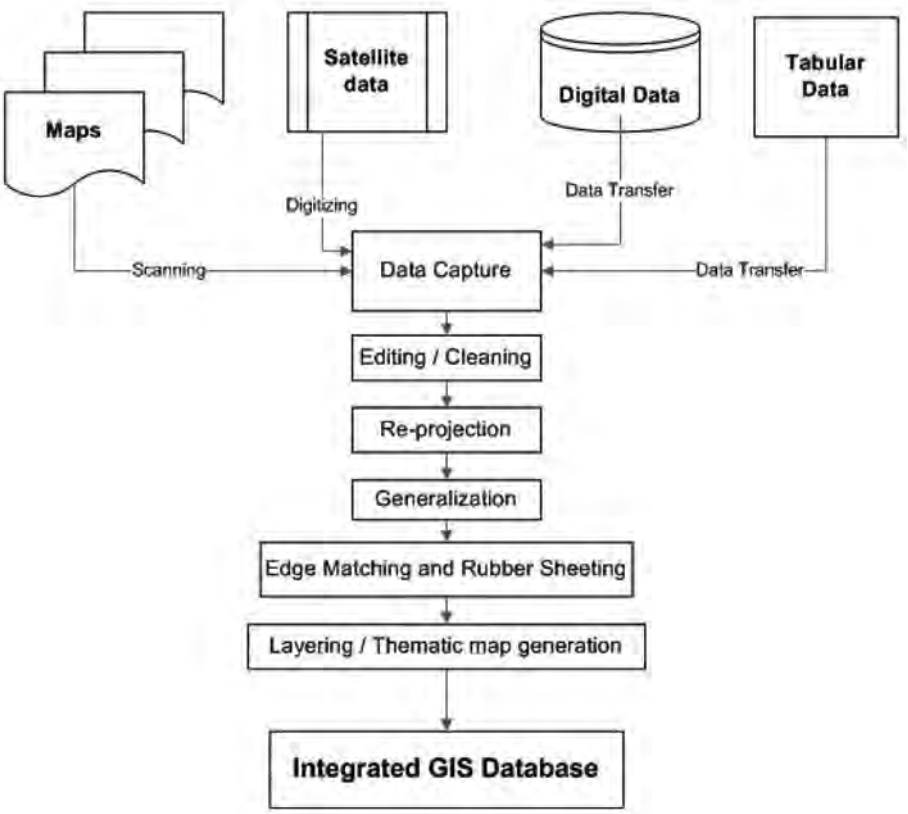

Figure 5.1 A schematic process flow of GIS based Thematic Mapping

Following are the Geomorphological, Geotechnical and Seismological themes considered for the microzonation:

i) Geology and Geomorphology (Base map)

ii) Effective Shear wave Velocity (calculated from SPT data)

iii) Liquefaction Potential / Factor of Safety

iv) Landuse Map

v) Basement configuration and Thickness of Valley Fill

vi) Landslide Hazard Zonation

vii) Site Response (considered at Predominant Frequency)

viii) Predominant Frequency

ix) Peak Ground Acceleration (PGA calculated using F-K integration)

5.2 LANDUSE

Guwahati, the capital of Assam and gateway to the east has continued to hold a place of prominence throughout the history due to its very strategic location. Nestled on the southern bank of the mighty Brahmaputra, where the river gets probably the narrowest in its westward journey, and surrounded all around by hills, Guwahati has been growing in prominence all along, and today is one of the fastest growing city of India. It has established itself as the business and commercial capital of the northeast India. Especially after shifting of capital of Assam from Shillong to Guwahati in 1972, there has been spurt of growth in the city. Population of Guwahati has crossed 15 lakhs as per the 2001 census.

For preparation of Landuse map of the city, the 1990 landuse map prepared by the Assam State Remote Sensing Application Center, Guwahati was used as primary guide to carry out the baseline classification and ground checking to arrive at an appropriate landuse. Keeping in mind the microzonation, old Survey of India topographic sheets pertaining to 1927, and 1968 editions were used to obtain the possible land fill areas. Satellite image, as described in the Para on Base Map was used for detailed classification of different landuse classes. A detailed road to road GPS based survey was conducted to arrive at cultural parameters such as residential, commercial and institutional areas in order to further sub-classify the broad habitation areas shown in greenish hue on the image. Ground checking was also conducted to collect data on other landuse classes such as water bodies, swamps, and agricultural field. A survey of the industrial areas was also conducted.

The followings are the landuse classes derived:

Residential Areas, Commercial Areas, Industrial Areas, Public Utility Areas, Educational Areas, Residential Areas in hill, Army/Police reserve, Airport, Field/Open areas, Agricultural land, Hills with Dense Forest, Hills with Light Forest, River, Sandbars, River Island, Waterbody/Beel and Swampy areas.

The landuse map was developed in-house at AMTRON and is shown in Figure 5.2.

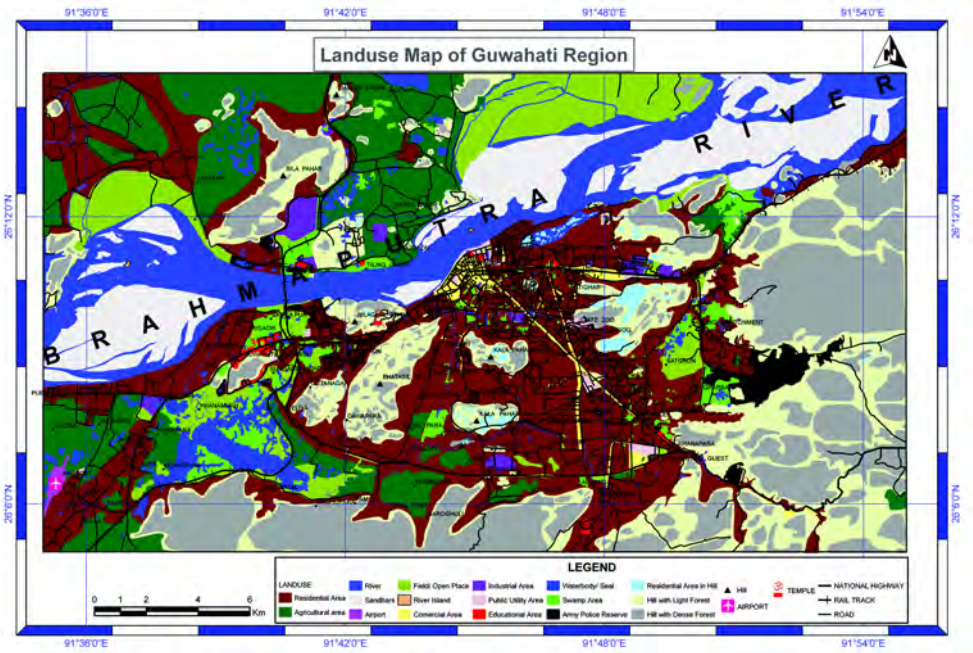

Figure 5.2 Landuse map of Guwahati Region

5.3 Geology and Geomorphology (BASE MAP)

In order to facilitate compilation and collation of data and maps from varied sources on a single platform, the first task was to bring out a Base map of the area surrounding Guwahati where microzonation was contemplated. For this purpose, DST took up the matter with the Survey of India who provided the 1:25,000 scale topographic sheets. The required information, coverage wise, such as roads, contour, railways, streams and certain administrative boundaries were traced on a transparency and digitized using onscreen digitization techniques. Further, IRS PAN and LISS III satellite images were acquired in digital format for the Greater Guwahati region. The images were corrected and georeferenced with respect to the topographic map points and GPS readings taken of the ground control points. Thereafter, the LISS and the PAN scenes were merged to produce a sharpened high resolution FCC image having a ground resolution of 5.8m. The stream network, road network, river and water bodies

were, thereafter updated using the satellite image. Further, an extensive GPS based point survey was done in the greater Guwahati to capture all possible road networks, important places, and other requisite features on the ground. Based on the above exercise, a comprehensive map of Guwahati was prepared. This map has been used all throughout the microzonation exercise. All other maps, data and GPS point surveys were collated and corrected with respect to this base map, which made it possible to weed out errors in various data sets as shown in Figure 5.3.

Broadly the area consists of two main geological formations viz.,

a) Precambrian granitic rocks forming the hill tracts and isolated hillocks and

b) Quaternary alluvium occupying the valleys, deposited over the uneven eroded and faulted basement of granitic rocks.

The granite and granite gneissic rocks are well foliated and jointed, allowing deep weathering along the joint and fault planes, and covered in most places by 1 to 3m thick ferrugenous soil capping.

The Quaternary alluvium, perhaps, form the flood plain deposit of the Brahmaputra River. This deposit could be classified into five aggradational units based on lithological characters, state of weathering, order of superposition and unconformity between them. They are, in order of increasing antiquity.

1. Active Flood Plain and Levee Deposit (AFP),
2. Digaru Surface (T1),
3. Bordang Surface (T2),
4. Sonapur Surface (T3), and
5. Pediment Surface (PD).

The Geotechnical properties of these units are of major concern in the work of seismic microzonation.

The rocks of active flood plains consist of alternate layers of silt/fine sand and clay/ silty clay. The rocks of Digaru Surface are represented mostly by silt and fine sand

and are underlain by the Bordang Surface below an unconformity. The Bordang Surface consists of white silty clay at the top and medium to coarse grained sand at the bottom. The Sonapur Surface constitute the oldest unit of all the fluvial deposits of Brahmaputra valley, mostly exposed near the foot hills showing contact with the pediment forming colluviums or with the granite rocks. It comprises of bedded sand, silt, and clay in varying proportion with maximum amount of clay. The Pediment Surface is formed of weathered and eroded alluvial materials deposited mostly along the foothills.

It is difficult to distinguish these litho-units at depth from the study of sludge collected during digging of boreholes up to 120m depths for ground water exploration. However, it has been seen that sand, silt, clay, and gravel alternate in irregular proportion with extensive lateral variations. It may be mention here that seismic resistivity sounding surveys by GSI could identify three layers of rocks at depth with resistivity characteristics of 200, 100 and 25 Ohm-meter in the central and western part of the valley.

The important geological structures relevant to seismic microzonation are faults inferred to have cut across the valley fill of Quaternary Alluvium. Important faults are (1) NE-SW trending fault cutting across the Deepor Beel, which runs for about 15km along Chotanagar – Maligaon area. It demarcates the boundary between the Nilachal and Fatasil hills; (2) a $N10^0E$-$S10^0W$ tending fault running for about 10km between the Kalapahar hill and the Fatasil hill; (3) a $N40^0E$-$S40^0W$ trending fault passing along the Tepar Beel, running for about 20km from the southern foot hill to the river Brahmaputra and (4) another important fault runs almost E-W from near Khanapara westward to the Deepor Beel in between the southern hills and the isolated hills of Kalapahar and Fatasil etc.

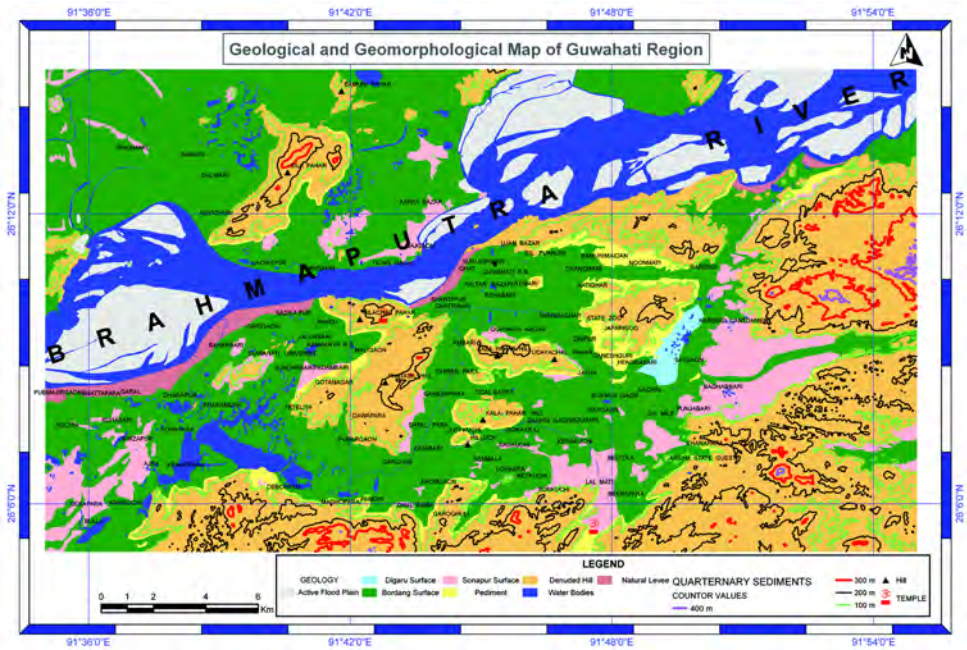

Figure 5.3 Geology and Geomorphology map of Guwahati Region (Base Map)

The overall topography of the area is rugged with high relief due to presence of steep sided hillocks carved out of the Meghalaya Plateau that occupies the southern and the eastern fringe of the area under consideration. The denuded and continuous hill tracts from Rani to Khanapara RF in the south and the Amchang Hills RF in the east rise in altitude from 200 to 400m above MSL. Isolated hillocks within the valley occasionally rise up to 300m above MSL. The highest hillock is located in the north-western part of the area (Silapahar-381m) and the lowest elevated hillock, Odalbakra – 145m, lies in the center of the area. The relative relief is high varying between 80 and 300m. The general elevation of the valley area varies from 25 to 50m above MSL.

The major landform units can be mapped as

a) Denuded hills,

b) Valley filled alluvium with almost flat surface, and

c) Swampy landmass/beels/water bodies.

It is important in the present context that many of the hillocks have been cut into small terraces and are occupied for habitation, and the swampy lands/water bodies have been filled up in many places for construction of houses due to tremendous pressure of population. A few of the hillocks have scarp or steeply inclined face. They are Engineering College hill, Gitanagar hill and Japorigong hill. The isolated hillocks have NE-SW trending dendritic pattern of drainage of moderate density. Due to deep weathering along joints and faults the hill slopes have become unstable making them vulnerable to rock and debris slides, especially during heavy rains accompanied by earthquake shaking as shown in Figure 5.3.

5.4 BASEMENT CONFIGURATION AND THICKNESS OF VALLEY FILL

Basement contour map was prepared from the data provided by GSI obtained through resistivity survey and that from the DGM obtained through drilling for ground water Figures 5.4, 5.5 and 5.6. In general, depth of basement increases from east to west in south bank and reaches up to –300m. In north bank basement depth reaches up to –600m in Singimari – Dadara area and attains the shape of a circular basin in the northwest corner of the area.

The basement forms $N10^0W$-$S10^0E$ trending steep 'V' shaped valley with maximum depth of –150m in between the Fatasil and Kalapahar hillocks that is traversed by a fault. Another NE-SW trending valley occurs in between the engineering college hill and the Fatasil hill that extends up to the junction of Neelachal hill and the Fatasil hill with maximum depth of –250m. This valley is also underlain by a fault. A NE-SW trending valley passing along the Tepar beel by the western side of the Japorigong hills reaches the depth of –100m and it is relatively wide. An E-W deep valley passes from Panjabri to Kahabari across the Deepor beel. Towards east the basins has highs and lows but to the west the basin gradually get deeper and attains the depth of –300m. A fault also runs along this valley. Thus it is seen that the valley area has variable depth of basement having steep gradient along some zones like the western, eastern and the southern margins of the Fatasil hill; western margin of the Kalapahar hill and the northern periphery of the Rani-Khanapara hill tract. These zones will have pronounced basin edge effect during earthquake shaking Figures 5.7 and 5.8 present Basement Contour and zonation map of Guwahati Region.

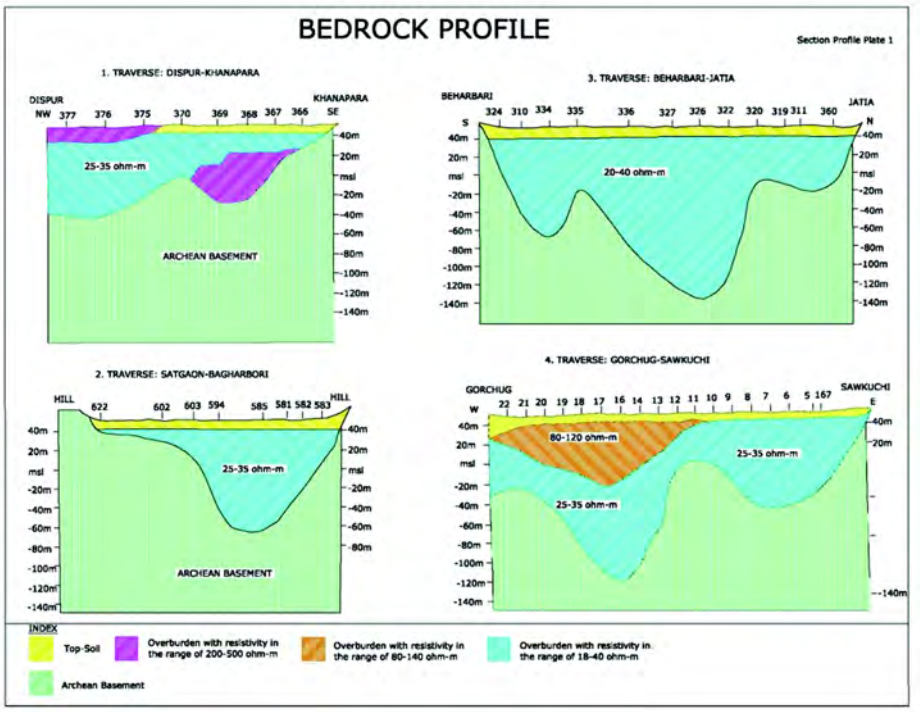

Figure 5.4 Bedrock section profile (1)

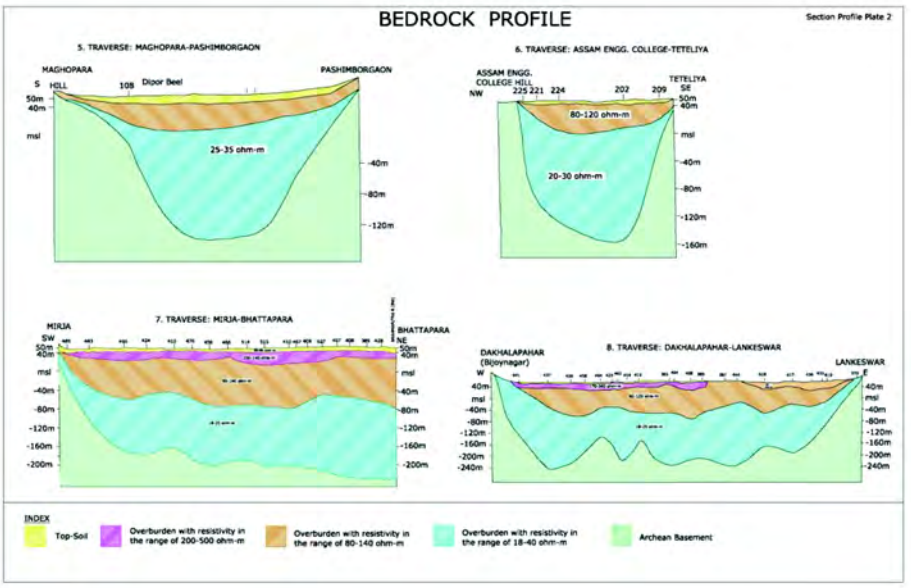

Figure 5.5 Bedrock section profile (2)

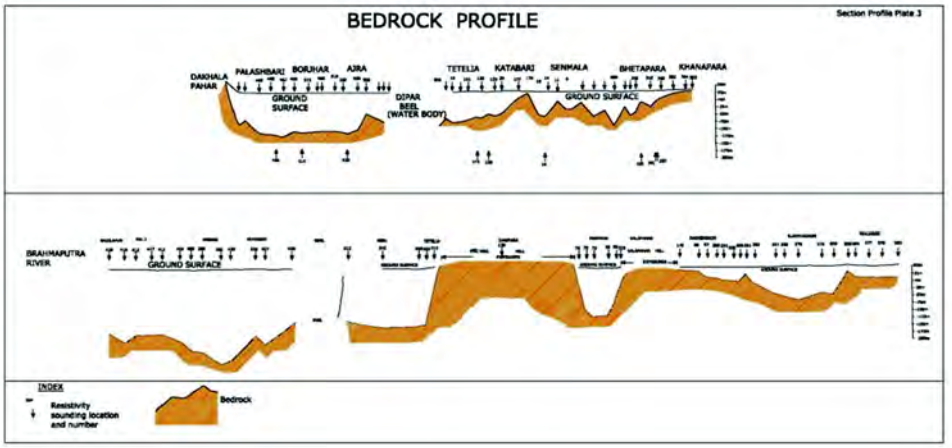

Figure 5.6 Bedrock section profile (3)

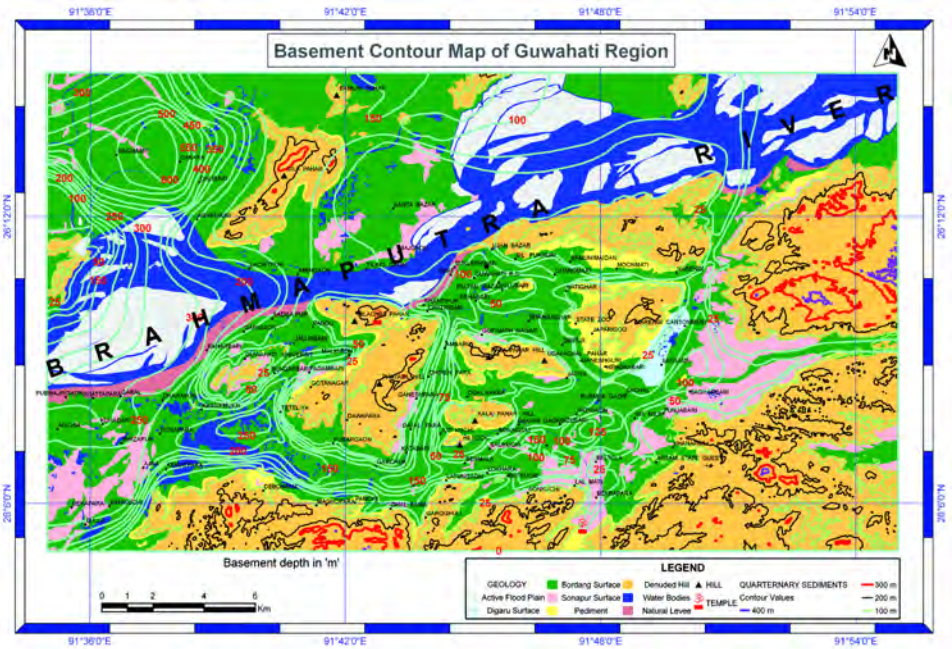

Figure 5.7 Basement contour map of Guwahati Region

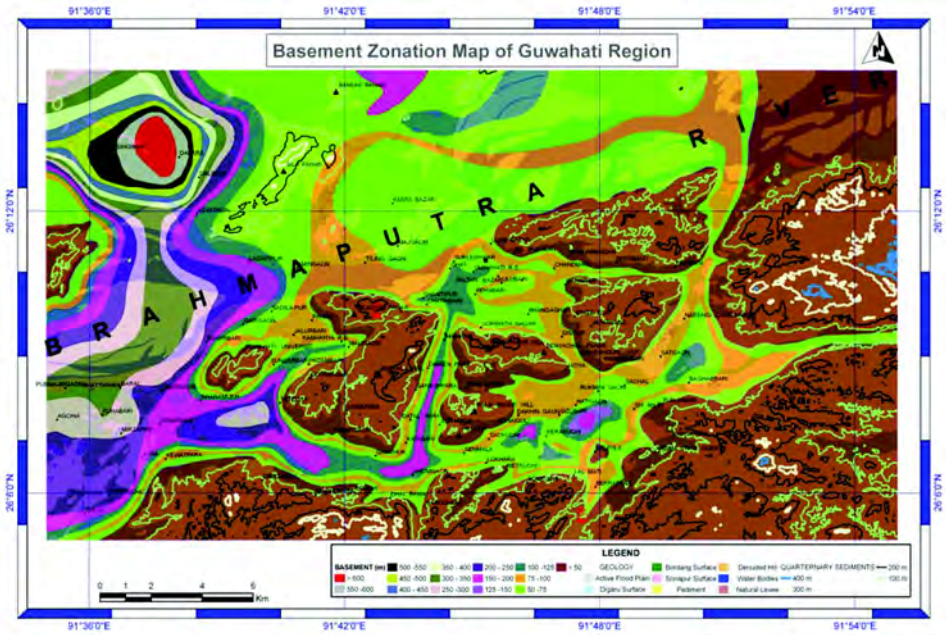

Figure 5.8 Basement zonation map of Guwahati Region

5.5 SEISMOTECTONICS

The city of Guwahati is located in an area surrounded on all sides by highly active tectonic blocks as shown in Figure 5.9. Generally speaking the area is buttressed in between the Himalayan collision zone to the north and the northeast, Indo-Myanmar subduction interface of Indian plate to the east and the Meghalaya Plateau – Mikir hills tectonic block to its south. Strictly speaking the Guwahati area falls in the domain of Meghalaya Plateau and Mikir hill block. Juxtaposition of ongoing collision-subduction tectonic processes has made the area one of the most intense seismic zones of the world.

Analysis of contemporary tectonics in the region reveals that active Himalayan frontal thrusts and cross faults cutting across these thrusts have been generating many relatively shallow, small and moderate earthquakes. Strike-slip movements along a NW-SE trending fault (Po Chu) in the Mishmi block had produced the 1950 Great

Assam earthquake (Mw 8.7) inflicting catastrophic damage in the Upper Assam area. All the other thrusts/faults in this block viz. Mishmi thrust, Lohit thrust and Tidding suture can be classified as capable faults.

The active subduction process along the Indo-Myanmar mobile belt and the conjugate faults lying across this belt has been producing many large and major earthquakes that shook the Guwahati region.

The tectonic block of Maghalaya Plateau-Mikir hill represents the northeastern most exposed element of the Indian shield, occupying a crucial position in between the northern collision and the eastern subduction zones of the Indian plate. This block is under tremendous stress and is seismically active. The Guwahati area being located in the northern margin of this block is vulnerable to severe earthquake damage. The N-S faults cutting across the Plateau such as the Jamuna or Dhubri fault, Dhudnoi/ Chedrang fault, and Kulsi fault in the Meghalaya Plateau are very active; NW-SE Kopili fault passing in between the Plateau and the Mikir hill and the NW-SE Bomdila fault passing along the northern margin of Mikir hill, both traversing across the Himalayan thrust and fold belt as well as the Indo-Myanmar mobile belt are very important.

The Jamuna or Dhubri fault has been the source for 1931 (Mw 7.1) Dhubri earthquake. Movement along the Dhudnoi or Chedrang fault generated the 1897 Great Assam earthquake. The Kopili fault has the record of producing the 1869 Cachar earthquake (Mw>7) and 1943 earthquake (Mw>7). Moreover, recent recording of earthquake events clearly demonstrate that Kopili fault is highly active at present. Another important active fault is the NE-Sylhet and its associated faults falling in the tectonic domain of Bengal basin. This fault had generated the 1918 Srimangal earthquake (Mw 7.6). Similar earthquake may affect the Guwahati city. The E-W Dauki fault system, a regional structure of great importance, though seems to be dormant at present may produce large earthquakes that may affect the Guwahati city. Focal mechanism solutions of the past earthquakes reveal that most of the events were due to strike slip motion in these terrains (Nandy and Dasgupta, 1991; Nandy, 2001).

Thus, it is seen that the Guwahati city area is vulnerable to catastrophic near source great and large earthquakes. It may be mentioned here that recent release of stress

along a 1200km long subduction interface in the southern part of the Indo-Maynmar-Andaman-Sunda subduction zone by the 26th December, 2004, Mw 9.0 earthquake has made it highly probable that next rupture may take place along the northern sector of the subduction zone in Indo-Myanmar region.

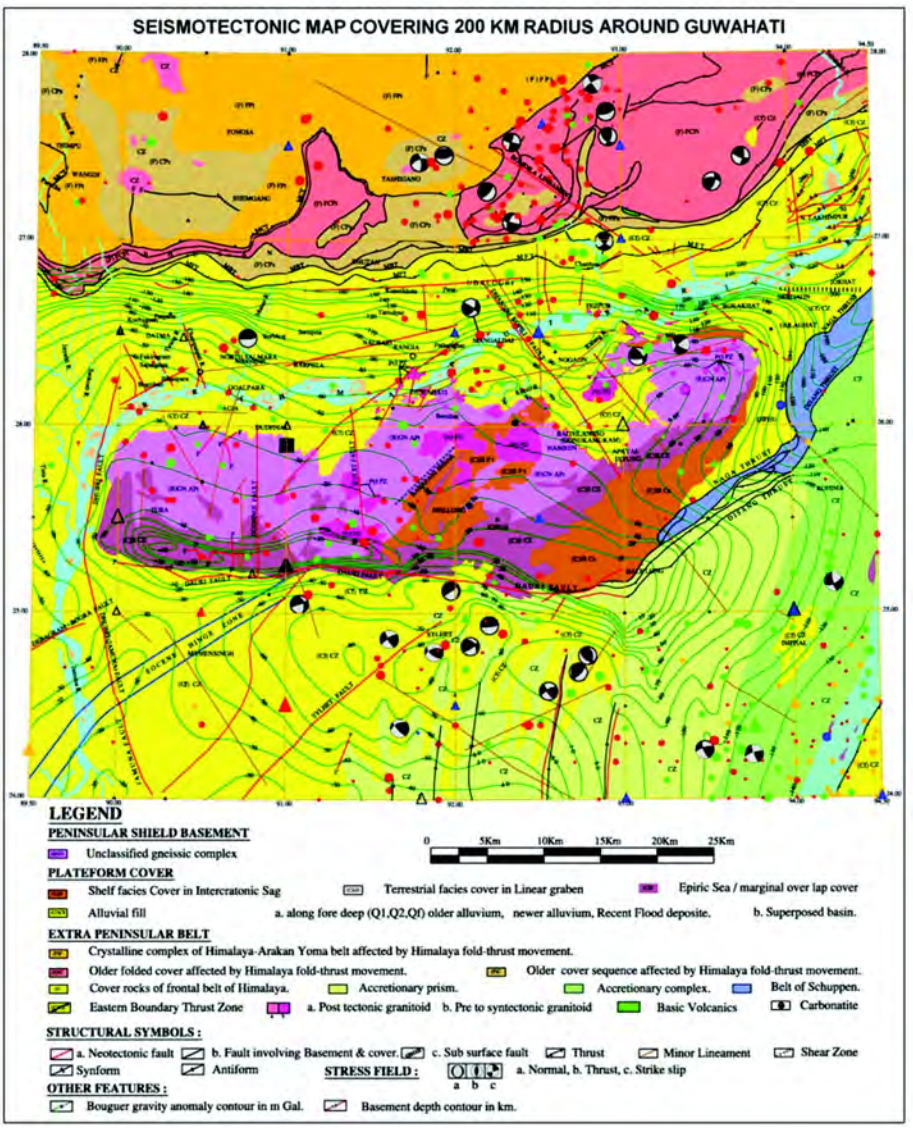

Figure 5.9 Seismotectonic map of the Guwahati Region

5.6 LANDSLIDE HAZARD ZONATION

Detailed work by Keffer (1984) on 40 historical earthquakes and numerous landslides induced by them revealed that most of the slides get triggered at intensity VI and above (MM Scale) with very few slides occurring at lower intensity zones.

The thickness of weathered zone/soil is fairly high in the granite hillocks in and around the Guwahati city. Many of the landslide incidences (baring a few in the Kalapahar area) are due to anthropogenic activities. A total of six landslides of different categories have been recorded. Most of them are slump type followed by debris slide and rock fall. Except one located SW of Deepor Beel, all are fresh slides. Slides located at Kalapahar, Kahangkar basti, Rupnagar and 10th mile on G-S road are of planer failure type whereas others are circular slip type.

A prominent landslide located at the foothills of Nabagraha temple caused slipping of the boundary wall of house in 2002. In July 1999, 4 persons were killed at north Kalapahar. In the vicinity of this place more people were killed by landslide in 1987. In 1982 landslide due to heavy rains and earthquake killed 4 people at Birubari.

Twenty two landslides are concentrated in and around the Guwahati City, especially in its central part. Kalapahar area experienced 10 slides followed by Dhirenpara having 4 slides. Area along the G-S road has the record of 9 landslides.

Based on geo-environmental parameters like slope angle, lithology, structure, relative relief, landuse-landcover, hydrological correlation, seismicity, rainfall and landslide incidences were considered for preparation of landslide hazard zonation map. Eight thematic maps were first prepared viz., facet map, slope morphometry map, relative relief map, lithological map, structural map, landuse-landcover map, drainage map, landslide incidence map, on 1:25,000 scales and then enlarged to 1:50,000 scales. The landslide hazard zonation map has been prepared according to Total Estimated Hazard (TEH) of each face by superimposing the slope facet map successively one by one over all the thematic maps. The TEH of the facet is calculated after adding the values of Landslide Hazard Evaluation factor (LHEF) of all 9 geo-environmental parameters encompassing the particular facet. The derived landslide hazard zonation map thus prepared showed only three categories of hazard zone such as Low Category of Hazard Zone (LHZ), Moderate Hazard Zone (MHZ) and High Hazard Zone (HHZ) as shown in Figure 5.10.

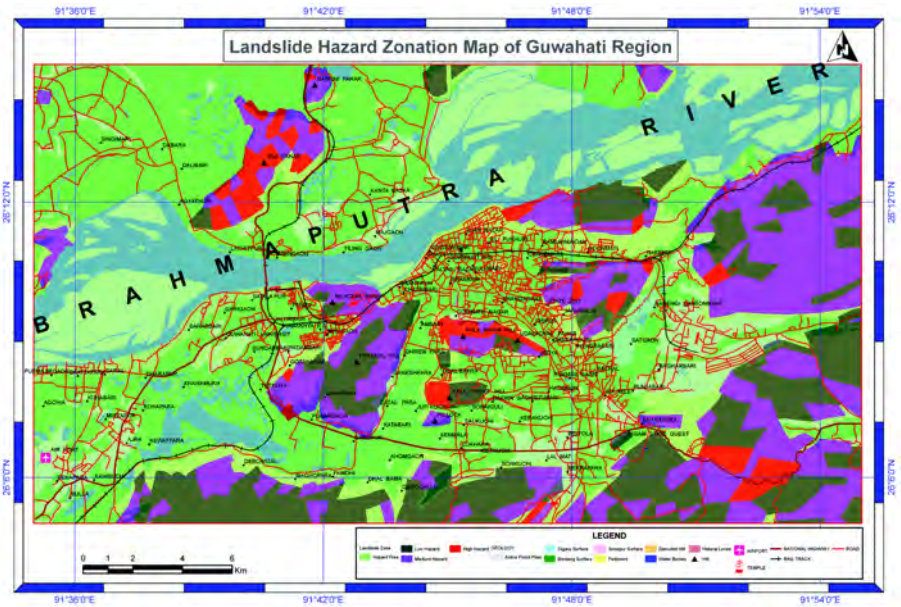

Figure 5.10 Landslide Hazard Zonation map of Guwahati Region

5.7 SHEAR WAVE VELOCITY (V_S^{30})

Shear wave velocity contour and distribution map of Guwahati Region is shown in Figures 5.11 and 5.12.

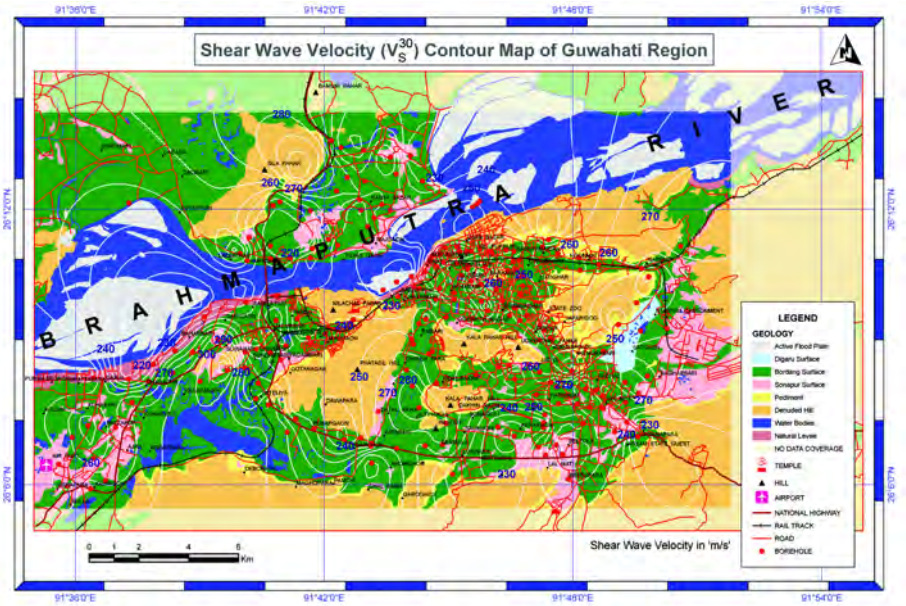

Figure 5.11 Shear wave velocity contour map of Guwahati Region

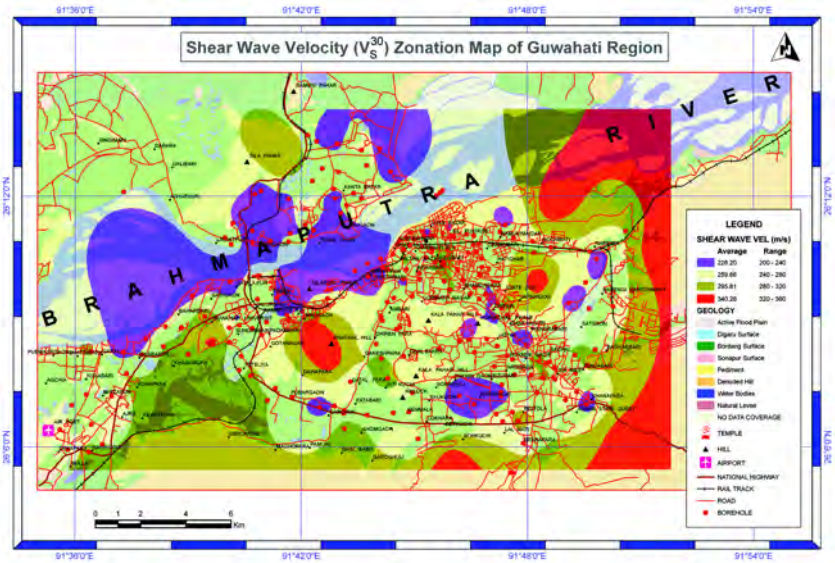

Figure 5.12 Shear wave velocity distribution map of Guwahati Region

5.8 PREDOMINANT FREQUENCY

Predominant frequency contour and distribution map of Guwahati Region is given in Figures 5.13 and 5.14 respectively.

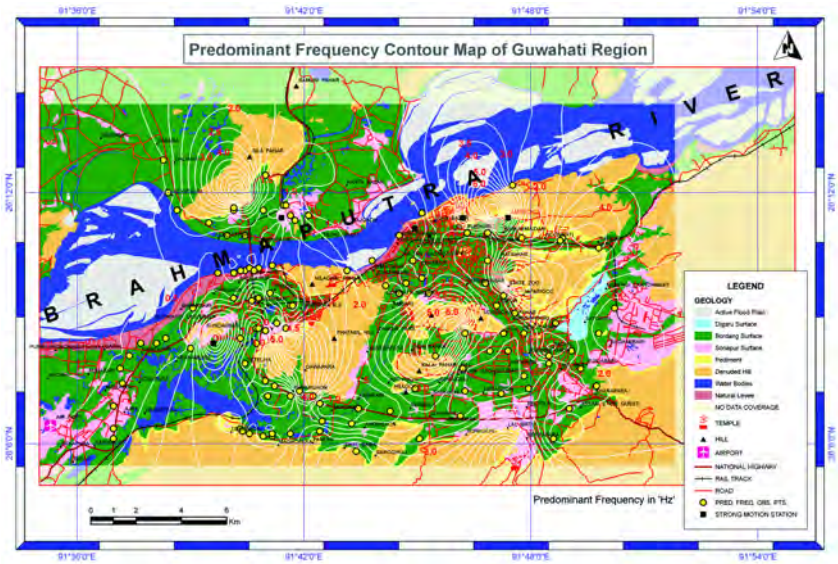

Figure 5.13 Predominant frequency contour map of Guwahati Region

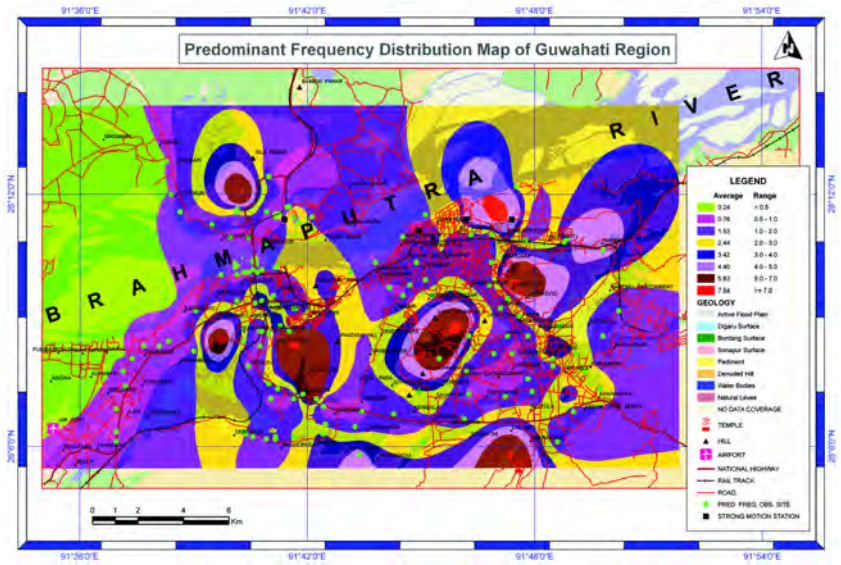

Figure 5.14 Predominant frequency distribution map of Guwahati Region

5.9 SITE RESPONSE

The site response is another seismological theme which is already discussed in Chapter 3. Site response contour and distribution map is presented in Figures 5.15 and 5.16 respectively.

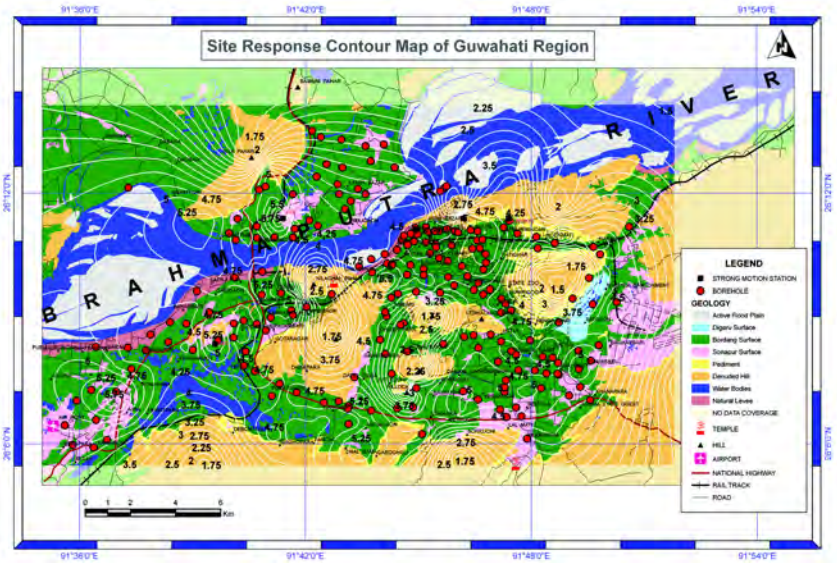

Figure 5.15 Site response contour map of Guwahati Region

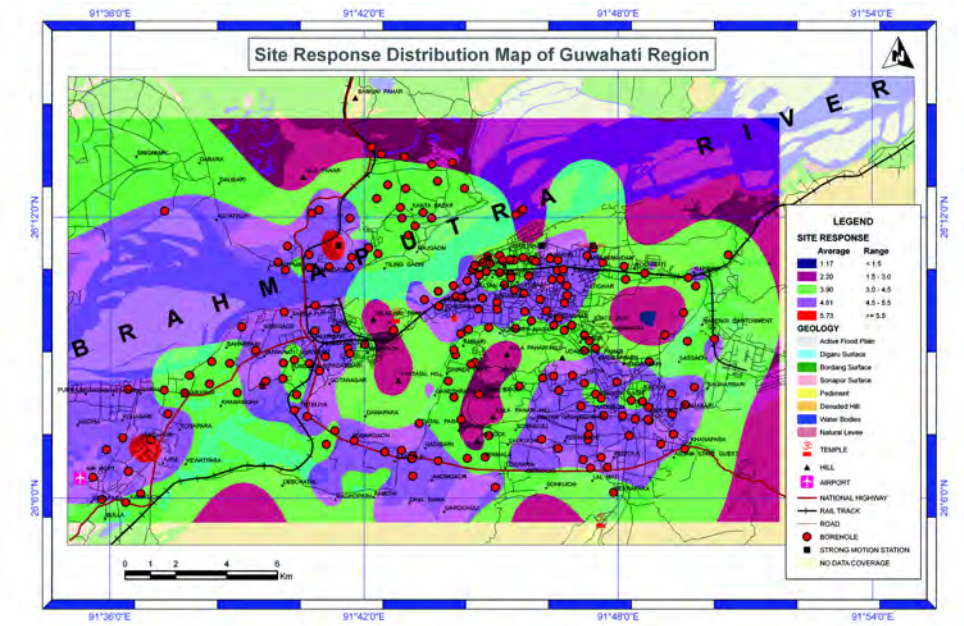

Figure 5.16 Site response distribution map of Guwahati Region

5.10 FACTOR OF SAFETY

A component subjected to a solitary load will be considered in the first instance. This load is interpreted in the context of the component's nature and duty. Therefore, load usually implies a transverse force in the case of a beam component, or a longitudinal compressive force in a column, or a torque in the case of a shaft, or a pressure in a fluid containment vessel, and so on.

There are two completely different manifestations of the load which have important consequences for the component:

- The extrinsic actual load is the load exerted on the component by its surrounds.
- The intrinsic maximum load is the largest load that the component can withstand without failure; the maximum load is a property of the component, a function of its dimensions and material.

Clearly, a component is safe only if the actual load applied to the component does not exceed the component's inherent maximum sustainable load. The degree of safety is usually expressed by the safety factor 'n' given as,

n = maximum load / actual load = F_{max} / F

and it follows that :

if n = 1 then the component is on the point of failure

if n < 1 then the component is in a failed state

if n > 1 then the component is safe.

Accordingly the study region is classified in two zones namely safe and unsafe. The Factor of Safety contour and distribution map is shown in Figures 5.17 and 5.18 respectively.

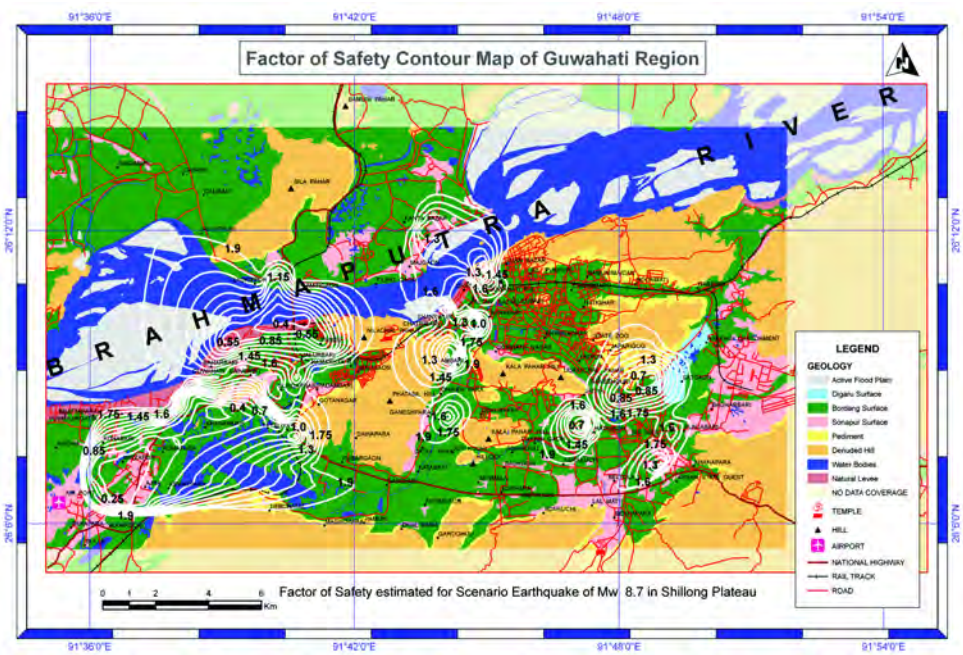

Figure 5.17 Factor of safety contour map of Guwahati Region

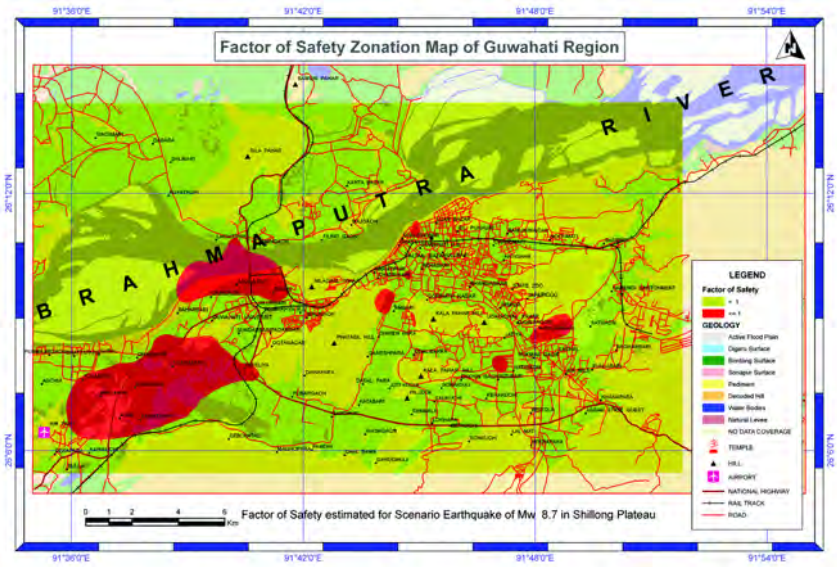

Figure 5.18 Factor of safety zonation map of Guwahati Region

5.11 SITE CLASSIFICATION

Site classification of Guwahati Region is already discussed in Chapter 3 and shown in Figure 5.19.

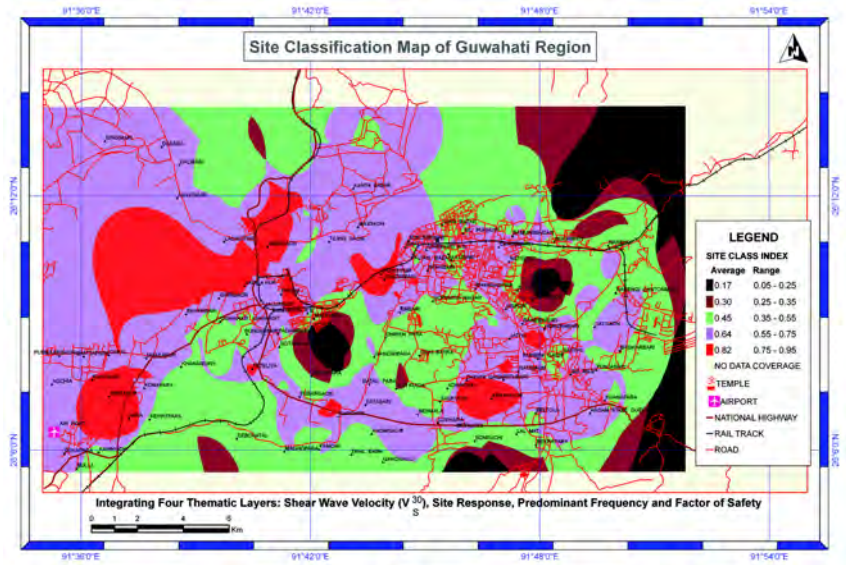

Figure 5.19 Site classification map of Guwahati Region

5.12 PEAK GROUND ACCELERATION

PGA is estimated in Guwahati Region by two methods as discussed in Chapter 4, but for the microzonation purpose PGA estimated by F-K integration is used and is also shown in Figure 5.20.

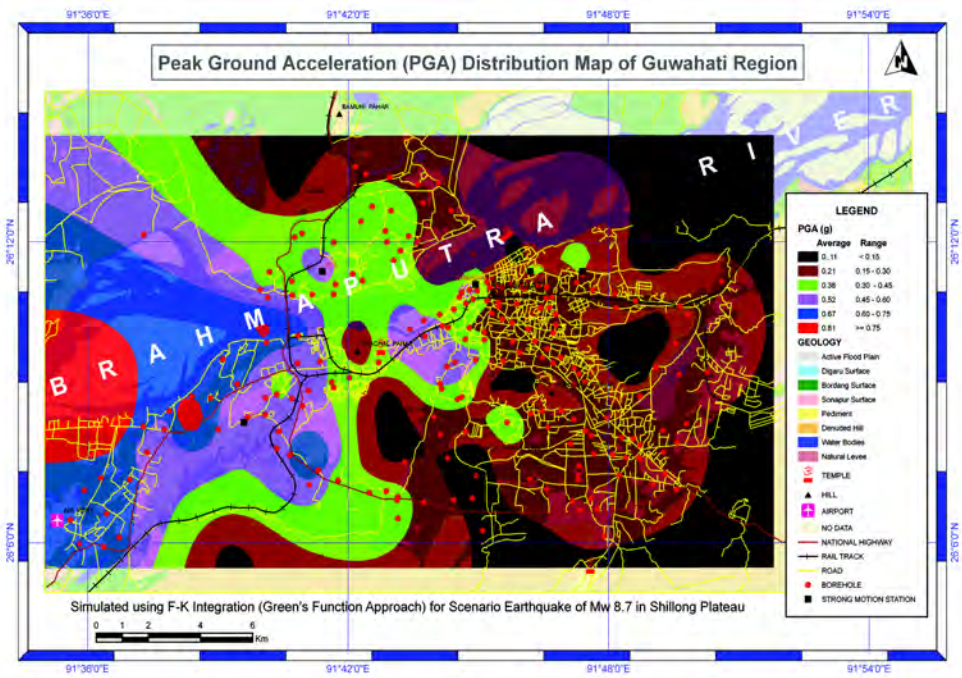

Figure 5.20 Peak Ground Acceleration (computed by F-K integration) map of Guwahati Region

CHAPTER 6

Seismic Microzonation on GIS Platform

6.1 INTRODUCTION

Seismic microzonation is a process that involves incorporation of geological, seismological and geotechnical concerns into economically, sociologically and politically justifiable and defensible landuse planning for earthquake effects so that architects and engineers can site and design structures that will be less susceptible to damage during major earthquakes. This exercise is similar to the macro level hazard evaluation requiring more rigorous inputs about site specific geological conditions, ground response to earthquake motions and their effect on the safety of constructions taking into consideration the design aspects of buildings, ground conditions which would enhance the earthquake effects like the liquefaction of soils, the ground water conditions and the static and dynamic characteristics of foundation or of the stability of slopes in the hilly terrain. To be useful, microzonation should provide general guidelines for the types of new structures that are most suited to an area. It should also provide information on the relative damage potential of the existing structures in a region. It follows, therefore, that if the principles of microzonation are correctly and judiciously applied, they could be useful in establishing criteria for landuse planning and a strategy for the formulation of a systematic and informed decision-making process, for the sitting and development of new communities in areas that are made hazardous by nature.

Seismic microzonation employs the following methodologies:

1. Liquefaction hazard mapping,

2. Prognosis of Scenario Earthquake Magnitude (SEM),

3. Attenuation relationship and Ground Motion Synthesis,

4. Site-specific ground motion studies, namely estimation of site effects, Peak Ground Acceleration (PGA), Peak Ground Velocity (PGV) and Response Spectra, and

5. Geomorphological characterization.

Seismic Microzonation mapping essentially requires (a) bedrock topography, (b) subsoil profile, (c) soil site classification, (d) PGA and PGV mapping, (e) liquefaction potential mapping, (f) geomorphological characterization, and (g) seismic hazard scenario. A typical Seismic Microzonation framework from seismicity to vulnerability assessment is depicted in the roadmap as given in Figure 6.1.

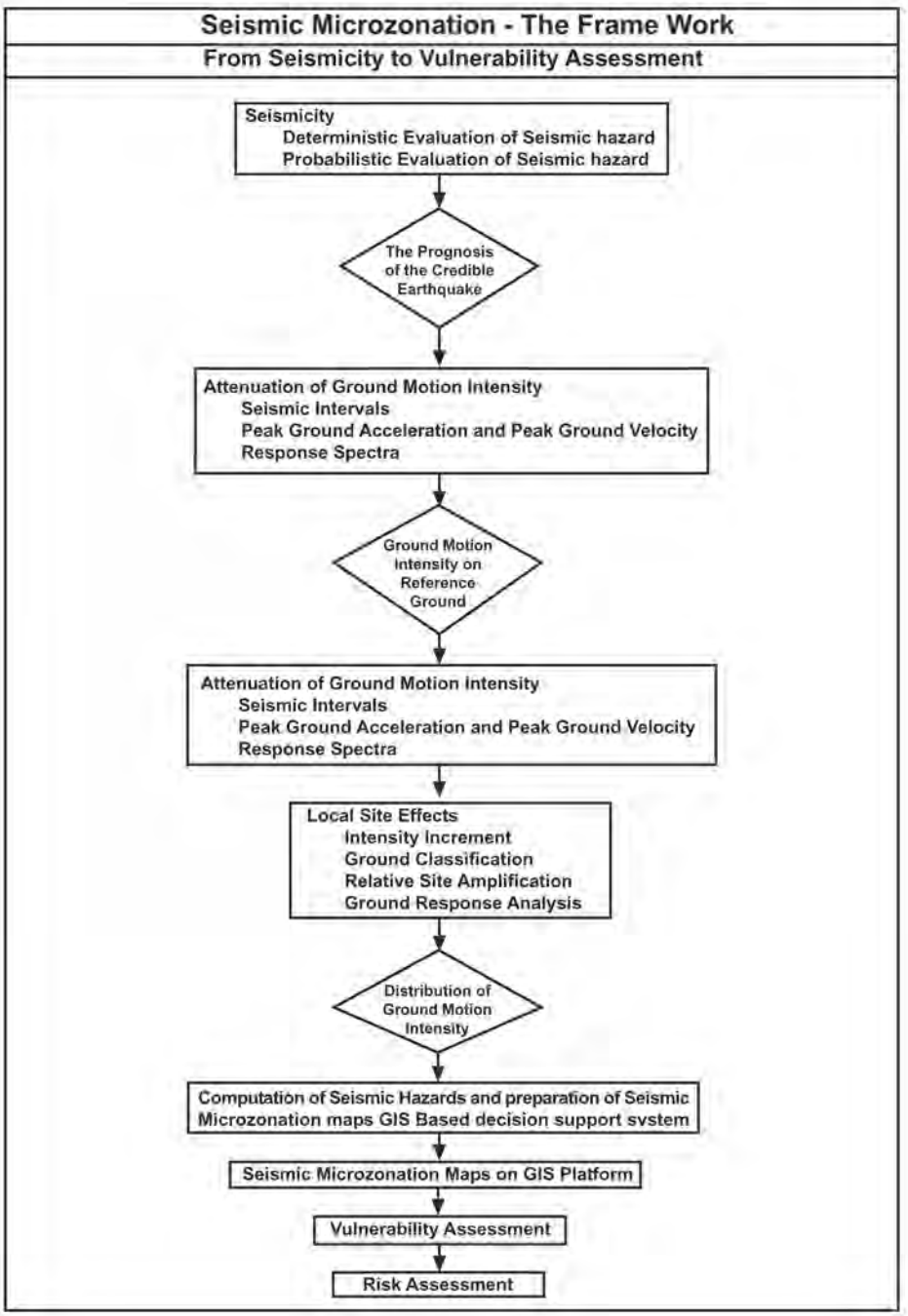

Figure 6.1: A typical seismic microzonation framework from Seismicity to Risk Assessment

6.2 GIS INTEGRATION LOGIC

6.2.1 Saaty's Analytical Hierarchy Process

The Analytical Hierarchy Process (AHP) employs a matrix of pair-wise comparisons (ratios) between the factors. This matrix is constructed by eliciting values of relative importance on a scale of 1 to 9 ; 1 meaning that the two factors are equally important, and 9 indicating that one factor is more important than the other. If a factor is less important than others, it is indicated by reciprocals of the 1 to 9 values (i.e., 1/1 to 1/9). The process of allocating weights is a subjective one and can be done in participatory mode in which a group of decision makers may be encouraged to reach a consensus of opinions about the relative importance of factors.

The matrix developed by pair-wise comparisons between the factors can be used to derive the individual normalized weights of each factor. It is performed by calculating the principal eigenvector of the matrix. This results in a matrix of values that are in the range of 0 to 1 and sum to '1' in each column. The weights for each attribute can be calculated by averaging the values in each row of the matrix. These weights will also sum to '1' and can be used in deriving the weighted sums of rating or scores for each region of cells or polygon of the mapped layers.

Since the values within each thematic map/layer vary significantly, they are classified into various ranges or types, which are known as the features of a layer. These features are then assigned ratings or scores within each layer, normalized to ensure that no layer exerts an influence beyond its determined weight. Therefore, a raw rating for each feature of every layer is allocated initially on a standard scale such as 1 to 10 and then normalized using the relation,

$$x_j = \frac{R_j - R_{min}}{R_{max} - R_{min}} \quad \ldots\ldots\ldots\ldots\ldots\ldots\ldots\ldots\ldots\ldots\ldots\ldots\ldots\ldots\ldots\ldots \quad (6.1)$$

where, R_j is the raw score, R_{min} and R_{max} are the minimum and maximum scores of a particular layer.

6.3 GIS INTEGRATION AND MICROZONATION MODEL

For Seismic Microzonation and Hazard delineation of the above themes, both Geomophological and Seismological themes are reclassified into a 1st phase geohazard map and 2nd phase Seismic Microzonation map with PGA distribution for a SEM of Mw 8.7. A typical two phase Microzonation procedure from hazard zonation to regional hazard zonation mapping on GIS platform and finally to Seismic Microzonation is shown in Figure 6.2.

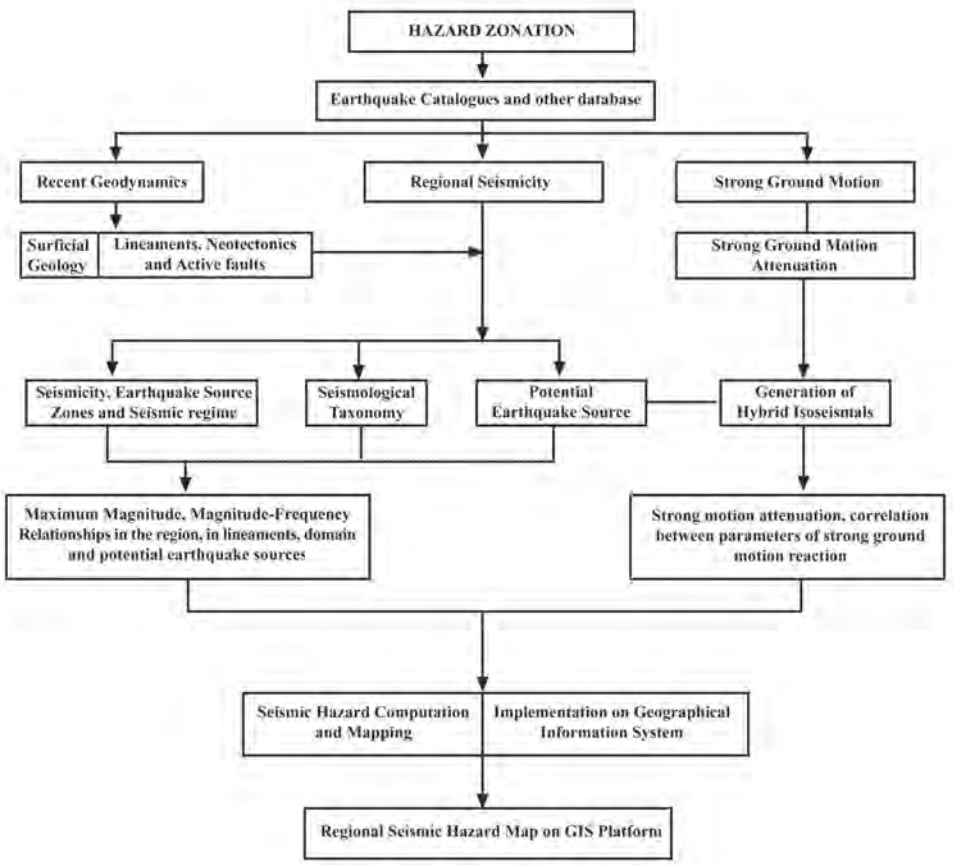

Figure 6.2 Microzonation Framework for Seismic Hazard Mapping

The Geological vector layers that have been used for microzonation include Geology and Geomorphology (GG), Basement (BS), Landslide hazard (LS) and Land Use (LU), while the seismological themes are Shear wave velocity (V_s^{30}), Site Response (SR), Peak Ground Acceleration(PGA), Predominant Frequency (PF), and Factor of Safety (FS).

The Geological and Seismological themes are weighted in scale of 9:1 depending on their contribution to the seismic hazard, the highest being attached to Geological & Geomorphological layer with a normalized weight of 0.2000. Basement has got the next weightage with a normalized value of 0.1778; Landslide hazard and Landuse have got the next weightage with normalized value of 0.1556 and 0.1333 whereas the V_s^{30}, PGA, SR, PF and FS are assigned the values 0.1111, 0.0889, 0.0667, 0.0444 and 0.0222 respectively.

A matrix of pair-wise comparisons (ratio) between the factors is built, which is used to derive the individual normalized weights of each factor. The pair-wise comparison is performed by calculating the principal eigen vector of the matrix and the elements of the matrix are in the range of 0 to 1 summing to '1' in each column. The weights for each theme can be calculated by averaging the values in each row of the matrix. These weights will also sum to '1' and can be used in deriving the weighted sum of rating or scores of each region of cells or polygons of the mapped layers. Since the values within each thematic map/layer vary significantly, those are classified into various ranges or types known as the features of a layer. These features are then assigned ratings (r) or scores within each layer, normalized to 0-1 as shown in Table 6.1 below.

Table 6.1 : Normalized feature ratings of the thematic maps

Theme	Weight	Feature	Rating	Normalized Rating
Geology (GG)	**0.2000**	River, Water Bodies & Swampy area	8	1.0000
		Active Flood Plain	7	0.8571
		Natural Levee	6	0.7143
		Pediment	5	0.5714
		Sonapur Surface	4	0.4286
		Digaru Surface	3	0.2857
		Bordang Surface	2	0.1429
		Denuded Hills	1	0.0000
Basement (BS)	**0.1778**	>600	7	1.0000
		500-600	6	0.8333
		400-500	5	0.6667
		300-400	4	0.5000
		200-300	3	0.3333
		100-200	2	0.1667
		<50-100	1	0.0000
Landslide Hazard (LS)	**0.1556**	High Hazard Zone	4	1.0000
		Medium Hazard Zone	3	0.6667
		Low Hazard Zone	2	0.3333
		River, Sand Bar & Hazard Free Zone	1	0.0000
Landuse (LU)	**0.1333**	Residential Area	7	1.0000
		Educational, Army / Police Reserve, Commercial area	6	0.8333

Theme	Weight	Feature	Rating	Normalized Rating
		Sandbars, River Island & Swampy area	5	0.6667
		Field/ open space & Agricultural Area	4	0.5000
		Residential Areas in Hill	3	0.3333
		Hill with dense & light forest	2	0.1667
		River, water bodies/ Beel	1	0.0000
Shear Wave Velocity (V_s^{30})	**0.1111**	200-240 m/s	4	1.0000
		240-280 m/s	3	0.6667
		280-320 m/s	2	0.3333
		320-360 m/s	1	0.0000
Peak Ground Acceleration (PGA)	**0.0889**	>= 0.75 g	6	1.0000
		0.60 – 0.75 g	5	0.8000
		0.45 – 0.60 g	4	0.6000
		0.30 – 0.45 g	3	0.4000
		0.15 – 0.30 g	2	0.2000
		< 0.15 g	1	0.0000
Site Response (SR)	**0.0667**	>= 5.5	5	1.0000
		4.5 - 5.5	4	0.7500
		3.0 - 4.5	3	0.5000
		1.5 - 3.0	2	0.2500
		<1.5	1	0.0000

Theme	Weight	Feature	Rating	Normalized Rating
Predominant Frequency (PF)	**0.0444**	<0.5 Hz	8	1.0000
		0.5-1.0 Hz	7	0.8571
		1.0-2.0 Hz	6	0.7143
		2.0-3.0 Hz	5	0.5714
		3.0-4.0 Hz	4	0.4286
		4.0 - 5.0 Hz	3	0.2857
		5.0 - 7.0 Hz	2	0.1429
		> 7.0 Hz	1	0.0000
Factor of Safety (FS)	**0.0222**	£1	1	1
		>1	0	0

The seismic hazard zonation map is obtained through the integration of all the above themes using the following relation

$$PSHI = GG_wGG_r + BS_wBS_r + LS_wLS_r + LU_wLU_r + V_s^{30}{}_w V_s^{30}{}_r + PGA_wPGA_r + SR_wSR_r + PF_wPF_r + FS_wFS_r / Ó_w \quad (6.2)$$

The notations have their usual meanings.

Five zones are mapped as shown in Figure 6.3 where average Hazard index is 0.55, 0.44, 0.35, 0.26 and 0.16. We termed these zones as very high, high, moderate, low and very low hazard regions. Figure 6.4 shows microzonation map of Guwahati region overlaid by PGA computed by Green's Function approximation.

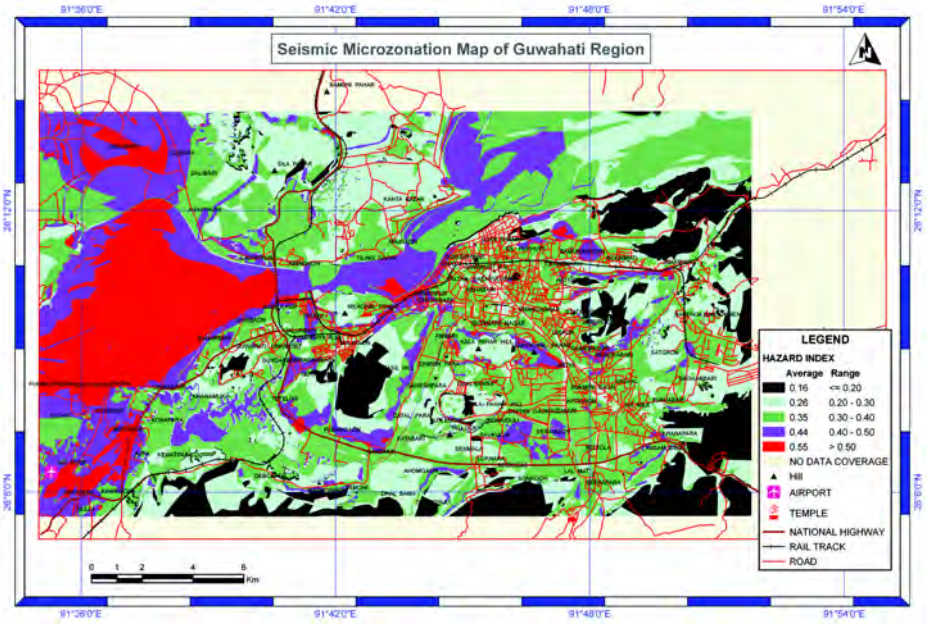

Figure 6.3 Seismic Microzonation Map of Guwahati Region (using PGA computed by F-K integration)

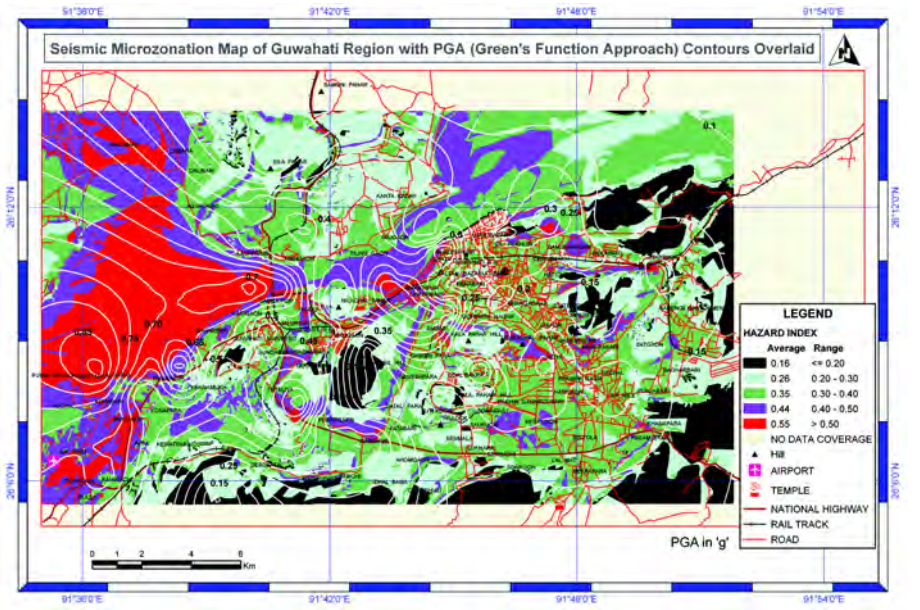

Figure 6.4 Seismic Microzonation Map of Guwahati Region with PGA (Green's Function Approach) contours overlaid

CHAPTER 7

Generation of Strong Motion Data for Greater Guwahati City Region

7.1 INTRODUCTION

Buildings and other structures in Guwahati city are facing highest seismic risk. Therefore, collection of strong motion data and analysis of site response of Guwahati city is essential for better estimation of hazard level in the Greater Guwahati region and this will provide valuable input for improvement of earthquake resistant design of structures. The geology and seismotectonics of the region have been well documented by Nandy (2001). Figure 7.1 shows the seismicity map of the NE India and adjoining region.

7.2 FREE-FIELD GROUND MOTION

In this work, twelve numbers of Strong Motion Accelerograph stations are to be installed at twelve sites in different part of the Greater Guwahati City area for recording free-field ground acceleration during earthquakes. These twelve sites have been selected on the basis of sub-soil and bedrock characteristics. RCC sheds as shown in Figure 7.2 have been constructed in nine sites and in all such sites accelerographs (Figure 7.3) have already been installed. At one of the sites, IIT Guwahati, first event has been recorded on 18th September 2005. The source of the event has been located at Indo-Myanamar border (24.64°N, 94.81°E). The magnitude and focal depth of the event were Mw = 5.7 and 82km respectively. The peak ground acceleration of the recorded motion is 0.013*g*.

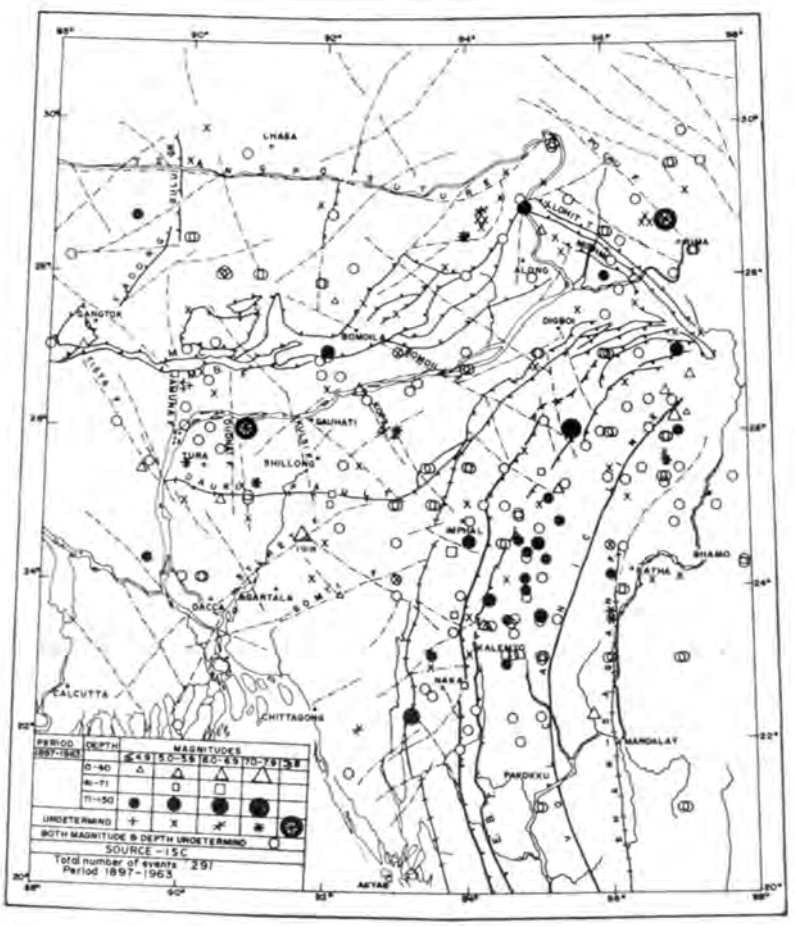

Figure 7.1 Seismicity map of the NE India and adjoining region (after Nandy, 2001)

Figure 7.2 SMA station at IIT Guwahati

Figure 7.3 SM Recorder (Etna)

Subsequently, six events have been recorded in different strong motion stations of the array established under the ongoing project. Details of the sources of these events along with the corresponding magnitude have been furnished in the Table 7.1. The sample ground motions recorded during these events are shown in the Figures 7.4 - 7.11.

Table 7.1: Details of the sources of the recorded events

Date	Magnitude (Mw)	Epicenter	Focal Depth (km)
11/2/2006	3.1	27.6°N, 92.3°E	43.5
14/2/2006	5.1	27.7°N, 88.8°E	20.1
23/2/2006	5.7	27.2°N, 92.0°E	33.0
12/8/2006	4.9	24.696°N, 92.755°E	46.2
06/11/2006	5.2	24.736°N, 95.223°E	122.6
10/11/2006	4.9	24.559°N, 92.320°E	43.1

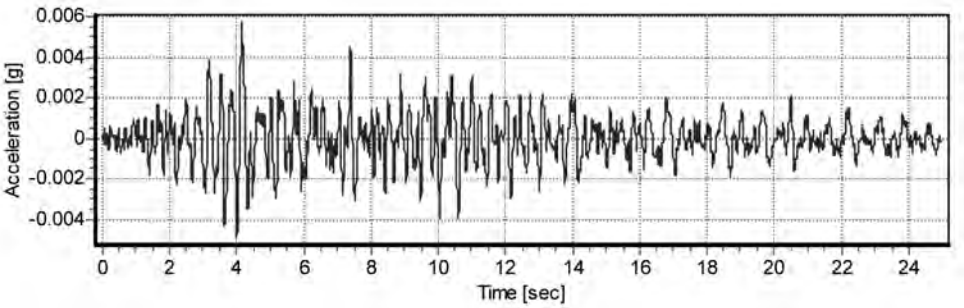

(a) North-South Component (PGA= 0.00574383g)

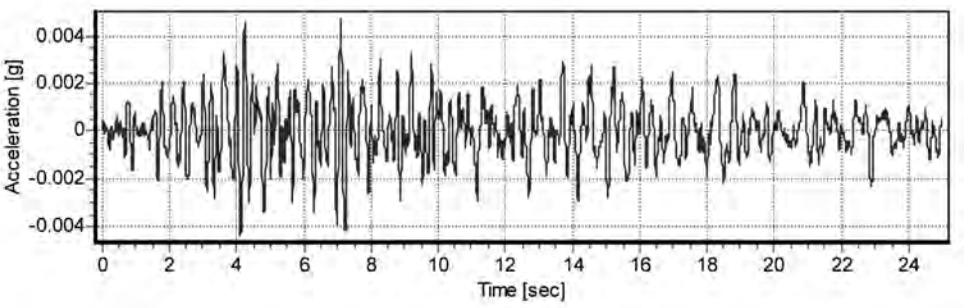

(b) East-West Component (PGA= 0.00480412g)

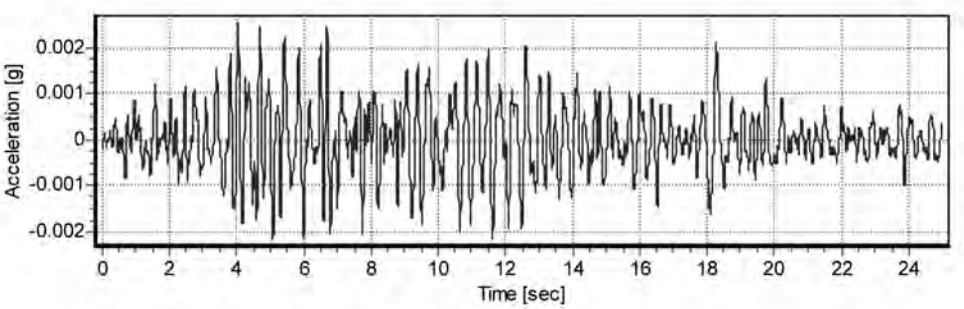

(c) Vertical Component (PGA= 0.002539g)

Figure 7.4 Strong motion accelerograms recorded at station - AEC, Guwahati (26.141911°N, 91.661072°E) on 14-02-2006

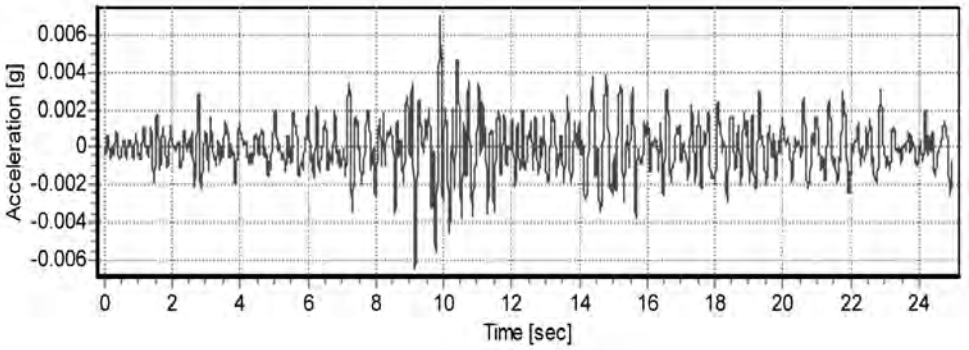

(a) North-South Component (PGA= 0.00701352g)

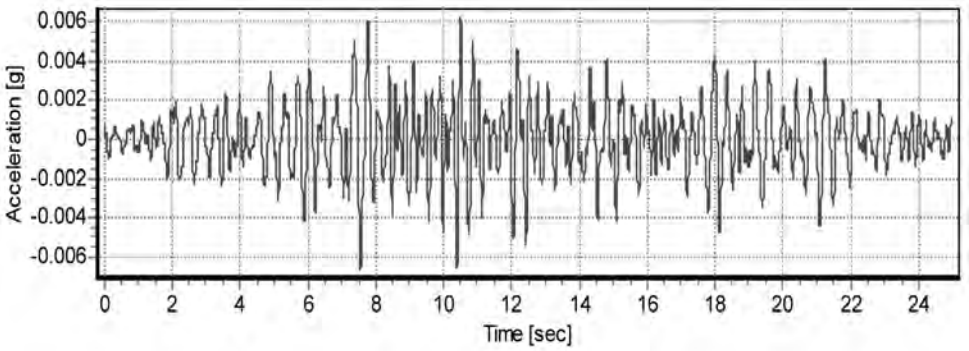

(b) East-West Component (PGA= 0.00665233g)

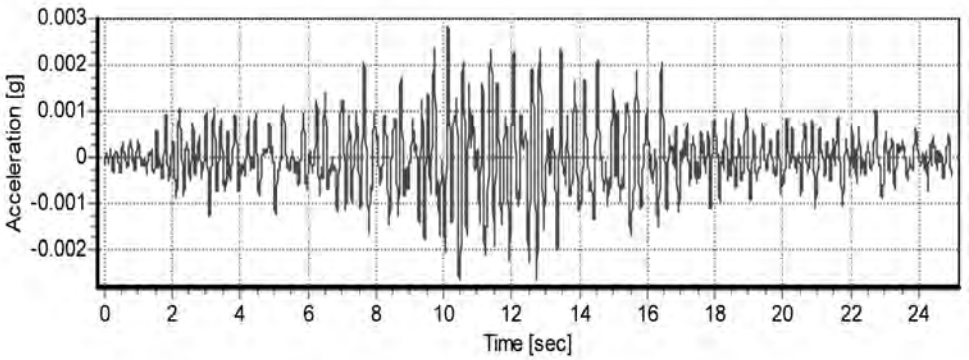

(c) Vertical Component (PGA= 0.00283862g)

Figure 7.5 Strong motion accelerograms recorded at station - AMTRON, Guwahati (26.185734°N, 91.786102°E) on 14-02-2006

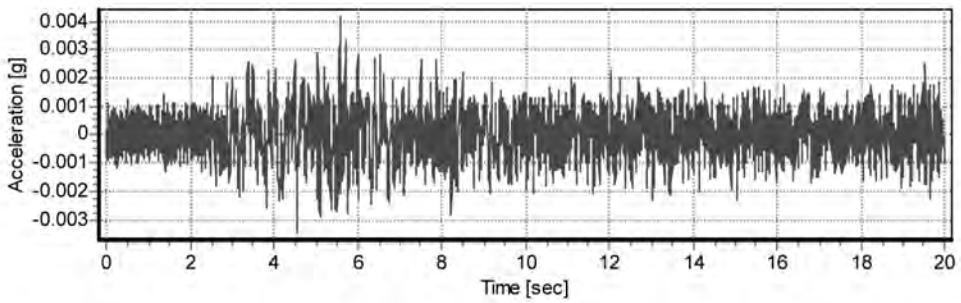

(a) North-South Component (PGA= 0.00415908g)

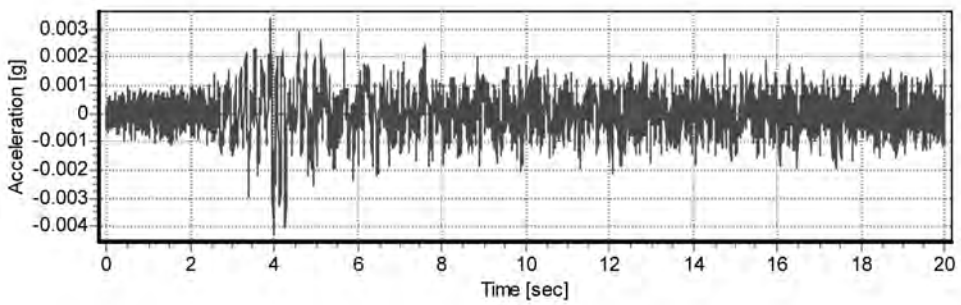

(b) East-West Component (PGA= 0.00428824g)

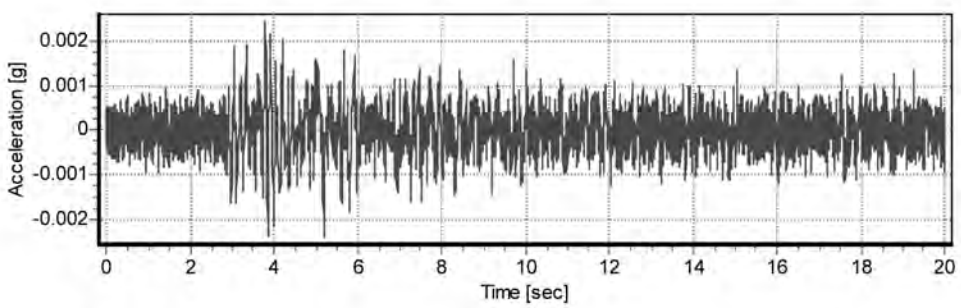

(c) Vertical Component (PGA= 0.00242985g)

Figure 7.6 Strong motion accelerograms recorded at station – Cotton College, Guwahati (26.187580°N, 91.743896°E) on 16-11-2006

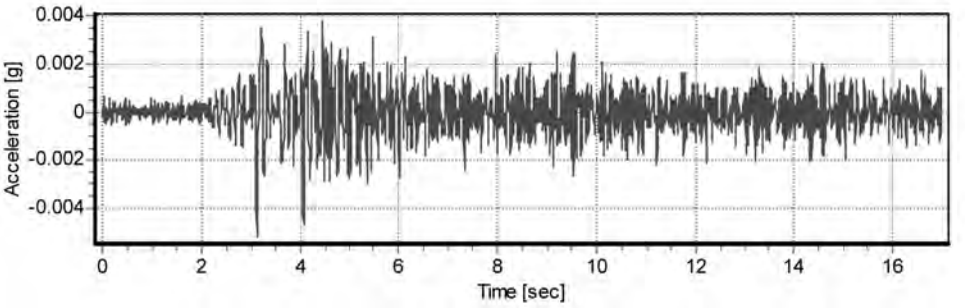

(a) North-South Component (PGA= 0.00521703g)

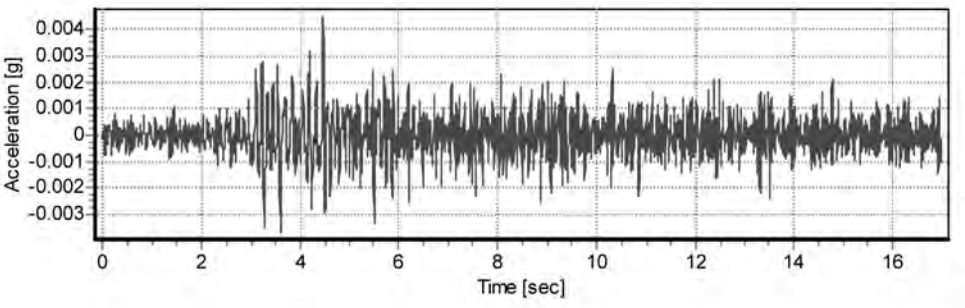

(b) East-West Component (PGA= 0.00449623g)

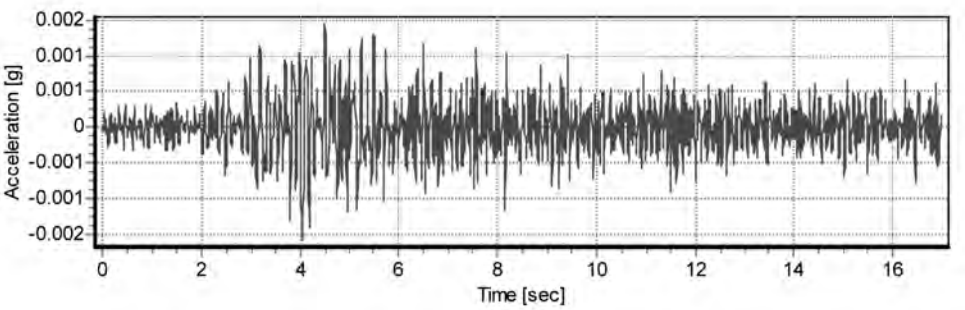

(c) Vertical Component (PGA= 0.00158163g)

Figure 7.7 Strong motion accelerograms recorded at station – IIT Guwahati Hill Top (26.187580° N, 91.743896 ° E) on 06-11-2006

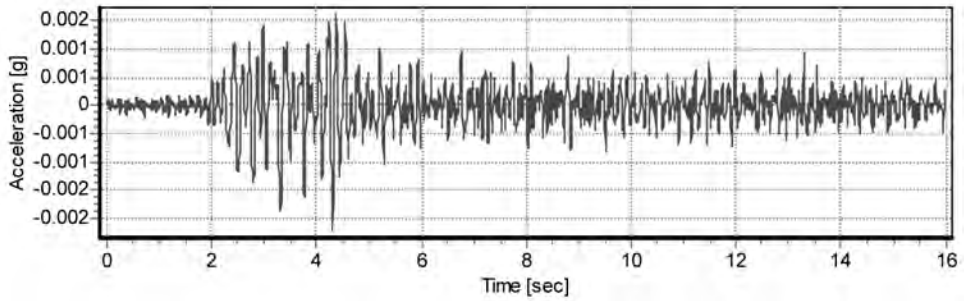

(a) North-South Component (PGA= 0.00223029g)

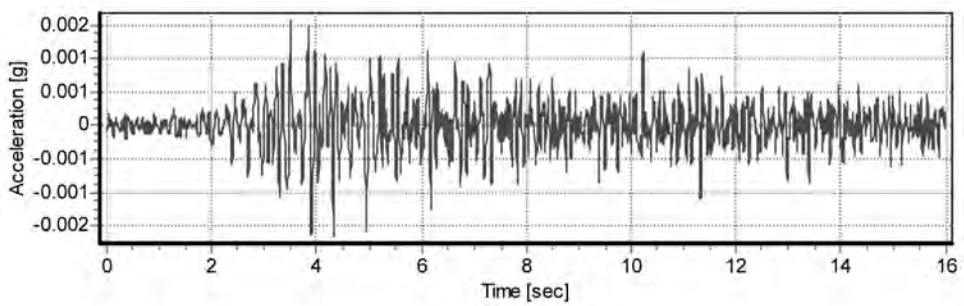

(b) East-West Component (PGA= 0.00165971g)

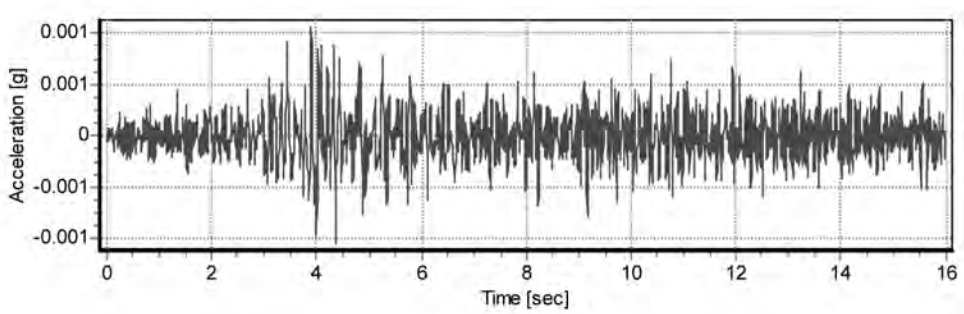

(c) Vertical Component (PGA= 0.00105951g)

Figure 7.8 Strong motion accelerograms recorded at station – IIT Guwahati (MED) (26.187481°N, 91.690567°E) on 06-11-2006

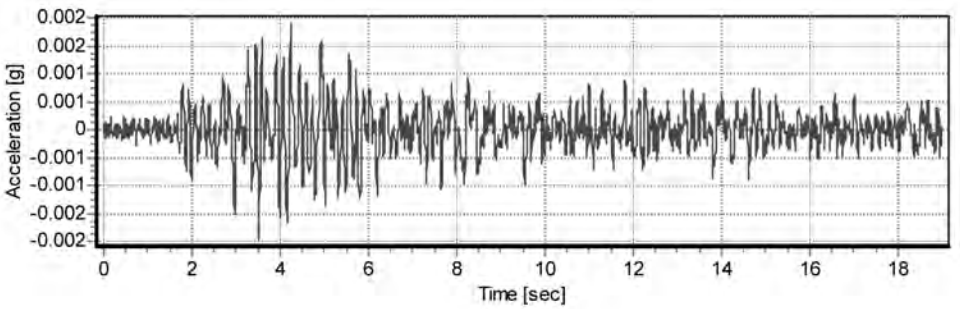

(a) North-South Component (PGA= 0.00196243g)

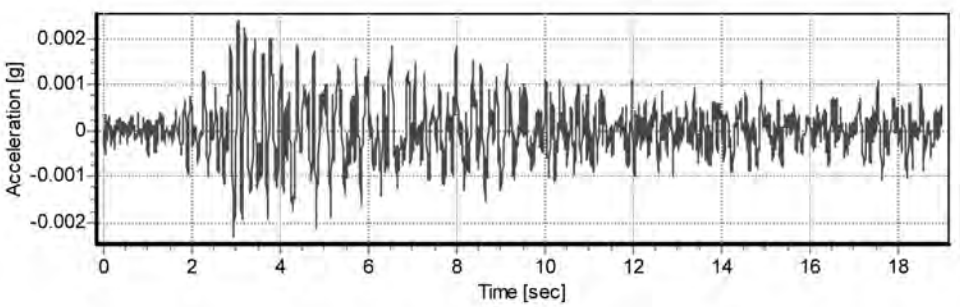

(b) East-West Component (PGA= 0.00238582g)

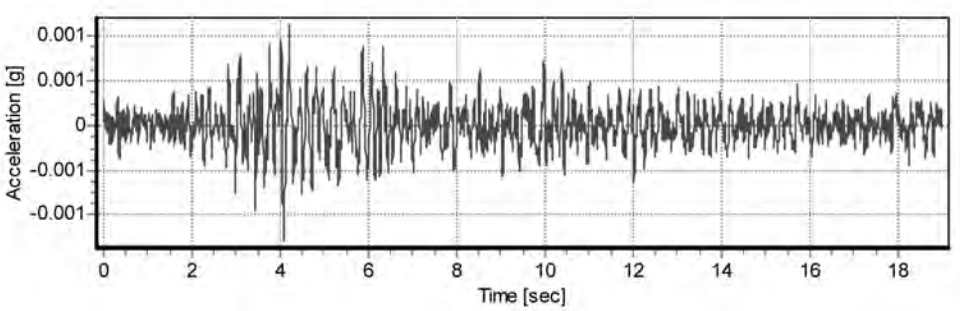

(c) Vertical Component (PGA= 0.00129389g)

Figure 7.9 Strong motion accelerograms recorded at station – CEO: Irrigation Guwahati (26.184713°N, 91.772697°E) on 06-11-2006

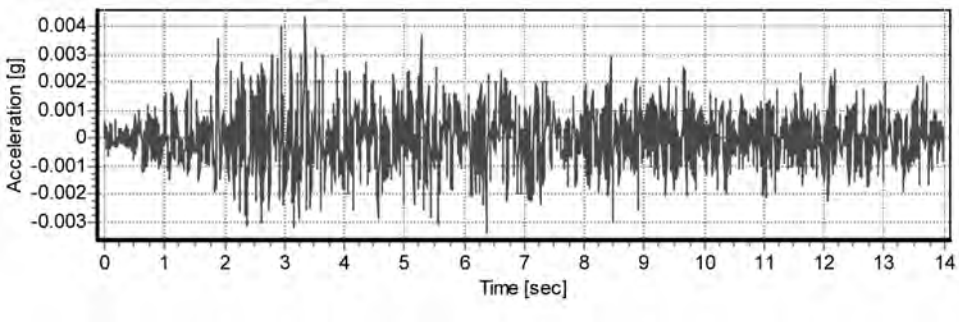

(a) North-South Component of (PGA= 0.00435117g)

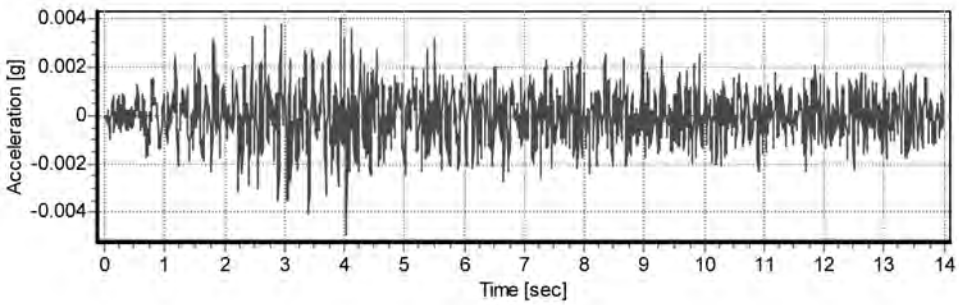

(b) East-West Component (PGA= 0.00493412g)

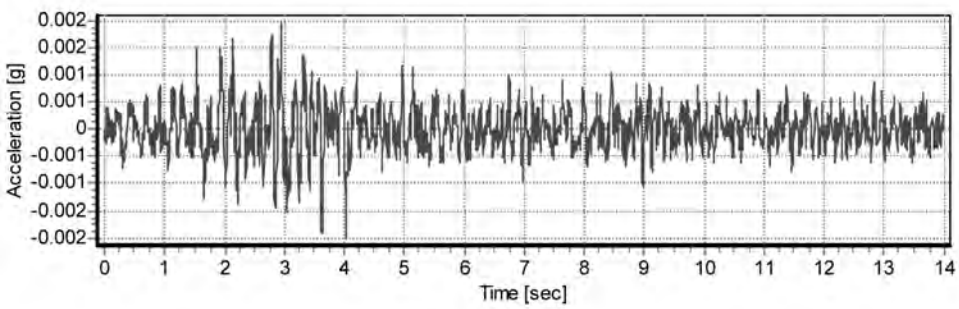

(c) Vertical Component (PGA= 0.00201165g)

Figure 7.10 Strong motion accelerograms recorded at station – RRL Guwahati (26.158409°N, 91.735542°E) on 06-11-2006

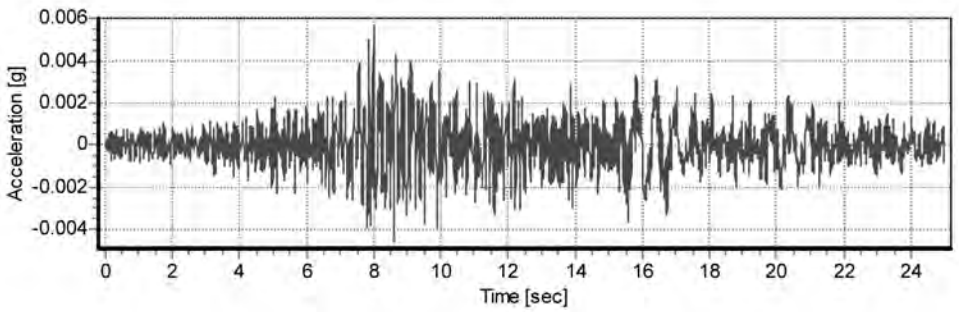

(a) North-South Component (PGA= 0.00567693g)

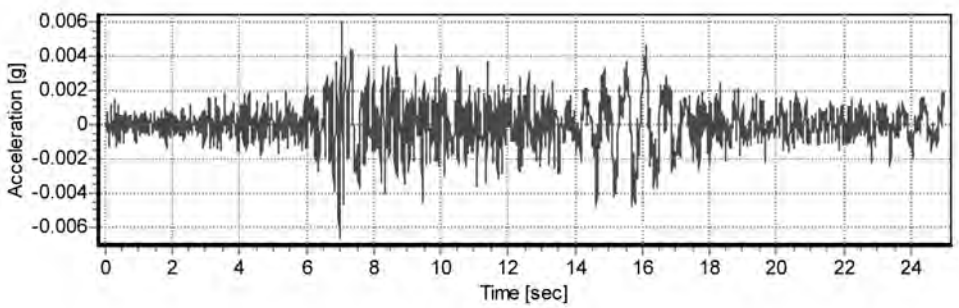

(b) East-West Component (PGA= 0.0066388g)

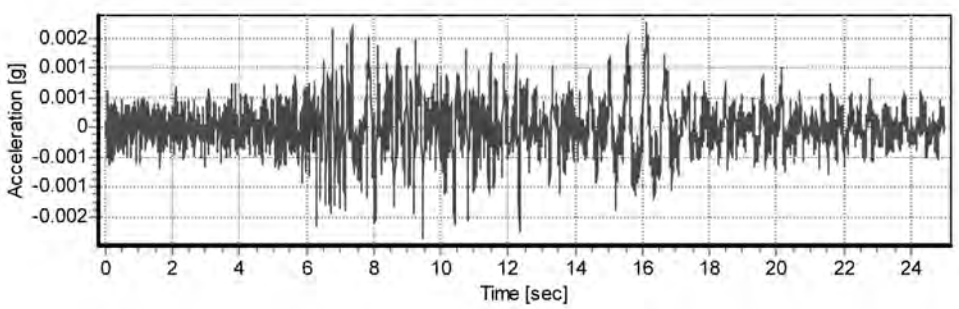

(c) Vertical Component (PGA= 0.00187761g)

Figure 7.11 Strong motion accelerograms recorded at station – S. D. Kalakhetra, Guwahati (26.132675°N, 91.821747°E) on 12-08-2006

7.3 AVERAGE NORMALIZED PSEUDO ACCELERATION SPECTRUM

Response spectrum is a practical means of characterizing ground motions and their effects on structures. The response spectrum provides a convenient means to summarize the peak responses of all possible linear single degree of freedom systems to a particular component of ground motion. In this study, pseudo acceleration spectra for eight strong motion stations have been developed using recorded ground motions at the respective stations. These spectra are then normalized by the respective peak ground accelerations. Finally, average normalized pseudo acceleration spectra obtained for each of the eight strong motion stations are shown in Figures 7.12 - 7.19. The spectrum shapes are representative of the sub-soil conditions of the respective sites.

7.4 GROUND MOTION ESTIMATION AT GUWAHATI DUE TO A HYPOTHETICAL Mw 7.5 EARTHQUAKE IN THE INDO-MYANMAR BORDER REGION

Out of the seven geologic-tectonic provinces in the NE region, the Myanmar-India region is basically a subduction zone. It appears to be continuous with Andaman-Nicobar ridge to the south. The past seismicity data indicates that Myanmar-India region is capable of producing earthquakes of moment magnitude 7.5 (Bhattacharya and Kayal, 2003). Recently, the strong motion instrument installed in IIT Guwahati triggered due to a Mw 5.7 earthquake with its epicenter in the Myanmar-India border region. The three components acceleration time histories are shown in Figure 7.20. After the 26th December, 2004 Sumatra-Andaman earthquake, there have been speculations among the seismologists that some adjustments are taking place in this subduction zone and there can be a great earthquake in the NE region. In view of this, it would be important to understand how the ground would respond in case of an earthquake event of magnitude Mw = 7.5 occurring in the Myanmar-India border region, at a distance of 350km from Guwahati.

In engineering practice, acceleration time history is the most sought after information during an earthquake. It is well known that high frequency accelerations resulting from complex faulting and medium irregularities are impossible to

be modeled in a simple deterministic manner. The complex layering and inhomogeneous make up of the near regional path overshadows many other effects to lead to random process like accelerograms. Nevertheless, within the scope of linear system theory, Green's function or impulse response function holds the key to the final solution. This function is the surface level response of the region under consideration to a buried impulsive double couple applied at an arbitrary point. Thus, small magnitude earthquakes with point-like sources could provide a clue to the regional Green's Function. In practice, since a point source is an idealization, suitable scaling is necessary in estimating Empirical Green's Function (EGF). Hartzell (1978) proposed that records of small magnitude earthquakes occurring near the main shock fault plane could be taken as EGF in simulating the ground motion for the target region. In this approach, the main shock fault plane is divided into sub-faults of equal size. The number of such sub-faults is determined from the scaling law of Kanamori and Anderson (1975). Each sub-fault is taken to produce the recorded accelerogram of the aftershock or small magnitude event, with a correction factor as suggested by Frankel (1995). Each such accelerogram is delayed at the surface station to account for rupture time and travel time from the various sub-faults that make up the main fault. The complete details of the EGF methodology are available in Iyengar and Raghukanth (2005). The details of the Mw 5.7 earthquake, used here as EGF and the hypothetical earthquake are given in Table 7.1. The strike and dip of the fault plane is taken as 281° and 46° which are same as that of the Mw 5.7 earthquake. The length and width of the fault plane for the hypothetical event estimated from magnitude are taken as 110km x 50km (Wells and Coppersmith, 1994). The simulated acceleration time histories for Guwahati city during the hypothetical event are shown in Figure 7.21. This method estimates the PGA at Guwahati city due to a hypothetical earthquake of Mw 7.5 occurring in Myanmar-India region as 0.1g. Similar studies will be undertaken for simulation of ground motions around greater Guwahati Region corresponding to all possible sources in the NE region.

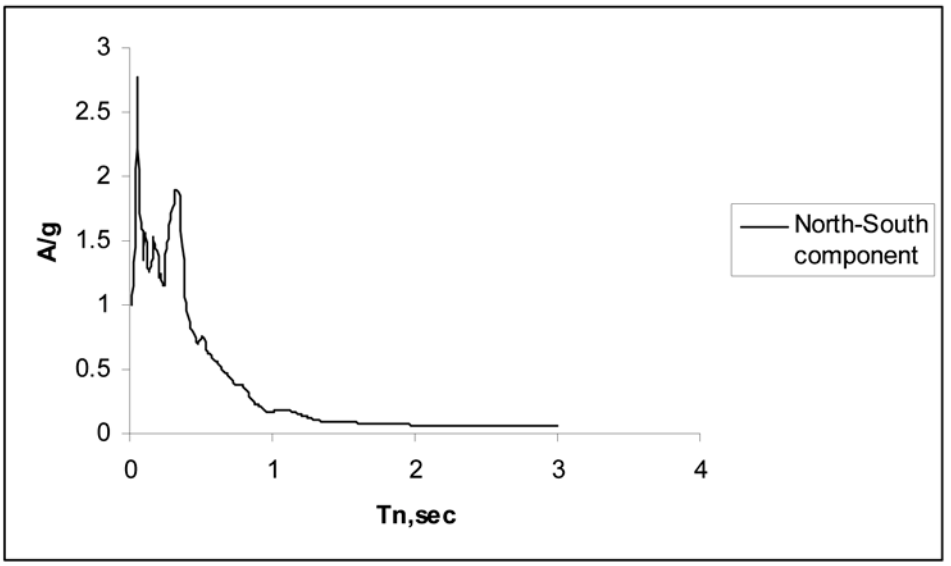

(a)

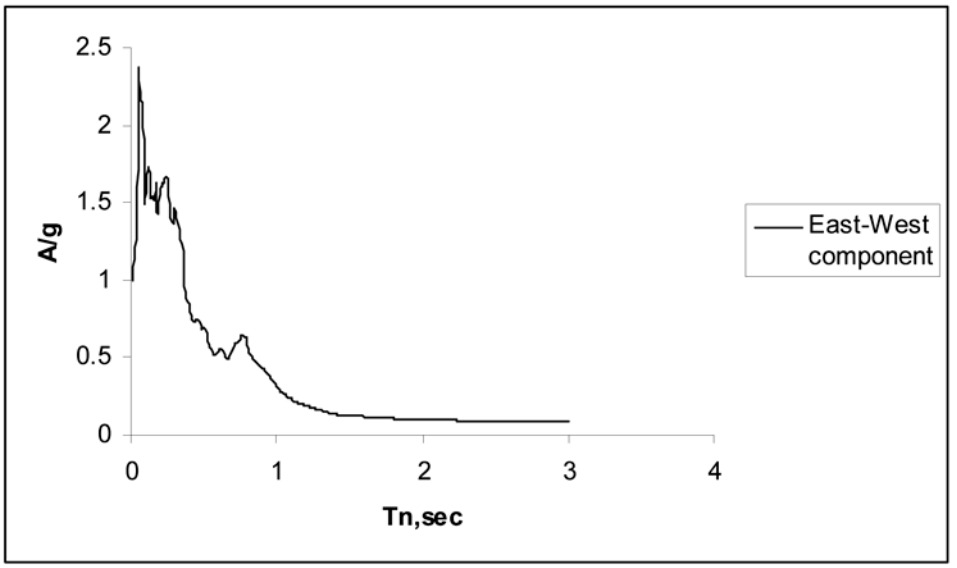

(b)

Figure 7.12 Average normalized pseudo-acceleration response spectrum for AEC Guwahati site (26.141911°N, 91.661072°E)

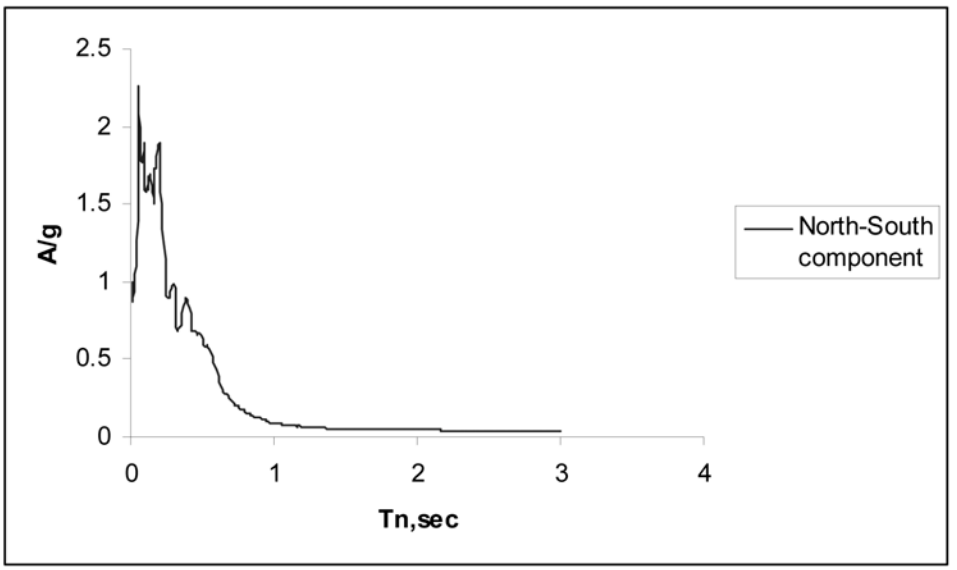

(a)

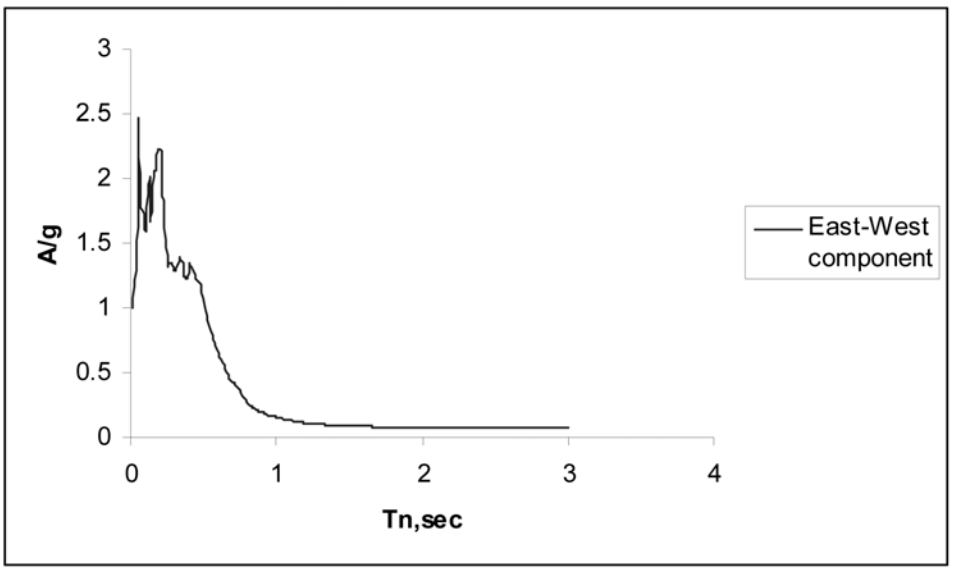

(b)

Figure 7.13 Average normalized pseudo-acceleration response spectrum for AMTRON Guwahati site (26.185734°N, 91.786102°E)

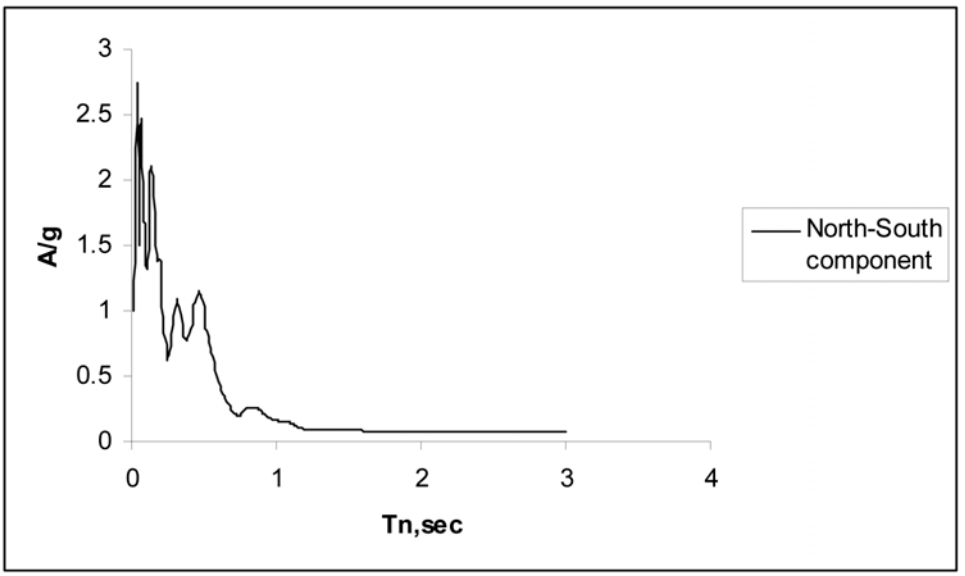

(a)

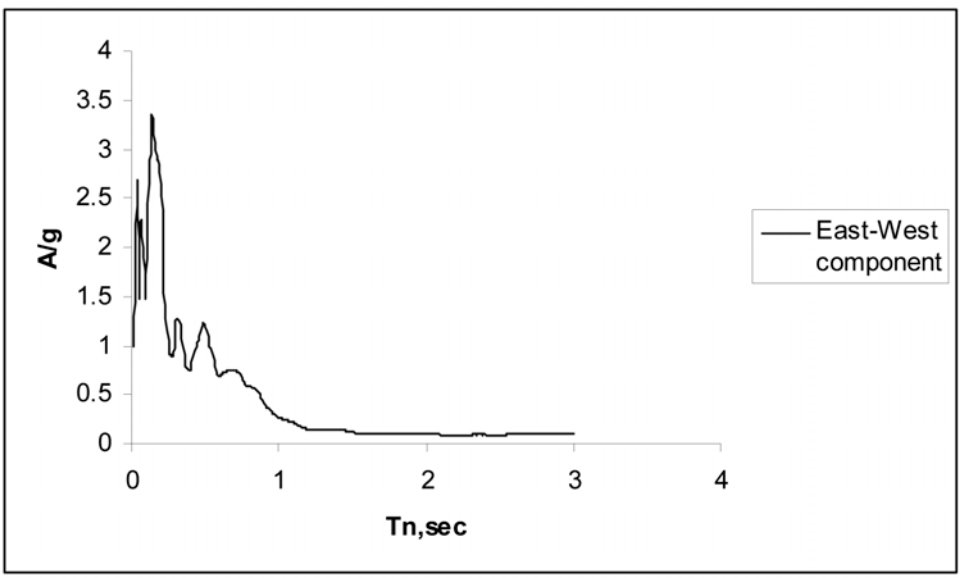

(b)

Figure 7.14 Average normalized pseudo-acceleration response spectrum for Cotton College Guwahati site (26.187580°N, 91.743896°E)

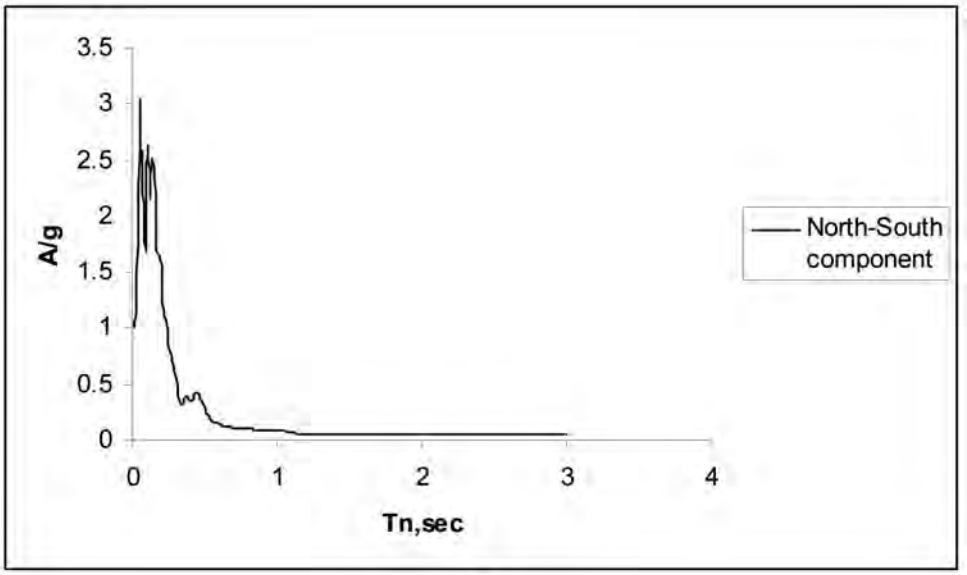

(a)

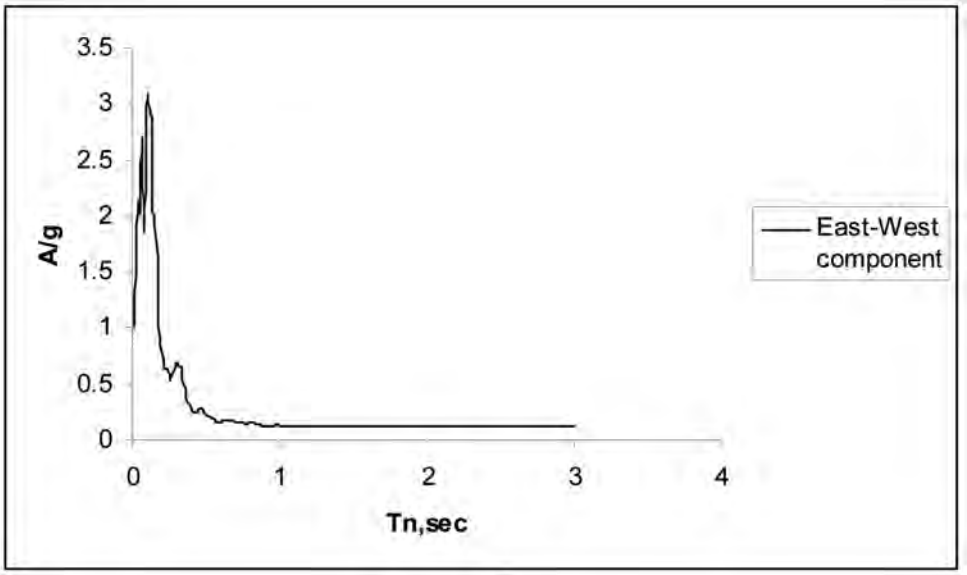

(b)

Figure 7.15 Average normalized pseudo-acceleration response spectrum for IIT Guwahati hill top site (26.193830°N, 91.692047°E)

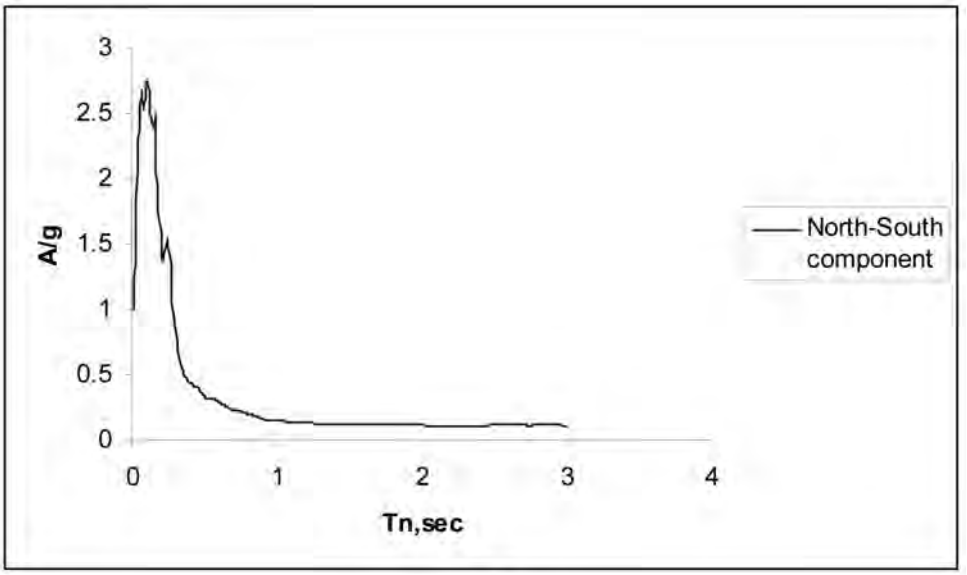

(a)

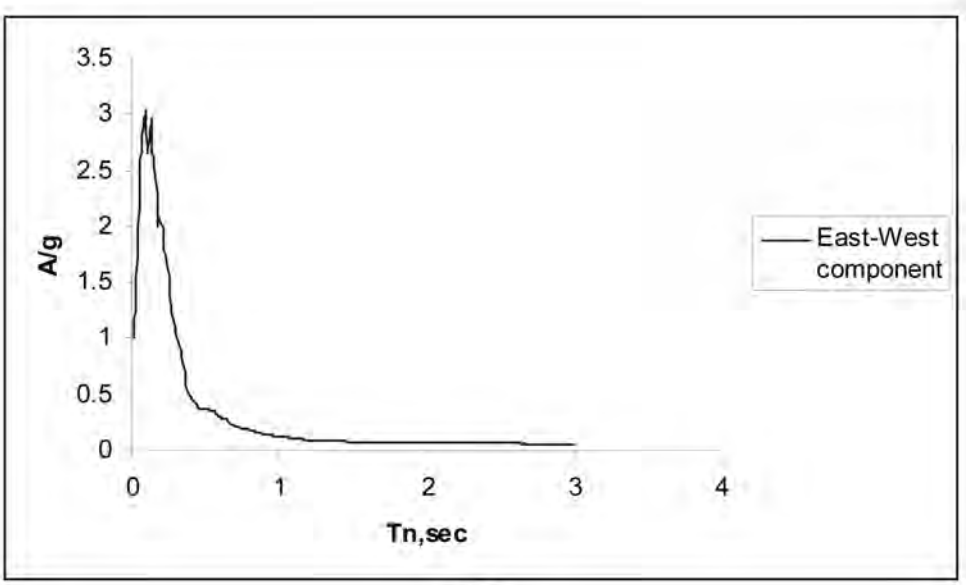

(b)

Figure 7.16 Average normalized pseudo-acceleration response spectrum for IIT Guwahati -MED site (26.187481°N, 91.690567°E)

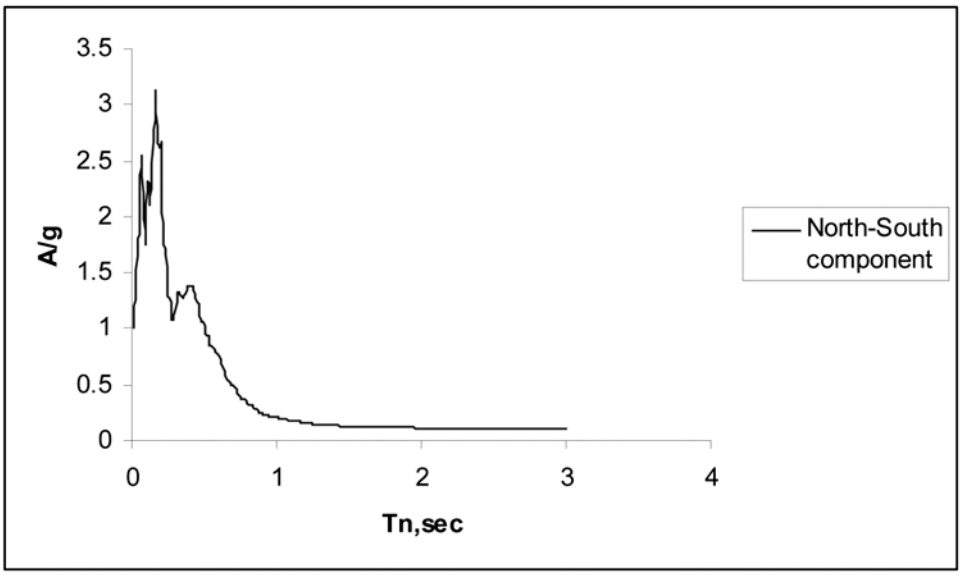

(a)

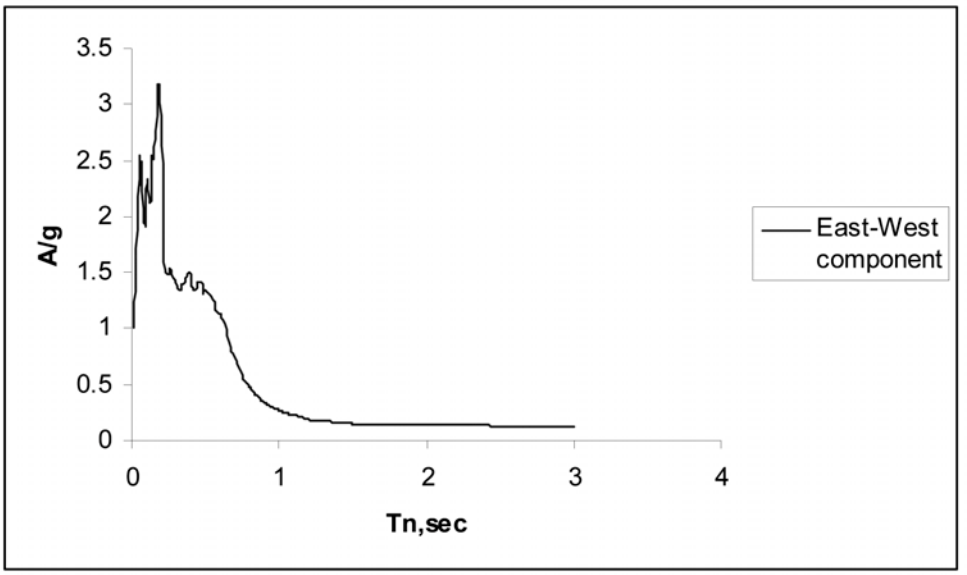

(b)

Figure 7.17 Average normalized pseudo-acceleration response spectrum for CEO- Irrigation Guwahati site (26.184713°N, 91.772697°E)

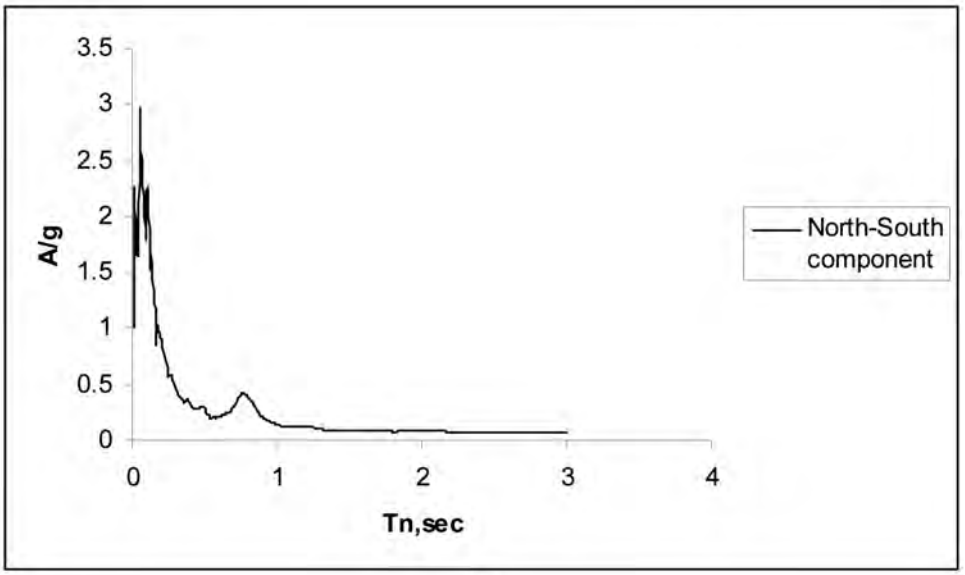

(a)

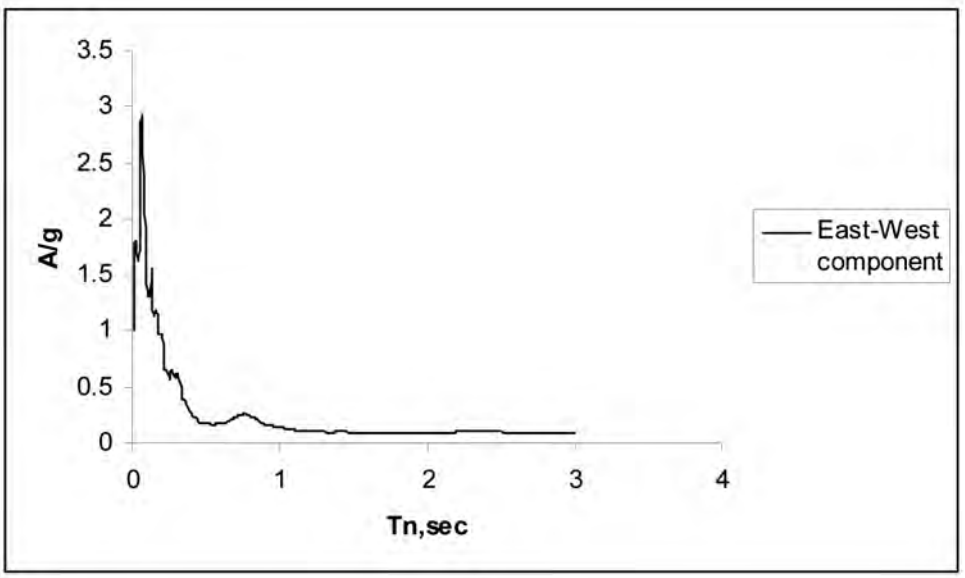

(b)

Figure 7.18 Average normalized pseudo-acceleration response spectrum for RRL Guwahati site (26.158409°N, 91.735542°E)

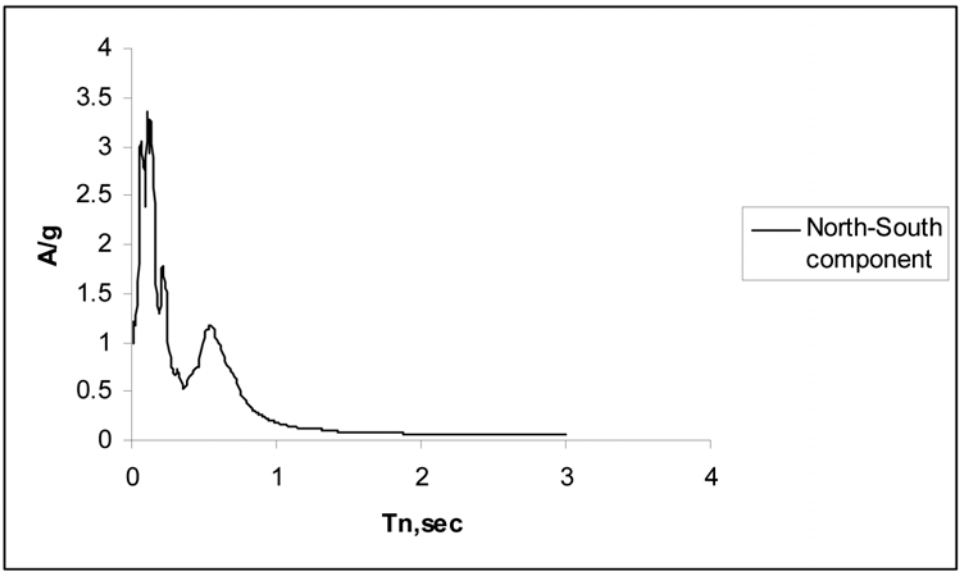

(a)

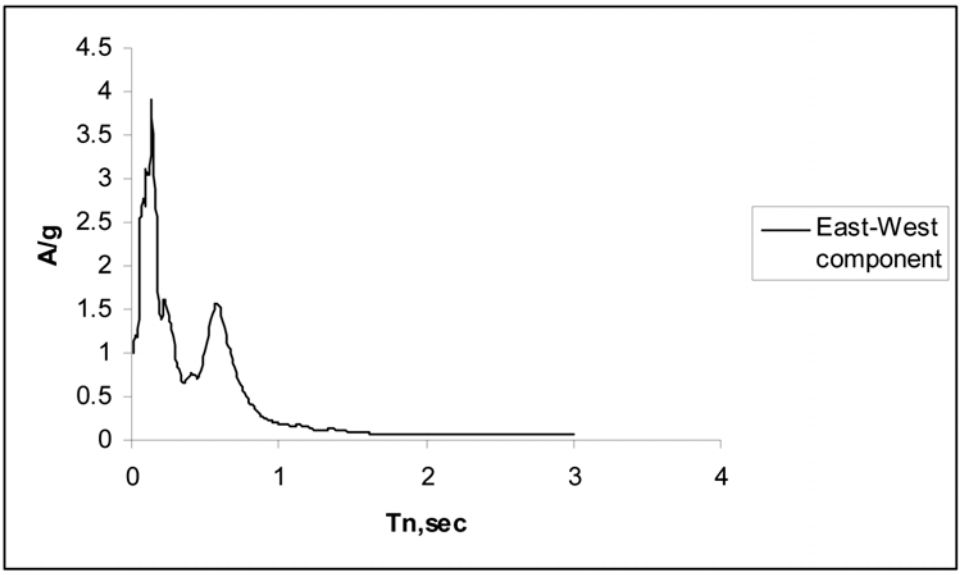

(b)

Figure 7.19 Average normalized pseudo-acceleration response spectrum for S.D. Kalakhetra Guwahati site (26.132675°N, 91.821747°E)

Table 7.2: Parameters of the hypothetical earthquake and the EGF

Date	Magnitude (M_w)	Epicenter		Focal Depth (km)
Hypothetical	**7.5**	**24.64°N**	**94.81°E**	**82**
18 / 9 / 2005	**5.7**	**24.64°N**	**94.81°E**	**82**

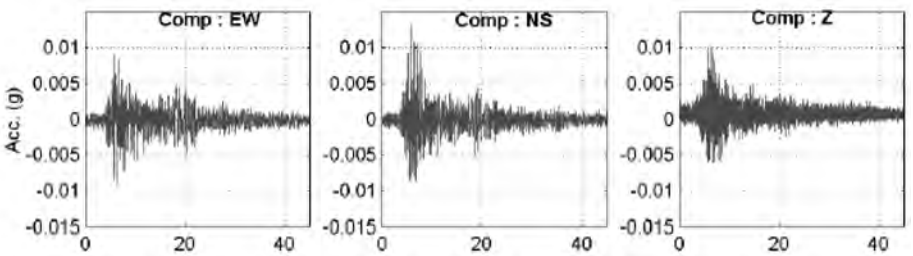

Figure 7.20 Three components of accelerograms of the event recorded on September 18, 2005

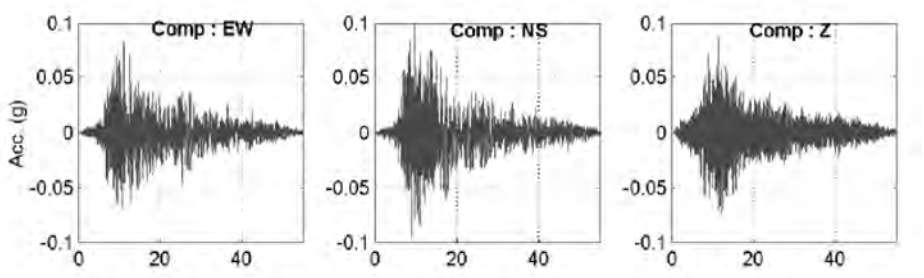

Figure 7.21 Simulated accelerograms at IIT Guwahati due to the hypothetical Earthquake of magnitude M_w = 7.5 in Indo-Myanmar Border

CHAPTER 8

Seismic Vulnerability of Buildings for Guwahati

8.1 INTRODUCTION

The primary emphasis in disaster management has been placed on the performance of structures, the failure of which would pose direct risk to life and property. Survey and assessment of existing building stocks for earthquake vulnerability risk is necessary to formulate the seismic hazard map of a city.

The seismic vulnerability study comprises mainly review of the existing buildings of Guwahati in the light of guidelines for earthquake resistant construction in India, construction practices being adopted in Guwahati urban area, building typologies, designing of questionnaire for detail survey of buildings of the Guwahati municipal area, selection of representative building samples for detailed analysis and NDT, and creation of database. Subsequently, seismic vulnerability of existing building stock estimated quantitatively and qualitatively. The quantitative approach covers demand-capacity computation, while qualitative procedure estimates structural scores using Rapid Screening Procedures (RSP). The results are mapped using ArcInfo and GIS, which are later synergized with seismic hazard microzonation to deliver seismic risk.

8.2 EXISTING BUILDING SCENARIO IN GUWAHATI URBAN AREA

India has a very complex socio-cultural environment and its built environment encompasses the widest possible range from non-engineered dwellings built with traditional skills to the most modern buildings, and Guwahati is no exception. The Guwahati urban area under study (the municipal area) is spread over 262 sq. km. comprising of 60 wards.

8.2.1 **Building Category** (source: Vulnerability Atlas of India,1999)

The specifications, which are predominantly seen in and around Guwahati are underlined and put in bold letters.

Type-A: Buildings in field-stone, **rural structures–bamboo reinforced biomass wall cladding – thatched/ CI sheet roof** , unburnt brick house, clay houses

Type-B: Ordinary brick building – **Brick Masonry Wall – 6"X6" corner columns with lintel bend and tie – timber trussed CI sheet roof,** buildings of the large block and prefabricated type, half-timbered structures, building in natural hewn stone

Type-C: Reinforced Concrete Building – Engineered & Non-Engineered, well built wooden structures

Type-X: Other types not covered in A, B, C.

The majority of houses in the villages around Guwahati urban area is of 'Assam Type' categorized in TYPE-B - (a) brick masonry wall, 6"X6" R.C. Column, lintel band, tie and with Timber truss. (b) bamboo reinforced Biomass Wall cladding with roofs made of thatch of bamboo supported on bamboo purloins. This building has very low vulnerability.

The existing building stock in municipal area of Guwahati city is comprised of RC framed structure (TYPE-C - around 80%). These dwelling units are mainly 2 to 3 storey with 3.0 to 3.3 m storey height. Most of the residential dwelling units are non-engineered, but has earthquake resistant elements in-built viz. tie beams and column sizes are minimum 250mm X 250mm. In most of such buildings, the column reinforcements are 4-16 TOR. There are few such buildings, which were built around 1965-70 and are reinforced with mild steel.

There has been phenomenal increase in construction of multi-storied apartment and commercial buildings, which are mostly G+5 to G+7 RC building. These buildings are engineered in a sense that the buildings are designed by engineers as per IS:1893-1984, which has been made mandatory by GMDA about 10 years ago.

Figure 8.1 Existing building typologies in Guwahati urban area

Figure 8.2 Existing building typologies in Guwahati urban area

8.3 PAST ATTEMPTS FOR ASSESSMENT OF VULNERABILITY

The Vulnerability Atlas of India (1999) detailed out housing vulnerability tables wherein damage risk levels for earthquakes are defined based on the intensity scales such as Very High, High, Moderate, Low, and Very Low, and the categorization of houses has been carried out based on the distribution of houses by predominant materials of roof and wall, according to 1991 Census of India. The state-wise Vulnerability Atlas, describing district-wise damage risk due to earthquake, wind and flood has been prepared. A demographic distribution map of Guwahati region is shown in Figure 8.3. Accordingly, the earthquake damage risk associated for Guwahati urban area varies from very low, low and medium for Type-A, Type-B, and Type-C houses respectively. There has not been any other reported literature on seismic vulnerability of existing building stocks of Guwahati urban area, which is one of the important modules for any Seismic Hazard and Risk Management (SHRM) study. A combination of local hazard intensity and vulnerability of existing house types has

been used for carrying out risk analysis given in the district-wise tables. The Vulnerability Atlas, thus, provides ready macro-level information for use by the authorities for natural disaster mitigation and preventive actions. The types of housing as existing in each district has been taken from the 1991 Census of India and categorized from vulnerability consideration. The vulnerability of these types to various intensities of the hazards was estimated by and the damage risk in each district has been presented in a separate table. The area of the district prone to various hazard intensities has also been shown. In the present study we achieved a preliminary seismic risk map using the PGA computed by F-K integration method as shown in Figure 8.5. The Microzonation map was integrated with Demographic distribution of the region. Table 8.1 is showing the normalized feature rating for risk estimation of the region. The preliminary seismic risk map presented here is recommended for decision making purpose.

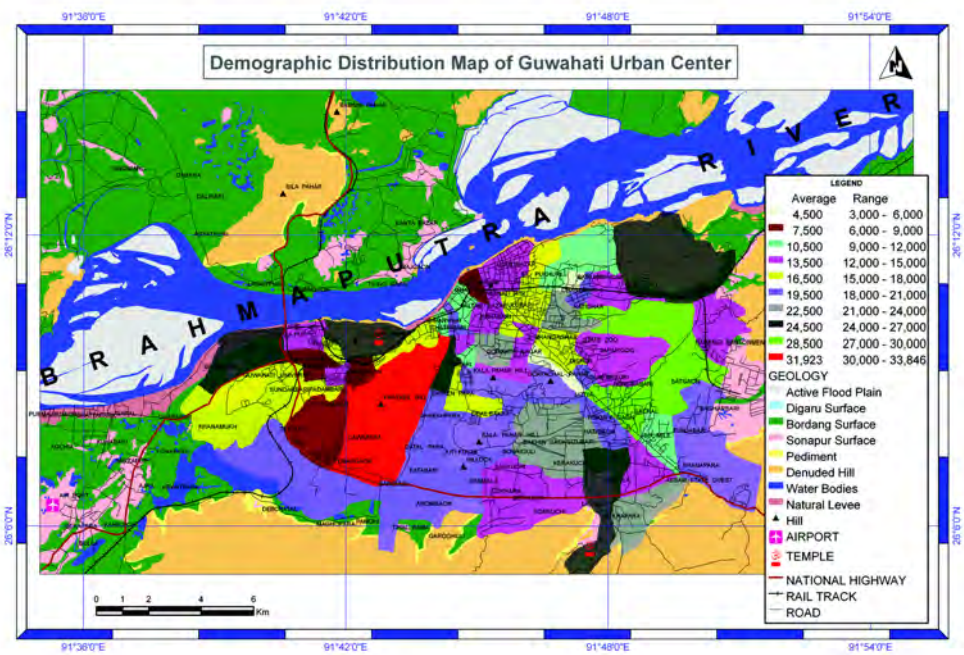

Figure 8.3 Demographic distribution map of Guwahati Region

8.4 THE MACRO - HAZARD MAPS

The monitoring of earthquake hazards In India is carried out by Indian Meteorological Department (IMD). In addition, noteworthy contributions are made by Geological Survey of India and the Department of Earthquake Engineering, IIT Roorkee in this regard. The Bureau of Indian Standards Committees on Earthquake Engineering has a Seismic Zoning Map. The earthquake hazard maps are drawn for each State and UT separately. Various district boundaries are clearly shown for easy identification of the hazard risk prone areas. The intensities of earthquakes on MSK scale are drawn on the maps to show various intensity zones.

8.5 SEISMIC EVALUATION METHODOLOGY

Indian buildings built over past two decades are seismically deficient because of lack of awareness regarding seismic behavior of structure, constant upgradation of knowledge as regards earthquake resistant design and construction. Also seismic design is not practiced in most of the buildings being built. It calls for seismic evaluation of existing building stocks in an area.

Evaluation is a complex process, which has to consider not only the design of building but also the deterioration of the material and damage caused to the building, if any. The difficulties faced in the seismic evaluation of a building are manifold. There is no reliable information/database available for existing building stock, construction practices, in-situ strength of material and components of the building. The seismic evaluation mainly relies on set of general evaluation statements. The unavailability of a reliable estimate of earthquake parameters, to which the building is expected to be subjected during its residual life poses another challenge. Probabilistic approach to evolve needful parameters, would call for elaborate studies. Hence, for preliminary appraisal, the ground motion parameters available in the present code (BIS, 2002) have been estimated at the macro level. As regards the effect of local soil conditions, which are known to greatly modify the earthquake ground motion, experiences of ground accentuation and data generated through collateral studies on site response have been considered. Also, in view of above constraints, the present study is limited to seismic evaluation of representative buildings of different typology viz. Type-A (Mud/RR Masonry, Adobe), Type-B (Brick

Masonry Buildings), and Type-C (RCC Buildings), and projects a generalized pattern of building response to future seismic ground motion in different wards/zones of Guwahati urban area.

The approach for assessment of seismic vulnerability of buildings involves estimation of seismic vulnerability of existing building stock quantitatively and qualitatively. The quantitative approach, covers demand-capacity computation (ATC-40, 1996), while qualitative procedure estimates structural scores based on national and international state-of-the-art procedures viz. Rapid Screening Procedure (ATC-21, 1988; ATC-21-1,1988). The seismic evaluation leading to seismic vulnerability of existing building stock at Guwahati has been estimated quantitatively and qualitatively. The general procedures for seismic evaluation of existing buildings adopted in the present study are: site visit and data collection; selection and review of evaluation statements; follow-up fieldwork; and analysis of buildings by quantitative and qualitative approach. The work presented here is aimed at carrying out seismic vulnerability of existing building stock to prognosticate the damage pattern of existing building stocks of Guwahati urban area in the advent of future earthquake.

8.6 QUALITATIVE APPROACH - RAPID VISUAL SCREENING OF BUILDINGS

The methodology adopted in carrying out the survey and indexing damage potential to various buildings is in line with the proposed methodology by Ministry of Home Affairs (MHA), India and is based on the classification of buildings as per MSK Intensity scale. The Rapid Visual Screening Form as shown in Table 8.1 was used for collecting building data. A total of 4500 nos. of sample buildings spread over 60 ward were surveyed and the building data has been electronically warehoused for future analytical work.

The study found that most of the residential buildings in Guwahati are constructed based on socio-economic consideration rather than engineering approach. The majority of building stock (about 80%) composed of Type-C buildings. The TYPE-A and TYPE-B buildings in residential area (about 20 %) are though non-engineered, they have earthquake resistant construction features inbuilt in them.

General construction of RC framed buildings are of nominal concrete of M15 grade (1:2:4) ranging from 3 to 4 story with story height of 3.00 to 3.30m (Type-C Structures) having RCC slab of 100-120mm thickness and 125-250mm thick brick masonry in cement mortar (1:6) as infill. The apartment buildings authorized by GMDA and GMC are well engineered, as the procedure of obtaining permission for such buildings are rigorous with a structural engineer as RTP (Registered Technical Personnel) in addition to the registered architect. The geotechnical investigation for such buildings is mandatory – rendering the substructure design more reliable. These RC buildings are designed for earthquake load as per IS: 1893 – 1984/2002. The detailing part of these buildings is of-course not as good as their design effort and around 20% of these buildings are deficient in ductility provisions as enumerated in IS: 1920-1993 (BIS, 1993a).

As mentioned earlier, there has been phenomenal increase in construction of multi-storied apartment and commercial buildings, which are mostly G+5 to G+7 RC building. These buildings are engineered in a sense that the buildings are designed by engineers as per IS:1893 , which has been made mandatory by GMDA about 10 years ago, but 20% of them are found deficient while quantitative analysis was done as per newly amended IS:1893-2002. Implementation of BIS code provisions regarding earthquake resistant design (BIS, 2002) and construction as given in IS: 4326-1993 (BIS, 1993b) were found to be absent almost in all the non-engineered TYPE-C residential buildings.

TABLE 8.1

SAMPLE OF RAPID VISUAL SCREEING FORMS

MORE THAN 4500 SUCH FORMS ARE GENERATED AND DIGIATLLY WAREHOUSED FOR GIS MAPPING. ALL THIS FORMS ARE ALSO CONVERTED TO DATA FILES IN MICROSOFT EXCEL & ACCESS FORMAT FOR COLLATION, AND DATA ATTRIBUTION

Seismic Zone V

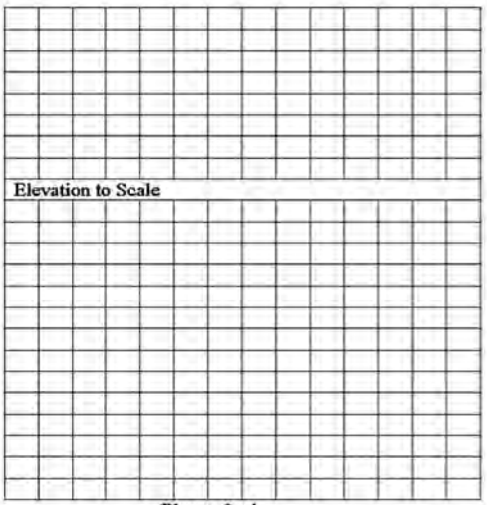

Building Name _____
Use _____
Address: _____
_____ Pin _____
Other Identifiers _____
No. Stories _____ Year Built _____
Total Floor Area (sq.m)_____

PHOTOGRAPH

OCCUPANCY		SITE	FALLING HAZARDS
Resi.:Ord/Imp. School Health Assembly Office Commercial Historic Emer. Service Industrial	Max. Number of Persons 0-10 11-50 51-100 >100 Residents _____ Floating _____	High W.T. (within 8 m) Liquefiable (if sandy soil) Land Slide Prone	☐ Chimneys ☐ Parapets ☐ Cladding ☐ Other

Probable Maximum Grade of Damage

Building Type	Masonry Building				RC or Steel Frame Building				URM infill	Wood
	A,A+	B,B+	C,C+	D	C,C+	D	E,E+	F		
Damage grade in Zone V	G5	G5	G4	G3	G4	G3	G2	G1	G4	G4

Note: +sign indicates higher strength hence somewhat lower damage expected than that stated. Also average damage in one building type in the area may be lower by one grade point than the probable maximum indicated.

Surveyor will identify the Building Type, encircle it, also the corresponding damage grade and tick mark the recommendation.

Recommended Action :

1) A, A+ or B, B+ : evaluate in detail for need of reconstruction or possible retrofitting to achieve type C or D
2) C, C+: evaluate in detail for need of retrofitting to achieve type D
3) URM infill: evaluate for need of reconstruction or possible retrofitting to level D
4) Wood: evaluate in detail for retrofitting

Surveyor's Signature _____
Name: _____
Date: _____

8.6.1 Questionnaire – Add on to Rapid Visual Screening

Designing of questionnaire comprising of set of evaluation statements is the first and foremost step for any seismic vulnerability analysis. The questionnaire helped the surveyor to determine any weak links in the structure that could precipitate structural or component failure. For pre-earthquake seismic evaluation of existing building stocks there is no standard questionnaire at international & national levels. Hence, a need was felt to design exhaustive questionnaire to uncover the flaws and weaknesses of buildings/built environment. In the backdrop of available practices being adopted all over the globe, a comprehensive questionnaire has been designed. The questionnaire involves the use of sets of evaluation statements which cover structural configuration and specification, condition of structure and ambience, scenario of distress in non-structural components, seismic vulnerability parameters, damage during previous earthquake and repairs carried out thereof, and assessment of scientist/surveyor. The questions are in the form of fill-in-the-blanks and evaluation statements highlighting building characteristics which are essential to avoid failures during earthquake.

8.7 SITE VISIT & BUILDING SURVEY - ADMINISTRATIVE UNITS OF GUWAHATI URBAN AREA

The region delineated under Guwahati Metropolitan Area measures 262 sq. km. includes Guwahati Municipal Corporation (GMC) area, North Guwahati Town Committee, Amingaon Census Town and 21 revenue villages which are under : Abhaypur, Rudreswar, Namati Jalah, Gouripur, Silamohekaiti, Tilingaon, Shila, Ghorajan, Mikirpara, Kahikuchi, Kahikuchi, Mirjapur, Jugipara, Borjhar, Garal Gaon, Dharapur, Janisimalu & Jansimalu (NC), Kalitakuchi(NC), Kharghuli, Bonda, Bondagaon and Bonda Grant, (I&II) and Birkuchi. In addition to the above area, there is Narangi Cantonment area, Guwahati Refinery (IOCL) area, and NF railway Colony.

In order to evaluate seismic vulnerability of huge number of building stocks in Guwahati urban area, house to house survey was carried out – involving physical measurement to get accurate building footprint, chain-age of building reference

point, and collection of socio-economic data. The comprehensive house to house survey was limited to Guwahati Municipal area, which is divided into 60 numbers of municipal wards as delineated by Guwahati Municipal Corporation. These 60 wards are taken as zone in the present analysis. In addition, Marengo Cantonment Area, Refinery area, NF railway area and surrounding revenue villages have been considered as a separate zone. Detailed house to house survey of existing buildings stocks of each ward has been conducted. These entire wards do not show any cluster formation making it imperative to collect data from each building carrying out house to house survey. This exercise took considerable time to complete. The other demarcated area viz. cantt. Refinery and railway colony area in Maligaon has well defined cluster formation and therefore building footprints are being generated from satellite imagery. Surveys of representative samples from these areas are carried out. The revenue villages around Guwahati are kept out of the survey as all these villages are mostly dominated by houses built from bamboo reinforced biomass as cladding and thatched/GI sheet roofing, which have very low vulnerability. However, footprints of these building stocks are being incorporated from satellite imagery with the detail attribution except the building type to get complete picture.

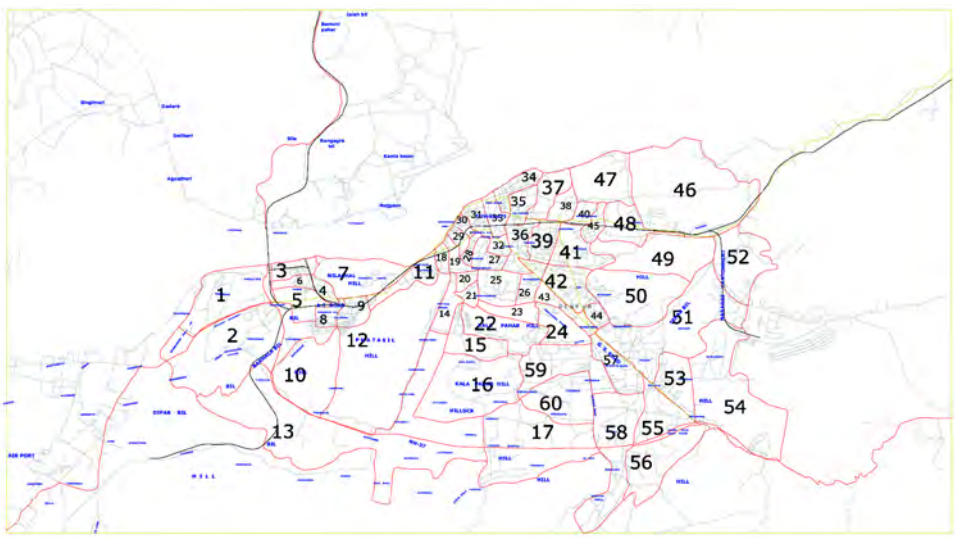

Figure 8.4 Guwahati urban area with wards delineated

Table 8.2: The weights and normalized ratings for integrations of risk assessment

Theme	Weight	Feature	Rating	Normalized Rating
Microzonation	**0.50**	>= 0.50	5	1.0000
		0.40 – 0.50	4	0.7500
		0.30 – 0.40	3	0.5000
		0.20 – 0.30	2	0.2500
		< 0.20	1	0.0000
Demography	**0.50**	30,000 - 33,846	10	1.0000
		27,000 - 30,000	9	0.8889
		24,000 - 27,000	8	0.7778
		21,000 - 24,000	7	0.6667
		18,000 - 21,000	6	0.5556
		15,000 - 18,000	5	0.4444
		12,000 - 15,000	4	0.3333
		9,000 - 12,000	3	0.2222
		6,000 - 9,000	2	0.1111
		3,000 - 6,000	1	0.0000

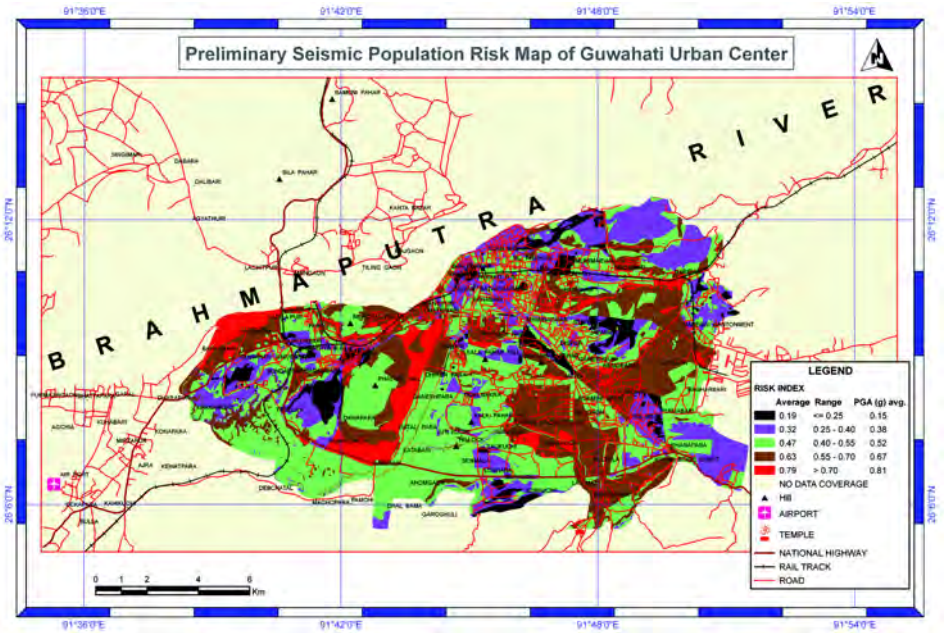

Figure 8.5 Preliminary Seismic Population Risk map of Guwahati urban center (Using the PGA computed by wave number integration method)

8.8 DETAILED SURVEY OF SELECTED BUILDINGS

Apart from filling-up of questionnaire for the selected buildings, surveyor has to inspect the health of structure critically to assess its seismic resistance. In the process, surveyor has to face several difficulties. The foremost problem is of uncovering the structure. In many buildings the structure is concealed by architectural finishes, and the surveyor will have to get into attics, and crawl spaces. Non-availability of plans, and design calculations are yet another problem, and is particularly frustrating with respect to reinforced concrete work. Assessing material quality and associated allowable stresses are also difficult preposition, and one has to rely on local available reports/information or otherwise one has to go for destructive testing, which is seldom possible. Destructive and non-destructive testing of reinforced concrete and masonry elements are necessary to determine strength and quality of construction. The rebound hammer was used to assess the

compressive strength of concrete structural members, wherever access is provided in reinforced concrete structure. If reinforcement details are available, a limited amount of exposure of critical reinforcement is needed to verify conformity to the plans/structural details. If the plans are not available, the quality of reinforcement is assessed by exposing reinforcement to a limited extent.

The Rapid Visual Screening Procedure (RVSP) is aimed to identify potentially hazardous buildings in the study area, without going into detailed analysis. RVSP utilizes a methodology based on visual inspection of a building and noting the structural configuration. The methodology begins with identifying the primary structural lateral load resisting system and materials of the building. The method generates a Structural Score 'S', which consists of a series of 'scores' and modifiers based on building attributes that can be seen during detailed survey. The Structural Score 'S' is related to probability of the building sustaining life-threatening damage in the event of occurrence of a severe earthquake in the region. A low S score suggests that the building is vulnerable and needs detailed analysis, whereas a high 'S' score indicates that the building is probably adequate. RVSP helps in developing a list of potentially hazardous buildings without a high cost of detailed analysis of each building.

The sample survey was carried out for about 4500 buildings spread over 60 wards of Guwahati municipal area, out of which about 5% are of Type A, 15 % are of Type B and 80% are of Type-C.

8.9 QUANTITATIVE APPROACH – DEMAND CAPACITY RATIO

For quantitative approach, DCR computation has been used for mainly Type C buildings and later it is related with the possible failure modes. Few Type B buildings were taken up for DCR analysis to understand the vulnerability of typical masonry structure existing in the area.

8.10 QUANTITATIVE SEISMIC VULNERABILITY OF MASONRY BUILDINGS

Since earthquake is a random process, all the load bearing walls in a structure are to be evaluated for their shear resistance. The demand placed by an earthquake i.e. lateral forces at various levels, as per IS:1893-2002, along with gravity load calculations were carried out for sample buildings, and later check in terms of Demand Capacity ratio (DCR) for shear resistance, combined stress, overturning, and stability of non-structural failures for long and short walls. The capacity of wall is defined as its allowable stress depending upon mortar type in accordance with the relevant codal provisions. The DCR greater than unity, indicates that the building is seismically vulnerable in respective criterion, whereas DCR less than one implies the building to be safe under earthquake loads. As indicated earlier, earthquake demands for better shear resistance and hence the DCR in shear should be less than one, otherwise the building will have diagonal (X) cracking. The DCR greater than one for combined stresses means that the building is not even designed for gravity loads and would lead to collapse on seismic shaking. The failures in overturning corroborate falling of walls. The check for non-structural element implies the falling hazard of parapet wall. The above analogy has been used to estimate seismic vulnerability in terms of various failure modes i.e. collapse, excessive cracking, falling of walls including parapet walls. The city of Guwahati fortunately does not have many load bearing structures, and the only area where such structures are located are the NF Railway colony, where all the official residences are on load bearing wall structure ranging from one to even three stories.

8.11 QUANTITATIVE SEISMIC VULNERABILITY OF RC BUILDINGS

In order to critically evaluate the RC framed buildings, selected building sample were modeled using sophisticated structural analysis software under combination of earthquakes and other wards for computing the member end forces in each structural member. Apart from the dead and live loads, the structure is analyzed for design basis earthquake (DBE) loads, the earthquake loads which can reasonably be expected to occur at least once during the lifetime of the structure. Accordingly dead load, live load and their combination as suggested in IS-1893-2002 have

been considered for analysis. The analysis directly computes member end forces and then each member is designed for worst load combination. The design module of analysis engine gives the longitudinal and transverse reinforcement for each member. This reinforcement corresponds to the demand of a member due to earthquake forces, whereas the actual reinforcement provided in a particular member would correspond to capacity. In order to calculate the DCRs, the calculated reinforcement of structural members has been compared with provided reinforcement. The DCRs for longitudinal and transverse reinforcement reflect DCRs for flexure and shear of member. The DCRs calculated for flexure and shear give the idea about inherent ductility and strength of member to ensure safety & serviceability during severe shocks.

The DCR greater than one for flexure indicates that the longitudinal reinforcement in columns & beams are inadequate leading to failure. The possibility of failure of such buildings is excessive cracking leading to collapse. Whereas DCR greater than one in shear indicates that the lateral ties provided are not sufficient leading to brittle failures i.e. catastrophic failure. In this case, there is possibility of diagonal cracking in structural elements. The check for non-structural element implies the falling hazard of parapet wall. Based upon above analogy, DCRs for flexure, shear and non-structural members leading to estimate seismic vulnerability in terms of failure modes i.e. excessive cracking, diagonal cracking and falling hazard respectively for few representative RC buildings have been computed.

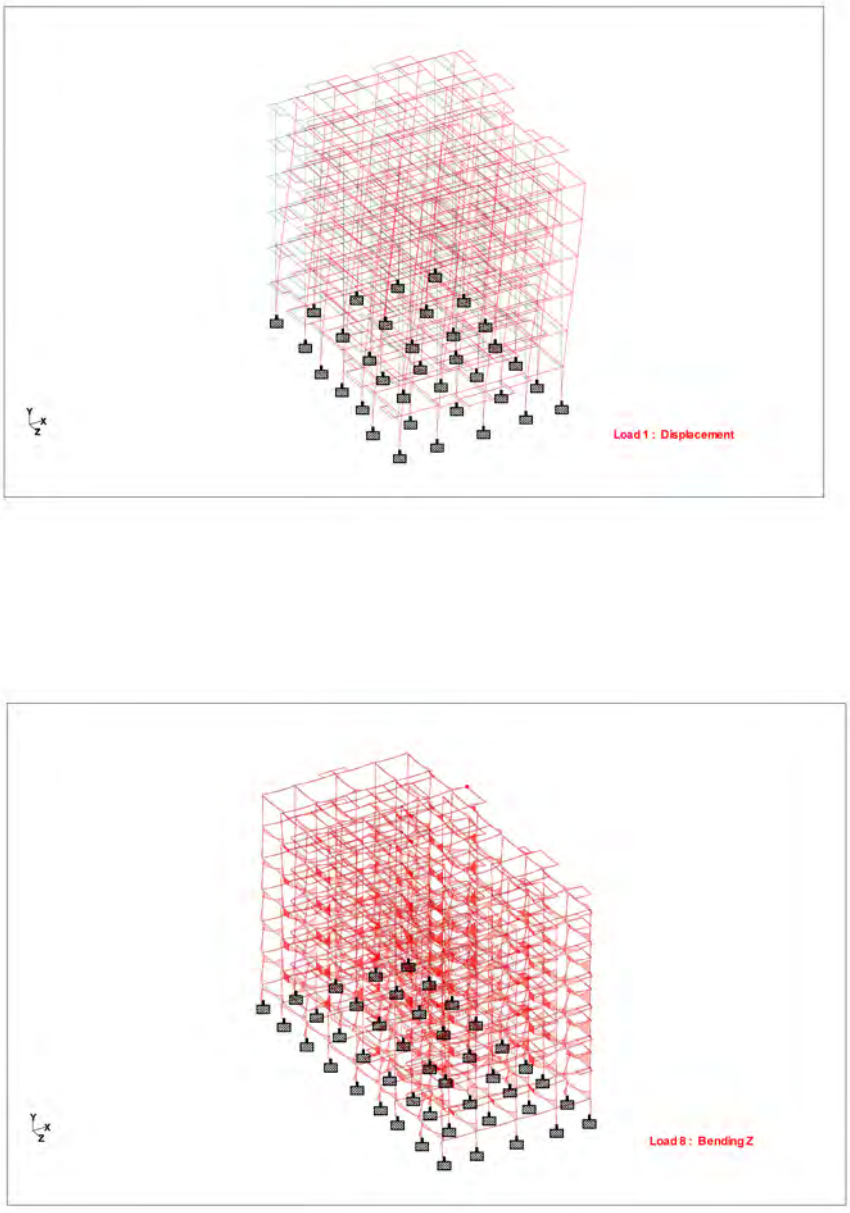

Figure 8.6 DCR ANALYSIS - Few TYPE-C Buildings (Carried out for 25 buildings)

8.12 PROGNOSTIC DAMAGE SCENARIO OF GUWAHATI URBAN AREA – ONGOING

The prognostic damage scenario of a ward reflects the structural and non-structural damages induced in the existing building stocks. The damage scenario of a ward given here is based on representative building surveyed for different building typologies and not final and conclusive. It would require the inputs from all the working subgroups to finally project prognostic damage scenario.

Based on the survey and analysis of data, the seismic vulnerability of Guwahati urban area obtained through qualitative approach. It is found that Type-A, Type-B & Type-C buildings are 10%, 40%, & 30% vulnerable respectively from engineering (design and construction) perpectives.

In order to present the prognostic damage scenario for Guwahati urban area using quantitative approach, the failure modes of different type of buildings are being collated. All the Type-A houses are 10% vulnerable since they are built from materials, which has very low vulnerability to earthquake damage. Unlike in other parts of India – rural housing in general in northeastern are very light and devoid of use of load bearing walls and stones. The roofing is very light rendering them very safe against earthquake. For Type-B buildings, the postulated failure modes have been categorized as Excessive Cracking (EC); Falling of Walls (FW); Falling Hazard of non-structural members (FH); and combination thereof - Excessive Cracking + Falling of Wall (EC+FW); Excessive Cracking + Falling Hazard (EC+FH); Falling of Wall + Falling Hazard (FW + FH); Excessive Cracking + Falling of Wall + Falling Hazard (EC + FW + FH); and safe buildings (which do not have any failure). At the first instance, ward wise seismic vulnerability is being derived, and later the ensemble is projected to present prognostic damage scenario for Guwahati urban area. Similarly, the various failure modes for assessing seismic vulnerability of Type-C buildings are identified as excessive cracking (EC), diagonal cracking (DC); falling hazard of non-structural members (FH); and combination thereof and safe buildings. The prognostic damage scenario for Type-C buildings in Guwahati urban area also being worked out and mapped to present Prognostic Seismic Vulnerability Map of Buildings in Guwahati. The vulnerability map can be effectively used to project the risk associated with existing building stock in Guwahati Urban area. Further, these

maps may act as guidance for future planning, risk reduction and disaster mitigation and management. The Prognostic Seismic Vulnerability Map needs to be concurrently and continuously updated with the availability of more geo-scientific and engineering data.

CHAPTER 9

Concluding Remarks

The seismic ground motion hazard mapped in the Guwahati Region is microzoned with local and regional site conditions incorporated through GIS. The process of overlaying, union and finally integration of various geomorphological and seismological thematic maps are complicated spatial operations that are optimally performed on GIS environment. The union of geological and geomorphological units, landuse, landslide hazard and basement zonation provide the background site condition of the Guwahati Region on which the seismological (site response, predominant frequency, peak ground acceleration) and geotechnical (V_s^{30} and Factor of Safety) attributes are overlaid.

The seismicity analysis of northeast India has been performed and the entire northeast is classified into four source zones namely zone 1 (Himalayan source), Zone 2 (Mishmi block), Zone 3 (Eastern Boundary Thrust Zone) and Zone 4 (Shillong plateau). Each has a potential of generating a great earthquake of magnitude greater than eight and that can devastate the entire region. An examination of the spatial distributions reveals relatively higher b values on the upper Tibet-Himalayan area. Low values are seen in the thrust zones especially in the Central Eastern Boundary Zone of Arakan Yoma Range indicating high stress buildup in the zone. The historical Shillong earthquake of Mw 8.7 is employed as the scenario earthquake. The presented Seismic Microzonation of Guwahati region is, therefore, a seismic scenario for an earthquake magnitude Mw 8.7 that represents a near source which may nucleate from the focus of the 1897 Great Shillong Earthquake historically known for its catastrophic effect. The Microzonation map given in Figure 6.3 obtained by integrating geological and seismological themes presents five hazard zones namely very low with the average hazard level 0.16, low with average hazard level 0.26, moderate with average hazard

level of 0.35, high with hazard level 0.44 and very high having hazard level greater than 0.55.

Very high hazard zone comes under the site class IIIA where average shear wave velocity (V_s^{30}) is 228m/s with site amplification is larger than 5.5 and average predominant frequency is 1.15Hz. Surface geology of this zone is predominantly active flood plain with pediment, Sonapur surface and some patches of Bordang surface. In this zone PGA level is very high and greater than 0.81g. Western part of Guwahati region comes under this zone that covers the area namely Bhattapara, Garal, Bulla, Singibari, Azpa, Baharbari, Khanapara etc.

High hazard zone comes under site class IIIB where average shear wave velocity (V_s^{30}) is 260m/s and average predominant frequency is 2.93Hz with average site amplification of 4.81. Here the surface geology of this zone is predominantly Sonapur surface, water bodies and pediments. Average PGA level in the zone is 0.52g. This zone resemble the very high hazard zone and it covers area like Lachitpur, Teteliya, Mirzapur, Dekapara etc. Guwahati airport incidentally falls within the high hazard zone.

Moderate hazard zone comes under site class IIIC with average shear wave velocity (V_s^{30}) is 296m/s. Surface geological feature of the zone is predominantly Bordang surface with average site amplification of 3.1. Average predominant frequency and PGA are 5.41Hz and 0.38g respectively. Moderate hazard zone covers the entire Bordang surface and its habitants like Dispur, Gopinath Nagar, Rehabari, Shantipur, Chatribari with important installations namely AMTRON, BSNL, Guwahati University and Irrigation department.

Low and very low hazard zone are under site class IIID which is almost covered by Hillocks. Average shear wave velocity in the zone is 340m/s while average predominant frequency is 7.1 Hz. This zone has very low PGA level of 0.11g with low site amplification of the value less than 1.5. This hazard zone encompasses the region near eastern flank of Brahmaputra River, in the periphery of hills like Fatasil hill, Kalapahar hill and some area in the eastern part of the region.

A preliminary seismic population risk map is prepared by integrating microzonation and demographic distribution of region assigning equal weightage to both of the themes. High risk zone covers the area namely Baharbari, Garigaon, Sadilapur, Dawapara, Pubargaon etc. some part of Fatasil hill comes under high risk zone because of higher demography distribution. Maximum part of the urban centre are under moderate risk zone like area near Kalapahar hills, Assam state guest house, Ganeshpara, Odalbakra, Rehabari with important installations namely BSNL, AMTRON, Guwahati University and Irrigation Department.

The hazard and risk map presented here may be useful for land use planning and making hazard mitigation decisions. This map is generally better spatial representation of seismic hazard including site specific analysis, and may be used for recognizing hazardous areas at regional scale. The geologic site condition map is an initial model to describe areas that may exhibit different seismic shaking characteristics during future earthquakes.

Bibliography

Abrahamson, N.A., and W.J. Silva (1997), Empirical response spectral attenuation relations for shallow crustal earthquakes, *Seism. Res. Lett*., *69*, 94-127.

Acharyya, S.K., and K.K. Ray (1977), Geology of Darjeeling Sikkim Himalaya: Guide to Excursion No. 4, *4th International Gondwana Symposium*, New Delhi, 1-25.

Agrawal, S.K., and C. Ajay (2004), Estimation of Seismic Vulnerability of Buildings in Delhi, *World Congress on Natural Disaster Mitigation*, Institution of Engineers (I), Kolkata.

Aki, K. (1965), Maximum likelihood estimate of b in the formula log N = a - bM and its confidence limits, *Bull. Earthq. Res. Inst. Tokyo Univ.*, *43*, 237-239.

Aki, K. (1969), Analysis of the seismic coda of local earthquakes as scattered waves, *J. Geophys. Res.*, *74*, 615-631.

Aki, K. (1988), Local site effects on strong ground motion, *Earthquake Engineering and Soil Dynamics II – Recent Advances in Ground Motion Evaluation*, June 27-30, Park City, Utah.

Aki, K. (1993), Local site effects on weak and strong ground motion, *Tectonophysics*, 218, 93-111.

Aki, K., and B. Chouet (1975), Origin of coda waves: Source, attenuation and scattering effects, *J. Geophys. Res.*, *80*, 3322-3342.

Aki, K., and K. Irikura (1991), Characterization and mapping of earthquake shaking for seismic zonation, *Proc. 4th Intern. Conf. Seismic Zonation,* EERI, Oakland, *1*, 61-110.

Albarello, D. (2001), Detection of spurious maxima in the site amplification characteristics estimated by the HVSR technique, *Bull. Seism. Soc. Am*., *91*, 2001, 718-724.

Algermissen, S.T., and D.M. Perkins (1976), A probabilistic estimate of maximum acceleration in rock in the contiguous United States, *U.S. Geol. Surv. Open-file Report,* 76–416, p. 45.

Alvarez, L., F. Vaccari, and G.F. Panza (1999), Deterministic seismic zoning of eastern Cuba, *Pure Appl. Geophys.*, *156*, 469–486.

Ambraseys, N.N. (1995), The prediction of earthquake peak ground acceleration in Europe, *Earthq. Eng. Struct. Dyn.*, *24*, 467-490.

Ambraseys, N.N. (2001), The earthquake of 10 July 1894 in the Gulf of Izmit (Turkey) and its relation to the earthquake of 17 August 1999, *J. Seismol.*, *5*, 117-128.

Ambraseys, N.N., and C.F. Finkel (1995), The Seismicity of Turkey and Adjacent Areas, *EREN*, Istanbul, p. 240.

Ambraseys, N.N., and C.P. Melville (1982), *A history of Persian Earthquakes*, C*ambridge Earth Science Series*, Cambridge, U.K.

Ambraseys, N., and R. Bilham (2000), A note on the Kangra Ms=7.8 earthquake of 4 April 1905., *Curr. Sci.*, *79*, 101-106.

Ambraseys, N.N., K.A. Simpson, and J.J. Bommer (1996), The Prediction of Horizontal Response Spectra in Europe, *Earthq. Eng. Struct. Dyn., 25*, 371-400.

Anderson, D.L., A. Ben-Menahem, and C.B. Archambeau (1965), Attenuation of seismic energy in the upper mantle, *J. Geophys. Res*., *70*, 1441-1448.

Anderson, J.G., and J. E. Luco (1983), Parametric study of near-field ground motions for oblique-slip and dip-slip dislocation models, *Bull. Seism. Soc. Am*., *73*, 45-57.

Anderson, J.G., P. Bodin, J. N. Brune, J. Prince, S.K. Singh, R. Quaas, and M. Onate (1986), Strong ground motion from the Michoacan, Mexico, earthquake, *Science, 233*, 1043-1049.

Andrews, D.J. (1986), Objective determination of source parameters and similarity of earthquakes of different size, *Earthquake Source Mechanics*, S. Das, J. Boatwright, and C.H. Scholz (Eds.), AGU, Washington D.C., 259-268.

Ansary, M.A., E. Yamazaki, and T. Katayama (1995), Statistical analysis of peak and directivity of earthquake ground motion, *Earthq. Eng. Struct. Dyn., 24,* 1527-1539.

Aoudia, A., F. Vaccari, P. Suhadolc, and M. Meghraoui (2000), Seismogenic potential and earthquake hazard assessment in the Tell Atlas of Algeria, *J. Seismol., 4*, 79-98.

Atakan, K., and J. Havskov (1996), Local site effects in the northern North Sea based on single-station spectral ratios of OBS recordings, *Terra Nova, 8*, 22-33.

Atakan, K., B. Brandsdottir, P. Halldorsson, and G. O. Fridleifsson (1997), Site response as a function of near-surface geology in the south Iceland seismic zone, *Nat. Haz., 15*, 139-164.

ATC-21 (1988), *Rapid Visual Screening of Buildings for Potential Seismic Hazards: A Handbook*, Applied Technology Council, Redwood city, CA, USA.

ATC-40 (1996), *Seismic Evaluation and Retrofit of Concrete Buildings, Vol. 1*, Applied Technology Council, Redwood city, CA, USA.

Athanasopoulos, G.A., P.C. Pelekis, and E.A. Leonidou (1999), Effects of surface topography on seismic ground response in the Egion (Greece) 15 June 1995 earthquake, *Soil Dyn. Earthq. Eng.*, *18*, 135-149.

Atkinson, G.M., and D.M. Boore (1995), New ground motion relations for eastern North America, *Bull. Seis. Soc. Am.*, *85*, 17-30.

Atkinson, G.M., and D.M. Boore (1997), Some comparisons between recent ground motion relations, *Seis. Res. Lett*., 68, 24-40.

Auden, J.B. (1959), Earthquakes in relation to the Damodar Valley Project, *Proc. 1st Symp. Earthq. Eng.* University of Roorkee, Roorkee.

Aviles, C.A., C.H. Scholz, and J. Boatwright (1987), Fractal Analysis applied to Characteristic segments of the San Andreas fault, *J. Geophys. Res*., *92*, 331-344.

Aviles, J., and L.E. Perez-Rocha (1998), Site effects and soil-structure interaction in the Valley of Mexico, *Soil Dyn. Earthq. Eng.*, *17*, 29-39.

Avouac, J., and P. Tapponnier (1993), Kinetic model of active deformation in central Asia, *Geophys. Res. Lett*., *20*, 895-898.

Bakir, S, H. Sucuoglu, and T. Yilmaz (2002), An overview of local site effects and the associated building damage in Adapazari during the 17 August 1999 Izmit earthquake, *Bull. Seis. Soc. Am*., *91*, 509-526.

Balassanian, S.Y., A.H. Martirosyan, S.N. Nazaretian, A.R. Arakelian, A.S. Avanessian V.A. Igumnov, and E. Ruttener (1998), Seismic Hazard Assessment in Armenia, *Nat. Haz., 18*, 227-236.

Banerjee S.K. (1957), Earthquakes in the Himalayan Region, *Ind. Assoc. for the Cultivation of Sci.*, Calcutta.

Bapat, A., R.C. Kulkarni, and S.K. Guha (1983), *Catalogue of earthquakes in India and neighbourhood from historical period up to 1979*, Indian Soc. Earthq. Tech., Roorkee, India.

Bard, P.Y. (1994), Effects of surface geology on ground motion: recent results and remaining issues, *Proc. 10th Europ. Conf. on Earthq. Eng.,* G. Duma (Ed.), Vienna, 305–323.

Bard, P.Y. (1997), Local effects on strong ground motion: basic physical phenomena and estimation methods for microzoning studies, *SERINA-Seismic Risk: An Integrated Seismological, Geotechnical and Structural Approach,* ITSAK (Ed.), Thessaloniki.

Bard, P.Y. (2000), Local effects on strong ground motion: Basic physical phenomena and estimation methods for microzonation studies, *Lecture notes*.

Bard, P.Y., and F.J. Chávez-García (1993), On the decoupling of surficial sediments from surrounding geology at Mexico City, *Bull. Seism. Soc. Am*., *83*, 1979-1991.

Bath, M., and S.J. Duda (1964), Earthquake volume, Fault plane area, seismic energy, strain, deformation and related quantities, *Ann. Geofis., 17*, 353-368.

Ben-Menahem, A., E Aboodi, and R. Schild (1974), Source of the Great Assam Earthquake and Interplate Wedge Motion, *Phys. Earth and Planet. Int.*, *9*, 265-289.

Beresnev, I.A., K.L. Wen, and Y.T. Yeh (1995), Seismological evidence for nonlinear elastic ground behavior during large earthquakes, *Soil Dyn. Earthq. Eng.*, *14*, 103-114.

Berge-Thierry, C., P. Bernard, and A. Herrero (2001), Simulating strong ground motion with the ‘k’ kinematic source model: An application to the seismic hazard in the Erzincan basin, Turkey, *J. Seismol.*, *5*, 85-101.

Bhatia, S.C., M.R. Kumar, and H.K. Gupta (1999), A probabilistic seismic hazard map of India and adjoining regions, *Ann. Geofis.*, *42*, 1153–1164.

Bhattacharya, P.M., and Kayal, J.R. (2003), Mapping the b-value and its correlation with the fractal dimension in the Northeast region of India, *J. Geol. Soc. Ind.*, *62*, 680–695.

Bilham, R. (1995), Location and magnitude of the 1833 Nepal earthquake and its relation to the rupture zones of contiguous Great Himalayan Earthquakes, *Curr. Sci., 69*, 155-187.

Bilham, R. (1998), Slip parameters for the Rann of Kachchh, India, 16 June 1819, earthquake, quantified from contemporary accounts, *Coastal Tectonics,* I. S. Stewart and C. Vita-Finzi (Eds.), *146*, 295-318

Bilham, R., and P. England (2001), Plateau pop-up during the Great 1897 Assam earthquake, *Nature*, *410*, 806-809.

Bilham, R., and V.K. Gaur (2000), The geodetic contribution to the study of seismotectonics in India, *Curr. Sci.*, *79*, 1259-1269.

Bilham, R., F. Blume, R. Bendick, and V.K. Gaur (1998), The geodetic constraints on the translation and deformation of India: implications for future great Himalayan earthquakes, *Curr. Sci.*, *74*, 213-229.

Bilham, R., R. Bendick, and K. Wallace, (2003), Flexure of the Indian Plate and intraplate earthquakes, *Proc. Indian Acad. Sci. (Earth Planet Sci.)*,*112*,1-14 .

Bilham, R., V.K. Gaur, and P. Molnar (2001), Himalayan Seismic Hazard, *Science*, *293*, 1442-1444.

BIS (1993a), IS:1920-1993: *Ductility Detailing of Reinforced Concrete Structures Subjected to Seismic Forces-Code of Practice*, Bureau of Indian Standards, New Delhi.

BIS (1993b), IS:4326-1993: *Code of Practice for Earthquake Resistant and Construction of Buildings*, Bureau of Indian Standards, New Delhi.

BIS (2002), IS:1893-2002: *Criteria for Earthquake Resistant Design of Structure*, Bureau of Indian Standards, New Delhi.

Boatwright, J. (1978), Detailed spectral analysis of two small New York State earthquakes, *Bull. Seism. Soc. Am.*, *68*, 1117-1131.

Boatwright, J., L.C. Seekins, T.E. Fumal, Liu Hsi-Ping, and C.S. Mueller (1991a), Ground motion amplification in the Marina district, *Bull. Seism. Soc. Am*., *81*, 1980-1997.

Boatwright, J., J.B. Fletcher, and T.E. Fumal (1991b), A general inversion scheme for source, site and propagation characteristics using multiply recorded sets of moderate-sized earthquakes, *Bull. Seism. Soc. Am.*, *81*, 1754-1782.

Bolt, B.A. (1993), *Earthquake and Geological discovery*, Scientific American Library, New York.

Bommer, J.J. (2003), Uncertainty about the Uncertainty in Seismic Hazard Analysis, *Eng. Geol., 70*, 165-168.

Boore, D.M., W.B. Joyner, and T.E. Fumal (1997), Equations for estimating horizontal response spectra and peak acceleration from western North American earthquakes: A summary of recent work, *Seism. Res. Lett., 68*, 128-153.

Boore, D.M. (1972), A Note on the Effect of Simple Topography on Seismic SH Waves, *Bull. Seism. Soc. Am*., *62*, 275-284.

Boore, D.M. (1973), The Pacoima Dam accelerogram of the February 9, 1971, San Fernando earthquake implications of local site topography, *Bull. Seism. Soc. Am.*, *63*, 1603-1609.

Boore, D.M. (2003), A compendium of *P*- and *S*-wave velocities from surface-to-borehole logging: summary and reanalysis of previously published data and analysis of unpublished data, *U. S. Geol. Surv. Open-File Rept. 03-191*, p.13, http://quake.usgs.gov/_boore.

Boore, D.M., W.B. Joyner, and T.E. Fumal (1993), Estimation of response spectra and peak ground accelerations from western North America earthquakes: an interim report, *U. S. Geol. Surv. Open-File report*, 93-509.

Boore, D.M., W.B. Joyner, and T.E. Fumal (1994), Estimation of response spectra and peak ground accelerations from western North America earthquakes: an interim report, part 2, *U. S. Geol. Surv. Open-File report*, 94-127.

Borcherdt, R.D. (1970), Effects of local geology on ground motion near San Francisco Bay, *Bull. Seism. Soc. Am*., *60*, 29-61.

Borcherdt, R.D. (1994), Estimates of site-dependent response spectra for design (methodology and justification), *Earthq. Spectra* ,*10*, 617-653.

Borcherdt, R.D., and G. Glassmoyer (1992), On the characteristics of local geology and their influence on ground motions generated by the Loma Prieta earthquake in the San Francisco Bay region, California, *Bull. Seism. Soc. Am.*, *82*, 603-641.

Borcherdt, R.D., G. Glassmoyer, A. Der Kiureghian, and E. Cranswick (1989), Results and data from seismologic and geologic studies following earthquakes of December 7, 1988 near Spitak, Armenia, S.S.R., *US Geol. Surv. Open-File Rept*., 89-163.

Bordet, P. (1973), On the position of the Himalayan Main Central Thrust within Nepal Himalayas, paper presented in Seminar on Geodynamics of the Himalayan Region, Hyderabad, 140-155.

Bouchon, M., and J. S. Barker (1996), Seismic response of a hill: The Example of Tarzana, California, *Bull. Seism. Soc. Am.*, *86*, 66-72.

Bouckovalas, G.D. and G.P. Kouretzis (2001), Stiff soil amplification effects in the 7 September 1999 Athens (Greece) earthquake, *Soil Dyn. Earthq. Eng., 21*, 671-687.

Boughacha, M.S., M. Ouyed, A. Ayadi, and H. Benhallou (2004), Seismicity and seismic hazard mapping of northern Algeria: Map of Maximum Calculated Intensities (MCI), *J. Seismol., 8*, 1-10.

Bouhadad, Y., and N. Laouami (2002), Earthquake Hazard Assessment in the Oran Region (Northwest Algeria), *Nat. Haz., 26*, 227-243.

Brune, J.N. (1970), Tectonic Stress and the spectra of seismic shear waves from earthquakes, *J. Geophys. Res*., *75*, 4997-5009.

Bullore M.D. (1904), The Seismic Phenomena in British India and Their Correction with Its Geology, *Mem. Geol. Surv. Ind.,* p. 3.

Bune, V.I., N.A. Vvedenskaya, I.V. Gorbunova, N.V. Kondorskaya, N.S. Landyreva, and I.V. Fedorova (1970), Correlation of MLH and mpv by Data of the Network of Seismic Stations of the USSR, *Geophy. J. Int.*, *19*, 533–542.

Burrough, P.A. (1986), *Principles of Geographical Information Systems for Land Resources Assessment*, Glarendon Press, Oxford, UK, p. 194.

Burrough, P.A., and R.A. Mcdonnell (1998), *Principles of geographic information system,* Oxford University Press, New York, USA, p. 333.

Bus, Z., G. Szeidovitz, and F. Vaccari (2000), Synthetic seismograms based deterministic seismic zoning for the Hungarian Part of the Pannonian Basin, *Pure Appl. Geophys.*, *157*, 205–220.

Campbell, K.W. (1981), Near-source attenuation of peak horizontal accelerations, *Bull. Seism. Soc. Am*., *71*, 2039-2070.

Campbell, K.W. (1988), Predicting strong ground motion in Utah. *Evaluation of Regional and Urban Earthquake Hazard Risks in Utah*, W. W. Hays and P. L. Gori (Eds.), *US Geol. Surv. Profess. Pap.*, L1-L31.

Campbell, K.W. (1989), The dependence of peak horizontal acceleration on magnitude, distance and site effects for small-magnitude earthquakes in California and eastern North America, *Bull. Seism. Soc. Am., 79*, 1311-1346.

Campbell, K.W. (1990), Empirical prediction of near-source soil and soft-rock ground motion for the Diablo Canyon power plant site, San Luis Obispo County, California, *Report Prepared for Lawrence Livermore National Laboratory,* Dames and Moore, Evergreen, Colorado.

Campbell, K.W. (1992), *Recommended models for predicting strong ground motion and MMI in the San Francisco bay area*, Report Prepared for EQE International, Dames and Moore, Evergreen, Colorado.

Campbell, K.W. (1993), Empirical prediction of near-source ground motion from large earthquakes, *Proceedings, International Workshop on Earthquake Hazard and Large Dames in the Himalaya, Jan, 15-16, 1993, New Delhi*, V.K. Gaur (Ed.), The Indian National Trust for Art and Cultural Heritage (INTACH), New Delhi, 93-103.

Campbell, K.W. (1997), Empirical near-source attenuation relationships for horizontal and vertical components of peak ground acceleration, peak ground velocity and Pseudo-absolute acceleration response spectra, *Seism. Res. Lett., 68*, 154-177.

Campbell, K.W. (2003), Prediction of Strong Ground Motion using the Hybrid Empirical Method and its use in the development of Ground-Motion (Attenuation) relations in eastern North America, *Bull. Seism. Soc. Am., 93*, 1012-1033.

Campbell, K.W., and Y. Bozorgnia (2003), Updated Near-Source Ground-Motion (Attenuation) Relations for the Horizontal and Vertical Components of Peak Ground Acceleration and Acceleration Response Spectra, *Bull. Seism. Soc. Am., 93*, 314-331.

Caserta, A., F. Bellucci, G. Cultrera, S. Donati, F. Marra, G. Mele, B. Palombo, and A. Rovelli (2000), Study of site effects in the area of Nocera Umbra (Central Italy) during the 1997 Umbria-Marche seismic sequence, *J. Seismol.*, *4*, 555-565.

Castro, R.R., F. Pacor, A. Sala, and C. Petrungaro (1996), S-wave attenuation and site effects in the region of Friuli, Italy, *J. Geophys. Res., 101*, 22355-22369.

Castro, R.R., J.G. Anderson, and S.K. Singh (1990), Site response, attenuation and source spectra of S-waves along the Guerrero, Mexico, subduction zone, *Bull. Seism. Soc. Am.*, *80*, 1481-1503.

Castro, R.R., M. Mucciarelli, F. Pacor, and C. Petrungaro (1997), S-wave site-response estimates using horizontal-to-vertical spectral ratios, *Bull. Seism. Soc. Am.*, *87*, 256-260.

Chandler, A.M., L.S. Chan, and N.T.K. Lam (2001), Deterministic seismic hazard parameters and engineering risk implications for the Hong Kong region, *J. Asian Earth Sci., 20*, 59-72.

Chandra, U. (1980), Attenuation of intensities in India, *Proc. 7th WCEE*, *2*, 521-524, Istanbul, Turkey.

Chauhury H.M., and H.N. Srivastava (1976), Seismicity and Focal Mechanism of Some Recent Earthquakes in Northeast India, *Ann. Geoph.*, 29-41.

Chavez-García, F.J., L.R. Sanchez, and D. Hatzfeld (1996), Topographic site effects and HSVR: A comparison between observations and theory, *Bull. Seism. Soc. Am.*, *86*, 1559–1573.

Chen, W.F., and C. Scawthorn (2003), *Earthquake Engineering Handbook*, CRC Press.

Chin, B., and K. Aki (1991), Simultaneous study of the Source, Path and Site effects on strong ground motion during the 1989 Loma Prieta earthquake: A preliminary result on pervasive nonlinear site effects, *Bull. Seism. Soc. Am.*, *81*, 1859-1884.

Coppersmith, K.J. (1991), Seismic Source Characterization for Engineering Seismic Hazard Analysis, *Proc. of the 4th International Conference on Seismic Zonation*, *vol. 1*, August 25-29, 1991, EERI, Oakland, CA, 3-60.

Coppersmith, K.J., P.C. Thenhaus, J.E. Ebel, W.K. Wedge, J.H. Williams, and N.C. Hester (1993), Regional Seismotectonic Settings, Seismic Hazard Assessment in the central and eastern United states, *Monograph 1: Hazard Assessment*, S.T. Algermissen and G.A Bollinger (Eds.), Central United States Earthquake Consortium, Memphis, TN, 35-80.

Cornell, C.A. (1968), Engineering Seismic Risk Analysis, *Bull. Seism. Soc. Am*., *58*, 1583-1606.

Costa, G., G.F. Panza, P. Suhadolc, and F. Vaccari (1993), Zoning of the Italian territory in terms of expected peak ground acceleration derived from complete synthetic seismograms, *Geophysical Exploration in Areas of Complex Geology,* R. Cassinis, K. Helbig, and G.F. Panza (Eds.), *J. Appl. Geophys.*, *30*, 149–160.

Crouse, C.B. (1991a), Ground-motion attenuation equations for earthquakes on the Cascadia subduction zone, *Earthq. Spectra*, *7*, 201-235.

Crouse, C.B. (1991b), Erratum: Ground-motion attenuation equations for earthquakes on the Cascadia subduction zone, *Earthq. Spectra, 7*, 506.

Curry, J.R., D.G. Moore, L.A. Lawver, F.J. Emmel, R.W. Raitt, M. Henry, and R. Kieckhefer (1979), Tectonics of the Andaman Sea and Burma, *Am. Assoc. Petr. Geol. Mem*., *29*, 189-198.

Dahle, A., H. Bungum, and L.G. Dvamme (1990), Attenuation models inferred from intraplate earthquake recordings, *Earthq. Eng. Struct. Dyn.*, *19*, 1125-1141.

Davis, B.E. (1996), *Geographic Information Systems: A Visual Approach*. OnWord Press, Albany, New York, p. 400.

De, R. (2000), A microearthquake survey in the Himalayan Foredeep region, Sikkim Himalaya, *J. Geophys.*, *XXI*, 1-8.

De, R., and J.R. Kayal (2003), Seismotectonic Model of the Sikkim Himalaya: Constraint from microearthquake surveys, *Bull. Seism. Soc. Am., 91*, 1395-1400.

DeMets, C., R.G. Gordon, D.F. Argus, and S. Stein (1994), Effect of recent version to the geomagnetism reversal time scale on estimates of current plate motions, *Geophys. Res. Lett*., *21*, 2191-2194.

Downes, G.L. (1995), Atlas of Isoseismal Maps of New Zealand Earthquakes, Institute of Geological and Nuclear Sciences, Lower Hutt.

Duan, B., D.D. Oglesby and S.K. Park (2003), A new optimization scheme for site response estimation, *Geophys. Res. Abstracts, 5*, p. 11296.

Dutta, T.K. (1964), Seismicity of Assam - Zones of Tectonic Activity, *Bull. N.G.R.I.*, *2*, p.152.

Dutta, T.K. (1967), Seismicity of Assam in Relation to Geotectonic Processes - Nature of Instability of the Assam Wedge. *Bull. Int. Inst. Seis. and Earth. Eng.*, *4*, p. 63.

Dutta, T.K., and M.M. Saikia (1976) The Eastern Limit of the Himalayan Orogenic Belt - the Indo-Burman Orogen and its Geodynamic Development. Himalayan Geology, *6*, p. 303.

Dutta, U., N. Biswas, A. Martirosyan, A. Papageorgiou, and S. Kinoshita (2003), Estimation of earthquake source parameters and site response in Anchorage, Alaska from strong-motion network data using generalized inversion method, *Phys. Earth Planet. Inter.*, *137*, 13-29.

Dutta, U., N. Biswas, A. Martirosyan, S.K. Nath, M. Dravinski, A. Papageorgiou, and R. Combellick (2000), Delineation of spatial variation of shear wave velocity with high-frequency Rayleigh waves in Anchorage, Alaska, *Geophys. J. Int.*, *143*, 365-375.

Duval, A.M., J.P, Meneroud, S. Vidal, and P.Y. Bard (1995), Usefulness of microtremor measurements for site effect studies, *Proc. 10th Euro. Conf. on Earthq. Engn.*, Duma (Ed.), Rotterdam, 521-527.

EERI (1994)*, Northridge earthquake, January 17, 1994, Preliminary reconnaissance report,* Earthquake Engineering Research Institute, Oakland, Calif*.*

EERI (1995), *The Hyogo-ken Nanbu Earthquake January 17, 1995 Preliminary Reconnaissance Report*, Earthquake Engineering Research Institute, Oakland, Calif.

El-Sayed, A., F. Vaccari, and G.F. Panza (2001), Deterministic seismic hazard in Egypt, *Geophys. J. Int.*, *144*, 555-567.

Epstein B., and C. Lomnitz (1966), A Model for the Occurrence of Large Earthquakes, *Nature*, 211 954.

Erdik, M., Y.A. Biro, T. Onur, K. Sesetyan, and G. Birgoren (1999), Assessment of earthquake hazard in Turkey and neighboring regions, *Annali di Geofisica, 42*, 1125-1138.

Esteva, L., C. Lomnitz, and E. Rosenblueth (1958), *Seismic Risk and Engineering decision*, Elsevier, New York.

Everdeen J.F. (1970), Study of Regional Seismicity and Associated Problem, *Bull. Siesm. Soc. Am.*, *60*, 393.

Faccioli, E. (1991), Seismic amplification in the presence of geological and topographic irregularities. *Proc. 2nd Int. Conf. Recent Adv. Geotech. Earthq. Eng.Soil Dyn.*, March 11-15, St. Louis, Missouri, Ed. S. Prakash, Univ. of Missouri-Rolle, 1779-1797.

Faccioli, E. (1995), Induced Hazards: Earthquake triggered Landslides, Proc. 5th Intern. Conf. on Seismic Zonation, Nice, France, Oct. 17–19, 1908–1931.

Faccioli, E., R. Paolucci, and V. Pessina (2002), Engineering assessment of seismic hazard and long period ground motions at the Bolu Viaduct Site following the November 1999 earthquake, *J. Seism., 6*, 307-327.

Field, E.H. (1996), Earthquake site-response study in Giumri (formerly Leninakan), Armenia, using ambient noise observations, *Intern. Jour. Rock Mechanics and Mining Sciences and Geomechanics Abstracts, 33*, 122A-122A.

Field, E.H., and K.H. Jacob (1993), The theoretical response of sedimentary layers to ambient seismic noise, *Geophys. Res. Lett.*, *20*, 2925-2928.

Field, E.H., and K.H. Jacob (1995), A comparison and test of various site response estimation techniques, including three that are not reference site dependent, *Bull. Seism. Soc. Am.*, *85*, 1127 - 1143.

Field, E.H., A.C. Clement, V. Aharonian, P.A. Friberg, L. Carroll, T.O. Babaian, S.S. Karapetian, S.M. Hovanessian, and H.A. Abramian (1995a), Earthquake site-response study in Giumri (formerly Leninakan), Armenia, using ambient noise observations, *Bull. Seism. Soc. Am*., *85*, 349-353.

Field, E.H., J.G. Anderson, T.L. Henyey, D.D. Jackson, W.B. Joyner, Y. Lee, H. Magistrale, B. Minster, K.B. Olsen, J.H. Steidl, L.A. Wald, and C.J. Wills (2000), Accounting for site effects in probabilistic seismic hazard analyses of southern California: Overview of the SCEC Phase III Report, *Bull. Seism. Soc. Am., 90*, S1 - S31.

Field, E.H., K.H. Jacob, and S.E. Hough (1992), Earthquake Site Response Estimation: A weak motion case study, *Bull. Seism. Soc. Am*., *82*, 2283-2307.

Field, E.H., P.A. Johnson, I.A. Beresnev, and Y. Zeng (1997), Nonlinear ground-motion amplification by sediments during the 1994 Northridge earthquake, *Nature,* 390, 599-602.

Field, E.H., S.E. Hough, K.H. Jacob, and P.A. Friberg (1995), Site response in Oakland, California, near the failed section of the Nimitz freeway *Intern. Jour. of Rock Mechanics and Mining Sciences and Geomechanics Abstracts*, *32*, 361A-362A.

Finn, W.D. (1991), Geotechnical engineering aspects of seismic microzonation. *Proc. 4th Int. Conf. Seismic Zonation*, August 25-29, EERI, Oakland CA, 199-250.

Finn, W.D., and A.M. Nichols (1988), Seismic response of long-period sites: lessons from the September 19, 1985, Mexican earthquake, *Can. Geotech. J., 25*, 28-137.

Fitch, T.J. (1970), Earthquake Mechanism in the Himalayan, Burmese and Anadaman Regions and Continental Tectonics of Central Asia., *J. Geophys. Res.*, *75*, 2699.

Fitch, T.J. (1972), Plate convergance, transcurrent faults and internal deformation adjacent to southeast Asia and the western pacific, *Geophys. Res*., *77*, 4432-4460.

Foresman, T.W. (1997), *The History of Geographic Information Systems: Perspectives from the Pioneers*, Prentice Hall, Englewood Cliffs, New Jersey, USA, p.320

Frankel, A. (1995a), Mapping Seismic Hazard in the central and eastern United States, *Bull. Seism. Soc. Am*., *66*, 8-21.

Frankel, A. (1995b), Simulating strong motion of large earthquakes using recordings of small earthquakes: the Loma Prieta Mainshock as test case, *Bull. Seism. Soc. Am*., *85*, 1144-1160.

Frankel, A. (1996), National Seismic Hazard Maps: Documentation June 1996, *U.S. Geol. Surv. Open-File Rep*., 96-532.

Frankel, A., C. Mueller, T. Barnhard, D. Perkins, E.V. Leyendecker, N. Dickman, S. Hanson, and M. Hopper (2000), USGS National Seismic Hazard Maps, *Earthq. Spectra, 16*, 1-19.

Fukushima, Y., and T. Tanaka (1990), A new attenuation relation for peak horizontal ground acceleration of strong ground motion in Japan, *Bull. Seism. Soc. Am*., *80*, 757-783.

Fukushima, Y., and T. Tanaka (1991), A new attenuation relation for peak horizontal acceleration of strong earthquake ground motion in Japan, *Shimizu Tech. Res. Bull., 10*, 1-11.

Fukushima, Y., M. Mori, S. Matsuzaki, S. Kobayashi, and Y. Ohno (2001), Semi-empirical estimation of ground motion using observed records at a site in Shikoku, Japan, *J. Seism.*, *5*, 63-72.

Fumal, T.E., and J.C. Tinsley (1985), Mapping shear-wave velocities of near-surface geologic materials. *Evaluating Earthquake Hazards in the Los Angeles Region — An Earth-Science Perspective*, J.I. Ziony (Ed.), US Geological Survey Prof. Paper, *1360*, 127-149

Gahalaut, V.K., and R. Chander (1997), On interseismic elevation changes and strain accumulation for great thrust earthquakes in the Nepal Himalaya, *Geophys. Res. Lett*., *24*, 1011-1014.

Gansser, A. (1964), *Geology of the Himalayas*, Interscience Publ., New York, p. 289.

Gaur, V.K., and R.K.S. Chouhan (1968), Quantitative measures of seismicity applied to Indian regions, *Bull. Ind. Soc. Earthq. Tech.*, 5, 63–78.

Gayskiy, Y.N., and A.P. Katok (1965), Primeneniye te0rii ekstremalnykh znazcheniy dlya ocenki povtoryaemosti silnykh zemletryaseniy. Sb. Dinamika zemnoy kory AN SSSR, Nauka, M. 9.

Geli, L., P.Y. Bard, and B. Jullien (1988), The effect of topography on earthquake ground motion: a review and new results, *Bull. Seism. Soc. Am*., *78*, 42-63.

Gibowicz, S.J., and S. Lasocki (2001), Seismicity induced by mining: ten years later, *Adv. Geophy.*, R. Dmoska, and B. Saltzmann (Eds.), *44*, 39-181.

Gorshkov, G.P. (1961), Problems on Seismotectonics and Seismic Regionalization of the Union of Burma. *AN USSR Bull. Soy. po sejsmol.* (in Russian), *12,* p.127.

GSI (1939), The Bihar-Nepal earthquake of 1934, *Geol. Surv. India Mem.*, *7*, p. 280.

GSI (1993), Bihar-Nepal earthquake, August 20, 1988, in *Geol. Surv. India, Sp. Pub.,* D.R. Nandy, A.K. Choudhury, C. Chakraborty, and P.L. Narula (Eds.), *31*, p. 104.

GSI (2000), Seismotectonic Atlas of India and its Environs, P.L. Narula, S.K. Acharyya, and J. Banerjee (Eds.), *Geo. Surv. Ind. Spl. Pub.*, Kolkata.

Gueguen, P., J.L. Chatelain, B. Guillier, H. Yepes, and J. Egred (1998), Site effect and damage distribution in Pujili (Ecuador) after the 28 March 1996 earthquake, *Soil Dyn. Earthq. Eng.*, *17*, 329-334.

Guha, S.K. (1962), Seismic regionalization of India, *Proc. 2nd Symp. Earthq. Eng.,* Roorkee, 191–207.

Gupta, I.D., and M.D. Trifunac (1988), Attenuation of intensity with epicentral distance in India, *Soil Dyn. Earthq. Eng.*, *7*, 162-169.

Gupta, S.C., and A. Kumar (2002), Seismic wave attenuation characteristics of three Indian regions: A comparative study, *Curr. Sci.*, *82*, 407-413.

Gutenberg, B., and C.F. Richter (1944), Frequency of earthquakes in California, *Bull. Seism. Soc. Am.*, *34*, 185–188.

Gutenberg, B., and C.F. Richter (1954), *Seismicity of Earth and Associated Phenomena*, Princeton University Press, Princeton, New Jersey.

Gutierrez, C., and S.K. Singh (1992), A site effect study in Acapulco, Guerrero, Mexico: comparison of results from strong-motion and microtremor data, *Bull. Seism. Soc. Am*., *82*, 642-659.

Gyi, L.T. (1973), Seismic Zoning Map of the Union of Burma, *Bull. Int. Inst. Seis. and Earth. Eng.*, *9*, p. 218.

Hamdache, M. (1998), Seismic hazard estimation in Northern Algeria, *Nat. Haz.,18*, 1998, 119-144.

Hanks, T.C., and H. Kanamori (1979), A moment magnitude scale, *J. Geophys. Res*., *84*, 2348-2350.

Hanna, K.C., and R.B. Culpepper (1998)*, GIS and Site Design: New Tools for Design Professionals*, John Wiley & Sons Ltd., New York, USA, p. 240.

Harkrider, D.G. (1976), Potentials and Displacements for Two Theoretical Seismic Sources, *Geophy. J. R. Astr. Soc.*, *47*, 97–133.

Hartzell, S.A., A. Leeds, A. Frankel, and J. Michael (1996), Site response for urban Los Angeles using aftershocks of the Northridge earthquake, *Bull. Seism. Soc. Am.*, *86*, 168-192.

Hartzell, S.A., D. Carver, and R.A. Williams (2001), Site response, shallow shear-wave velocity and damage in Los Gatos, California, from the 1989 Loma Prieta earthquake, *Bull. Seism. Soc. Am.*, *91*, 468-478.

Hartzell, S.H. (1978), Earthquake aftershocks as Green's functions, *Geophys. Res. Lett*, *5*, 1-4.

Hartzell, S.H. (1992), Site response estimation from earthquake data, *Bull. Seism. Soc. Am.*, *82*, 2308-2327.

Haskell, N.A. (1960), Crustal reflection of plane SH waves, *J. Geophys. Res.*, *65*, 4147-4150.

Haskell, N.A. (1963), Radiation pattern of Rayleigh waves from a fault of arbitrary dip and direction of motion in a homogeneous medium, *Bull. Seis. Soc. Am.*, *53*, 619 - 642.

Haskell, N.A. (1964), Total energy and energy spectral density of elastic wave radiation from propagating faults, *Bull. Seis. Soc. Am.*, *54*, 1811-1841

Havskov, J., and L. Ottemoeller (2000), SEISAN earthquake analysis software, *Seis. Res. lett.*, *70*, 532-534.

Heaton, T.H., F. Tajimaand, and A.W. Mori (1986), Estimating ground motions using recorded accelerograms, *Surv. Geophys.*, *8*, 25-83.

Helmberger, D.V. (1968), The crust-mantle transition in the Bering Sea, *Bull. Seism. Soc. Am.*, *58*, 179-214.

Herrmann, R.B. (1978), A note on causality problems in the numerical solution of elastic wave propagation in cylindrical coordinate systems, *Bull. Seism. Soc. Am., 68*, 117-124.

Herrmann, R.B. (1979), SH wave generation by Dislocation sources-a numerical study, *Bull. Seism. Soc. Am.*, *69*, 1-15.

Herrmann, R.B., and B. Mandal (1986), A study of wavenumber integration techniques, *Earthq. Notes*, *57*, 33-40.

Herrmann, R.B., and C.Y. Wang (1985), A comparison of synthetic seismograms, *Bull. Seism. Soc. Am., 75*, 41-56.

Hohl, P. (1998), *GIS Data Conversion: Strategies, Techniques and Management*. OnWord Press, Albany, New York, p. 423.

Hong, P.N. (2001), Probabilistic Seismic Hazard Assessment along the Southeastern Coast of Vietnam, *Nat. Haz.*, *24*, 53-74.

Horike, M., B. Zhao, and H. Kawase (2001), Comparison of site response characteristics inferred from microtremors and earthquake shear waves, *Bull. Seism. Soc. Am., 91*, 1526-1536.

Hough, S.E., R.D, Borcherdt, P.A. Friberg, R. Busby, E. Filed, and K.H. Jacob (1990), The role of sediment-induced amplification in the collapse of the Nimitz freeway during the October 17, 1989 Loma Prieta earthquake, *Nature*, *344*, 853-855.

Hudson, D.E. (1969), Strong-Motion Earthquake Accelerograms Digitized and Plotted Data, Volume I - Uncorrected Accelerograms, Part A - Accelerograms IA1 through IA20, California Institute of Technology, Earthquake Engineering Research Laboratory, Pasadena, California.

Hwang, H., and J.R. Huo (1997), Attenuation relations of ground motion for rock and soil sites in eastern United States, *Soil Dyn. Earthq. Eng., 16*, 363-372.

Ibs-von Seht M., and J. Wohlenberg (1999), Microtremor measurements used to map thickness of soft sediments, *Bull. Seism. Soc. Am.*, *89*, 250 - 259.

IMD (2000), Chamoli earthquake of March 29, 1999 and its aftershocks, *Meteorological Monograph*, India Meteorological Department, Seismology No. 2/2000.

ISC (2006), On-line Bulletin, *http://www.isc.ac.uk/Bull*, Internatl. Seis. Cent., Thatcham, United Kingdom.

Ito, K., and M. Matsuzaki (1990), Earthquakes as self-organized critical phenomena, *J. Geophys. Res., 95*, 6853-6860.

Iyengar, R.N. (2000), Seismic Status of Delhi Megacity, *Curr. Sci.*, *78*, 568–574.

Iyengar, R.N., and S.T.G. Raghukanth (2005), Strong Ground Motion Estimation during the Kutch, India Earthquake, *PAGEOPH (In Press).*

Jangpangi, B.S. (1979), Stratigraphy and Structure of Bhutan Himalaya, *Tectonic Geology of Himalaya*, P.S. Saklani (Ed.), 221-242.

Johnston, A.C., K.J. Coppersmith, L.R. Kanter, and C.A. Cornell (1994), *The earthquakes of stable continent interiors, Vol. 1*, Assessment of large Earthquake Potential, Electric Power Research Institute, Palo Alto, CA.

Joshi, A. (2003), Predicting strong motion parameters for the Chamoli earthquake of 28th March 1999, Garhwal Himalaya, India, from simplified finite fault model, *J. Seis., 7*, 1-17.

Joyner, W.B., and D.M. Boore (1981), Peak horizontal acceleration and velocity from strong motion records including records from the 1979 Imperial Valley, California, earthquake, *Bull. Seism. Soc. Am*., *71*, 2011-2038.

Joyner, W.B., and D.M. Boore (1988), Measurement, characteristics and prediction of strong ground motion, *Proc. Earthq. Eng. Soil Dyn. II, Geotechnical Div/ASCE*, Park City, Utah, 43-102.

Kagan, Y., and L. Knopoff (1976), Statistical search for non-random features of the seismicity of strong earthquakes, *Phys. Earth Planet. Interiors, 12*, 291-318.

Kagan, Y.Y. (1991), Seismic moment distribution, *Geophys. J. Int.*, *106*, 123-134.

Kagan, Y.Y. (1993), Statistics of characteristics earthquakes, *Bull. Seism. Soc. Am*, *83*, 7-24

Kagan, Y.Y. (1997), Statistical aspects of Parkfield earthquake sequence and Parkfield prediction experiment, *Tectonophysics*, *270*, 207-219.

Kagan, Y.Y., and D.D. Jackson (2000), Probabilistic forecasting of earthquakes, *Geophys. J. Int.*, *143*, 438-453.

Kaila, K.L., and D. Sarkar (1977), Earthquake intensity attenuation pattern in India, *Proc. Symp. Analysis of Seismicity and Seismic Risk*, 173-191, Liblice, Czechoslovakia.

Kaila, K.L., and M. Rao (1979), Seismic zoning maps of Indian subcontinent, *Geophys. Res. Bull.*,*17*, 293–301.

Kanamori, H., and D.L. Anderson (1975), Theoretical basis of some empirical relations in seismology, *Bull. Seism. Soc. Am.*, *65*, 1073-1095.

Karnik V. (1972), A Note on the Morphology and Activity of Seismic Zones in the Aegean Region, *Nature Phys. Sc*., *239*, p. 72.

Karnik V., and Z. Schenkova (1974), Application of the Theory of Largest Values to Earthquake Occurrence in the Balkan Region, *Studia geoph, et geod.*, *18*, p. 134.

Karnik, V., and C. Radu (1977), Time Variation of Earthquake Activity in the Balkan Region, *Studia geoph, et geod*, *21*, p. 285.

Kato, K., K. Aki, and M. Takemura (1995), Site amplification from coda waves: Validation and Application to S-wave Site response, *Bull. Seism. Soc. Am*., *85*, 467-477.

Kayabali K. (1996), Soil liquefaction evaluation using shear wave velocity, *Eng. Geology*, *44*, 121-127.

Kayal, J.R., S.S. Arefiev, S. Barua, D. Hazarika, N. Gogoi, A. Kumar, S.N. Chowdhury, and S. Kalita (2006), Shillong plateau earthquakes in northeast India region: complex tectonic model, *Curr. Sci.*, *91*, 109-114.

Kayal, J.R. (1996), Precursor seismicity, foreshocks and aftershocks of the Uttarkashi earthquake of October 20, 1991 at the Garhwal Himalaya, *Tectonophys., 263*, 339-345.

Kayal, J.R. (2000), Seismotectonic structure in the western Himalaya, Deep continental studies in India, *DST News Lett., 10*, 2-5.

Kayal, J.R. (2001), Microearthquake activity in some parts of the Himalaya and the tectonic model, *Tectonophys.*, *339*, 331-351.

Kayal, J.R., B. Ghosh, P. Chakrabarty, and R. De (1995), Aftershock study of the Uttarkashi earthquake of October 20, 1991 by a temporary microearthquake network, *Geol. Soc. India Memo*., *30*, 25-41.

Kayal, J.R., O.P. Singh, P.K. Chakraborty, and G. Karunakar (2002), Aftershock sequence of the Chamoli earthquake of March 1999 in the Garhwal Himalaya, *Bull. Seism. Soc. Am.*, *93*, 109-117.

Kebede, F., and T. van Eck (1997), Probabilistic seismic hazard assessment for the Horn of Africa based on seismotectonic regionalisation, *Tectonophys.*, *270*, 221-237.

Keffer (1984) Landslides caused by earthquakes, *Geol. Soc. Am. Bull.*, *95*, 406 – 421.

Keilis-Borok, V.I. (1968), Seysmologiya i logika. Vych. seysmologiya, vyp. 4, Nauka, M. 317

Khattri, K., M. Wyss, V.K. Gaur, S.N. Saha, and V.K. Bansal (1985), Seismic Gap in Assam, Northeast India, *Bull. Seis. Soc. Am.*, *75*, 1469-1470.

Khattri, N., and M. Wyss (1978), Precursory Variation of Seismicity Rate in the Assam Area, *Indi. Geol.*, *6*, 615.

Khattri, K.N. (1987), Great earthquakes, seismicity gaps and potential for earthquake disaster along the Himalaya plate boundary. *Earthquake Prediction,* K. Mogi and K.N. Khattri (Eds.), *Tectonophys.*, *138*, 79-92.

Khattri, K.N. (1999), An evaluation of earthquakes hazard and risk in northern India, *Him. Geo., 20*, 1-46.

Khattri, K.N., A.M. Rogers, D.M. Perkins, and S.T. Algermissen (1984). A seismic hazard map of India and adjacent areas*, Tectonophys.*, *108*, 93-134.

Khattri, K.N., and M. Weiss (1978), Precursory variation of seismic rate in Assam Area, India, *Geology*, *6*, 685-688.

Kijko, A. (2003), Estimation of the Maximum Earthquake Magnitude, m_{max}, *PAGEOPH*, in print

Kijko, A., and B. J. Mitchell (1983), Multimode Rayleigh wave attenuation and Q in the crust of the Barents shelf, *J. Geophys. Res.*, *88*, 3315-3328.

King, J.L., and B.E. Tucker (1984), Observed variations of earthquake motion across a sediment-filled valley, *Bull. Seism. Soc. Am.*, *74*, 137-151.

Knopoff, L., and Kagan Y. (1977), Analysis of the theory of extremes as applied to earthquake problems, *Geophys. Res., 82*, 5647-5657

Kobayashi, K. (1980), A method for presuming deep ground soil structures by means of longer period microtremors, *Proc. of the 7th WCEE*, Sept. 8-13, Istanbul, Turkey, *1*, 237-240.

Konno, T., K. Kato, and R.L. Nigbor (1999), Soil site response, *Nuclear Eng. Design*, *192*, 285-294.

Koravos, G.Ch., I.G. Main, T.M. Tsapanos, and R.M.W. Musson (2003), Maximum earthquake magnitudes in the Aegean area constrained by tectonic moment release rates, *Geophys. J. Int.*, *152*, 94-112.

Korte, G.B. (1997), *The GIS Book: Understanding the Value and Implementation of Geographic Information Systems*, OnWord Press, Albany, New York, p. 440.

Kracke, D., R. Heinrich, G. Jentzsch and D. Kaiser (2000), Seismic Hazard Assessment of the East Thuringian Region/Germany – Case Study, *Studia Geophysica et Geodaetica*, *44*, 537-548.

Kramer, S.L. (2003), *Geotechnical Earthquake Engineering,* Pearson Publication, p. 653.

Krinitzsky, E.L. (2003), How to combine deterministic and probabilistic methods for assessing earthquake hazards, *Eng. Geology*, *70*, 157-163.

Krishnan, M.S. (1956), *Geology of India and Burma*, Higginbthams, Madras.

Kudo, K. (1995), Practical estimates of site response, state-of-the-art report., *Proc. 5th Int. Conf. Seismic Zonation*, Nice, France 3.

Kumar, G. (1981), Stratigraphy and tectonics of lesser Himalaya of Kumaon, Uttar Pradesh, *Contemporary Geoscientific Res. Himalaya*, *1*, 61-70.

Lachet, C., and P.Y. Bard (1994), Numerical and theoretical investigations on the possibilities and limitations of Nakamura's technique, *J. Phy. Earth*, *42*, 377-397.

Lachet, C., D. Hatzfeld, P.Y. Bard, N. Theodulidis, C. Papaioannou, and A. Savvaidis (1996), Site effects and microzonation in the city of Thessaloniki (Greece) Comparison of different approaches, *Bull. Seism. Soc. Am*., *86*, 1692-1703.

Lachet, C., M. Bouchon, N. Theodulidis, and P.Y. Bard (1995), Horizontal to vertical ratio and geological conditions, *Proc. 10th Eur. Conf. Earthq. Eng.*, Duma (Ed.), Rotterdam, 285-289.

Langston, C.A. (1979), Structure under Mount Rainier, Washington, inferred from teleseismic body waves, *J. Geophys. Res., 84*, 4749 - 4762.

Lapajne, J.K., B.S. Motnikar, and P. Zupancic (1996), Preliminary Seismic Hazard Maps of Slovenia, *Nat. Haz.*, *14*, 155-164.

Lee, W.H.K., H. Meyers, and K. Shimazaki (1998), *Historical Seismograms and Earthquakes of the World*, Academic Press, New York.

Legrand, D., A. Cisternas, and L. Dorbath (1996), Multifractal analysis of the 1992 Erzincan aftershock sequence, *Geophy. Res. Lett.*, *23*, 933-936.

Lermo, J., and F.J. Chávez-García (1992), Site effect evaluation using microtremors: a review (abstract), *EOS*, *73*, 352.

Lermo, J., and F.J. Chávez-García (1993), Site effect evaluation using spectral ratios with only one station, *Bull. Seism. Soc. Am*., *83*, *5*, 1574-1594.

Lermo, J., and F.J. Chávez-García (1994), Are microtremors useful in site response evaluation?, *Bull. Seism. Soc. Am*., *84*, 1350-1364.

Leydecker, G., and J.R. Kopera (1999), Seismological hazard assessment for a site in Northern Germany, an area of low seismicity, *Eng. Geology*, *52*, 293-304.

Lindley, G.T., and R.J. Archuleta (1995), Variation of seismic site effects in the Santa Cruz Mountains, California, *Int. Jour. Rock Mech. Mining Sce. Geomech. Abstracts*, *32*, 362A-362A.

Longley, P., and M. Batty (1997), *Spatial Analysis: Modelling in a GIS Environment*, John Wiley & Sons Ltd., New York, USA, p. 392.

Lyon-Caen, H., and P. Molner (1985), Gravity anomalies, flexure of the Indian plate and structure, support and evolution of the Himalaya and Ganga basin, *Tectonics*, *4*, 513-538.

Lyubushin, A.A., T.M. Tsapanos, V.F. Pisarenko, and G.C. Koravos (2002), Seismic Hazard for Selected Sites in Greece: A Bayesian Estimate of Seismic Peak Ground Acceleration, *Nat. Haz., 25*, 83-98.

Main, I.G. (1995), Earthquakes as critical phenomena: Implications for probabilistic Seismic Hazard Analysis, *Bull. Seism. Soc. Am*., *85*, 1299-1308

Main, I.G. (1996), Statistical physics, Seismogenesis and seismic hazard, *Rev. Geophys*., *34*, 433-462

Main, I.G., D. Irving, R. Musson, and A. Reading (1999), Constraints on the frequency-magnitude relation and maximum magnitudes in the UK from observed seismicity and glacio-isostatic recovery rates, *Geophys. J. Int.*, *137*, 535-550.

Makropoulos, K.C., and P.W. Burton (1985a), Seismic Hazard in Greece I. Magnitude Recurrence, *Tectonophys*., *117*, 105-257.

Makropoulos, K.C., and P.W. Burton (1985b), Seismic Hazard in Greece. II. Ground Acceleration, *Tectonophys.*, *117*, 259-294.

Mäntyniemi, P., V. Mârza, A. Kijko, and P. Retief (2003), A New Probabilistic Seismic Hazard Analysis for the Vrancea (Romania) Seismogenic Zone, *Nat. Haz.*, *29*, 371-385.

Marble, D.F., and D.J. Pequet (1983), Geographic Information System and Remote Sensing, *Manual. Rem. Sens.* Am. Soc., Photogrammetry, Falls Church, VA.

Markusiæ, S., P. Suhadolc, M. Herak, and F. Vaccari (2000), A contribution to seismic hazard in Croatia from deterministic modelling, *PAGEOPH*, *157*, 185–204.

Marrara, F., and P. Suhadolc (1998), Site amplifications in the city of Benevento (Italy): comparison of observed and estimated ground motion from explosive sources, *J. Seism.*, *2*, 125-143.

Matsuoka, M., and S. Midorikawa (1994), The digital national land information and seismic microzoning, *22nd Symp. Earthq. Ground Motion*, 23-34 (in Japanese with English abstract).

Mc Harg, I. (1969), *Design with Nature*, National History Press, New York.

McKenzie, D.P., and J.G. Sclatcr (1971), Evolution of the Indian Ocean since the Late Cretaceous, *Geoph. J. R. Astr. Soc.*, *24*, p. 437.

Menke, W. (1989), *Geophysical Data Analysis: Discrete Inverse Theory*, Academic, New York.

Midorikawa, S., and H. Kobayashi (1979), On estimation of strong earthquake motions with regard to fault rupture, *Trans. of A.I.J.*, *282*, 71-81 (in Japanese with English abstract).

Milne, W. A., and A.G. Davenport (1969), Distribution of Earthquake Risk in Canada, *Bull. Seism. Soc. Am*., *59*, 729.

Mithal, R.S., and L.S. Srivastava (1959), Geotectonic position and earthquakes of Ganga-Brahmputra region, *Proc. 1st Symp. Earthquake Eng.,* Roorkee.

Mitra, S., K. Priestley, V.K. Gaur, S.S. Rai, and J. Haines (2006), Variation of Rayleigh wave group velocity dispersion and seismic heterogeneity of the Indian crust and uppermost mantle, *Geophys. J. Int.*, *164*, 88–98

Mogi, K. (1962), Magnitude-frequency relationship for elastic shocks accompanying the fractures of various materials and some related problems in earthquakes. *Bull. Eq. res. Inst. Univ. Tokyo*, *40*, 831-883

Molas, G.L., and F. Yamazaki (1995), Attenuation of earthquake ground motion in Japan including deep focus events, *Bull. Seism. Soc. Am*., *85*, 1343-1358.

Molas, G.L., and F. Yamazaki (1996), Attenuation of response spectra in Japan using new JMA records, *Bull. Earthq. Resistant Struct. Res. Center*, *19,* 115-128.

Molchan, G.M. (1997), Earthquake prediction as a decision-making problem, *PAGEOPH*, *149*, 233-247.

Molnar, P., and P. Taponnier (1975), Conozoic tectonics of Asia, Effects of continental collision, *Science*, *189*, 419-426.

Molnar, P., and P. Tapponnier (1977), Relation of tectonics of eastern Chiena to the India-Eurasia collision, application of slipline field theory to large scale continental tectonics, *Geology*, *5*, 212-216.

Molnar, P., and W.P. Chen (1982), Seismicity and mountain building, *Mountain Building Processes,* K. Hsu (Ed.), Academic Press, New York, 41-57.

Molnar, P., T.J. Fitch, and F.T. Wu (1973), Fault Plane Solutions of Shallow Earthquakes and Contemporary Tectonics, *Asia. Earth Planet. Sci. Lett.*, *19*, 101.

Mucciarelli, M. (1998), Reliability and applicability of Nakamura's technique using microtremors: an experimental approach, *J. Earthq. Eng.*, *2*, 625 –638.

Muço, B., F. Vaccari, G. Panza, and N. Kuka (2002), Seismic zonation in Albania using a deterministic approach, *Tectonophys.*, *344,* 277-288.

Mukhopadhyay, M., and S. Dasgupta (1988), Deep structures and tectonics of Burmese arc, Constraints from earthquake and gravity data, *Tectonophys.*, *149*, 299-322.

Musson, R.M.W., and P.W. Winter (1996), Seismic Hazard Maps for the U.K., *Nat. Haz.*, *14*, 141-154.

Nakamura, Y. (1989), A Method for Dynamic Characteristics Estimations of Subsurface Using Microtremors on the ground Surface, *QR RTRI*, *30*, 25-33.

Nakamura, Y. (1996), Real-time information systems for seismic hazard mitigation UrEDAS, HERAS and PIC*, Q.R. of R.T.R.I., 37-3*, 112-127.

Nandy, D.R. (1973), Geology and Structural Lineaments of the Luhit Himalaya (Arunachal Pradesh) and Adjoining Area; A Tectonic Interpretation, *Seminar on Geodynamics of the Himalayan Region*, Hyderabad.

Nandy, D.R. (2001), Geodynamics of Northeastern India, *ACB Publications*, Kolkata, India.

Nandy, D.R., and S. Dasgupta (1991) Seismo-tectonic domains of northeast India and adjacent areas, *Phys. Chem. Earth*, *18*, 371-384

Nath, S.K. (2004), Seismic Hazard Mapping and Microzonation in the Sikkim Himalaya through GIS Integration of Site Effects and Strong Ground Motion Attributes, *Nat. Haz.*, *31*, 319-342.

Nath, S.K., D. Chatterjee, N.N. Biswas, M. Dravinski, D.A. Cole, A. Papageorgiou, J.A. Rodriguez, and C.J. Poran (1997), Correlation Study of Shear wave velocity in near surface geologic formations in Anchorage, Alaska, *Earthq. Spectra*, *13*, 55-75.

Nath, S.K., M. Vyas, I. Pal, and P. Sengupta (2004), A Hazard Scenario in the Sikkim Himalaya from Seismotectonics, Spectral Amplification, Source Parameterization and Spectral Attenuation Laws using Strong Motion Seismometry, *J. Geophys. Res.*, *110*, B01301, doi: 10.1029/2004/2004JB003199.

Nath, S.K., M. Vyas, I. Pal., and P. Sengupta (2005), A Seismic Hazard Scenario In The Sikkim Himalaya from Seismotectonics, Spectral Amplification, Source Parameterization, and Spectral Attenuation Laws Using Strong Motion Seismometry, *J. Geophys. Res.*, 110, B01301, doi: 10.1029/2004jb003199.

Nath, S.K., N.N. Biswas, M. Dravinski, and A. Papageorgiou, (2002), Determination of S-wave site response in Anchorage, Alaska in the 1-9 Hz frequency band, *Pure Appl. Geophys.* 159, 2673-2698.

Nath, S.K., P. Sengupta, and J.R. Kayal (2002), Determination of Site Response at Garhwal Himalaya from the aftershock sequence of 1999 Chamoli Earthquake, *Bull. Seism. Soc. Am.*, *92*, 1071-1081.

Nath, S.K., P. Sengupta, S. Sengupta, and A. Chakrabarti (2000), Site response estimation using Strong Motion network: A step towards microzonation of Sikkim Himalayas, *Seismology 2000, Curr. Sci.*, *79*, 1316-1326.

Nath, S.K., P. Sengupta, S.K. Srivastav, S.N. Bhattacharya, R.S. Dattatrayam, R. Prakash, and H.V. Gupta (2003), Estimation of S-wave site response in and around Delhi region from weak motion data. *Proc. Indian Acad. Sci. (Earth Planet. Sci)*, *112*, 441-462.

National Bureau of Soil Survey (1994), *Master Plan for Irrigation Development, Sikkim*, Govt. of Sikkim, Agricultural Finance Corporation Ltd, Report, *2*, 35-47.

Nogoshi, M., and T. Igarashi (1971), On the amplitude characteristics of microtremor (Part 2), *Jour. Seism. Soc. Japan*, *24*, 26-40 (in Japanese with English abstract).

Nordquist, J.M. (1945), Theory of Largest Values Applied to Earthquake Magnitudes, *Trans. Am. Geoph. Un.*, 26-29.

Nuannin, P., O. Kulhanek, and L. Persson (2005), Spatial and temporal b value anomalies preceding the devastating off coast of NW Sumatra earthquake of December 26, 2004, *Geophys. Res. Lett.*, *32*, L11307, doi: 10. 1029/2005GL022679.

Oldham, R.D. (1882), A catalogue of Indian earthquakes from the earliest time to the end of A.D. 1869, by the late Thomas Oldham edited by R. D. Oldham, *Mem. Geol. Surv. India*, *19*, 163-215.

Oldham, R.D. (1899), Report on the great earthquake of 12th June 1897 (incl. the reports by P. Bose, G.Grimes, H.Hayden, T. LaTouche and E. Vredenburg), *Mem. Geol. Survey of India*, *29,* p.1379, Calcutta.

Oldham, R.D. (1899), Report on the Great Earthquake of 12th June, 1897, *Mem. Geol. Surv. Ind.*, *29*, p. 1379, Calcutta.

Omachi, T., Y. Nakamura, and T. Toshinawa (1991), Ground motion characteristics in the San Francisco Bay area detected by micro tremor measurements, *Proc. 2nd Int. Conf. on Recent Adv. in Geot. Earth Eng. and Soil Dyn.,* 11-15 March, St. Louis, Missouri, 1643-1648.

Oncel, A.O., and O. Alptekin (1999), Effect of aftershocks on earthquake hazard estimation: An example from the North Anatolian Fault Zone, *Nat. Haz.*, *19*, 1-11.

Ordaz, M., and S.K. Singh (1992), Source spectra attenuation of seismic waves from Mexican earthquakes and evidence of amplification in the hill zone of Mexico City, *Bull. Seism. Soc. Am., 82*, 24-43.

Orozova, I.M., and P. Suhadolc (1999), A deterministic-probabilistic approach for seismic hazard assessment, *Tectonophys., 312*, 191-202.

Orozova, I.M., G. Costa, F. Vaccari, and P. Suhadolc (1996), Estimation of 1Hz maximum acceleration in Bulgaria for seismic risk reduction purposes, *Tectonophysics,* 258, 263–274.

Panza, G.F., F. Vaccari, G. Costa, P. Suhadolc, and D. Faeh (1996), Seismic input modelling for zoning and microzoning, *Earthq. Spectra, 12*, 529–566.

Papanastassiou, D. (1998), Seismic Hazard Assessment in the Area of Mystras-Sparta, South Peloponnesus, Greece, Based on Local Seismotectonic, Seismic, Geologic Information and on Different Models of Rupture Propagation, *Nat. Haz., 18*, 237-251.

Parolai, S., D. Bindi, and P. Augliera (2000), Application of the generalized inversion technique (GIT) to a microzonation study: Numerical simulations and comparison with different site-estimation techniques, *Bull. Seism. Soc. Am*., *90*, 286-297.

Parvez, I.A., A.A. Gusev, G.F. Panza, and A.G. Petukhin (2001), Preliminary determination of the interdependence among strong motion amplitude, earthquake magnitude and hypocentral distance for the Himalayan region, *Geophys. J. Int., 144*, 577–596.

Parvez, I.A., and A. Ram (1997), Probabilistic assessment of earthquake hazards in the north-east Indian Peninsula and Hindukush region, *Pure Appl. Geophys.*, *149*, 731–746.

Parvez, I.A., and A. Ram (1999), Probabilistic Assessment of earthquake hazards in the Indian Subcontinent, *Pure Appl. Geophys., 154*, 23-40.

Parvez, I.A., F. Vaccari, and G.F. Panza (2003), A deterministic seismic hazard map of India and adjacent areas, *Geophys. J. Int*., *155*, 489-508.

Parvez, I.A., F. Vaccari, and G.F. Panza (2004), Site-specific microzonation study in Delhi metropolitan city by 2-D modeling of SH and P-SV waves, *Pure Appl. Geophys.*, *161*, 1165-1184.

Parvez, I.A., G.F. Panza, A.A. Gusev, and F. Vaccari (2002), Strong-motion Amplitude in Himalayas and a Pilot Study for the Deterministic First-order Microzonation in a Part of Delhi City, *Curr. Sci.*, *82*, 158–166.

Pedersen, H., B. Le. Brun, D. Hatzfeld, M. Campillo, and P.Y. Bard (1994), Ground-Motion amplitude across ridges, *Bull. Seism. Soc. Am*., *84*, 1786-1800.

Pendse, C.G. (1948), Earthquakes in India and Neighbourhood, *India Met. Dept. Sci. Notes*, *10*, p.177.

Petersen, M.D., W.A. Bryant, C.H. Cramer, M.S. Reichle, and C.R. Real (1997), Seismic ground-motion hazard mapping incorporating site effects for Los Angeles, Orange and Ventura counties, California: a geographical information system application. *Bull. Seism. Soc. Am*., *87*, 249-255.

Phillips, W.S., and K. Aki (1986), Site amplification of coda waves from local earthquakes in central California, *Bull. Seism. Soc. Am*., *76*, 627-648.

Ponce, V.M. (1989), *Engineering Hydrology, Principles and Practices*, Prentice Hall, Englewood Cliffs, New Jersey.

Porter, L.D., and D.J. Leeds (2000), Correlation of strong ground motion for the 1994 Northridge earthquake, *Geophys. J. Int.*,*143*, 376-388.

Radulian, M., F. Vaccari, N. Mândrescu, G.F. Panza, and C.L. Moloveanu (2000), Seismic hazard of Romania: deterministic approach, *PAGEOPH*,*157*, 221–247.

Raina, V.K., and B.S. Srivastava (1980), A reappraisal of the geology of the Sikkim lesser Himalaya, *Stratigraphy and Correlation of lesser Himalayan formation,* K.S. Valdiya and S. B. Bhatia (Eds.), 201-220, Hindustan Publishing Corporation, Delhi.

Rajendran, K., C.P. Rajendran, S.K. Jain, C.V.R. Murty, and J.N. Arlekar (2000), The Chamoli earthquake, Garhwal Himalaya: Field observations and implications for seismic hazard, *Curr. Sci.*, 78, 45-51.

Raju, A.T.R. (1968), Geological Evaluation of Assam and Cambay Basins of India, *Bull. Am. Assoc. Petrol.*, *52*, 2422.

Rastogi, B.K. (2000), Chamoli earthquake of magnitude 6.6 on 29th March 1999, *J. Geol. Soc. India*, 55, 505-514.

Reasenberg, P.A. and L.M. Jones (1989), Earthquake hazard after a mainshock in California, *Science*, *243*, 1173-1176.

Reiter, L. (1990), *Earthquake Hazard Analysis: Issues and Insights*, Colombia University Press, New York.

Richter, C.F. (1958), *Elementary Seismology*, San Francisco, W.H. Freeman and Co., p. 345.

Riepl, J., P.Y. Bard, D. Hatzfeld, C. Papaioannou, and S. Nechtschein (1998), Detailed evaluation of site response estimation methods across and the sedimentary valley of Volvi (EURO-SEISTEST), *Bull. Seism. Soc. Am*., *88*, 488-502.

Romanelli, F., and F. Vaccari (1999), Site response estimation and ground motion spectrum scenario in the Catania area, *J. Seismol.*, *3*, 311-326.

Romeo, R., and A. Pugliese (2000), Seismicity, seismotectonics and seismic hazard of Italy, *Eng. Geology*, *55*, 241-266.

Saaty, T.L. (1980), *The Analytic Hierarchy Process,* McGraw-Hill International, New York, NY, USA.

Saaty, T.L. (1990), An Exposition of the AHP in Reply to the Paper 'Remarks on the Analytic Hierarchy Process, *Management Science*, *36*, 259-268.

Sadigh, K., C.Y. Chang, N.A. Abrahamson, S.J. Chiou, and M.S. Power (1993), Specification of Long-Period Ground Motions: Updated Attenuation Relationships for Rock Site Conditions and Adjustment Factors for Near-Fault Effects, In *Proc. ATC-17-1 Seminar on Seismic Isolation, Passive Energy Dissipation and Active Control, Vol. I, March 11-12, San Francisco*, Applied technology Council, Redwood City, CA, 11-23.

Sadigh, K., C.Y. Chang, Z.A. Egan, F. Makdisi, and R.R. Youngs (1997), Attenuation Relationships for Shallow Crustal Earthquakes Based on California Strong Motion Data, *Seism. Res. Lett*., *68*, 180-189.

Safak, E. (1995), A new model to simulate site effects, *Proc. 10th European Conference on Earthquake Engineering*, Duma (Ed.), Rotterdam, 297-303.

Safak, E. (2001), Local site effects and dynamic soil behavior, *Soil Dyn. Earthq. Eng.*, *21*, 453-458.

Sander, P. (1998), Hard rock aquifers in arid and semi arid zones, *Water Resources of Hard Rock Aquifers in Arid and (Semi-Arid) Zones-Studies and Reports in Hydrology*, J.W. Lloyd (Ed.), UNESCO Publishing, Paris, France, *58*, p. 224

Santo, T. (1969), On the Characteristic Seismicity in South Asia from Hindukush to Burma, *Bull. Int. Inst. Seis. and Earth*. *Eng.*, *2*, p. 14.

Schenkova, Z., and V. Karnik (1978), The Third Asymptotic Distribution of Largest Magnitudes in the Balkan Earthquake Provinces, *Pure Appl. Geoph*., *116*, 1314-1325

Schenkova, Z., and V. Schenk (1975), Return Periods of Earthquakes and Trends of Seismic Activity, *Pure Appl. Geoph*., *113,* p 683.

Schnabel, B., J. Lysmer, and H.B. Seed (1972), SHAKE – A Computer Program for Earthquake Response Analysis of Horizontally Layered Sites, *Report EERC,* p. 7212.

Schnabel, P.B., (1973), *Effects of Local Geology and Distance from Source on Earthquake Ground Motion*, Ph.D. Thesis, University of California, Berkeley, California.

Scholemmer, D., S. Wiemer, and M. Wyss (2005), Variations in earthquake-size distribution across different stress regimes, *Nature*, *437*, 539-542.

Scholz, C.H. (1968), The magnitude-frequency relation of microfracturing in rock and its relation to earthquake, *Bull. Seis. Soc. Am*., *58*, 399–415.

Seale, S.H., and R.J. Archuleta (1989), Site amplification and attenuation of strong ground motion, *Bull. Seis. Soc. Am*., *79*, 1673-1696.

Seed, H.B., and I.M. Idriss (1970), *Soil Moduli and Damping Factors for Dynamic Response Analyses, Rep. No. EERC-70/10*, Earthquake Engineering Research Center, University of California, Berkeley, California

Seekins, L.C., L. Wennerberg, L. Margheriti, and H.P. Liu (1996). Site amplification at five locations in San Francisco, California; a comparison of S-waves, codas and microtremors, *Bull. Seism. Soc. Am.*, 86, 627-635.

Sen, Z., and K. Al-Suba'I (2001), Seismic Hazard Assessment in the Tihamat Asir Region, Southwestern Saudi Arabia, *Math. Geology*, *33*, 967-991.

Shankar, R., and P. Narula (1999), Chamoli earthquake of 29th March 1999- A preliminary appraisal, *Ind. Minerals, 52*, 141-150.

Sharma, M.L (1998). Attenuation relationship for estimation of peak ground horizontal acceleration using data from strong motion arrays in India, *Bull. Seism. Soc. Am.*, *88, 1063-1069.*

Shi, Y., and B.A. Bolt (1982), The standard error of the magnitude-frequency b value, *Bull. Seism. Soc. Am.*, *72*, 1677-1687.

Shiono, K., Y. Ohta, and K. Kudo (1979), Observation of 1 to 5 sec microtremors and their applications to earthquake engineering, Part VI: existence of Rayleigh wave components, *Jour. Seism. Soc. Japan*, *32*, 115-124 *(in Japanese with English abstract).*

Shoji, Y., and M. Kamiyama (2002), Estimation of local site effects by generalized inversion scheme using observed records of 'Small-Titan', *Soil Dyn. Earthquake Eng.*, *22*, 855-864.

Singh, S.K., E. Mena, and R. Castro (1988), Some aspects of source characteristics of the 19 September 1985 Michoacan earthquake and ground motion amplification in and near Mexico City from strong motion data, *Bull. Seism. Soc. Am*., *78*, 451-477.

Singh, S.K., J. G. Ordaz, J. G. Anderson, M. Rodriguez, R. Quaas, E. Mena, M. Ottaviani, and D. Almora (1989), Analysis of near-source strong-motion recordings along the Mexican subduction zone, *Bull. Seism. Soc. Am*., *79*, 1697-1717.

Singh, S.K., J. Lermo, T. Dominguez, M. Ordez, J.M. Espinosa, E. Mena, and R. Quass (1988), The Mexico earthquake of September 19, 1985 - a study of amplification of seismic waves in the valley of Mexico with respect to a hill zone site, *Earthq. Spectra, 4*, 653-673.

Singh, S.K., W.K. Mohanty, B.K. Bansal, and G.S. Roonwal (2002), Ground motion in Delhi from future large/great earthquakes in the central seismic gap of the Himalayan Arc, *Bull. Seism. Soc. Am*., *92*, 555-569.

Sinharoy, S. (1988), Metamorphic implications for intercontinental underthrusting-models for inverted metamorphism in the Himalayas, *Ind. Mineral*, *42*, 214-231.

Slejko, D., R. Camassi, I. Cecic, D. Herak, M. Herak, S. Kociu, V. Kouskouna, J. Lapajne, K. Makropoulos, C. Meletti, B. Muço, C. Papaioannou, L. Peruzza, A. Rebez, P. Scandone, E. Sulstarova, N. Voulgaris, M. Zivcic, and P. Zupancic (1999), Seismic hazard assessment for Adria, *Annali di Geofisica*, *42*, 1085-1107.

Sousa, M.L., and C.S. Oliveira (1996), Hazard Mapping Based on Macroseismic Data Considering the Influence of Geological Conditions, *Nat.Haz.*, *14*, 207-226.

Speidel, D.H., and P.H. Mattson (1997), Problems for Probabilistic Seismic Hazard Analysis, *Nat. Haz.*, *16*, 165-179.

Spudich, P., W.B. Joyner, A.G. Lindh, D.M. Boore, B.M. Margaris, and J.B. Fletcher (1999), SEA99: A revised ground motion prediction relation for use in extensional tectonic regimes, *Bull. Seism. Soc. Am*., *89*, 1156-1170.

Star, S., K.C. McGwire, and J.E. Estes (1997), *Integration of Geographic Information Systems and Remote Sensing*. Cambridge University Press, Cambridge, UK, p. 248.

Stein, S., and M. Wysession (2003), *An Introduction to Seismology, Earthquakes, and Earth Structure*, Blackwell, Malden, MA.

Stucchi, M. (1993), *Historical investigations of European Earthquakes*, CNR – Istituto di Ricerca sul Rischio Sismico, Milano.

Sugito, M., G. Goda, and T. Masuda (1994), Frequency dependent equi-linearized technique for seismic response analysis of multi-layered ground, *Proc. JSCE*, *493*, 49-58 (in Japanese with English abstract).

Suyehiro, S., T. Asada, and M. Ohtake (1964), Foreshocks and aftershocks accopmpanying a perceptible earthquake in central Japan: On the peculiar nature of foreshocks, *Pap. Meteorol. Geophys.*, *19*, 427-435.

Sykes, L.R., E.S. Bruce, and C.H. Scholz (1999), Rethinking Earthquake Prediction, *Pure Appl. Geophys.*, *155*, 207–232.

Talebian, M. (1996), Seismic risk analysis of Japan: peak ground acceleration and uniform risk response spectra, *Internl. Jour. of Rock Mechanics and Mining Sciences and Geomechanics Abstracts, 33*, 218A-218A.

Tandon, A.N. (1954), Study of Great Assam Earthquake of August 15, 1950 and Its Aftershocks, *Ind. J. Meteorol. Geophys., 5*, 95-137.

Tandon, A.N. (1956), Zones of India liable to earthquake damage, *Ind. J. Meteorol. Geophys.*,*10*, 137–146.

Tandon, A.N., and H.N. Srivastava (1975), Focal Mechanism of Some Recent Himalayan Earthquakes and Regional Plate Tectonics, *Bull. Seis. Soc. Am*., *65*, 963-969.

Teves-Costa, P., L. Matias, and P.Y. Bard (1996), Seismic behavior estimation of thin alluvium layers using microtremor recordings, *Soil Dyn. Earthquake Eng.*,*15*, 201-209.

Than, K. (1975), Earthquake Mechanisms Pressure and Tension Axes in Indian Ocean and Related Regions, *Bull. Int. Inst. Seis. and Earth. Eng.*, *11*, p. 1.

Thenhaus, P.C. (1983), Summary of workshops concerning, regional seismic source zones of parts of the Conterminous United States, Convened 1979-1980, Golden, Colorado, *U.S. Geol. Surv*. *Circular*, p. 898.

Thenhaus, P.C. (1986), Seismic source zones in probabilistic estimation of the earthquake ground motion hazard: A classification with key issues, *Proc. Conference 34: Workshop on Prob. Earthq. Haz. Assess.*, 53-71.

Theodulidis, N.P., and B.C. Papazachos (1992), Dependence of strong ground motion on magnitude-distance, site geology and macroseismic intensity for shallow earthquakes in Greece: I, Peak horizontal acceleration, velocity and displacement, *Soil Dyn. Earthq. Eng., 11*, 387-402.

Thingbaijam, K.K.S., S.K. Nath, A. Yadav, A. Raj, M.Y. Walling, and W.K. Mohanty (2007), Recent Seismicity in Northeast India and its Adjoining Region, *J. Seism.*, Communicated.

Tonouchi, K., T. Sakayama, and T. Imai (1983), S wave velocity in the ground and the damping factor, *Bull. Int. Assoc. Eng. Geologists*, *26-27*, 327-333.

Toro, G.R, N.A. Abrahamson, and J.F. Schneider (1997), Model of strong ground motions from earthquakes in central and eastern North America: Best estimates and uncertainties, *Seism. Res. Lett.*, *68*, 41-57.

Toro, G.R., W.J. Silva, R.K. McGuire, and R.B. Herrmann (1992), Probabilistic seismic hazard mapping of the Mississippi embayment, *Seism. Res. Lett.*, *63*, 449-475.

Triantafyllidis, P., P.M. Hatzidimitriou, N. Theodulidis, P. Suhadolc, C. Papazachos, D. Raptakis, and K. Lontzetidis (1999), Site effects in the city of Thessaloniki (Greece) estimated from acceleration data and 1D soil profiles, *Bull. Seism. Soc. Am*., *89*, 521-537.

Trifunac, M.D. (1976), Preliminary empirical model for scaling Fourier amplitude spectra of strong ground acceleration in terms of earthquake magnitude, source-to station distance and recording site condition, *Bull. Seism. Soc. Am*., *66*, 1343-1373.

Trifunac, M.D., and M.I. Todorovska (2000), Can aftershock studies predict site amplification factors? Northridge, CA, Earthquake of 17 January 1994, *Soil Dyn. Earthq. Eng.*,*19*, 233–251.

Tsapanos, T.M. (2003), A seismic hazard scenario for the main cities of Crete island, Greece, *Geophys. J. Int., 153*, 403-408.

Tsapanos, T.M., and P.W. Burton (1991), Seismic hazard evaluation for specific seismic regions of the world, *Tectonophys.*, *194*, 153-169.

Tumarkin, A.G., and R.J. Archuleta (1997), Recent Advances in Prediction and Processing of Strong Ground Motions, *Nat. Haz.*, *15*, 199-215.

Usami, T. (1981), *Nihon Higai Jishin Soran (List of Damaging Japanese Earthquakes)*, University of Tokyo Press (in Japanese).

Utsu, T. (1965), A method for determining the value of b in the formula log N=a-bM showing the magnitude–frequency relation for the earthquakes. *Geophy. Bull. Hokkaido Univ.*, *13*, 99-103 (in Japanese with English abstract).

Utsu, T. (1971), Statistical Features of Seismicity, *International Handbook of Earthquake and Engineering Seismology*, W.H.K. Lee, H. Kanamori, P.C. Jennings, and C. Kisslinger (Eds.), Academic Press, *81*, 719-732.

Verma, R.K., and M. Mukhopadhyay (1977), An analysis of gravity field in Northeastern India, *Tectonophys.*, *42*, 283-317.

Verma, R.K., M. Mukhapadhyay, and M.S. AhluwaJia (1976), Seismicity, Gravity and Tectonics of North-East India and Northern Burma, *Bull. Seis. Soc. Am.*, *66*, 1683-1694.

Vorobieva, I.A. (1999), Prediction of a subsequent large earthquake, *Phy. Earth Planet. Interiors*, *111*, 197-206.

Vorobieva, I.A., and G.F. Panza (1993), Prediction of the occurrence of related strong earthquakes in Italy, *Pure Appl. Geophys.*, *141*, 25-41.

Vulnerability Atlas of India (1999), Building Materials & Technology Promotion Council, New Delhi.

Vyas, M., S.K. Nath, I. Pal, P. Sengupta and W.K. Mohanty (2004), GSHAP Revisited for the Prediction of Maximum Credible Earthquake in the Sikkim Region, *ACTA Geophys. Polo.*, *53*, 143-152.

Wadia, D.N. (1953), *Geology of India,* McMillan, London.

Wang, C.Y., and R.B. Herrmann (1980), A numerical study of P-, SV- and SH wave generation in a plane layered medium, *Bull. Seism. Soc. Am.*, *70*, 1015-1036.

Warren, N.W., and G.V. Latham (1970), An Experimental Study of Thermally Induced Microfracturing and its Relation to Volcanic Seismicity, *J. Geophys Res*., *75*, 4455-4464.

Wells, D.L., and K.L. Coppersmith (1994), New empirical relationships among magnitude, rupture length, rupture width, rupture area and surface displacement, *Bull. Seism. Soc. Am*., *84*, 974-1002

Wesnouski, S.G., C.H. Scholz, K. Shimazaki, and T. Matsuda (1983), Earthquake frequency distribution and the mechanics of faulting, *J. Geophys. Res*., *88*, 9331-9340.

Wood, H.O. (1908), Distribution of apparent intensity in San Francisco in The California Earthquake of April 18, 1906, *Report of the State Earthquake Investigation Commission*, Carnegie Inst. of Wash. Publ., *87*, Washington, D.C., 220-245.

Wyss, M. (1973), Towards a physical understanding of the earthquake frequency distribution, *J. Geophys. Res.*, *31*, 341–359

Yegulalp, T. M., and J.T. Kuo (1974), Statistical prediction of the occurrence of maximum magnitude earthquakes, *Bull. Seism. Soc. Am*., *64*, 393-414.

Yilmaztürk, A., and P.W. Burton (1999), An evaluation of seismic hazard parameters in southern Turkey, *J. Seismol.*, *3*, 61-81.

Youngs, R. R., S.J. Chiou, W.J. Silva, and J.R. Humphrey (1997), Strong ground motion attenuation relationships for subduction zone earthquakes, *Seism. Res. Lett.*, *68*, 58-73.

Zivciæ, P., P. Suhadolc, and F. Vaccari (2000), Seismic zonation of Slovenia based on deterministic hazard computation, *Pure Appl. Geophys.*, *157*, 171–184.

ANNEXURE I

Homogeneous Earthquake Catalogue (1866–2006) of Northeast India

Year	Month	Day	Longitude (°E)	Latitude (°N)	Depth (km)	Magnitude (Mw)
1866	05	23	87.00	25.00	-	5.5
1868	06	30	91.50	24.50	-	7.5
1870	04	11	99.00	30.00	-	6.7
1879	11	23	98.70	24.60	-	5.0
1897	06	12	91.00	26.00	60.0	8.7
1906	08	31	97.00	27.00	100.0	7.0
1908	12	12	97.50	26.50	35.0	7.5
1909	02	17	87.00	27.00	-	5.0
1911	12	07	88.00	23.00	-	5.0
1914	03	28	99.00	25.00	100.0	6.9
1918	07	08	91.00	24.50	60.0	7.6
1920	08	15	93.20	22.20	-	6.0
1923	06	22	94.00	22.70	35.0	6.0
1923	08	10	93.40	22.60	-	6.0
1923	09	09	91.00	25.25	35.0	7.1
1924	01	30	93.00	25.00	-	6.0
1924	02	14	96.00	26.00	-	6.0
1924	08	13	91.50	29.50	35.0	5.0
1924	09	02	95.00	23.00	-	6.0

Year	Month	Day	Longitude (^{o}E)	Latitude (^{o}N)	Depth (km)	Magnitude (Mw)
1924	10	08	91.00	30.50	35.0	6.5
1926	05	10	96.00	27.00	-	6.3
1926	08	18	94.50	24.50	-	6.0
1926	10	23	93.00	25.00	80.0	6.0
1927	03	15	95.00	24.50	130.0	6.5
1927	05	20	94.50	24.50	-	6.0
1927	07	15	96.00	27.00	-	6.0
1928	07	09	96.00	27.00	-	6.0
1928	08	30	96.00	27.00	-	6.0
1929	03	25	95.00	29.50	35.0	6.0
1929	10	19	96.00	26.70	-	6.0
1930	07	02	90.20	25.80	35.0	7.1
1930	07	03	90.20	25.80	-	6.0
1930	07	04	90.20	25.80	-	6.0
1930	07	08	90.80	25.80	-	6.0
1930	07	11	93.80	25.00	-	6.0
1930	07	13	90.80	25.80	-	6.0
1930	09	22	93.80	25.30	35.0	6.0
1931	01	27	96.80	25.60	35.0	7.6
1931	02	10	96.00	25.50	35.0	5.6
1931	05	27	98.50	27.50	35.0	5.6
1931	10	18	98.00	26.00	35.0	5.6
1932	01	03	98.50	25.50	35.0	5.6
1932	03	06	92.50	25.50	35.0	5.6
1932	03	24	90.00	25.00	35.0	5.6
1932	03	27	92.00	24.50	35.0	5.6
1932	08	14	95.50	26.00	120.0	7.0
1932	11	09	92.00	26.50	35.0	5.6

Year	Month	Day	Longitude (^{O}E)	Latitude (^{O}N)	Depth (km)	Magnitude (Mw)
1933	03	06	90.50	26.00	35.0	5.6
1933	08	11	98.50	25.50	35.0	6.5
1933	11	19	98.00	25.00	35.0	5.6
1934	01	19	98.25	25.50	35.0	6.0
1934	06	02	95.00	24.50	130.0	6.5
1934	12	15	89.25	31.25	35.0	7.1
1935	01	03	88.00	30.50	35.0	6.5
1935	03	21	89.50	24.25	80.0	6.2
1935	04	23	94.75	24.00	110.0	6.2
1935	05	21	89.25	28.75	140.0	6.2
1936	02	11	87.00	27.50	50.0	5.6
1936	05	10	96.80	26.30	-	6.0
1936	06	18	90.30	26.60	-	6.0
1936	06	19	96.90	26.40	-	6.0
1936	09	07	87.00	27.50	-	5.1
1937	03	09	92.00	27.00	-	6.0
1937	03	21	94.00	25.50	-	6.0
1937	08	31	96.80	25.90	-	6.0
1937	09	09	94.70	24.90	-	6.0
1938	01	29	87.00	27.50	35.0	5.5
1938	04	14	95.00	23.50	130.0	6.8
1938	05	06	95.00	24.50	100.0	5.8
1938	08	16	94.25	23.50	35.0	7.2
1938	11	21	95.00	30.00	35.0	6.0
1939	05	27	94.00	24.50	75.0	6.8
1939	06	19	94.00	23.50	35.0	5.6
1940	02	13	92.00	27.00	-	6.0
1940	05	11	94.10	24.90	80.0	6.0

Year	Month	Day	Longitude (^{o}E)	Latitude (^{o}N)	Depth (km)	Magnitude (Mw)
1940	08	02	90.50	28.00	-	6.0
1940	09	03	91.50	30.50	35.0	6.0
1940	10	04	91.50	30.50	35.0	6.0
1941	01	21	92.00	27.00	100.0	6.8
1941	01	27	92.50	26.50	180.0	6.5
1941	02	23	96.00	28.00	90.0	5.5
1941	05	16	99.00	24.00	35.0	6.9
1941	05	22	93.00	27.50	35.0	5.6
1941	12	26	99.00	21.50	35.0	7.0
1943	02	08	92.00	27.00	-	6.0
1943	10	23	94.00	26.80	35.0	7.2
1943	10	23	93.50	21.50	35.0	7.2
1944	12	24	92.20	24.70	-	6.0
1945	05	19	90.90	25.10	-	6.0
1946	03	16	92.60	26.40	-	6.0
1946	09	12	96.00	23.50	60.0	7.5
1947	03	08	94.70	24.90	-	6.0
1947	07	29	94.00	28.50	60.0	7.9
1947	09	09	96.80	25.90	-	6.0
1947	11	29	92.90	27.90	-	6.0
1950	02	13	95.30	29.80	-	6.0
1950	02	23	95.30	29.80	-	6.0
1950	02	26	90.50	28.00	-	6.0
1950	08	15	96.50	28.60	25.0	8.7
1950	08	15	97.10	27.30	-	6.0
1950	08	16	95.70	28.60	-	7.0
1950	08	16	92.50	27.50	-	6.7
1950	08	16	97.00	28.80	-	6.6

Year	Month	Day	Longitude (^{o}E)	Latitude (^{o}N)	Depth (km)	Magnitude (Mw)
1950	08	16	94.70	29.40	-	6.6
1950	08	16	95.80	29.10	-	6.4
1950	08	16	96.40	27.40	-	6.0
1950	08	16	91.90	27.90	-	6.0
1950	08	17	95.10	29.20	-	6.2
1950	08	17	96.80	25.90	-	6.0
1950	08	17	91.90	27.90	-	6.0
1950	08	18	96.40	29.40	-	6.6
1950	08	18	95.80	29.40	-	6.5
1950	08	19	96.60	28.70	-	6.0
1950	08	20	94.90	29.90	-	6.4
1950	08	20	95.10	29.20	-	6.0
1950	08	21	94.20	29.40	-	6.1
1950	08	21	97.00	27.50	-	6.0
1950	08	22	94.50	29.30	-	6.3
1950	08	22	97.20	27.40	-	6.3
1950	08	23	95.10	29.30	-	6.3
1950	08	23	96.90	27.20	-	5.9
1950	08	24	96.40	28.30	-	6.3
1950	08	25	95.10	29.20	-	6.0
1950	08	26	95.10	26.80	-	7.0
1950	08	26	95.00	32.00	-	6.0
1950	08	27	94.60	29.90	-	6.2
1950	08	29	95.10	29.20	-	6.0
1950	08	30	96.60	28.70	-	6.0
1950	08	31	95.70	28.20	-	6.1
1950	09	01	95.50	30.00	-	6.0
1950	09	02	96.60	29.90	-	6.5

Year	Month	Day	Longitude (^{o}E)	Latitude (^{o}N)	Depth (km)	Magnitude (Mw)
1950	09	03	94.20	28.70	-	6.0
1950	09	04	96.60	28.70	-	6.0
1950	09	05	92.00	29.30	-	6.0
1950	09	08	96.80	25.90	-	6.0
1950	09	10	95.10	29.20	-	6.0
1950	09	11	95.00	26.80	-	6.0
1950	09	13	95.30	27.80	-	7.0
1950	09	14	95.10	29.20	-	6.0
1950	09	30	94.30	28.70	-	6.7
1950	10	03	96.70	28.00	-	6.3
1950	10	08	96.10	28.90	-	6.6
1950	10	16	95.00	28.30	-	6.0
1950	10	29	94.70	27.80	-	6.0
1950	10	30	96.90	28.00	-	6.0
1950	11	02	97.30	30.60	-	6.3
1950	11	12	94.80	27.70	-	6.0
1950	11	16	96.40	27.50	-	6.0
1950	11	18	94.60	27.70	-	6.7
1950	12	24	91.70	24.40	-	6.3
1951	01	03	94.40	29.00	-	6.6
1951	01	04	94.20	28.60	-	5.6
1951	02	08	94.40	28.20	-	5.8
1951	02	15	98.00	29.00	-	5.3
1951	02	21	94.00	28.90	-	5.8
1951	03	06	95.10	28.80	-	6.4
1951	03	12	94.50	28.20	-	6.5
1951	03	16	96.20	31.20	-	6.0
1951	03	17	97.20	30.90	-	6.5

Year	Month	Day	Longitude (^{O}E)	Latitude (^{O}N)	Depth (km)	Magnitude (Mw)
1951	03	30	97.20	29.90	-	6.0
1951	04	06	97.50	30.50	-	6.0
1951	04	07	90.40	25.80	-	6.8
1951	04	14	94.10	28.20	-	6.4
1951	04	22	94.30	29.20	-	6.5
1951	05	28	87.00	29.00	-	6.0
1951	07	21	96.60	28.70	-	6.0
1951	07	31	95.50	31.20	-	6.0
1951	08	01	95.50	31.20	-	6.0
1951	09	24	96.80	25.90	-	6.0
1951	10	18	93.70	28.80	-	6.0
1951	11	06	96.00	29.00	-	6.0
1951	11	17	91.60	31.00	-	6.3
1951	11	19	91.60	31.00	-	6.0
1951	11	22	91.50	30.50	-	6.0
1951	11	23	91.50	30.50	-	6.0
1951	11	25	91.60	31.00	-	6.0
1951	12	03	92.00	30.00	-	6.0
1951	12	07	90.50	31.00	-	6.0
1951	12	26	90.50	31.00	-	6.3
1952	01	15	94.50	23.80	-	6.0
1952	02	06	95.50	31.20	-	6.0
1952	02	16	95.50	30.00	-	6.0
1952	03	06	90.80	29.60	-	6.0
1952	04	30	91.60	31.00	-	6.0
1952	04	30	94.50	25.50	-	6.0
1952	05	26	94.50	28.50	-	6.0
1952	06	02	91.50	30.50	-	6.0

Year	Month	Day	Longitude (°E)	Latitude (°N)	Depth (km)	Magnitude (Mw)
1952	06	15	91.00	31.50	-	6.0
1952	08	17	91.50	30.50	60.0	7.5
1952	08	25	94.00	28.00	-	6.0
1952	09	15	92.00	30.00	-	6.0
1952	11	07	94.00	25.50	-	6.0
1952	11	14	92.00	30.00	-	6.0
1952	11	28	95.20	25.00	-	6.0
1953	04	23	96.70	30.00	-	6.0
1953	10	08	97.20	29.90	-	6.0
1954	02	23	91.70	27.80	-	6.5
1954	03	21	95.20	24.40	180.0	7.5
1955	04	17	90.00	26.50	-	4.5
1955	05	04	97.00	27.20	-	6.0
1955	09	20	90.00	27.50	-	5.7
1955	11	23	90.00	26.50	-	5.0
1955	12	29	90.30	30.10	-	6.0
1956	01	21	93.50	23.50	-	6.1
1956	02	29	94.20	23.40	60.0	6.4
1956	03	14	90.80	25.20	-	5.0
1956	03	23	90.00	30.00	-	5.0
1956	07	12	94.00	22.60	100.0	6.3
1956	07	16	95.70	22.30	-	7.0
1956	08	22	95.20	28.10	-	5.8
1956	09	19	94.80	23.90	150.0	6.3
1957	07	01	93.80	24.40	-	7.3
1957	12	12	93.00	24.50	-	6.0
1958	01	04	92.00	27.00	-	6.0
1958	01	06	96.80	25.60	-	5.8

Year	Month	Day	Longitude (^{O}E)	Latitude (^{O}N)	Depth (km)	Magnitude (Mw)
1958	02	09	90.90	24.90	-	5.0
1958	02	13	92.50	27.60	-	5.5
1958	03	22	93.80	23.50	-	6.5
1958	10	28	96.30	25.20	-	6.0
1959	02	14	96.00	28.00	-	6.0
1959	02	22	91.50	28.50	-	5.7
1959	05	22	95.50	25.50	-	5.0
1959	06	07	94.00	24.00	-	5.5
1959	06	10	91.00	30.00	-	5.8
1959	08	27	96.00	25.00	-	5.8
1959	11	02	93.00	28.00	-	5.0
1960	05	26	93.00	27.00	-	5.0
1960	07	29	90.30	26.90	-	6.5
1960	08	21	88.60	26.40	-	5.5
1961	02	04	95.30	24.70	-	5.5
1961	06	11	98.60	25.20	-	5.8
1961	06	14	94.80	24.70	-	5.8
1961	09	29	87.00	28.00	-	6.0
1961	11	06	91.90	26.70	-	6.0
1961	12	25	90.00	27.00	-	6.0
1962	09	22	97.00	26.50	-	6.3
1962	10	30	93.30	26.60	-	6.0
1963	02	22	87.10	27.20	-	5.3
1963	06	19	90.50	24.90	-	6.2
1963	06	21	90.90	24.80	-	6.2
1963	10	14	95.30	25.20	-	5.3
1964	01	07	98.70	29.80	46.0	5.0
1964	01	07	98.90	30.10	-	4.5

Year	Month	Day	Longitude (^{o}E)	Latitude (^{o}N)	Depth (km)	Magnitude (Mw)
1964	01	15	95.50	25.20	78.0	4.0
1964	01	22	93.60	22.40	88.0	6.1
1964	01	22	93.80	21.90	-	5.5
1964	01	27	97.20	29.20	33.0	4.9
1964	02	01	87.80	27.30	33.0	4.8
1964	02	18	91.20	27.40	22.0	5.3
1964	02	18	91.40	27.20	-	4.3
1964	02	27	94.40	21.70	102.0	6.5
1964	03	20	94.40	23.60	86.0	5.7
1964	03	27	89.30	27.20	-	6.3
1964	03	27	95.80	25.90	93.0	5.4
1964	03	27	89.40	27.10	29.0	5.0
1964	03	27	89.00	26.80	-	4.5
1964	04	13	90.20	27.60	52.0	6.0
1964	04	15	88.10	21.50	-	5.3
1964	04	15	88.10	21.60	-	5.2
1964	04	15	89.60	23.80	15.0	5.1
1964	06	03	95.80	25.90	100.0	5.9
1964	06	13	94.00	23.00	60.0	5.2
1964	07	12	95.30	24.90	155.0	6.7
1964	07	13	94.70	23.70	117.0	6.0
1964	08	17	94.20	24.30	158.0	4.8
1964	08	30	88.40	27.10	-	5.0
1964	09	01	92.30	27.10	33.0	5.5
1964	10	06	94.60	30.30	33.0	4.5
1964	10	21	93.80	28.10	37.0	6.8
1964	10	21	93.70	28.00	37.0	5.9
1964	10	29	96.70	26.30	170.0	4.7

Year	Month	Day	Longitude (^{O}E)	Latitude (^{O}N)	Depth (km)	Magnitude (Mw)
1964	11	10	92.20	29.80	69.0	4.6
1964	11	25	96.30	26.60	80.0	5.4
1965	01	12	87.84	27.40	23.0	5.4
1965	01	12	87.68	27.31	18.0	4.8
1965	02	18	94.21	24.97	45.0	5.0
1965	02	25	94.64	23.63	94.0	4.7
1965	04	11	92.33	26.82	70.0	4.6
1965	04	30	95.84	28.42	33.0	4.1
1965	05	30	95.80	25.93	101.0	4.9
1965	06	04	95.22	31.78	33.0	4.4
1965	06	11	95.33	24.68	149.0	4.6
1965	06	15	95.51	29.67	30.0	4.9
1965	06	18	93.67	24.94	48.0	4.9
1965	07	05	94.80	21.20	13.0	4.2
1965	10	06	96.18	29.14	41.0	4.5
1965	11	06	91.70	27.10	40.0	4.0
1965	11	15	90.60	30.80	33.0	4.2
1965	12	05	94.46	23.34	97.0	4.7
1965	12	09	92.50	26.70	-	4.9
1965	12	09	92.51	27.43	-	4.8
1965	12	15	94.47	22.00	109.0	4.8
1965	12	17	94.50	22.00	114.0	4.7
1966	02	24	91.44	26.35	47.0	4.7
1966	03	07	98.62	29.19	20.0	4.8
1966	03	23	90.04	25.91	20.0	4.1
1966	04	23	90.47	25.90	45.0	4.4
1966	04	26	96.47	24.90	-	4.5
1966	05	06	92.80	22.10	43.0	4.4

Year	Month	Day	Longitude (^{o}E)	Latitude (^{o}N)	Depth (km)	Magnitude (Mw)
1966	05	23	95.54	24.21	25.0	4.4
1966	05	27	96.57	27.43	40.0	4.5
1966	06	05	93.50	24.60	45.0	4.0
1966	06	26	92.84	26.14	74.0	4.6
1966	07	05	92.60	27.84	33.0	4.5
1966	08	10	91.70	31.00	33.0	4.4
1966	09	11	95.60	26.90	-	4.5
1966	09	19	97.73	24.01	33.0	4.5
1966	09	20	97.68	24.09	32.0	4.7
1966	09	26	92.61	27.49	-	5.1
1966	10	02	94.81	24.41	75.0	4.6
1966	10	18	94.87	24.28	86.0	4.8
1966	10	22	94.28	23.04	72.0	4.8
1966	10	27	93.72	23.84	38.0	4.4
1966	11	08	96.60	25.90	42.0	4.2
1966	12	15	94.43	21.51	84.0	5.2
1967	01	04	94.19	23.55	54.0	4.8
1967	01	13	94.72	23.94	84.0	4.1
1967	01	30	96.14	26.10	39.0	5.0
1967	01	30	90.54	25.40	55.0	4.5
1967	02	08	93.80	23.13	51.0	4.7
1967	02	10	96.50	27.70	33.0	4.3
1967	02	25	92.52	27.38	33.0	4.4
1967	03	11	94.39	28.45	15.0	4.7
1967	03	14	94.29	28.41	20.0	5.3
1967	03	16	96.45	26.91	-	4.4
1967	04	15	95.00	24.04	-	4.4
1967	04	23	94.95	24.76	53.0	4.4

Year	Month	Day	Longitude (^{O}E)	Latitude (^{O}N)	Depth (km)	Magnitude (Mw)
1967	06	08	96.15	26.69	58.0	4.3
1967	06	17	94.68	23.05	122.0	4.3
1967	06	20	96.10	25.40	136.0	4.0
1967	06	26	94.80	23.50	-	4.1
1967	07	07	92.14	27.87	33.0	4.5
1967	08	15	93.56	31.05	36.0	5.1
1967	08	27	94.27	23.20	66.0	4.0
1967	09	06	91.90	24.00	-	4.5
1967	09	15	91.86	27.42	19.0	5.3
1967	09	22	94.70	31.96	33.0	4.5
1967	10	18	94.89	23.38	58.0	4.3
1967	11	10	91.75	25.46	44.0	4.4
1967	11	14	91.61	24.05	24.0	4.5
1967	12	10	94.88	22.49	153.0	4.6
1968	01	18	93.20	23.64	75.0	4.4
1968	01	23	95.65	26.01	96.0	4.5
1968	01	31	92.20	29.80	25.0	4.7
1968	02	12	95.36	22.87	-	4.1
1968	04	13	95.00	24.51	119.0	4.4
1968	05	02	92.28	26.23	51.0	4.3
1968	06	12	91.94	24.83	39.0	4.9
1968	06	28	94.93	30.29	26.0	4.5
1968	06	30	94.82	30.22	48.0	4.4
1968	07	04	94.94	30.25	33.0	4.4
1968	07	13	94.75	30.33	27.0	4.5
1968	07	14	94.77	30.25	48.0	4.5
1968	07	15	95.00	30.26	25.0	4.4
1968	07	16	94.79	30.28	32.0	4.3

Year	Month	Day	Longitude (^{o}E)	Latitude (^{o}N)	Depth (km)	Magnitude (Mw)
1968	07	19	94.85	30.27	30.0	4.5
1968	07	23	94.98	30.27	30.0	4.5
1968	07	25	94.67	30.40	33.0	4.4
1968	07	26	94.84	30.17	33.0	4.4
1968	08	09	94.23	25.28	45.0	4.3
1968	08	18	90.62	26.42	22.0	4.7
1968	08	20	94.87	30.07	33.0	4.5
1968	08	23	94.97	30.28	28.0	4.5
1968	08	24	94.66	30.38	-	4.5
1968	08	25	94.76	30.39	-	4.4
1968	08	29	94.89	30.21	33.0	4.5
1968	09	01	94.85	30.25	31.0	4.5
1968	09	03	95.07	30.25	18.0	4.5
1968	09	11	95.04	30.33	15.0	4.4
1968	09	16	96.08	28.66	60.0	4.5
1968	11	18	92.90	26.90	51.0	4.0
1968	12	27	91.61	24.12	27.0	4.7
1969	01	25	92.40	22.98	49.0	4.8
1969	02	07	94.14	27.46	33.0	4.6
1969	02	18	95.37	24.53	164.0	4.4
1969	02	22	92.36	26.54	38.0	4.3
1969	04	28	95.20	25.93	68.0	4.6
1969	06	01	91.77	25.72	33.0	4.5
1969	06	14	94.64	31.76	33.0	4.6
1969	06	30	92.71	26.93	44.0	4.6
1969	08	10	94.68	21.81	76.0	4.3
1969	08	15	94.66	30.34	33.0	4.5
1969	08	29	96.06	26.35	72.0	4.8

Year	Month	Day	Longitude (^{O}E)	Latitude (^{O}N)	Depth (km)	Magnitude (Mw)
1969	09	29	95.37	24.80	118.0	4.5
1969	09	30	94.80	25.20	50.0	4.5
1969	10	17	94.70	23.09	124.0	5.6
1969	10	22	95.64	28.99	33.0	4.4
1969	10	29	94.38	23.61	70.0	4.4
1969	11	05	90.24	27.66	13.0	4.6
1969	11	11	91.80	26.60	33.0	4.6
1969	11	24	99.00	30.50	51.0	4.3
1969	12	19	93.64	24.43	57.0	4.5
1970	01	19	97.06	26.99	32.0	4.3
1970	02	08	93.46	31.07	27.0	4.3
1970	02	19	93.96	27.40	12.0	5.0
1970	03	10	96.98	26.83	24.0	4.8
1970	03	13	93.99	24.91	59.0	4.5
1970	04	06	96.34	26.45	98.0	4.6
1970	05	29	94.06	23.96	49.0	4.7
1970	06	24	95.81	28.99	19.0	4.4
1970	07	07	94.64	24.34	95.0	4.1
1970	07	25	88.58	25.72	32.0	4.7
1970	07	29	95.37	26.02	68.0	5.9
1970	07	29	95.10	26.24	52.0	4.9
1970	07	29	95.33	26.04	33.0	4.6
1970	07	31	95.61	26.16	47.0	4.7
1970	08	01	98.70	28.90	63.0	4.3
1970	08	13	93.87	24.62	42.0	4.4
1970	08	28	91.55	24.78	39.0	4.5
1970	10	14	94.20	21.83	68.0	4.4
1970	12	01	93.50	21.30	-	4.1

Year	Month	Day	Longitude (°E)	Latitude (°N)	Depth (km)	Magnitude (Mw)
1970	12	25	96.42	24.49	-	4.3
1971	02	02	91.66	23.71	37.0	4.7
1971	03	31	96.68	26.11	41.0	4.4
1971	04	21	92.05	26.20	33.0	4.0
1971	05	17	94.82	24.34	163.0	4.4
1971	05	30	96.41	25.20	-	6.3
1971	05	30	96.43	25.22	44.0	5.2
1971	05	30	96.34	25.28	43.0	4.9
1971	05	31	96.51	25.22	-	6.1
1971	06	16	94.31	23.78	18.0	4.3
1971	06	26	94.78	24.60	74.0	4.7
1971	07	17	93.15	26.41	52.0	5.3
1971	10	10	95.92	23.00	46.0	5.3
1971	10	10	95.29	24.97	133.0	4.4
1971	10	14	95.86	23.06	47.0	5.6
1971	10	24	87.19	28.30	57.0	4.7
1971	10	31	90.65	26.18	33.0	4.4
1971	11	11	93.88	21.44	55.0	4.6
1971	12	04	87.95	27.93	29.0	4.8
1971	12	25	96.58	25.32	33.0	4.3
1971	12	29	94.73	25.17	46.0	5.3
1972	01	20	95.31	31.65	33.0	4.5
1972	03	07	94.95	23.30	141.0	4.0
1972	03	26	93.55	25.79	88.0	4.4
1972	04	01	94.83	22.94	155.0	4.1
1972	04	08	89.42	29.67	49.0	4.5
1972	04	17	95.34	25.58	110.0	4.6
1972	05	10	94.58	21.37	84.0	4.6

Year	Month	Day	Longitude (^{O}E)	Latitude (^{O}N)	Depth (km)	Magnitude (Mw)
1972	06	02	95.86	28.37	13.0	4.2
1972	06	08	92.44	29.59	73.0	4.4
1972	06	27	96.70	25.98	23.0	4.2
1972	07	11	94.60	24.24	61.0	4.3
1972	07	22	91.41	31.38	-	5.8
1972	07	22	91.48	31.46	33.0	4.4
1972	07	28	91.61	31.43	08.0	4.0
1972	08	21	88.02	27.23	33.0	4.7
1972	08	21	88.01	27.33	33.0	4.5
1972	11	01	96.37	26.44	94.0	4.9
1972	11	06	88.43	26.88	59.0	4.5
1972	11	11	95.58	24.75	172.0	4.6
1972	11	22	96.25	25.09	-	4.6
1972	12	18	94.35	21.25	76.0	4.9
1973	01	02	88.08	31.17	43.3	4.7
1973	02	10	94.53	24.43	66.8	4.0
1973	03	19	95.39	26.10	63.9	4.2
1973	03	22	87.15	28.12	33.0	4.6
1973	03	24	98.46	21.42	18.4	4.2
1973	05	31	93.52	24.31	-	5.3
1973	06	01	98.82	25.20	-	4.7
1973	06	01	98.51	24.85	26.4	4.2
1973	07	04	94.86	23.60	125.5	4.6
1973	07	04	92.60	27.49	29.5	4.5
1973	07	12	95.06	24.05	115.4	4.0
1973	07	27	94.49	23.28	60.2	5.0
1973	07	31	97.06	27.23	33.0	4.4
1973	08	01	89.17	29.59	62.9	4.5

Year	Month	Day	Longitude (°E)	Latitude (°N)	Depth (km)	Magnitude (Mw)
1973	08	15	95.52	26.41	60.5	4.1
1973	09	11	92.61	27.08	54.0	4.5
1973	10	09	93.55	27.69	33.0	4.5
1973	10	31	92.45	25.21	33.1	4.0
1973	11	02	91.70	25.72	21.0	4.3
1973	11	19	96.63	25.32	33.0	4.0
1973	12	04	94.08	22.65	62.5	4.2
1973	12	21	94.88	30.27	40.5	4.4
1973	12	26	93.38	22.43	31.4	4.5
1974	01	07	94.72	23.43	108.3	4.4
1974	01	20	92.90	22.80	19.5	4.5
1974	03	05	94.83	23.10	-	4.3
1974	03	20	95.84	23.05	-	4.4
1974	04	05	93.68	21.33	47.0	4.6
1974	04	07	96.58	25.54	-	4.0
1974	05	15	91.91	25.66	34.1	4.2
1974	05	25	95.08	24.56	110.5	4.2
1974	06	22	93.54	25.79	50.1	4.4
1974	07	09	92.32	27.34	53.0	4.3
1974	07	10	95.64	28.94	42.2	4.5
1974	07	23	93.31	22.01	35.0	4.4
1974	07	27	94.88	30.31	29.7	4.4
1974	08	24	96.37	25.76	18.6	4.4
1974	08	30	94.62	22.97	106.7	4.2
1974	09	21	91.04	25.63	27.0	4.4
1974	09	21	94.63	24.14	109.0	4.3
1974	11	16	95.43	24.90	128.3	4.3
1974	12	02	95.31	24.44	106.8	4.5

Year	Month	Day	Longitude (^{O}E)	Latitude (^{O}N)	Depth (km)	Magnitude (Mw)
1974	12	07	93.69	23.88	77.5	4.4
1974	12	21	97.46	25.49	33.0	4.2
1975	01	13	94.55	25.13	33.0	4.1
1975	01	14	97.24	30.56	18.6	4.4
1975	01	17	94.04	22.79	16.3	4.2
1975	01	23	88.37	27.44	33.0	4.2
1975	02	06	87.67	27.95	63.3	4.4
1975	02	09	96.82	29.74	33.0	4.3
1975	03	03	93.50	24.11	42.0	4.5
1975	03	03	94.48	22.35	61.4	4.2
1975	04	24	87.04	27.44	25.5	4.5
1975	04	30	97.00	30.75	15.0	4.2
1975	05	21	94.09	23.86	51.3	4.9
1975	05	30	96.92	26.55	52.7	5.3
1975	05	31	97.15	25.18	112.4	4.1
1975	06	03	96.95	26.59	09.5	5.0
1975	06	03	96.91	26.59	42.6	4.7
1975	06	03	96.96	26.60	37.0	4.4
1975	06	10	95.91	28.19	29.8	4.5
1975	06	24	87.50	27.74	33.0	4.5
1975	06	28	94.89	22.64	137.4	4.5
1975	06	28	95.56	29.06	48.2	4.4
1975	07	08	94.62	21.42	111.8	5.4
1975	07	08	94.80	21.37	113.9	4.0
1975	07	09	94.82	21.60	118.5	4.5
1975	07	23	96.36	26.58	21.7	4.8
1975	09	17	94.22	22.29	68.6	4.4
1975	10	21	94.34	22.92	52.3	4.5

Year	Month	Day	Longitude (°E)	Latitude (°N)	Depth (km)	Magnitude (Mw)
1975	11	19	94.85	21.55	114.5	4.2
1975	11	26	87.80	28.15	33.0	4.6
1975	12	13	94.27	23.62	61.6	4.8
1975	12	20	96.46	27.82	34.0	4.0
1975	12	29	97.07	26.73	33.8	5.0
1975	12	29	97.09	26.69	14.2	4.4
1976	01	25	93.42	30.99	33.0	4.7
1976	02	01	93.50	24.41	59.0	4.0
1976	03	30	94.27	24.26	56.0	4.6
1976	04	04	96.66	25.33	39.0	4.9
1976	04	05	95.42	21.82	44.0	5.5
1976	05	25	95.35	25.08	107.0	4.7
1976	05	29	98.90	24.50	-	7.5
1976	05	29	98.71	24.53	10.0	7.0
1976	05	29	98.93	24.55	32.0	5.2
1976	05	29	98.89	24.47	33.0	4.9
1976	05	29	98.77	24.39	33.0	4.9
1976	05	29	98.79	24.32	33.0	4.5
1976	05	29	98.65	24.47	33.0	4.0
1976	05	29	98.78	24.42	33.0	4.0
1976	05	30	98.81	24.42	28.0	5.1
1976	05	30	98.87	24.54	34.0	4.8
1976	05	30	98.76	24.75	33.0	4.0
1976	05	31	98.64	24.34	14.0	6.2
1976	05	31	98.77	24.38	20.0	5.5
1976	06	01	96.27	26.14	46.0	4.9
1976	06	03	98.67	24.24	33.0	4.8
1976	06	05	96.16	26.13	97.0	4.1

Year	Month	Day	Longitude (^{O}E)	Latitude (^{O}N)	Depth (km)	Magnitude (Mw)
1976	06	08	98.66	24.18	33.0	4.5
1976	06	09	98.75	24.89	33.0	5.9
1976	06	09	98.62	24.68	33.0	4.4
1976	06	20	98.64	24.56	17.0	4.7
1976	06	20	98.61	24.75	33.0	4.1
1976	06	23	88.79	21.42	23.0	5.3
1976	06	30	94.64	22.76	97.0	4.0
1976	07	03	98.68	24.19	33.0	5.4
1976	07	13	98.90	24.55	33.0	4.5
1976	07	21	98.70	24.78	09.0	6.3
1976	07	23	98.68	24.89	33.0	5.0
1976	08	01	98.70	24.81	33.0	4.4
1976	08	04	98.90	24.69	33.0	4.1
1976	08	05	92.39	28.07	61.0	4.7
1976	08	12	97.07	26.68	27.0	6.4
1976	09	14	89.56	29.80	82.0	5.5
1976	09	24	95.01	24.05	164.0	4.6
1976	10	12	98.81	24.48	33.0	5.0
1976	10	31	96.56	26.48	33.0	4.8
1976	11	06	96.44	26.52	66.0	4.5
1976	11	10	96.97	26.51	63.0	4.7
1976	12	06	94.56	24.20	97.0	4.7
1976	12	15	94.61	23.13	97.0	5.0
1976	12	17	92.44	27.75	33.0	4.7
1976	12	25	95.06	25.91	84.0	4.9
1977	01	05	95.15	25.49	105.0	4.5
1977	01	06	87.98	31.25	-	4.8
1977	01	07	98.56	24.28	16.0	4.3

Year	Month	Day	Longitude (°E)	Latitude (°N)	Depth (km)	Magnitude (Mw)
1977	02	03	96.58	25.73	19.0	4.1
1977	02	05	96.54	25.52	57.0	4.1
1977	02	06	92.95	24.33	-	4.4
1977	02	24	96.24	26.08	85.0	4.2
1977	03	05	93.01	31.47	33.0	4.1
1977	03	15	89.41	31.41	19.0	4.5
1977	03	16	89.38	31.30	33.0	4.6
1977	05	12	92.96	21.68	-	5.7
1977	06	05	88.43	26.07	-	4.5
1977	06	16	95.28	30.02	33.0	4.3
1977	06	30	97.10	26.91	36.0	4.6
1977	07	05	95.64	31.90	-	4.4
1977	07	05	97.42	27.15	45.0	4.3
1977	07	10	93.11	26.58	-	4.5
1977	07	21	94.85	30.32	15.0	4.6
1977	07	22	94.81	30.29	20.0	4.3
1977	08	03	94.90	30.27	21.0	4.5
1977	08	03	94.85	30.30	-	4.4
1977	08	04	94.82	30.30	10.0	4.5
1977	08	06	94.79	30.32	35.0	4.4
1977	08	08	94.85	30.30	44.0	4.3
1977	08	13	94.81	30.35	25.0	4.4
1977	08	14	98.08	28.40	33.0	4.7
1977	08	16	94.83	30.29	47.0	4.5
1977	08	18	94.82	30.31	33.0	4.5
1977	08	18	94.84	30.40	62.0	4.5
1977	08	21	94.82	30.32	38.0	4.5
1977	08	21	94.79	30.35	33.0	4.0

Year	Month	Day	Longitude (^{O}E)	Latitude (^{O}N)	Depth (km)	Magnitude (Mw)
1977	08	23	94.84	30.28	36.0	4.5
1977	08	24	94.81	30.30	33.0	4.4
1977	08	25	94.86	30.30	35.0	4.5
1977	08	28	94.94	30.26	46.0	4.5
1977	10	05	97.24	26.74	33.0	4.6
1977	10	13	93.33	23.47	-	4.9
1977	10	17	98.91	25.87	-	4.5
1977	10	27	93.25	31.20	35.0	4.6
1977	10	29	95.02	29.25	33.0	4.2
1977	11	13	93.00	26.51	52.0	4.7
1977	11	24	96.28	25.30	33.0	4.1
1977	11	29	94.71	21.73	109.0	4.1
1977	12	21	95.91	23.82	33.0	4.4
1977	12	22	96.95	26.37	27.0	4.5
1977	12	22	96.11	28.54	33.0	4.5
1977	12	23	92.31	23.71	33.0	4.7
1978	01	08	95.20	24.73	98.0	4.7
1978	01	29	95.64	24.53	-	4.3
1978	01	31	96.87	25.94	33.0	4.1
1978	02	03	94.70	23.02	92.0	4.7
1978	02	03	95.23	28.72	33.0	4.1
1978	02	09	94.76	23.93	86.0	4.9
1978	02	11	94.74	24.31	88.0	4.3
1978	02	22	94.13	23.30	83.0	5.0
1978	02	23	94.70	23.08	113.0	4.8
1978	03	02	96.96	27.28	62.0	4.2
1978	03	18	93.00	24.38	61.0	4.3
1978	03	28	94.54	24.46	53.0	4.8

Year	Month	Day	Longitude (^{o}E)	Latitude (^{o}N)	Depth (km)	Magnitude (Mw)
1978	03	28	92.74	23.15	33.0	4.5
1978	03	31	94.53	25.37	33.0	4.2
1978	04	07	92.38	22.80	49.0	4.5
1978	04	19	92.68	27.67	51.0	4.5
1978	04	19	92.59	27.65	33.0	4.2
1978	04	27	94.64	23.69	61.0	4.2
1978	04	27	96.05	22.09	34.0	4.0
1978	06	09	96.16	25.61	144.0	4.3
1978	06	10	94.65	22.88	113.0	4.8
1978	06	14	98.70	25.78	33.0	4.1
1978	07	03	94.57	23.13	54.0	4.0
1978	07	21	94.83	28.75	35.0	4.7
1978	07	23	94.63	22.89	149.0	4.4
1978	08	04	96.56	26.16	187.0	4.0
1978	08	10	96.94	26.46	38.0	4.7
1978	09	18	94.67	22.69	111.0	4.6
1978	09	22	94.72	23.72	102.0	4.3
1978	09	29	94.75	21.43	96.0	4.5
1978	10	10	93.69	24.37	49.0	4.5
1978	10	14	87.33	27.66	-	4.5
1978	10	20	94.68	24.18	98.0	4.8
1978	10	27	94.53	22.21	116.0	4.3
1978	11	18	92.59	26.55	55.0	4.1
1978	12	08	94.92	22.79	108.0	4.1
1978	12	14	93.73	22.68	75.0	4.0
1978	12	21	95.84	22.92	32.0	4.1
1978	12	29	92.85	23.47	33.0	4.0
1978	12	30	94.17	24.81	33.0	4.6

Year	Month	Day	Longitude (^{O}E)	Latitude (^{O}N)	Depth (km)	Magnitude (Mw)
1979	01	09	92.49	24.96	64.0	4.5
1979	01	13	91.89	27.39	33.0	4.0
1979	01	14	95.49	25.15	33.0	4.6
1979	01	28	91.02	24.87	-	4.0
1979	02	18	95.98	23.04	43.0	5.3
1979	02	26	91.23	25.98	54.0	4.0
1979	03	03	94.52	24.48	89.0	4.4
1979	03	04	93.50	24.56	33.0	4.3
1979	03	18	96.67	25.04	46.0	4.7
1979	03	25	94.09	22.30	81.0	4.2
1979	03	28	94.82	24.61	71.0	4.5
1979	04	02	90.68	26.46	33.0	4.5
1979	04	10	94.62	24.94	33.0	4.5
1979	04	11	88.84	25.98	33.0	4.5
1979	04	18	94.00	24.19	74.0	4.5
1979	04	25	96.63	27.43	24.0	4.3
1979	05	12	92.43	23.95	27.0	4.0
1979	05	18	95.84	23.73	33.0	4.3
1979	05	19	92.79	22.31	61.0	4.2
1979	05	29	94.74	24.50	82.0	4.6
1979	05	30	94.69	22.13	126.0	4.6
1979	05	31	95.16	25.28	102.0	4.4
1979	06	08	96.52	25.13	66.0	4.4
1979	06	19	87.48	26.74	02.0	4.9
1979	06	26	94.19	30.32	33.0	4.3
1979	07	13	95.22	24.88	109.0	4.3
1979	07	29	91.81	26.81	68.0	4.8
1979	08	01	95.60	26.18	96.0	4.3

Year	Month	Day	Longitude (°E)	Latitude (°N)	Depth (km)	Magnitude (Mw)
1979	08	04	94.89	30.30	39.0	4.5
1979	08	07	94.88	30.42	37.0	4.5
1979	08	08	98.85	25.11	10.0	5.0
1979	08	11	94.93	24.20	113.0	4.7
1979	08	12	94.92	30.23	54.0	4.4
1979	08	21	95.15	25.95	137.0	4.3
1979	09	08	98.72	31.84	33.0	4.0
1979	09	21	96.80	24.90	33.0	4.3
1979	09	29	95.77	24.01	33.0	4.6
1979	09	29	95.80	29.04	35.0	4.6
1979	10	09	94.95	21.80	138.0	4.1
1979	10	17	87.62	27.97	33.0	4.3
1979	10	17	96.85	23.63	-	4.2
1979	10	19	94.35	23.04	91.0	4.9
1979	11	07	93.95	22.10	80.0	4.2
1979	11	12	96.00	22.81	07.0	4.4
1979	11	16	88.69	27.95	39.0	4.3
1979	11	25	96.32	25.21	32.0	5.5
1979	12	03	94.90	24.41	-	4.6
1979	12	06	95.48	30.05	12.0	5.1
1979	12	21	97.04	27.10	32.0	5.5
1979	12	25	97.24	26.89	-	4.6
1980	01	01	98.60	26.08	-	4.1
1980	01	02	96.46	31.70	49.0	4.3
1980	01	06	98.64	25.87	47.0	4.3
1980	01	13	98.02	29.19	-	4.0
1980	01	27	95.17	24.69	167.0	4.1
1980	02	08	93.59	21.27	58.0	4.9

Year	Month	Day	Longitude (^{O}E)	Latitude (^{O}N)	Depth (km)	Magnitude (Mw)
1980	02	22	88.65	30.55	14.0	6.6
1980	02	22	88.68	30.62	39.0	4.5
1980	02	22	88.68	30.55	41.0	4.5
1980	02	22	88.74	30.67	-	4.5
1980	02	22	88.74	30.64	38.0	4.4
1980	02	22	88.78	30.61	21.0	4.3
1980	02	23	94.61	23.37	86.0	4.5
1980	02	23	88.77	30.56	33.0	4.0
1980	02	28	88.71	30.54	33.0	4.3
1980	03	01	96.30	28.64	33.0	4.3
1980	03	04	88.68	30.54	49.0	4.5
1980	03	26	94.41	28.63	48.0	4.2
1980	03	28	94.69	23.87	97.0	4.2
1980	04	04	93.76	21.30	64.0	4.7
1980	04	13	95.52	30.20	30.0	4.7
1980	04	14	95.47	30.18	02.0	4.4
1980	05	16	96.22	22.71	33.0	4.2
1980	05	20	94.20	23.72	83.0	5.4
1980	05	27	95.99	28.15	33.0	4.1
1980	06	03	88.65	30.75	-	5.6
1980	06	10	88.57	30.42	64.0	4.3
1980	06	11	90.31	25.79	69.0	4.0
1980	06	25	88.84	30.57	33.0	4.1
1980	07	16	94.79	22.51	33.0	4.4
1980	07	17	93.71	22.51	77.0	4.5
1980	08	01	96.15	23.92	37.0	4.9
1980	08	07	94.84	30.32	29.0	4.1
1980	08	09	94.94	30.25	26.0	4.0

Year	Month	Day	Longitude (°E)	Latitude (°N)	Depth (km)	Magnitude (Mw)
1980	08	10	94.91	30.32	57.0	4.3
1980	08	12	94.62	24.81	52.0	4.8
1980	08	18	94.95	26.65	57.0	4.6
1980	08	19	94.89	30.34	39.0	4.4
1980	08	23	94.89	30.35	34.0	4.3
1980	08	25	94.88	30.36	42.0	4.1
1980	08	26	94.91	30.36	19.0	4.2
1980	08	28	94.91	21.90	122.0	4.3
1980	08	29	94.94	30.32	44.0	4.3
1980	08	30	96.40	28.76	35.0	4.5
1980	08	30	94.89	30.40	34.0	4.2
1980	09	02	94.89	30.36	37.0	4.4
1980	09	03	94.93	30.29	49.0	4.2
1980	09	04	94.93	30.28	42.0	4.2
1980	09	09	94.93	30.27	41.0	4.3
1980	09	13	94.90	30.24	48.0	4.4
1980	09	14	95.33	24.89	109.0	4.5
1980	09	14	94.91	30.35	15.0	4.0
1980	09	19	94.92	30.27	43.0	4.1
1980	09	20	94.89	30.34	37.0	4.1
1980	09	24	94.89	30.34	24.0	4.1
1980	10	04	95.15	23.09	122.0	4.5
1980	10	08	87.72	31.43	34.0	4.6
1980	10	10	96.94	27.16	22.0	4.9
1980	10	23	95.00	22.58	127.0	4.1
1980	10	30	91.46	23.90	30.0	4.6
1980	11	19	88.80	27.40	-	6.6
1980	11	20	93.92	22.74	30.0	5.1

Year	Month	Day	Longitude (^{O}E)	Latitude (^{O}N)	Depth (km)	Magnitude (Mw)
1980	12	01	90.94	22.06	33.0	4.4
1980	12	11	95.97	24.22	170.0	4.2
1980	12	22	89.59	26.67	33.0	4.2
1980	12	26	88.88	29.08	67.0	4.2
1980	12	31	93.59	21.08	64.0	4.6
1981	02	01	96.34	24.77	21.0	4.6
1981	02	07	97.14	26.29	58.0	4.0
1981	02	08	88.61	30.60	33.0	4.5
1981	02	09	89.76	27.20	16.0	4.5
1981	02	28	93.66	26.03	40.0	4.6
1981	03	07	97.82	22.13	-	4.6
1981	03	07	94.88	24.66	81.0	4.0
1981	03	19	90.48	26.29	-	4.5
1981	03	26	89.08	22.35	-	4.5
1981	03	31	96.93	26.51	26.0	4.4
1981	04	04	95.14	25.02	115.0	4.1
1981	04	11	95.04	24.63	137.0	4.0
1981	04	25	95.34	24.90	146.0	5.1
1981	04	29	96.62	26.12	33.0	4.0
1981	05	01	94.56	22.94	98.0	4.1
1981	05	06	93.87	22.47	76.0	4.5
1981	05	06	93.15	23.70	33.0	4.0
1981	05	14	98.68	25.94	24.0	4.0
1981	06	17	93.68	23.72	67.0	4.6
1981	06	30	95.19	22.50	42.0	4.9
1981	07	07	97.90	25.13	42.0	5.1
1981	07	15	94.26	22.59	101.0	4.0
1981	07	18	94.65	24.79	81.0	5.0

Year	Month	Day	Longitude (°E)	Latitude (°N)	Depth (km)	Magnitude (Mw)
1981	07	30	94.68	22.95	113.0	4.3
1981	08	04	97.78	25.03	-	4.3
1981	08	14	97.96	25.15	38.0	5.1
1981	08	16	96.63	25.52	38.0	5.2
1981	08	16	96.65	25.48	41.0	4.1
1981	08	16	96.64	25.53	40.0	4.0
1981	08	18	96.20	25.47	33.0	4.6
1981	08	23	96.06	26.70	82.0	4.8
1981	08	23	94.43	22.89	90.0	4.5
1981	08	23	94.91	24.68	91.0	4.4
1981	08	28	97.71	24.92	70.0	4.0
1981	08	29	97.89	24.95	46.0	4.3
1981	09	05	95.56	26.51	37.0	4.2
1981	09	23	91.64	30.66	19.0	4.2
1981	09	27	95.47	26.60	33.0	4.3
1981	10	03	94.87	30.35	32.0	4.3
1981	10	09	94.44	23.67	117.0	4.6
1981	10	14	94.82	28.67	65.0	4.4
1981	10	19	88.12	31.32	33.0	4.2
1981	10	23	94.93	29.89	-	5.4
1981	10	24	95.02	29.90	33.0	5.0
1981	10	26	94.93	30.03	-	4.5
1981	11	15	95.13	25.65	70.0	4.4
1981	11	21	93.23	22.70	44.0	4.3
1981	11	21	89.12	29.53	50.0	4.3
1981	12	09	92.51	27.50	33.0	4.4
1981	12	11	95.08	25.02	122.0	4.3
1981	12	13	95.07	29.92	21.0	4.7

Year	Month	Day	Longitude (^{O}E)	Latitude (^{O}N)	Depth (km)	Magnitude (Mw)
1982	01	03	94.35	24.69	85.0	4.9
1982	01	11	92.06	24.70	40.0	4.0
1982	01	22	89.87	30.89	-	5.7
1982	01	24	94.67	21.41	120.0	4.9
1982	01	28	90.89	25.47	33.0	4.1
1982	01	31	96.46	25.11	43.0	4.3
1982	02	12	94.66	21.90	122.0	4.5
1982	02	16	98.22	23.86	-	4.0
1982	02	26	90.62	25.79	49.0	4.6
1982	02	26	92.29	26.30	33.0	4.5
1982	02	26	94.83	24.07	140.0	4.1
1982	03	24	88.70	30.55	33.0	4.3
1982	03	24	95.64	24.16	33.0	4.1
1982	03	30	95.58	23.56	42.0	4.9
1982	04	03	94.42	22.35	99.0	4.5
1982	04	05	88.84	27.38	-	5.2
1982	04	06	94.47	24.35	102.0	4.3
1982	04	22	95.00	29.94	14.0	5.4
1982	04	24	92.92	28.31	52.0	4.4
1982	05	02	95.06	29.90	38.0	4.6
1982	05	17	94.99	25.34	95.0	4.8
1982	05	22	93.96	24.10	76.0	4.3
1982	05	29	95.51	29.68	22.0	4.8
1982	06	01	94.72	24.65	79.0	4.0
1982	06	20	89.97	26.24	33.0	4.4
1982	06	25	94.45	23.06	102.0	4.1
1982	07	02	96.61	28.57	60.0	4.4
1982	07	05	96.49	26.95	-	4.5

Year	Month	Day	Longitude (^{o}E)	Latitude (^{o}N)	Depth (km)	Magnitude (Mw)
1982	07	06	90.31	25.88	08.0	4.4
1982	07	24	96.52	30.11	59.0	4.2
1982	08	18	89.26	27.04	51.0	4.8
1982	08	21	92.23	25.16	51.0	4.6
1982	08	30	96.70	25.38	39.0	5.0
1982	08	31	91.46	25.38	32.0	4.5
1982	09	04	95.93	22.92	41.0	5.1
1982	09	14	95.31	25.93	88.0	4.6
1982	09	20	95.94	22.88	25.0	5.2
1982	09	21	91.27	25.15	43.0	4.6
1982	10	07	94.40	23.42	102.0	4.3
1982	10	26	95.17	29.77	41.0	4.9
1982	11	14	94.57	22.06	105.0	4.5
1982	11	14	97.10	21.20	40.0	4.1
1982	11	18	91.75	26.38	-	4.7
1982	11	26	94.87	27.78	29.0	4.4
1982	11	29	94.59	22.23	132.0	4.5
1982	12	10	95.15	28.99	-	4.3
1982	12	11	94.48	24.52	66.0	4.2
1982	12	12	94.69	24.83	-	4.5
1982	12	15	96.00	25.71	-	4.7
1982	12	17	95.15	24.96	116.0	4.7
1982	12	25	96.38	26.40	110.0	4.5
1982	12	30	91.66	26.25	33.0	4.5
1982	12	30	91.69	26.01	61.0	4.3
1983	01	03	94.45	24.23	84.0	4.5
1983	01	12	97.00	26.90	31.0	4.6
1983	01	12	96.80	26.72	53.0	4.3

Year	Month	Day	Longitude (^{O}E)	Latitude (^{O}N)	Depth (km)	Magnitude (Mw)
1983	01	13	95.03	24.67	109.0	5.0
1983	01	14	95.86	29.08	43.0	4.4
1983	01	19	91.36	25.46	10.0	4.0
1983	01	25	96.42	26.40	121.0	4.5
1983	01	29	94.24	24.01	90.0	4.2
1983	01	31	95.04	24.72	70.0	4.6
1983	02	02	92.87	26.90	42.0	4.5
1983	02	20	95.96	22.79	-	4.3
1983	03	01	96.05	28.63	40.0	4.5
1983	03	05	93.89	22.83	50.0	4.5
1983	04	01	93.69	21.86	67.0	4.1
1983	04	04	96.79	26.46	33.0	4.0
1983	04	09	99.00	21.78	13.0	4.5
1983	04	13	93.41	25.61	33.0	4.4
1983	04	13	94.48	22.86	120.0	4.4
1983	04	17	94.36	22.03	93.0	4.4
1983	04	30	96.71	25.65	35.0	4.7
1983	05	01	92.24	25.09	-	4.4
1983	05	07	94.76	22.89	99.0	4.3
1983	06	16	95.62	26.03	98.0	5.2
1983	06	26	93.87	23.06	81.0	4.6
1983	07	23	91.25	25.37	59.0	4.2
1983	07	31	97.02	30.17	57.0	4.2
1983	08	03	98.54	21.76	-	4.7
1983	08	07	98.95	21.84	-	4.2
1983	08	13	98.03	21.34	-	4.2
1983	08	16	90.99	31.45	50.0	4.4
1983	08	21	94.43	22.73	124.0	4.5

Year	Month	Day	Longitude (^{o}E)	Latitude (^{o}N)	Depth (km)	Magnitude (Mw)
1983	08	23	95.12	24.55	128.0	4.8
1983	08	30	94.67	25.04	60.0	5.7
1983	09	18	94.79	23.05	61.0	4.5
1983	09	23	95.12	24.77	115.0	4.8
1983	10	02	92.52	28.05	38.0	4.4
1983	10	16	90.31	29.51	33.0	4.2
1983	10	21	94.38	22.00	97.0	4.8
1983	10	21	94.42	24.89	71.0	4.1
1983	11	16	96.12	26.16	135.0	4.9
1983	11	17	91.73	25.15	42.0	4.1
1983	12	22	95.52	26.00	151.0	4.1
1983	12	23	87.91	25.87	33.0	4.0
1984	01	07	94.49	21.54	116.0	4.2
1984	01	14	88.06	31.41	62.0	4.0
1984	01	15	96.37	28.64	23.0	4.2
1984	01	18	95.05	28.86	-	4.2
1984	01	20	96.36	28.65	28.0	4.8
1984	01	20	94.47	24.00	110.0	4.3
1984	01	21	96.61	30.26	10.0	5.1
1984	01	24	95.50	30.15	41.0	4.4
1984	02	05	94.71	22.72	93.0	4.4
1984	02	19	94.79	24.99	51.0	4.6
1984	02	20	95.70	28.96	22.0	4.3
1984	02	28	94.57	22.18	96.0	4.4
1984	03	05	94.62	24.52	68.0	5.0
1984	03	11	98.74	24.73	-	4.3
1984	03	21	93.30	26.76	15.0	4.3
1984	04	25	95.70	26.03	109.0	4.6

Year	Month	Day	Longitude (^{O}E)	Latitude (^{O}N)	Depth (km)	Magnitude (Mw)
1984	05	06	93.53	24.22	32.0	5.9
1984	05	07	94.57	24.87	89.0	4.3
1984	05	16	94.96	24.72	119.0	4.3
1984	05	21	91.51	23.66	13.0	4.8
1984	06	09	92.61	26.91	72.0	4.2
1984	07	04	92.74	25.80	33.0	4.3
1984	07	05	94.82	24.81	79.0	4.5
1984	07	07	94.33	24.81	74.0	4.2
1984	07	19	97.61	21.82	10.0	4.2
1984	07	24	95.86	26.02	33.0	4.3
1984	07	27	96.62	21.73	10.0	4.3
1984	07	28	96.34	21.77	33.0	4.6
1984	08	05	94.32	23.47	80.0	4.5
1984	09	08	96.59	22.72	33.0	4.4
1984	09	16	93.58	24.65	36.0	4.6
1984	09	22	92.15	26.49	29.0	5.0
1984	09	28	94.34	23.04	55.0	4.1
1984	09	30	91.51	25.44	34.0	4.7
1984	10	02	88.58	31.00	33.0	4.0
1984	10	03	93.44	25.37	59.0	4.4
1984	10	07	97.22	24.63	47.0	4.7
1984	10	18	94.50	24.03	117.0	4.2
1984	10	28	89.18	30.18	33.0	4.0
1984	11	01	94.64	22.24	117.0	4.1
1984	11	13	94.18	24.04	77.0	4.1
1984	11	15	92.72	26.72	84.0	4.4
1984	11	15	95.20	22.09	87.0	4.2
1984	11	21	96.49	25.42	33.0	4.4

Year	Month	Day	Longitude (^{o}E)	Latitude (^{o}N)	Depth (km)	Magnitude (Mw)
1984	11	28	97.08	26.65	-	5.9
1984	11	28	89.01	31.81	33.0	5.5
1984	11	28	95.02	24.61	115.0	5.0
1984	12	02	96.95	26.73	62.0	4.4
1984	12	03	96.84	27.41	84.0	5.0
1984	12	03	96.70	27.51	58.0	4.1
1984	12	08	94.84	24.33	107.0	4.0
1984	12	26	93.10	21.07	45.0	4.1
1984	12	30	92.85	24.66	-	5.7
1985	01	07	91.96	27.14	12.0	5.2
1985	01	07	91.77	27.20	33.0	4.3
1985	01	11	91.90	27.13	33.0	4.8
1985	01	21	94.38	24.70	94.0	4.6
1985	01	25	94.52	23.32	107.0	5.5
1985	02	03	94.54	25.42	62.0	4.5
1985	02	17	95.24	25.54	85.0	4.7
1985	02	21	96.04	28.35	15.0	5.0
1985	02	23	94.75	28.97	46.0	4.4
1985	03	04	94.61	23.74	99.0	4.0
1985	03	05	94.08	27.72	52.0	4.9
1985	04	02	94.46	24.31	97.0	4.4
1985	04	06	92.52	28.42	33.0	4.5
1985	04	17	96.01	23.96	39.0	4.6
1985	04	24	96.08	26.18	46.0	5.4
1985	05	10	94.27	22.04	87.0	4.0
1985	05	17	95.26	25.30	87.0	4.4
1985	05	25	88.48	27.63	33.0	4.3
1985	05	30	98.26	30.94	06.0	4.7

Year	Month	Day	Longitude (^{O}E)	Latitude (^{O}N)	Depth (km)	Magnitude (Mw)
1985	06	07	96.21	26.87	33.0	4.5
1985	06	17	90.20	25.65	22.0	4.3
1985	07	18	94.80	30.36	-	4.2
1985	07	19	94.91	30.38	33.0	4.6
1985	07	20	94.83	30.35	-	4.7
1985	07	20	94.86	30.29	35.0	4.5
1985	07	21	94.23	29.97	33.0	4.0
1985	07	26	94.87	30.33	26.0	4.2
1985	07	27	94.84	30.32	19.0	4.5
1985	07	28	88.61	30.15	66.0	4.2
1985	08	01	95.16	29.15	36.0	5.7
1985	08	23	97.59	25.33	40.0	5.0
1985	08	25	97.68	25.45	14.0	5.1
1985	09	05	97.71	25.40	20.0	5.3
1985	09	07	97.51	25.86	38.0	4.0
1985	09	09	97.53	25.85	33.0	4.2
1985	09	11	97.73	25.37	31.0	4.6
1985	10	02	89.73	27.19	45.0	4.1
1985	10	12	92.52	27.11	14.0	5.0
1985	10	12	92.62	27.19	10.0	4.5
1985	10	12	95.18	24.79	108.0	4.0
1985	10	14	97.21	26.50	33.0	4.6
1985	10	25	92.48	27.20	33.0	4.5
1985	10	31	92.51	27.10	18.0	4.7
1985	11	01	96.86	27.28	44.0	4.3
1985	11	03	91.52	23.61	-	4.5
1985	11	08	93.96	22.65	47.0	4.2
1985	11	09	94.61	21.26	108.0	4.0

Year	Month	Day	Longitude (°E)	Latitude (°N)	Depth (km)	Magnitude (Mw)
1985	11	26	94.67	25.06	33.0	4.1
1985	11	28	97.14	26.23	20.0	5.0
1985	12	22	93.24	24.10	-	4.6
1985	12	26	92.07	27.09	11.0	4.0
1986	01	02	92.63	22.49	28.0	4.2
1986	01	07	88.43	27.38	42.0	4.0
1986	01	08	93.96	23.38	82.0	4.4
1986	01	17	94.31	22.75	62.0	4.9
1986	01	18	95.56	21.10	22.0	5.3
1986	01	23	98.73	29.59	33.0	4.2
1986	01	27	95.90	22.88	10.0	5.2
1986	01	27	98.42	29.74	39.0	4.5
1986	02	05	98.42	29.82	20.0	5.1
1986	02	08	93.00	23.87	30.0	5.3
1986	02	08	93.86	22.06	76.0	4.0
1986	02	10	87.86	28.15	67.0	4.4
1986	02	13	94.62	21.52	122.0	4.4
1986	02	19	91.13	25.10	-	4.9
1986	03	06	97.11	26.69	51.0	4.3
1986	03	29	98.87	26.10	33.0	4.1
1986	04	04	88.20	30.81	44.0	4.2
1986	04	17	94.74	24.43	86.0	5.2
1986	04	18	95.61	21.23	10.0	4.3
1986	04	20	95.36	25.05	112.0	4.9
1986	04	26	94.51	22.85	102.0	4.5
1986	04	29	88.26	31.43	35.0	4.0
1986	05	09	94.46	21.64	97.0	4.5
1986	05	22	91.06	31.67	33.0	4.5

Year	Month	Day	Longitude (^{O}E)	Latitude (^{O}N)	Depth (km)	Magnitude (Mw)
1986	05	23	91.18	31.67	33.0	4.5
1986	06	23	96.89	26.25	32.0	4.3
1986	07	02	96.80	25.06	49.0	4.1
1986	07	16	91.58	27.57	33.0	4.5
1986	07	23	95.54	26.75	68.0	4.0
1986	07	26	94.19	23.71	38.0	5.1
1986	08	16	94.11	22.60	89.0	4.6
1986	08	16	94.22	22.67	85.0	4.6
1986	09	09	97.14	23.68	33.0	4.7
1986	09	10	92.15	25.38	47.0	4.6
1986	09	15	98.77	24.65	10.0	4.6
1986	09	30	94.02	23.41	72.0	4.2
1986	10	10	94.89	30.33	26.0	4.4
1986	10	12	94.86	30.38	33.0	4.5
1986	10	13	94.74	30.40	33.0	4.5
1986	10	14	91.97	25.03	33.0	4.4
1986	11	01	96.40	26.85	11.0	5.0
1986	11	08	92.21	27.17	48.0	4.2
1986	11	10	98.38	24.12	-	4.1
1986	11	22	94.76	25.27	65.0	4.3
1986	11	29	96.93	26.10	20.0	4.6
1986	12	22	95.09	29.87	33.0	4.5
1986	12	31	92.91	26.47	46.0	4.6
1987	01	09	95.19	28.62	33.0	4.3
1987	01	24	92.69	27.63	24.0	4.6
1987	02	07	94.75	23.68	108.0	4.6
1987	02	13	94.08	23.10	47.0	4.2
1987	02	15	94.83	24.25	109.0	4.8

Year	Month	Day	Longitude (°E)	Latitude (°N)	Depth (km)	Magnitude (Mw)
1987	03	01	95.85	28.67	17.0	4.7
1987	03	22	96.71	25.92	40.0	4.1
1987	03	26	96.37	24.93	43.0	4.6
1987	04	01	98.54	21.94	-	5.0
1987	04	03	95.18	24.87	140.0	4.4
1987	04	06	95.93	26.50	105.0	4.7
1987	04	23	87.01	27.93	48.0	4.4
1987	04	29	93.73	22.60	48.0	4.9
1987	04	29	94.64	24.07	107.0	4.7
1987	05	10	87.27	28.99	33.0	4.3
1987	05	16	98.37	26.24	27.0	4.3
1987	05	18	94.21	25.23	53.0	6.2
1987	05	20	96.71	26.92	81.0	4.2
1987	05	30	94.58	22.70	111.0	4.3
1987	06	10	94.39	23.60	33.0	4.4
1987	06	11	93.59	26.15	62.0	4.7
1987	06	14	94.74	21.15	113.0	4.0
1987	07	10	96.94	27.32	43.0	4.6
1987	07	16	92.33	23.55	33.0	4.1
1987	07	16	92.44	21.16	33.0	4.0
1987	07	17	92.68	27.76	-	4.7
1987	07	19	95.19	24.95	123.0	4.5
1987	08	06	94.31	23.45	110.0	4.4
1987	08	24	94.41	23.05	86.0	4.8
1987	08	26	94.33	21.83	123.0	4.1
1987	09	03	93.85	21.26	60.0	4.2
1987	09	05	93.81	23.84	76.0	4.5
1987	09	06	93.41	26.64	58.0	4.6

Year	Month	Day	Longitude (^{O}E)	Latitude (^{O}N)	Depth (km)	Magnitude (Mw)
1987	09	09	95.27	24.78	122.0	4.5
1987	09	13	92.84	27.32	33.0	4.1
1987	09	17	94.83	30.35	-	4.4
1987	09	19	94.81	30.34	-	4.2
1987	09	22	94.81	30.32	33.0	4.5
1987	09	23	95.67	22.25	33.0	4.3
1987	09	23	94.53	30.77	33.0	4.1
1987	09	25	90.37	29.84	19.0	5.2
1987	09	26	90.45	29.82	33.0	4.3
1987	09	26	94.30	21.92	103.0	4.2
1987	09	28	94.90	23.66	100.0	4.4
1987	09	29	90.41	29.91	33.0	4.5
1987	09	29	90.41	29.73	46.0	4.2
1987	10	06	90.42	29.90	10.0	5.0
1987	10	10	98.88	21.79	33.0	4.1
1987	10	15	92.77	27.38	27.0	4.1
1987	10	22	89.06	27.07	19.0	4.5
1987	11	01	90.01	29.63	33.0	4.0
1987	11	15	93.38	26.52	53.0	4.0
1987	11	23	93.57	30.26	33.0	4.5
1987	11	24	97.50	21.58	33.0	4.4
1987	11	28	95.78	25.56	33.0	4.1
1987	12	01	93.22	26.33	59.0	4.8
1987	12	11	90.92	26.04	57.0	4.3
1987	12	12	90.40	29.75	45.0	4.5
1987	12	22	95.28	29.91	-	4.1
1988	01	01	94.78	30.11	33.0	4.2
1988	01	10	90.29	29.75	50.0	5.3

Year	Month	Day	Longitude (°E)	Latitude (°N)	Depth (km)	Magnitude (Mw)
1988	01	10	90.44	29.89	10.0	4.9
1988	01	19	88.80	27.77	33.0	4.0
1988	01	20	93.73	23.39	92.0	4.1
1988	01	25	94.87	30.16	-	5.1
1988	02	06	91.56	24.67	33.0	5.9
1988	02	12	93.90	25.08	33.0	4.1
1988	02	15	93.93	21.53	73.0	4.4
1988	02	16	94.81	30.00	25.0	4.4
1988	02	17	94.37	24.29	111.0	4.5
1988	02	17	92.11	27.11	02.0	4.5
1988	02	17	92.99	26.73	46.0	4.2
1988	02	24	94.08	23.33	72.0	4.9
1988	02	24	95.63	25.98	112.0	4.2
1988	02	28	91.56	24.72	22.0	4.5
1988	03	06	95.41	25.97	106.0	4.4
1988	03	28	95.05	29.99	33.0	4.2
1988	04	06	92.47	28.27	33.0	4.0
1988	04	11	97.18	27.01	19.0	4.2
1988	04	18	93.88	24.88	60.0	4.1
1988	05	09	94.77	29.02	20.0	4.8
1988	05	10	94.78	29.04	23.0	4.7
1988	05	10	90.88	25.32	33.0	4.1
1988	05	11	96.50	25.31	53.0	4.7
1988	05	26	88.61	27.45	42.0	4.4
1988	06	06	94.73	29.05	10.0	4.1
1988	06	28	94.80	24.66	139.0	4.8
1988	07	03	94.26	22.07	83.0	4.5
1988	07	05	91.24	28.11	66.0	4.6

Year	Month	Day	Longitude (^{O}E)	Latitude (^{O}N)	Depth (km)	Magnitude (Mw)
1988	07	10	95.38	25.03	125.0	5.6
1988	07	11	95.96	26.24	33.0	4.5
1988	07	11	93.88	22.46	33.0	4.3
1988	08	06	95.15	25.13	100.0	7.2
1988	08	06	94.99	25.34	86.0	4.1
1988	08	07	94.90	25.05	107.0	4.6
1988	08	07	95.29	25.72	33.0	4.5
1988	08	08	95.34	25.08	95.0	4.9
1988	08	08	95.03	25.38	109.0	4.7
1988	08	13	95.13	25.29	91.0	4.7
1988	08	21	95.10	25.27	92.0	4.4
1988	08	29	87.51	26.39	33.0	4.2
1988	09	03	97.33	29.95	22.0	5.3
1988	09	04	94.98	25.15	86.0	4.1
1988	09	04	91.75	26.30	07.0	4.1
1988	09	17	95.09	25.21	100.0	4.6
1988	09	19	94.25	21.89	86.0	4.3
1988	09	27	88.37	27.19	28.0	5.0
1988	09	30	98.83	30.32	33.0	4.1
1988	10	09	94.72	24.68	46.0	4.3
1988	10	12	95.73	24.89	33.0	4.2
1988	10	19	94.89	30.05	33.0	4.6
1988	10	22	95.77	25.78	33.0	4.3
1988	11	07	88.47	31.90	33.0	4.0
1988	11	09	98.94	23.24	10.0	4.2
1988	11	27	93.72	23.52	33.0	4.8
1988	11	30	94.56	24.09	83.0	4.0
1988	12	04	95.02	25.12	100.0	4.9

Year	Month	Day	Longitude (^{o}E)	Latitude (^{o}N)	Depth (km)	Magnitude (Mw)
1988	12	13	87.97	27.14	52.0	4.2
1988	12	20	91.12	27.66	39.0	4.6
1988	12	22	98.95	23.05	12.0	4.3
1988	12	24	87.97	26.91	41.0	4.1
1988	12	27	94.74	23.25	124.0	4.7
1988	12	27	87.86	27.98	38.0	4.6
1988	12	28	96.99	26.97	29.0	4.2
1988	12	29	93.34	24.74	79.0	4.0
1988	12	30	93.92	22.42	65.0	4.4
1989	01	02	95.10	24.98	109.0	5.0
1989	01	07	98.83	23.28	18.0	4.0
1989	01	10	92.89	24.62	33.0	4.0
1989	01	19	94.62	30.00	33.0	4.5
1989	01	27	94.95	25.32	93.0	4.2
1989	02	03	89.94	30.19	19.0	5.6
1989	02	03	89.97	30.27	10.0	4.1
1989	02	04	90.09	30.19	10.0	4.4
1989	02	05	90.07	30.12	10.0	4.1
1989	02	12	96.90	26.20	20.0	5.0
1989	02	20	98.02	31.25	43.0	4.4
1989	02	22	98.94	25.98	46.0	4.2
1989	02	28	92.64	27.10	42.0	4.4
1989	03	01	97.98	21.74	11.0	6.0
1989	03	01	97.82	21.62	10.0	4.5
1989	03	08	92.77	26.94	59.0	4.4
1989	03	17	97.87	21.64	33.0	4.6
1989	03	17	97.73	21.95	33.0	4.4
1989	04	03	94.66	25.15	58.0	5.1

Year	Month	Day	Longitude (^{O}E)	Latitude (^{O}N)	Depth (km)	Magnitude (Mw)
1989	04	06	95.11	25.02	103.0	4.2
1989	04	08	96.75	26.41	33.0	4.2
1989	04	09	90.02	29.11	10.0	4.9
1989	04	13	92.43	24.40	10.0	5.2
1989	04	16	95.95	25.08	35.0	4.5
1989	04	18	95.79	29.00	18.0	4.3
1989	04	19	89.96	30.16	39.0	4.4
1989	04	21	95.54	21.66	58.0	4.4
1989	04	22	96.90	26.60	15.0	4.1
1989	04	24	94.84	24.38	119.0	4.7
1989	04	25	98.62	30.72	33.0	4.0
1989	04	25	98.99	30.42	39.0	4.0
1989	04	28	98.89	30.32	10.0	5.4
1989	04	29	91.58	25.61	33.0	4.0
1989	05	03	97.48	31.16	33.0	4.5
1989	05	16	93.58	21.06	33.0	4.1
1989	05	18	94.63	23.43	112.0	4.5
1989	05	22	87.86	27.38	-	5.0
1989	05	31	94.26	22.53	110.0	4.1
1989	06	11	90.70	26.39	50.0	4.9
1989	06	12	89.78	21.83	06.0	5.2
1989	06	12	95.18	24.77	33.0	4.0
1989	06	25	93.62	21.59	63.0	4.2
1989	06	28	94.37	23.79	66.0	4.8
1989	06	28	94.13	23.78	83.0	4.0
1989	07	02	95.87	24.47	52.0	4.2
1989	07	10	94.37	23.53	72.0	4.3
1989	07	15	94.54	22.79	96.0	4.6

Year	Month	Day	Longitude (°E)	Latitude (°N)	Depth (km)	Magnitude (Mw)
1989	07	15	94.45	23.72	33.0	4.3
1989	07	25	92.55	27.55	33.0	4.5
1989	07	30	94.03	24.46	33.0	4.4
1989	08	03	92.66	26.94	33.0	4.3
1989	08	05	95.90	24.88	33.0	4.5
1989	08	09	94.55	24.51	80.0	4.8
1989	09	19	92.65	26.88	25.0	4.5
1989	09	25	94.37	22.69	113.0	4.3
1989	10	10	87.49	28.36	38.0	4.4
1989	10	12	95.52	24.34	33.0	4.1
1989	11	11	94.33	21.09	95.0	4.2
1989	11	19	89.70	28.96	33.0	4.1
1989	11	27	96.53	25.79	36.0	4.4
1989	12	02	93.82	21.21	49.0	5.0
1989	12	03	93.71	21.19	47.0	5.0
1989	12	04	95.26	25.32	146.0	4.2
1989	12	08	93.80	21.19	59.0	4.9
1989	12	08	93.68	21.11	55.0	4.0
1989	12	09	94.58	22.88	114.0	4.6
1989	12	22	94.71	28.88	46.0	4.2
1989	12	29	94.57	24.70	85.0	4.8
1989	12	29	94.27	24.13	99.0	4.1
1989	12	31	94.30	22.63	57.0	4.1
1990	01	09	95.26	24.74	121.0	6.1
1990	01	09	88.11	28.15	36.0	4.7
1990	01	10	94.63	24.46	87.0	4.6
1990	01	10	94.51	22.47	118.0	4.5
1990	01	11	95.38	25.00	145.0	4.5

Year	Month	Day	Longitude (^{O}E)	Latitude (^{O}N)	Depth (km)	Magnitude (Mw)
1990	01	19	95.69	24.67	33.0	4.0
1990	01	23	96.52	25.14	35.0	5.2
1990	02	05	92.41	24.85	33.0	4.0
1990	02	09	98.94	26.05	10.0	4.5
1990	02	18	89.95	29.39	10.0	4.2
1990	02	22	93.13	24.95	52.0	4.7
1990	02	22	90.02	29.14	54.0	4.6
1990	02	23	90.02	29.38	10.0	4.0
1990	02	26	94.01	23.02	93.0	4.6
1990	02	26	94.19	25.29	51.0	4.5
1990	03	01	88.40	28.75	33.0	4.0
1990	03	08	96.64	25.45	24.0	5.5
1990	03	08	96.61	25.39	40.0	4.4
1990	03	10	97.40	30.58	41.0	4.4
1990	03	15	96.47	25.27	50.0	4.0
1990	04	08	94.35	23.85	82.0	4.3
1990	04	10	97.85	21.65	46.0	4.4
1990	04	26	94.57	24.01	85.0	4.1
1990	04	30	95.23	26.54	150.0	4.9
1990	05	06	89.98	29.99	33.0	4.5
1990	05	08	94.93	30.10	33.0	4.0
1990	05	13	88.11	31.47	33.0	4.2
1990	05	14	92.62	22.78	26.0	4.1
1990	05	22	89.96	30.16	-	4.3
1990	05	24	95.52	26.54	94.0	4.5
1990	06	04	94.50	23.64	85.0	4.7
1990	06	14	94.00	24.98	58.0	4.1
1990	06	20	98.54	24.80	33.0	4.0

Year	Month	Day	Longitude (°E)	Latitude (°N)	Depth (km)	Magnitude (Mw)
1990	06	24	94.13	23.01	89.0	4.3
1990	07	13	94.44	23.64	114.0	4.5
1990	07	31	95.62	24.25	33.0	4.3
1990	08	02	94.65	22.67	132.0	4.8
1990	08	02	95.23	24.89	159.0	4.4
1990	08	29	92.74	27.18	25.0	4.2
1990	09	02	92.67	26.58	57.0	4.8
1990	09	10	95.42	24.05	75.0	4.0
1990	10	03	94.29	23.25	77.0	4.5
1990	10	29	92.44	26.47	37.0	4.5
1990	11	03	96.88	27.60	42.0	4.4
1990	11	10	94.84	25.36	102.0	4.7
1990	11	15	93.00	23.81	26.0	5.2
1990	11	29	94.64	24.37	82.0	4.7
1990	12	10	94.42	23.36	79.0	4.1
1990	12	11	92.26	27.75	33.0	4.3
1990	12	28	93.80	22.97	49.0	4.3
1990	12	29	92.59	26.68	27.0	4.2
1991	01	03	95.21	24.32	33.0	4.8
1991	01	05	95.96	23.55	18.0	7.2
1991	01	05	96.04	23.97	43.0	5.7
1991	01	05	96.02	23.82	-	4.3
1991	01	10	95.90	23.55	-	4.2
1991	01	23	95.22	24.72	118.0	5.3
1991	01	23	92.53	24.42	33.0	4.0
1991	01	26	97.10	24.71	34.0	4.4
1991	01	28	95.39	26.08	-	4.9
1991	01	30	95.13	22.49	33.0	4.1

Year	Month	Day	Longitude (^{O}E)	Latitude (^{O}N)	Depth (km)	Magnitude (Mw)
1991	01	31	93.29	23.81	33.0	4.3
1991	02	02	91.17	25.51	26.0	4.6
1991	02	12	97.02	29.54	44.0	4.3
1991	02	13	96.06	23.72	37.0	4.1
1991	02	13	96.89	29.75	28.0	4.1
1991	03	01	95.99	23.87	16.0	4.4
1991	03	07	95.06	24.73	133.0	4.2
1991	03	11	94.74	25.81	33.0	4.6
1991	03	15	87.55	28.34	64.0	4.7
1991	04	09	92.96	26.41	50.0	4.5
1991	04	13	92.52	26.72	56.0	4.5
1991	04	21	95.82	23.18	33.0	4.1
1991	04	27	94.79	29.74	42.0	4.3
1991	05	11	93.68	24.26	44.0	4.7
1991	05	11	96.24	26.46	115.0	4.5
1991	05	25	95.18	25.29	84.0	4.5
1991	05	28	94.95	25.32	115.0	4.4
1991	06	08	96.61	29.31	174.0	4.5
1991	06	23	93.19	26.59	46.0	4.5
1991	06	25	94.02	21.52	58.0	4.0
1991	07	09	94.48	22.14	131.0	4.2
1991	07	18	94.83	30.37	09.0	4.4
1991	07	18	94.71	30.40	33.0	4.1
1991	07	19	95.21	25.14	110.0	4.6
1991	07	20	94.81	30.39	-	4.5
1991	07	20	94.77	30.30	33.0	4.2
1991	07	23	94.83	30.33	14.0	4.0
1991	07	24	94.39	22.27	91.0	4.6

Year	Month	Day	Longitude (°E)	Latitude (°N)	Depth (km)	Magnitude (Mw)
1991	07	24	94.78	30.38	22.0	4.5
1991	07	24	93.58	21.47	33.0	4.5
1991	07	25	94.76	30.39	16.0	4.5
1991	07	28	94.80	30.34	34.0	4.5
1991	07	29	95.16	24.59	128.0	4.3
1991	07	29	94.74	30.34	33.0	4.3
1991	07	29	94.82	30.34	20.0	4.3
1991	07	30	94.81	30.37	26.0	4.5
1991	07	31	98.86	24.86	33.0	4.2
1991	08	04	96.00	23.92	37.0	4.6
1991	08	07	88.66	25.27	10.0	4.2
1991	08	22	91.18	25.29	45.0	4.4
1991	09	01	96.38	26.39	33.0	4.4
1991	09	02	90.47	24.54	78.0	4.4
1991	09	07	93.89	24.15	64.0	4.6
1991	09	09	95.00	28.84	-	4.6
1991	09	12	95.71	29.69	38.0	4.3
1991	09	19	92.14	26.23	33.0	4.5
1991	09	26	90.27	25.59	33.0	4.5
1991	09	27	96.79	26.30	33.0	4.4
1991	09	30	94.42	22.74	89.0	4.5
1991	10	26	96.43	24.01	120.0	4.2
1991	11	09	94.31	22.73	107.0	4.3
1991	11	11	92.86	26.14	33.0	4.1
1991	11	15	92.60	21.02	82.0	4.3
1991	11	17	93.18	24.68	60.0	4.4
1991	11	17	94.74	23.53	91.0	4.1
1991	11	21	96.41	26.61	82.0	4.5

Year	Month	Day	Longitude (^{O}E)	Latitude (^{O}N)	Depth (km)	Magnitude (Mw)
1991	12	04	93.91	23.97	65.0	4.8
1991	12	07	93.81	22.89	79.0	4.5
1991	12	07	93.83	24.00	52.0	4.5
1991	12	14	94.58	23.74	94.0	4.4
1991	12	15	93.88	30.03	33.0	4.5
1991	12	20	93.12	24.69	39.0	5.0
1991	12	21	87.96	27.80	65.0	4.2
1991	12	24	92.52	30.11	20.0	4.1
1992	01	05	94.49	21.50	99.0	4.2
1992	01	13	92.50	24.42	45.0	4.3
1992	01	16	94.73	21.85	10.0	4.2
1992	01	25	98.68	26.06	43.0	4.4
1992	02	06	95.64	29.61	15.0	5.0
1992	02	08	95.46	29.34	57.0	4.0
1992	02	09	95.63	29.65	12.0	4.5
1992	02	09	95.68	29.64	10.0	4.3
1992	02	25	92.23	25.17	33.0	4.6
1992	03	01	94.56	23.40	74.0	4.2
1992	03	07	89.31	29.68	92.0	4.5
1992	03	08	94.65	23.11	93.0	4.3
1992	03	22	95.62	25.96	33.0	4.0
1992	03	23	97.41	26.79	33.0	4.5
1992	03	24	94.31	23.23	123.0	4.4
1992	03	25	95.25	24.82	100.0	4.3
1992	03	28	98.71	21.29	41.0	4.1
1992	04	04	87.96	28.12	25.0	4.6
1992	04	09	96.60	28.14	33.0	4.0
1992	04	13	88.31	31.95	35.0	4.5

Year	Month	Day	Longitude (^{o}E)	Latitude (^{o}N)	Depth (km)	Magnitude (Mw)
1992	04	15	94.93	24.27	131.0	5.2
1992	04	15	90.52	25.32	33.0	4.0
1992	04	20	92.11	26.99	33.0	4.4
1992	04	20	95.23	26.72	42.0	4.3
1992	04	20	91.15	26.64	14.0	4.0
1992	04	23	98.93	22.43	12.0	6.4
1992	04	23	98.88	22.43	10.0	6.3
1992	04	23	98.89	22.30	33.0	4.8
1992	04	26	94.03	23.46	108.0	4.3
1992	05	09	93.96	23.74	56.0	4.1
1992	05	27	94.16	22.54	33.0	4.3
1992	05	28	94.53	22.75	100.0	4.5
1992	05	28	92.06	23.14	07.0	4.2
1992	06	08	94.22	23.36	116.0	4.5
1992	06	08	94.06	28.50	13.0	4.5
1992	06	10	96.71	25.65	33.0	4.5
1992	06	13	93.16	21.81	56.0	4.2
1992	06	15	95.97	24.00	17.0	6.6
1992	06	21	89.20	30.65	35.0	4.0
1992	06	23	95.64	23.55	87.0	4.4
1992	07	02	94.81	24.47	144.0	4.3
1992	07	02	95.55	25.07	13.0	4.1
1992	07	08	93.68	21.06	37.0	4.7
1992	07	09	90.02	21.05	29.0	4.8
1992	07	09	93.22	22.70	10.0	4.3
1992	07	14	93.44	23.61	20.0	4.1
1992	07	24	90.19	29.40	23.0	4.5
1992	07	30	90.18	29.57	31.0	6.0

Year	Month	Day	Longitude (^{O}E)	Latitude (^{O}N)	Depth (km)	Magnitude (Mw)
1992	07	30	90.11	29.83	32.0	4.3
1992	07	30	90.26	29.85	33.0	4.2
1992	07	30	90.29	29.85	33.0	4.1
1992	08	04	90.38	29.84	10.0	4.0
1992	08	08	91.90	25.35	50.0	4.0
1992	08	08	90.28	29.89	33.0	4.0
1992	08	10	95.69	23.98	33.0	4.5
1992	08	16	92.09	30.12	30.0	4.7
1992	08	21	93.55	22.56	25.0	4.0
1992	09	06	95.01	24.53	122.0	5.0
1992	09	08	94.93	28.60	46.0	4.4
1992	09	15	93.78	21.31	51.0	4.7
1992	09	21	93.05	23.34	44.0	4.1
1992	09	25	98.37	23.67	52.0	4.1
1992	10	04	96.41	28.94	29.0	4.3
1992	10	04	94.41	24.62	60.0	4.1
1992	10	05	94.60	24.21	20.0	4.1
1992	10	24	94.22	23.59	124.0	4.4
1992	10	30	95.97	23.75	04.0	4.4
1992	10	31	93.44	27.20	21.0	4.5
1992	11	11	92.80	27.65	67.0	4.2
1992	11	11	94.36	22.55	97.0	4.1
1992	12	12	91.39	25.48	-	4.2
1992	12	20	98.09	21.52	33.0	4.3
1992	12	22	94.73	24.53	103.0	4.1
1992	12	26	94.80	21.01	124.0	4.0
1993	01	01	94.69	22.98	115.0	4.9
1993	01	09	98.87	29.97	33.0	4.3

Year	Month	Day	Longitude (°E)	Latitude (°N)	Depth (km)	Magnitude (Mw)
1993	01	18	90.38	30.84	10.0	6.1
1993	01	18	90.44	30.94	17.0	4.5
1993	01	18	90.41	30.97	-	4.2
1993	01	23	95.67	25.79	111.0	4.4
1993	01	27	93.87	24.13	49.0	4.2
1993	02	12	92.35	23.51	33.0	4.1
1993	02	14	95.08	22.53	33.0	4.1
1993	02	15	87.51	25.89	30.0	4.5
1993	02	15	90.40	30.85	20.0	4.4
1993	02	16	90.16	30.55	33.0	4.2
1993	02	17	94.61	22.90	119.0	4.5
1993	02	17	92.57	26.02	16.0	4.2
1993	03	01	92.98	22.81	24.0	4.2
1993	03	03	90.33	25.56	33.0	4.2
1993	03	05	90.75	28.90	27.0	4.0
1993	03	17	95.82	23.54	35.0	4.1
1993	03	18	94.14	23.93	77.0	4.6
1993	03	20	87.33	29.03	12.0	6.4
1993	03	20	87.34	29.01	21.0	4.7
1993	03	21	87.47	29.06	33.0	4.0
1993	03	27	95.02	24.64	109.0	4.9
1993	03	31	87.33	29.10	16.0	4.8
1993	04	01	94.46	23.21	91.0	5.3
1993	04	01	94.45	23.15	97.0	4.5
1993	04	02	96.52	25.31	33.0	4.6
1993	04	11	94.20	24.01	79.0	4.6
1993	04	12	95.38	28.80	17.0	4.3
1993	04	13	94.22	22.34	90.0	4.4

Year	Month	Day	Longitude (^{O}E)	Latitude (^{O}N)	Depth (km)	Magnitude (Mw)
1993	04	13	96.28	26.47	91.0	4.0
1993	04	14	94.87	24.76	121.0	4.7
1993	04	14	96.53	26.53	22.0	4.4
1993	04	19	95.94	24.57	33.0	4.0
1993	05	01	95.87	24.63	66.0	4.1
1993	05	03	98.07	29.76	10.0	4.7
1993	05	08	95.64	29.05	33.0	4.4
1993	05	11	94.27	22.27	97.0	4.1
1993	05	23	98.79	31.59	47.0	4.4
1993	05	24	96.18	28.91	43.0	4.6
1993	05	26	98.71	31.72	33.0	4.2
1993	05	27	93.60	21.91	54.0	4.1
1993	05	28	93.10	26.62	56.0	4.3
1993	06	12	97.02	29.12	49.0	4.1
1993	06	18	92.45	27.30	25.0	4.2
1993	06	19	95.12	25.45	33.0	4.0
1993	06	23	92.66	27.79	27.0	4.1
1993	06	24	94.58	23.43	111.0	4.0
1993	07	08	93.56	23.83	74.0	4.1
1993	07	14	93.90	23.10	59.0	4.8
1993	07	31	91.87	27.34	71.0	4.1
1993	08	02	93.64	22.84	79.0	4.5
1993	08	06	94.08	23.37	104.0	4.0
1993	08	17	95.67	26.08	109.0	4.5
1993	08	27	95.90	23.10	19.0	4.6
1993	09	01	97.12	27.50	59.0	4.4
1993	09	04	94.81	30.35	-	4.9
1993	09	05	87.27	27.33	32.0	4.2

Year	Month	Day	Longitude (°E)	Latitude (°N)	Depth (km)	Magnitude (Mw)
1993	09	06	94.27	23.49	92.0	5.0
1993	09	06	94.79	30.38	09.0	4.0
1993	09	11	95.10	24.62	60.0	4.3
1993	09	20	92.81	27.94	41.0	4.5
1993	10	02	96.32	25.03	45.0	4.0
1993	10	17	95.32	25.45	33.0	4.2
1993	10	18	98.17	30.03	13.0	4.4
1993	12	02	95.10	23.75	33.0	4.5
1993	12	09	96.55	25.96	33.0	4.2
1993	12	12	92.04	27.29	30.0	4.3
1993	12	15	94.12	23.30	133.0	4.4
1993	12	20	93.87	22.48	86.0	4.5
1993	12	22	94.92	25.04	113.0	4.3
1993	12	31	95.34	29.36	34.0	4.5
1994	01	04	95.97	26.35	108.0	4.3
1994	01	11	97.21	25.21	10.0	6.3
1994	01	11	97.14	25.24	39.0	4.3
1994	01	11	97.08	25.25	32.0	4.2
1994	01	12	97.27	25.17	15.0	4.4
1994	01	20	93.37	24.94	70.0	4.4
1994	01	23	95.75	29.99	44.0	4.4
1994	01	29	94.71	24.44	128.0	4.2
1994	02	15	96.05	24.99	-	4.5
1994	03	05	94.94	24.69	108.0	4.5
1994	03	11	93.28	22.15	69.0	4.1
1994	03	24	91.27	26.22	48.0	4.4
1994	03	27	96.16	24.50	39.0	4.4
1994	03	29	96.53	26.70	90.0	4.4

Year	Month	Day	Longitude (^{O}E)	Latitude (^{O}N)	Depth (km)	Magnitude (Mw)
1994	04	06	96.84	26.16	-	5.9
1994	04	06	96.86	26.19	62.0	4.7
1994	04	09	94.81	24.63	102.0	4.4
1994	04	14	95.58	24.98	192.0	4.7
1994	04	15	90.48	26.07	45.0	4.4
1994	04	18	92.94	26.22	59.0	4.1
1994	04	24	93.21	24.30	32.0	4.2
1994	05	05	95.68	25.66	105.0	4.5
1994	05	05	94.44	24.78	60.0	4.1
1994	05	06	93.61	26.39	33.0	4.0
1994	05	14	98.55	29.54	15.0	4.0
1994	05	17	95.02	25.50	33.0	4.6
1994	05	19	95.30	25.62	108.0	4.7
1994	05	20	94.68	30.68	33.0	4.0
1994	05	25	87.93	27.62	51.0	4.1
1994	05	28	94.13	24.52	69.0	4.4
1994	06	01	92.96	23.04	33.0	4.4
1994	06	02	94.90	25.19	100.0	4.3
1994	06	09	92.19	24.35	53.0	4.1
1994	06	28	95.14	24.79	173.0	4.1
1994	07	09	98.01	24.72	33.0	4.1
1994	07	24	92.78	25.18	27.0	4.4
1994	08	03	93.98	21.50	39.0	5.6
1994	08	05	92.51	26.67	40.0	4.0
1994	08	08	95.21	24.71	116.0	5.5
1994	08	29	96.55	26.71	114.0	4.5
1994	09	03	94.53	24.72	89.0	4.4
1994	09	21	96.86	26.45	23.0	4.1

Year	Month	Day	Longitude (^{o}E)	Latitude (^{o}N)	Depth (km)	Magnitude (Mw)
1994	09	23	94.90	21.52	124.0	4.3
1994	09	23	98.51	22.19	31.0	4.2
1994	10	11	92.00	30.21	39.0	4.3
1994	10	18	94.45	24.13	106.0	4.8
1994	10	18	94.52	24.17	92.0	4.3
1994	10	20	96.51	25.13	33.0	4.3
1994	10	21	93.07	22.27	33.0	4.2
1994	10	24	92.38	27.13	30.0	4.4
1994	10	25	92.23	27.13	29.0	4.8
1994	11	02	95.38	24.85	158.0	4.5
1994	11	21	96.67	25.54	14.0	6.0
1994	11	25	93.31	21.56	43.0	4.4
1994	12	06	94.68	29.02	-	4.3
1994	12	30	88.26	30.43	17.0	4.0
1995	01	01	87.71	27.94	58.0	4.5
1995	01	12	88.21	30.21	34.0	4.1
1995	01	14	94.43	22.33	93.0	4.1
1995	01	17	93.63	24.14	-	4.4
1995	01	20	92.50	27.42	40.0	4.0
1995	02	02	88.04	30.15	10.0	4.3
1995	02	08	95.06	25.07	59.0	4.4
1995	02	17	92.40	27.64	37.0	5.1
1995	03	11	94.51	24.11	114.0	4.1
1995	03	11	88.25	30.11	09.0	4.0
1995	03	13	94.58	22.07	139.0	4.0
1995	03	16	88.09	30.12	51.0	4.3
1995	03	16	88.05	30.04	15.0	4.1
1995	03	18	97.47	27.61	33.0	4.5

Year	Month	Day	Longitude (^{O}E)	Latitude (^{O}N)	Depth (km)	Magnitude (Mw)
1995	03	21	90.34	30.77	-	4.6
1995	03	24	87.41	28.64	123.0	4.2
1995	03	26	92.38	27.61	10.0	4.4
1995	03	26	90.41	30.72	39.0	4.1
1995	03	29	94.23	24.60	49.0	4.5
1995	04	04	96.16	25.11	25.0	4.7
1995	04	09	94.71	24.52	72.0	4.3
1995	04	09	97.99	29.66	33.0	4.0
1995	04	10	94.56	24.48	43.0	4.1
1995	04	14	88.10	30.06	44.0	4.2
1995	04	21	94.72	24.68	39.0	4.1
1995	04	24	88.22	29.95	25.0	4.1
1995	04	28	95.41	24.90	132.0	4.1
1995	04	28	88.13	29.98	-	4.0
1995	05	04	94.97	25.40	170.0	4.4
1995	05	06	95.29	24.96	118.0	5.8
1995	05	06	95.10	24.95	120.0	4.3
1995	05	08	95.12	24.90	119.0	4.8
1995	05	09	95.10	25.24	79.0	4.8
1995	05	09	90.81	26.11	33.0	4.2
1995	05	13	94.52	22.78	116.0	4.2
1995	05	21	95.27	25.05	112.0	4.5
1995	05	30	95.67	27.14	33.0	4.5
1995	06	07	94.08	23.71	-	4.5
1995	06	17	94.14	23.14	36.0	4.7
1995	06	26	94.66	23.63	120.0	4.2
1995	06	27	95.25	25.53	15.0	4.3
1995	06	28	91.91	28.38	28.0	4.1

Year	Month	Day	Longitude (°E)	Latitude (°N)	Depth (km)	Magnitude (Mw)
1995	06	29	98.99	21.92	33.0	5.6
1995	07	03	92.33	27.24	19.0	4.5
1995	07	04	94.84	30.35	-	4.2
1995	07	05	93.72	23.08	84.0	4.0
1995	07	06	94.71	30.24	25.0	4.5
1995	07	10	94.40	28.81	112.0	4.3
1995	07	11	98.96	21.89	11.0	4.6
1995	07	11	98.27	21.26	08.0	4.3
1995	07	11	94.58	24.25	165.0	4.0
1995	07	15	98.95	21.99	32.0	4.1
1995	07	16	94.85	30.37	09.0	4.2
1995	07	19	94.82	30.36	-	4.9
1995	07	19	95.13	24.77	126.0	4.0
1995	07	20	92.26	23.08	27.0	4.0
1995	07	23	98.88	22.03	34.0	4.3
1995	07	29	93.57	23.21	61.0	4.1
1995	07	30	88.21	30.25	48.0	6.4
1995	07	30	94.56	22.96	112.0	4.8
1995	07	30	88.04	30.03	33.0	4.1
1995	07	30	92.67	27.05	88.0	4.0
1995	08	07	98.60	21.71	05.0	4.1
1995	08	08	90.07	26.07	55.0	4.1
1995	08	13	94.53	24.41	81.0	4.0
1995	08	30	95.04	25.29	58.0	4.2
1995	09	05	96.71	27.08	33.0	4.0
1995	09	19	88.25	30.33	-	4.3
1995	09	20	96.65	25.37	21.0	4.7
1995	09	24	97.41	29.03	59.0	4.3

Year	Month	Day	Longitude (^{O}E)	Latitude (^{O}N)	Depth (km)	Magnitude (Mw)
1995	09	26	96.84	27.14	31.0	4.6
1995	09	29	92.62	27.54	33.0	4.1
1995	10	05	88.24	30.17	53.0	4.5
1995	10	09	97.75	24.93	05.0	4.2
1995	10	19	94.42	22.68	87.0	4.3
1995	10	23	93.94	28.44	-	4.1
1995	11	01	95.67	22.46	15.0	4.7
1995	11	07	96.96	24.38	94.0	4.2
1995	11	09	96.82	27.49	69.0	4.0
1995	11	18	93.08	23.87	33.0	4.2
1995	12	01	91.95	24.25	20.0	4.3
1995	12	01	92.14	26.23	54.0	4.1
1995	12	04	91.97	27.25	52.0	4.3
1995	12	06	91.54	24.76	47.0	4.4
1995	12	09	95.11	21.67	33.0	4.0
1995	12	12	96.07	26.87	33.0	4.7
1995	12	25	89.31	31.09	49.0	4.1
1995	12	27	88.14	30.15	58.0	4.4
1996	01	09	95.03	24.69	117.0	4.4
1996	01	12	94.34	21.53	86.0	4.5
1996	01	26	91.51	30.87	43.0	5.4
1996	01	28	94.06	22.76	120.0	4.3
1996	02	05	97.02	21.13	33.0	4.1
1996	02	08	93.22	23.81	76.0	4.5
1996	02	08	94.70	23.41	119.0	4.3
1996	02	11	95.03	24.16	160.0	4.0
1996	02	16	92.06	28.76	-	4.1
1996	02	17	90.60	26.08	45.0	4.0

Year	Month	Day	Longitude (°E)	Latitude (°N)	Depth (km)	Magnitude (Mw)
1996	02	23	93.63	24.41	250.0	4.0
1996	03	04	96.11	24.32	-	4.2
1996	03	04	92.66	23.56	33.0	4.0
1996	03	05	92.96	26.35	77.0	4.0
1996	03	12	88.24	30.09	63.0	4.6
1996	03	13	88.38	30.07	10.0	4.0
1996	03	19	96.36	24.97	33.0	4.3
1996	03	20	93.65	23.69	33.0	4.1
1996	03	21	94.29	21.20	96.0	4.0
1996	04	06	96.25	30.01	15.0	4.2
1996	04	07	96.30	29.99	11.0	4.5
1996	04	22	92.02	30.04	17.0	4.2
1996	04	25	95.19	24.84	111.0	4.4
1996	04	26	87.80	27.84	25.0	4.2
1996	05	01	94.87	29.87	57.0	4.0
1996	05	10	88.15	30.03	-	4.8
1996	05	10	88.06	30.01	48.0	4.4
1996	05	11	88.11	30.05	09.0	4.6
1996	05	11	88.24	30.15	62.0	4.4
1996	05	11	88.11	30.17	54.0	4.1
1996	05	11	94.62	22.72	120.0	4.0
1996	05	14	92.27	26.44	58.0	4.8
1996	05	14	88.03	29.94	43.0	4.1
1996	05	17	88.02	30.01	47.0	4.5
1996	05	17	88.09	30.05	39.0	4.1
1996	05	17	88.11	30.14	33.0	4.0
1996	05	21	92.14	29.32	-	4.4
1996	05	21	93.18	27.05	32.0	4.1

Year	Month	Day	Longitude (^{O}E)	Latitude (^{O}N)	Depth (km)	Magnitude (Mw)
1996	06	03	93.98	27.94	31.0	4.1
1996	06	09	92.26	28.38	58.0	4.7
1996	06	15	93.35	21.62	43.0	4.2
1996	06	18	94.44	22.76	101.0	4.1
1996	06	27	92.29	27.19	-	4.3
1996	06	27	93.97	23.00	36.0	4.0
1996	06	27	92.20	27.18	13.0	4.0
1996	06	28	95.39	24.90	125.0	4.2
1996	06	30	94.48	23.97	18.0	4.5
1996	07	03	88.19	30.11	-	6.0
1996	07	03	88.24	30.19	60.0	4.7
1996	07	03	88.26	30.03	41.0	4.2
1996	07	03	88.17	30.12	33.0	4.1
1996	07	04	88.17	30.07	27.0	4.6
1996	07	04	88.09	30.04	48.0	4.2
1996	07	05	87.79	29.86	46.0	4.1
1996	07	05	92.48	21.85	28.0	4.0
1996	07	06	87.98	29.87	95.0	4.7
1996	07	08	94.77	21.33	120.0	4.8
1996	07	08	88.23	30.15	30.0	4.1
1996	07	08	88.20	30.22	73.0	4.0
1996	07	12	87.88	30.18	33.0	4.3
1996	07	12	92.29	27.15	14.0	4.2
1996	07	12	87.98	30.12	33.0	4.1
1996	07	12	88.33	30.28	43.0	4.0
1996	07	13	88.03	30.02	24.0	4.0
1996	07	17	92.28	26.32	41.0	4.1
1996	07	18	88.18	30.17	72.0	4.4

Year	Month	Day	Longitude (^{o}E)	Latitude (^{o}N)	Depth (km)	Magnitude (Mw)
1996	07	22	88.09	30.02	57.0	4.4
1996	07	23	87.71	31.40	21.0	4.1
1996	07	24	98.97	25.94	39.0	4.0
1996	07	26	96.21	25.11	13.0	5.3
1996	07	27	94.78	21.30	103.0	4.8
1996	07	28	95.34	25.92	79.0	4.8
1996	07	28	94.02	23.58	51.0	4.1
1996	07	31	88.21	30.24	58.0	5.4
1996	07	31	88.13	30.10	33.0	5.4
1996	08	04	93.16	26.43	43.0	4.3
1996	08	06	95.23	24.91	108.0	4.8
1996	08	07	96.54	23.99	41.0	4.2
1996	08	07	88.10	30.16	43.0	4.1
1996	08	09	96.26	22.06	05.0	4.0
1996	08	18	90.15	25.84	39.0	4.1
1996	08	20	94.74	23.95	128.0	4.1
1996	08	25	88.10	30.28	65.0	4.4
1996	08	28	98.74	21.54	62.0	4.1
1996	08	29	88.27	30.30	48.0	4.6
1996	09	08	96.23	24.79	13.0	4.4
1996	09	11	92.82	27.66	-	4.3
1996	09	12	92.51	27.01	40.0	4.5
1996	09	13	88.54	27.32	33.0	4.2
1996	09	14	96.63	25.55	38.0	4.2
1996	09	14	92.71	27.62	50.0	4.0
1996	09	24	88.40	23.42	-	4.3
1996	09	25	88.80	27.60	32.0	4.8
1996	10	03	87.60	28.34	35.0	4.3

Year	Month	Day	Longitude (^{O}E)	Latitude (^{O}N)	Depth (km)	Magnitude (Mw)
1996	10	07	98.25	25.46	33.0	4.1
1996	10	14	88.21	30.09	64.0	4.2
1996	10	17	98.93	21.94	33.0	4.5
1996	10	27	94.99	30.10	53.0	4.3
1996	10	27	93.62	21.59	43.0	4.3
1996	10	31	94.58	23.04	103.0	4.6
1996	11	09	98.87	21.88	35.0	4.6
1996	11	09	92.38	22.11	14.0	4.0
1996	11	17	95.14	24.26	127.0	4.9
1996	11	19	92.68	24.57	27.0	5.0
1996	11	19	93.25	26.46	40.0	4.1
1996	11	20	95.95	28.86	29.0	4.2
1996	11	23	87.93	30.60	33.0	4.2
1996	11	24	92.74	26.84	43.0	4.5
1996	11	26	98.93	28.73	38.0	4.3
1996	12	01	98.46	21.53	40.0	4.3
1996	12	05	96.42	25.44	97.0	4.1
1996	12	10	94.93	25.27	114.0	4.4
1996	12	15	94.00	23.58	56.0	4.4
1996	12	17	94.17	22.77	58.0	4.0
1996	12	20	93.44	23.62	-	4.0
1996	12	23	90.12	26.07	33.0	4.3
1996	12	24	87.91	30.44	-	4.3
1997	01	06	93.18	21.43	33.0	4.0
1997	01	11	96.29	25.20	33.0	4.0
1997	01	12	91.25	26.53	16.0	4.4
1997	01	15	96.06	25.44	-	4.3
1997	01	18	96.80	30.30	36.0	4.4

Year	Month	Day	Longitude (°E)	Latitude (°N)	Depth (km)	Magnitude (Mw)
1997	01	25	88.09	30.06	39.0	4.2
1997	01	30	94.67	25.17	85.0	4.1
1997	02	02	96.60	25.35	70.0	4.4
1997	02	08	92.60	31.65	58.0	4.1
1997	02	09	94.62	24.14	117.0	4.0
1997	02	15	94.51	23.93	108.0	4.5
1997	02	15	94.15	24.17	64.0	4.1
1997	02	18	94.94	22.84	42.0	4.4
1997	02	19	94.96	22.84	38.0	4.4
1997	02	20	96.72	30.22	30.0	4.3
1997	03	05	90.38	30.77	-	4.6
1997	03	07	95.43	29.93	63.0	4.5
1997	03	10	92.68	27.42	38.0	4.2
1997	03	10	92.57	27.33	18.0	4.2
1997	03	13	88.85	31.02	56.0	4.4
1997	03	22	87.96	30.34	33.0	4.3
1997	03	22	87.99	29.92	34.0	4.0
1997	03	23	98.27	27.02	-	4.3
1997	03	25	98.30	25.08	33.0	4.2
1997	04	04	90.38	23.09	-	4.2
1997	04	06	94.44	21.33	98.0	4.5
1997	04	12	97.43	30.36	51.0	4.3
1997	04	13	97.44	30.41	66.0	4.5
1997	04	13	97.50	30.40	60.0	4.1
1997	04	14	94.48	22.59	110.0	4.8
1997	04	15	94.62	22.66	129.0	4.6
1997	04	15	97.07	30.07	119.0	4.1
1997	04	21	94.87	23.32	137.0	4.3

Year	Month	Day	Longitude (^{O}E)	Latitude (^{O}N)	Depth (km)	Magnitude (Mw)
1997	04	21	96.86	24.41	-	4.0
1997	04	25	96.21	26.48	100.0	4.5
1997	05	04	92.53	27.54	24.0	4.0
1997	05	06	93.60	25.15	52.0	4.7
1997	05	08	92.28	24.89	-	5.6
1997	05	12	93.45	25.83	-	4.4
1997	05	16	97.00	30.29	33.0	4.9
1997	05	19	93.89	25.03	65.0	4.5
1997	05	29	96.68	26.49	120.0	4.3
1997	06	02	92.65	28.04	27.0	4.5
1997	06	06	94.08	24.19	95.0	4.5
1997	06	15	89.91	23.98	35.0	4.3
1997	06	22	96.67	30.14	25.0	4.3
1997	06	24	97.24	30.22	54.0	4.6
1997	06	24	96.87	30.20	73.0	4.5
1997	06	24	97.08	30.39	68.0	4.4
1997	06	24	97.01	30.41	53.0	4.1
1997	06	24	96.24	26.35	71.0	4.0
1997	06	24	92.32	25.06	67.0	4.0
1997	06	26	96.77	30.21	21.0	4.2
1997	06	26	96.86	30.33	39.0	4.1
1997	06	26	90.35	30.78	17.0	4.0
1997	06	27	96.95	30.31	54.0	4.2
1997	07	01	95.38	25.00	124.0	4.2
1997	07	02	96.29	30.27	34.0	4.2
1997	07	02	96.94	30.37	26.0	4.1
1997	07	04	96.84	30.27	74.0	4.2
1997	07	04	96.96	30.32	68.0	4.1

Year	Month	Day	Longitude (°E)	Latitude (°N)	Depth (km)	Magnitude (Mw)
1997	07	08	88.21	29.92	80.0	4.3
1997	07	08	96.21	25.51	13.0	4.0
1997	07	10	94.95	29.82	15.0	4.5
1997	07	11	94.86	21.74	152.0	5.2
1997	07	18	91.80	26.83	-	4.1
1997	07	20	89.95	25.40	-	4.0
1997	07	24	95.67	26.09	100.0	4.4
1997	07	24	96.90	30.33	26.0	4.1
1997	07	31	93.22	23.91	33.0	4.7
1997	07	31	93.20	23.89	46.0	4.4
1997	08	04	91.48	28.22	30.0	4.2
1997	08	05	90.98	23.19	33.0	4.2
1997	08	05	94.68	24.39	85.0	4.0
1997	08	06	92.93	26.02	58.0	4.5
1997	08	08	93.64	22.01	90.0	4.1
1997	08	09	97.00	30.33	42.0	4.8
1997	08	09	96.82	30.46	64.0	4.2
1997	08	09	94.78	22.31	115.0	4.0
1997	08	10	97.12	30.19	80.0	4.2
1997	08	11	96.86	30.24	58.0	4.1
1997	08	14	96.94	30.33	58.0	4.1
1997	08	14	96.88	30.25	43.0	4.0
1997	08	17	96.99	30.30	80.0	4.5
1997	08	18	94.83	24.63	117.0	4.0
1997	08	25	94.16	27.55	-	4.0
1997	09	04	94.51	24.47	114.0	4.4
1997	09	13	88.13	30.07	33.0	4.8
1997	09	15	88.21	30.10	43.0	4.6

Year	Month	Day	Longitude (^{O}E)	Latitude (^{O}N)	Depth (km)	Magnitude (Mw)
1997	09	17	97.48	25.83	33.0	4.0
1997	09	18	88.10	28.84	71.0	4.5
1997	09	28	94.97	25.32	118.0	4.3
1997	10	02	93.57	21.48	56.0	4.0
1997	10	05	88.13	30.40	33.0	4.2
1997	10	08	93.46	25.05	66.0	4.4
1997	10	09	96.60	22.65	20.0	4.2
1997	10	26	93.51	23.99	63.0	4.5
1997	10	30	89.73	29.54	45.0	4.2
1997	11	04	94.18	27.09	-	4.6
1997	11	08	96.22	26.49	104.0	4.6
1997	11	08	95.84	28.80	17.0	4.5
1997	11	08	96.95	30.25	53.0	4.4
1997	11	10	89.43	24.22	33.0	4.5
1997	11	10	92.36	23.04	-	4.1
1997	11	11	95.34	26.48	85.0	4.1
1997	11	12	96.65	27.86	-	4.1
1997	11	20	93.80	23.14	67.0	4.2
1997	11	21	92.68	22.22	30.0	5.9
1997	11	21	93.08	21.23	50.0	4.2
1997	11	22	92.66	22.20	53.0	4.5
1997	11	23	96.09	26.18	64.0	4.5
1997	11	25	96.95	27.01	51.0	4.2
1997	11	27	87.31	27.56	33.0	4.4
1997	11	28	94.67	21.93	125.0	4.4
1997	12	02	95.13	25.11	112.0	4.6
1997	12	08	87.27	27.50	33.0	4.6
1997	12	27	96.13	26.41	117.0	4.2

Year	Month	Day	Longitude (^{o}E)	Latitude (^{o}N)	Depth (km)	Magnitude (Mw)
1997	12	29	94.77	23.53	120.0	4.1
1997	12	30	96.59	25.40	33.0	5.8
1997	12	30	96.55	25.29	40.0	4.7
1998	01	02	94.50	23.23	88.0	4.0
1998	01	06	91.76	25.91	61.0	4.2
1998	01	10	96.44	26.52	114.0	4.2
1998	01	13	93.48	28.56	69.0	4.2
1998	01	21	97.66	24.48	16.0	4.3
1998	02	01	87.14	28.19	75.0	4.2
1998	02	08	94.41	24.43	11.0	4.3
1998	02	12	87.91	26.63	37.0	4.3
1998	02	16	98.59	25.85	20.0	4.3
1998	02	16	94.20	23.12	109.0	4.2
1998	02	18	94.23	23.18	30.0	4.5
1998	02	21	95.80	27.37	100.0	4.4
1998	02	22	88.23	30.25	33.0	4.7
1998	02	22	88.32	30.25	12.0	4.3
1998	02	28	87.67	26.95	53.0	4.1
1998	03	01	94.56	23.60	109.0	4.2
1998	03	06	94.40	24.54	49.0	4.0
1998	03	11	94.92	25.15	88.0	4.5
1998	03	15	87.05	29.06	33.0	4.1
1998	04	10	94.98	24.91	123.0	4.5
1998	04	10	94.96	30.46	25.0	4.3
1998	04	15	96.42	25.31	33.0	4.2
1998	04	18	95.75	25.03	20.0	4.1
1998	04	23	94.67	24.93	39.0	4.1
1998	05	02	95.26	24.94	107.0	4.4

Year	Month	Day	Longitude (^{O}E)	Latitude (^{O}N)	Depth (km)	Magnitude (Mw)
1998	05	02	94.20	31.96	33.0	4.3
1998	05	02	93.71	28.19	150.0	4.0
1998	05	06	97.51	24.54	15.0	4.2
1998	05	16	97.81	24.17	29.0	4.2
1998	06	06	89.29	30.51	33.0	5.0
1998	06	06	89.36	30.39	33.0	4.9
1998	06	07	96.33	26.50	46.0	4.0
1998	06	11	93.12	24.33	33.0	4.0
1998	06	18	94.83	24.98	102.0	4.1
1998	06	19	93.61	23.90	61.0	4.2
1998	06	30	94.70	22.93	121.0	4.6
1998	07	02	97.78	30.12	38.0	4.1
1998	07	02	93.69	21.03	45.0	4.1
1998	07	08	91.07	27.32	33.0	4.4
1998	07	13	98.37	21.32	28.0	4.1
1998	07	13	98.36	21.50	21.0	4.0
1998	07	17	94.40	22.76	106.0	4.3
1998	07	20	88.25	30.18	58.0	6.0
1998	07	20	88.02	30.13	33.0	4.8
1998	07	20	87.95	30.31	-	4.6
1998	07	20	88.23	30.43	33.0	4.5
1998	07	20	88.07	30.13	18.0	4.5
1998	07	20	88.07	30.25	33.0	4.4
1998	07	20	88.05	30.19	27.0	4.3
1998	07	20	88.02	30.11	18.0	4.2
1998	07	20	87.79	30.25	41.0	4.2
1998	07	20	88.22	30.04	72.0	4.2
1998	07	20	88.13	30.08	18.0	4.1

Year	Month	Day	Longitude (°E)	Latitude (°N)	Depth (km)	Magnitude (Mw)
1998	07	21	88.21	30.30	42.0	4.8
1998	07	23	88.09	30.18	23.0	4.1
1998	07	27	93.59	24.26	21.0	4.1
1998	07	29	87.94	30.23	60.0	4.0
1998	07	30	87.99	30.17	33.0	4.6
1998	07	31	87.80	28.18	78.0	4.1
1998	08	04	94.39	23.48	43.0	4.0
1998	08	07	88.26	30.31	55.0	4.6
1998	08	10	96.54	25.38	15.0	4.0
1998	08	16	87.95	29.77	33.0	4.5
1998	08	18	91.10	27.65	35.0	4.7
1998	08	23	88.16	30.26	36.0	4.3
1998	08	25	88.16	30.27	53.0	5.8
1998	08	25	88.18	30.06	-	4.7
1998	08	25	88.13	30.04	49.0	4.5
1998	08	25	88.20	30.03	49.0	4.4
1998	08	25	88.62	31.13	33.0	4.4
1998	08	25	88.04	29.97	33.0	4.4
1998	08	25	88.23	30.07	38.0	4.3
1998	08	25	88.23	30.01	18.0	4.3
1998	08	25	88.17	30.07	61.0	4.3
1998	08	25	88.11	30.05	39.0	4.3
1998	08	25	88.09	30.25	27.0	4.2
1998	08	25	88.14	29.92	49.0	4.1
1998	08	28	88.22	30.29	24.0	5.1
1998	08	29	94.74	30.30	22.0	4.3
1998	08	30	88.19	30.14	53.0	5.3
1998	08	30	88.10	30.07	15.0	4.9

Year	Month	Day	Longitude (^{O}E)	Latitude (^{O}N)	Depth (km)	Magnitude (Mw)
1998	09	07	88.22	30.34	53.0	4.6
1998	09	08	88.13	30.39	14.0	4.1
1998	09	10	88.47	27.34	24.0	4.4
1998	09	13	95.93	24.01	23.0	4.6
1998	09	24	94.43	23.39	109.0	4.1
1998	09	26	92.81	27.76	-	4.5
1998	09	28	92.77	27.79	14.0	4.4
1998	09	30	88.12	30.01	34.0	4.8
1998	10	05	88.26	30.26	23.0	5.2
1998	10	16	90.75	25.62	46.0	4.0
1998	10	16	94.60	23.71	72.0	4.0
1998	10	21	94.40	24.39	87.0	4.4
1998	10	24	88.08	30.38	20.0	4.5
1998	10	30	94.15	23.90	105.0	4.2
1998	11	10	93.83	21.06	65.0	4.3
1998	11	17	95.05	25.42	128.0	4.0
1998	11	24	94.51	26.35	55.0	4.2
1998	11	26	87.86	27.69	35.0	4.2
1998	11	29	94.88	29.52	13.0	4.1
1998	12	01	87.68	28.06	67.0	4.6
1998	12	02	93.50	26.40	10.0	4.6
1998	12	02	94.98	25.03	98.0	4.1
1998	12	04	92.29	26.60	40.0	4.0
1998	12	11	95.15	24.72	148.0	4.0
1998	12	21	92.75	22.30	33.0	4.0
1999	01	05	94.58	22.67	111.0	4.2
1999	01	07	94.34	23.45	120.0	4.2
1999	01	12	93.66	22.45	33.0	4.1

Year	Month	Day	Longitude (^{o}E)	Latitude (^{o}N)	Depth (km)	Magnitude (Mw)
1999	01	12	94.38	25.72	55.0	4.0
1999	01	19	96.92	27.11	35.0	4.0
1999	01	20	96.19	26.67	61.0	4.4
1999	01	20	92.63	26.43	57.0	4.2
1999	01	25	97.81	25.03	33.0	4.7
1999	01	28	87.31	28.22	41.0	4.0
1999	02	03	95.94	28.95	30.0	4.6
1999	02	08	92.85	22.16	-	4.3
1999	02	08	92.74	22.17	33.0	4.2
1999	02	11	92.85	22.29	41.0	4.3
1999	02	16	95.37	25.71	91.0	4.0
1999	02	19	94.59	25.35	99.0	4.2
1999	02	19	96.00	29.93	18.0	4.1
1999	02	21	93.67	26.45	41.0	4.1
1999	02	22	93.64	23.26	25.0	5.0
1999	02	28	88.15	31.17	-	4.1
1999	03	11	94.06	25.93	106.0	4.2
1999	03	13	90.63	30.50	27.0	4.5
1999	03	25	87.28	28.12	57.0	4.2
1999	03	29	94.26	23.14	100.0	4.1
1999	04	05	93.72	24.94	31.0	5.6
1999	04	05	93.51	25.00	33.0	5.1
1999	04	07	96.25	26.48	73.0	4.5
1999	04	07	95.97	26.34	14.0	4.5
1999	04	10	87.85	28.04	33.0	4.0
1999	04	14	93.74	24.50	45.0	4.4
1999	04	14	93.81	24.73	33.0	4.2
1999	04	15	93.33	25.80	110.0	4.4

Year	Month	Day	Longitude (^{O}E)	Latitude (^{O}N)	Depth (km)	Magnitude (Mw)
1999	04	15	93.62	25.60	54.0	4.3
1999	04	30	94.14	25.26	33.0	4.4
1999	04	30	93.99	25.24	58.0	4.0
1999	05	09	95.51	24.93	165.0	4.2
1999	05	11	92.76	26.49	15.0	4.4
1999	05	11	92.85	26.56	33.0	4.2
1999	05	25	94.47	23.37	114.0	4.3
1999	05	31	98.65	29.01	51.0	4.7
1999	05	31	98.61	29.02	52.0	4.5
1999	06	09	94.92	25.26	80.0	4.5
1999	06	19	94.35	24.18	80.0	4.2
1999	06	20	92.94	26.33	22.0	4.2
1999	06	26	91.95	26.81	49.0	4.2
1999	06	28	96.60	26.81	-	4.0
1999	07	05	93.78	23.14	122.0	4.1
1999	07	05	93.55	22.87	48.0	4.1
1999	07	22	92.02	21.53	10.0	4.8
1999	07	22	91.90	21.62	10.0	4.7
1999	07	22	92.02	21.53	10.0	4.2
1999	07	28	93.23	25.77	11.0	4.6
1999	07	28	93.34	25.75	61.0	4.1
1999	08	28	89.80	22.92	15.0	4.5
1999	08	30	97.08	21.98	22.0	4.2
1999	09	05	87.53	28.07	33.0	4.5
1999	09	05	87.53	28.07	33.0	4.2
1999	09	05	87.52	28.32	79.0	4.1
1999	09	05	87.52	28.32	79.0	4.0
1999	09	09	93.94	23.26	57.0	4.0

Year	Month	Day	Longitude (°E)	Latitude (°N)	Depth (km)	Magnitude (Mw)
1999	09	20	87.98	27.24	23.0	4.6
1999	09	27	98.97	29.27	25.0	4.2
1999	10	01	94.12	24.30	33.0	4.0
1999	10	03	88.29	30.01	-	4.4
1999	10	03	88.12	30.17	33.0	4.0
1999	10	05	91.98	26.29	33.0	5.2
1999	10	05	91.93	26.26	33.0	4.5
1999	10	06	94.76	23.67	134.0	4.0
1999	10	08	94.48	22.75	115.0	4.0
1999	10	09	91.78	26.18	70.0	4.2
1999	10	09	92.08	26.38	19.0	4.0
1999	10	10	97.01	27.59	-	4.3
1999	10	10	97.40	27.54	72.0	4.2
1999	10	15	90.06	29.61	33.0	4.4
1999	10	15	90.46	29.68	22.0	4.3
1999	10	15	90.46	29.68	22.0	4.0
1999	10	17	93.72	21.89	13.0	4.2
1999	10	19	94.94	24.78	116.0	4.2
1999	10	19	95.24	24.98	145.0	4.0
1999	10	26	92.95	30.13	96.0	4.5
1999	11	05	94.62	21.95	112.0	4.5
1999	11	13	91.55	28.59	45.0	4.0
1999	11	24	93.53	21.85	58.0	4.3
1999	12	02	94.40	21.13	65.0	4.3
1999	12	20	97.72	24.55	35.0	4.5
1999	12	22	94.77	24.11	116.0	4.3
1999	12	23	96.89	26.86	25.0	4.0
1999	12	26	94.56	24.68	100.0	4.2

Year	Month	Day	Longitude (^{O}E)	Latitude (^{O}N)	Depth (km)	Magnitude (Mw)
1999	12	31	91.77	21.45	30.0	4.2
2000	01	02	92.57	27.60	-	4.6
2000	01	03	92.81	22.12	46.0	4.0
2000	01	09	95.37	31.03	09.0	4.1
2000	01	22	95.39	30.96	33.0	4.4
2000	01	22	95.17	31.19	20.0	4.1
2000	01	23	92.47	22.69	100.0	4.5
2000	01	25	88.36	27.68	32.0	4.6
2000	01	25	92.65	27.68	-	4.6
2000	01	25	92.28	27.48	95.0	4.3
2000	01	25	92.68	27.70	10.0	4.2
2000	01	26	95.49	30.89	33.0	5.2
2000	01	26	92.61	27.69	13.0	4.5
2000	01	30	92.03	29.32	33.0	4.8
2000	02	03	96.45	26.50	97.0	4.0
2000	02	14	93.80	22.30	38.0	4.0
2000	02	20	95.22	31.02	24.0	4.5
2000	02	20	95.39	31.03	32.0	4.2
2000	02	27	94.13	23.03	39.0	4.5
2000	03	03	94.45	22.72	100.0	4.2
2000	03	13	87.73	27.67	92.0	4.7
2000	03	17	91.86	26.71	70.0	4.5
2000	03	18	94.92	25.24	94.0	4.4
2000	03	28	94.58	23.94	111.0	4.8
2000	03	28	93.69	22.26	71.0	4.1
2000	03	30	94.46	24.66	70.0	4.4
2000	04	09	94.98	30.23	-	5.0
2000	04	09	95.00	30.19	18.0	4.9

Year	Month	Day	Longitude (°E)	Latitude (°N)	Depth (km)	Magnitude (Mw)
2000	04	10	88.34	30.15	25.0	4.2
2000	04	18	89.76	25.94	46.0	4.1
2000	04	22	95.16	25.87	52.0	4.0
2000	04	27	94.42	22.47	35.0	4.0
2000	05	03	94.51	23.85	33.0	4.1
2000	05	11	96.81	26.01	-	4.4
2000	05	11	94.23	25.41	38.0	4.0
2000	05	14	91.75	28.25	25.0	4.3
2000	05	23	87.16	31.00	30.0	4.3
2000	05	29	87.13	31.01	25.0	4.6
2000	05	29	87.11	30.93	42.0	4.2
2000	05	31	94.58	22.19	121.0	4.0
2000	06	03	87.26	31.24	12.0	4.6
2000	06	05	97.28	30.57	23.0	4.3
2000	06	07	97.19	26.80	33.0	6.3
2000	06	08	97.14	26.63	-	5.1
2000	06	14	97.01	26.83	20.0	4.8
2000	07	02	94.71	24.52	73.0	5.2
2000	07	04	90.67	24.11	100.0	4.0
2000	07	17	92.31	27.02	33.0	4.5
2000	07	20	95.27	25.70	99.0	4.3
2000	08	02	93.51	22.04	30.0	4.1
2000	08	13	94.74	24.69	75.0	4.5
2000	08	16	92.38	26.67	33.0	4.5
2000	09	10	92.69	28.39	33.0	4.7
2000	10	06	97.80	24.38	33.0	5.4
2000	10	08	88.15	30.42	33.0	4.9
2000	10	09	97.99	30.42	33.0	4.8

Year	Month	Day	Longitude (^{O}E)	Latitude (^{O}N)	Depth (km)	Magnitude (Mw)
2000	10	11	94.80	23.85	-	4.5
2000	10	15	96.41	27.00	70.0	4.2
2000	10	18	88.20	29.95	16.0	4.0
2000	10	19	97.56	24.41	23.0	4.1
2000	10	25	95.79	28.90	28.0	4.1
2000	11	09	91.41	25.31	48.0	4.3
2000	11	09	92.38	22.42	19.0	4.3
2000	11	13	92.86	21.70	-	5.5
2000	11	16	97.51	24.23	35.0	4.6
2000	11	24	95.58	26.34	83.0	4.5
2000	12	02	98.06	29.62	20.0	4.1
2000	12	05	94.61	23.94	35.0	4.0
2000	12	11	98.86	25.70	27.0	4.1
2000	12	22	93.90	23.22	71.0	4.2
2000	12	28	96.57	30.60	32.0	4.3
2001	01	04	98.75	21.47	41.4	4.3
2001	01	24	92.69	27.55	20.9	4.0
2001	03	03	93.68	23.90	32.4	4.2
2001	03	10	91.81	27.98	42.8	4.2
2001	03	16	94.80	30.32	14.6	4.3
2001	04	06	92.62	26.47	42.7	4.0
2001	04	10	94.93	24.59	92.8	4.5
2001	04	10	98.95	24.77	17.0	4.5
2001	04	26	94.76	24.72	35.8	4.2
2001	04	28	87.13	28.77	25.0	4.6
2001	04	29	87.18	28.76	51.7	4.0
2001	05	26	95.01	25.41	64.9	4.3
2001	06	13	94.92	23.55	38.7	4.1

Year	Month	Day	Longitude (^{o}E)	Latitude (^{o}N)	Depth (km)	Magnitude (Mw)
2001	06	14	95.58	26.08	108.1	4.0
2001	06	20	92.23	26.63	60.5	4.0
2001	06	29	93.58	23.27	41.8	4.0
2001	06	30	95.33	24.88	144.1	4.2
2001	08	12	94.94	24.45	106.4	4.5
2001	08	31	95.66	26.70	57.6	5.0
2001	09	10	96.88	28.95	07.8	4.1
2001	09	29	95.15	21.19	25.0	4.1
2001	10	10	98.96	24.82	-	4.1
2001	10	19	93.69	21.08	47.4	4.9
2001	10	25	94.38	22.80	97.9	4.1
2001	10	26	92.89	26.26	47.3	4.0
2001	11	06	91.97	27.39	21.4	4.4
2001	12	02	88.18	27.22	24.5	4.6
2002	01	03	94.09	23.29	79.0	4.0
2002	01	07	94.50	24.24	149.0	4.6
2002	01	09	90.49	24.67	100.0	5.1
2002	01	12	94.37	24.10	121.0	4.0
2002	01	18	93.53	23.75	33.0	5.0
2002	01	28	93.70	23.69	33.0	4.3
2002	01	29	92.27	21.54	145.0	4.6
2002	01	31	87.88	29.93	46.0	4.0
2002	02	06	88.14	31.13	28.0	4.0
2002	03	10	94.24	21.21	87.0	4.9
2002	03	21	88.01	29.98	70.0	4.3
2002	03	23	87.97	30.22	24.0	4.4
2002	03	27	88.13	29.88	33.0	4.0
2002	03	27	93.07	26.60	38.0	4.0

Year	Month	Day	Longitude (^{O}E)	Latitude (^{O}N)	Depth (km)	Magnitude (Mw)
2002	03	28	88.09	30.02	65.0	4.0
2002	03	31	87.92	29.93	27.0	4.3
2002	04	02	96.11	25.53	33.0	4.7
2002	04	02	87.28	29.42	59.0	4.3
2002	04	09	88.12	30.04	65.0	4.0
2002	04	11	97.07	27.23	33.0	4.0
2002	04	17	94.70	24.42	56.0	4.0
2002	04	22	96.42	29.97	147.0	4.2
2002	04	27	96.83	30.29	33.0	4.3
2002	05	05	90.93	22.58	10.0	4.5
2002	05	07	93.86	21.60	59.0	4.1
2002	05	09	87.92	29.97	42.0	4.0
2002	05	26	96.03	23.94	33.0	4.6
2002	06	07	95.18	24.84	153.0	4.0
2002	06	16	87.96	29.92	13.0	4.0
2002	06	20	88.87	25.87	38.0	5.1
2002	06	20	91.28	25.32	23.0	4.1
2002	07	03	89.36	30.15	33.0	4.1
2002	07	04	94.54	22.83	107.0	4.5
2002	07	04	94.54	22.83	107.0	4.3
2002	07	07	94.51	22.36	132.0	5.4
2002	07	09	98.86	31.72	10.0	4.5
2002	07	09	87.95	29.86	45.0	4.4
2002	07	11	90.80	25.81	10.0	4.6
2002	07	14	94.09	23.87	48.0	4.5
2002	07	14	93.81	23.41	71.0	4.3
2002	07	14	94.09	23.87	48.0	4.1
2002	07	16	87.69	27.65	33.0	4.1

Year	Month	Day	Longitude (^{o}E)	Latitude (^{o}N)	Depth (km)	Magnitude (Mw)
2002	07	18	98.28	21.22	33.0	4.6
2002	07	18	98.22	21.20	28.0	4.3
2002	07	20	92.18	25.12	31.0	4.6
2002	07	20	92.18	25.12	31.0	4.0
2002	07	29	93.50	23.38	33.0	4.0
2002	07	30	98.81	31.83	29.0	4.1
2002	08	01	88.03	29.93	33.0	4.2
2002	08	03	93.22	22.17	52.0	4.1
2002	08	06	87.99	30.06	44.0	4.5
2002	08	14	97.92	21.20	26.0	4.1
2002	08	16	88.00	30.11	21.0	4.1
2002	08	16	98.38	31.05	28.0	4.0
2002	08	20	92.80	27.21	54.0	4.1
2002	08	22	88.22	29.93	50.0	4.5
2002	08	31	88.06	29.88	16.0	4.7
2002	10	05	95.27	24.85	159.0	5.4
2002	10	05	94.63	24.41	49.0	4.3
2002	10	11	93.81	23.01	71.0	4.5
2002	10	11	87.92	29.82	39.0	4.4
2002	10	11	88.40	31.22	69.0	4.2
2002	10	14	91.75	24.71	45.0	4.2
2002	10	16	93.50	21.18	41.0	5.1
2002	10	17	97.63	29.73	49.0	4.0
2002	10	22	93.49	22.60	66.0	4.1
2002	10	24	93.51	21.47	66.0	4.0
2002	10	29	88.19	31.17	72.0	4.3
2002	10	30	93.88	23.33	93.0	5.3
2002	11	01	93.80	22.52	75.0	4.2

Year	Month	Day	Longitude (^{o}E)	Latitude (^{o}N)	Depth (km)	Magnitude (Mw)
2002	11	14	92.43	27.44	79.0	4.3
2002	11	16	92.47	26.28	26.0	4.5
2002	11	16	90.45	29.79	11.0	4.4
2002	11	16	90.34	29.67	-	4.3
2002	11	16	90.37	29.66	-	4.0
2002	11	16	90.44	29.80	10.0	4.0
2002	11	18	94.65	21.47	35.0	4.0
2002	11	29	90.31	29.68	10.0	4.6
2002	11	30	95.07	28.62	31.0	4.6
2002	12	12	93.66	23.52	69.0	5.5
2002	12	14	96.61	25.42	20.0	4.1
2002	12	16	87.99	29.87	33.0	4.3
2002	12	16	90.44	29.71	-	4.1
2002	12	24	96.48	30.43	20.0	4.3
2002	12	25	93.98	23.23	76.0	5.3
2002	12	29	94.07	22.76	115.0	5.3
2003	02	05	89.76	27.21	33.0	4.7
2003	02	15	90.59	25.93	10.0	4.0
2003	03	18	94.89	25.30	92.0	4.6
2003	03	25	89.38	27.26	51.0	5.4
2003	03	31	91.95	26.62	74.0	4.0
2003	05	23	92.29	26.91	86.0	4.0
2003	05	29	92.73	27.23	22.0	4.2
2003	05	30	92.77	27.02	58.0	4.3
2003	06	04	93.73	23.23	43.0	4.5
2003	06	23	88.15	27.77	80.0	4.5
2003	07	08	88.13	27.29	17.0	4.5
2003	07	08	88.13	27.29	17.0	4.3

Year	Month	Day	Longitude (^{o}E)	Latitude (^{o}N)	Depth (km)	Magnitude (Mw)
2003	07	26	92.33	22.89	-	6.5
2003	07	26	92.33	22.89	-	5.6
2003	07	27	92.34	22.84	-	5.4
2003	07	27	92.34	22.84	-	4.4
2003	07	27	92.24	22.79	-	4.1
2003	07	27	92.20	22.62	49.0	4.0
2003	07	27	92.30	22.85	38.0	4.0
2003	07	29	95.92	26.25	34.0	4.3
2003	07	29	95.92	26.25	34.0	4.1
2003	08	01	92.28	22.85	15.0	4.3
2003	08	01	92.28	22.85	15.0	4.2
2003	08	08	96.87	26.64	13.0	4.7
2003	08	08	96.87	26.64	13.0	4.1
2003	08	18	95.56	29.55	29.0	5.5
2003	08	18	95.56	29.55	29.0	5.3
2003	08	18	95.56	29.55	29.0	5.2
2003	08	18	95.59	29.44	33.0	4.3
2003	08	18	95.59	29.44	33.0	4.2
2003	08	18	95.39	29.52	33.0	4.2
2003	08	18	95.59	29.44	33.0	4.0
2003	08	19	96.72	25.54	-	4.0
2003	08	20	92.74	27.44	33.0	4.6
2003	08	24	96.31	25.03	17.0	4.4
2003	08	24	94.78	24.77	77.0	4.4
2003	08	24	94.78	24.77	77.0	4.4
2003	08	24	96.31	25.03	17.0	4.3
2003	08	26	93.56	25.03	36.0	4.5
2003	08	26	93.56	25.03	36.0	4.5

Year	Month	Day	Longitude (^{O}E)	Latitude (^{O}N)	Depth (km)	Magnitude (Mw)
2003	08	27	93.52	22.92	49.0	4.1
2003	08	30	95.78	23.74	71.0	4.4
2003	09	05	98.83	22.16	10.0	4.1
2003	09	13	94.35	24.20	86.0	4.5
2003	09	29	87.90	27.39	33.0	4.4
2003	10	06	95.26	29.73	44.0	4.1
2003	10	15	94.87	24.60	125.0	4.0
2003	10	29	95.92	26.02	78.0	4.4
2003	11	06	96.83	21.00	10.0	4.0
2003	11	08	93.66	23.61	50.0	4.0
2003	11	09	92.91	21.84	37.0	4.5
2003	11	11	94.10	22.97	81.0	4.1
2003	11	19	94.96	24.61	145.0	4.4
2003	11	29	93.36	25.84	35.0	4.3
2003	12	06	90.39	25.57	27.0	4.1
2003	12	19	92.31	22.80	33.0	4.0
2003	12	20	94.11	22.01	76.0	4.1
2003	12	23	89.21	31.16	-	4.1
2003	12	27	88.11	27.28	67.0	4.1
2003	12	30	96.37	25.32	47.0	4.4
2004	02	19	96.58	25.40	15.0	4.2
2004	02	27	87.60	28.13	78.0	4.3
2004	03	07	91.22	31.65	16.0	5.2
2004	03	20	94.79	23.63	95.7	4.4
2004	04	09	95.03	24.62	105.4	4.0
2004	04	13	95.07	24.68	107.9	4.4
2004	05	24	95.11	24.63	111.3	4.3
2004	05	24	97.14	27.05	01.4	4.3

Year	Month	Day	Longitude (°E)	Latitude (°N)	Depth (km)	Magnitude (Mw)
2004	05	27	89.22	26.28	10.0	4.2
2004	06	03	95.04	25.26	80.0	4.4
2004	06	14	94.27	23.23	78.8	4.3
2004	06	19	95.47	25.24	33.5	4.2
2004	06	28	96.47	26.52	81.6	4.3
2004	07	15	96.60	25.41	48.2	4.0
2004	07	23	88.12	30.18	-	4.5
2004	08	20	94.30	26.28	-	4.0
2004	09	10	93.35	23.89	59.4	4.0
2004	09	17	93.15	23.78	-	4.0
2004	09	18	93.31	23.87	40.8	4.3
2004	09	20	93.62	21.53	91.7	4.2
2004	09	23	96.31	31.12	31.6	4.4
2004	09	24	96.34	27.46	70.8	4.1
2004	09	27	95.52	29.77	13.9	4.9
2004	09	27	98.98	24.81	12.4	4.2
2004	10	08	89.40	25.79	95.7	4.8
2004	10	08	94.30	24.30	-	4.5
2004	10	08	95.78	25.31	56.5	4.4
2004	10	10	87.73	27.73	10.0	4.1
2004	10	12	97.27	29.53	49.7	4.2
2004	10	26	92.89	31.75	10.0	4.5
2004	10	27	98.71	29.23	24.0	4.4
2004	10	27	98.62	28.97	10.0	4.1
2004	11	04	94.48	23.39	110.0	4.1
2004	11	05	93.71	24.09	-	4.4
2004	11	27	98.18	25.15	37.4	4.4
2004	12	01	89.46	30.55	10.0	4.3

Year	Month	Day	Longitude (^{O}E)	Latitude (^{O}N)	Depth (km)	Magnitude (Mw)
2004	12	07	92.43	24.41	72.2	4.0
2004	12	09	92.54	24.76	-	5.4
2004	12	26	91.77	23.97	33.0	5.1
2004	12	28	87.93	23.84	10.0	4.5
2004	12	29	87.28	23.37	10.0	5.2
2004	12	31	88.08	23.68	10.0	4.9
2004	12	31	87.60	23.52	10.0	4.4
2005	01	01	87.05	23.51	10.0	4.5
2005	01	01	87.29	21.56	10.0	4.4
2005	01	01	88.25	27.01	33.0	4.3
2005	01	04	98.75	24.84	24.0	4.2
2005	01	06	96.60	25.43	44.2	4.4
2005	01	07	98.86	25.12	36.5	4.4
2005	01	07	87.09	23.33	10.0	4.3
2005	01	07	87.14	22.97	10.0	4.3
2005	01	07	94.80	23.58	129.0	4.1
2005	01	12	87.60	23.35	10.0	4.5
2005	01	14	94.58	21.98	110.2	4.0
2005	01	15	87.26	23.53	10.0	4.8
2005	01	18	94.70	22.97	-	4.6
2005	01	20	87.25	23.88	10.0	4.7
2005	01	20	87.19	22.91	10.0	4.2
2005	02	03	95.56	26.13	-	4.8
2005	02	07	89.81	30.30	10.0	4.5
2005	02	07	95.60	31.29	10.0	4.0
2005	02	08	94.33	22.97	97.3	4.1
2005	02	15	94.54	24.43	-	4.8
2005	02	15	92.52	24.55	35.2	4.7

Year	Month	Day	Longitude (°E)	Latitude (°N)	Depth (km)	Magnitude (Mw)
2005	02	21	89.15	26.06	10.0	4.0
2005	03	11	90.49	27.34	52.6	4.1
2005	03	12	87.20	22.99	10.0	4.4
2005	03	23	95.29	26.08	-	4.7
2005	03	25	94.84	25.48	-	4.9
2005	03	26	87.93	28.26	70.7	4.5
2005	04	01	87.41	23.66	10.0	4.8
2005	04	05	92.39	22.49	10.0	4.1
2005	04	12	94.45	22.43	111.6	4.3
2005	04	13	87.12	23.72	10.0	4.5
2005	04	16	87.01	23.40	10.0	4.8
2005	04	19	94.48	23.71	90.1	4.2
2005	05	01	87.28	23.33	10.0	4.5
2005	05	03	91.06	25.76	-	4.0
2005	05	08	90.26	30.10	-	4.3
2005	05	15	92.56	31.53	33.0	4.4
2005	05	27	95.74	23.13	10.0	4.1
2005	05	29	92.42	26.93	56.0	4.0
2005	06	01	94.63	28.88	-	5.7
2005	06	03	92.64	31.70	10.0	4.0
2005	06	14	95.69	26.07	83.7	4.5
2005	06	14	87.92	27.21	44.4	4.3
2005	06	20	94.54	22.55	88.6	4.1
2005	06	24	93.14	26.48	54.2	4.0
2005	07	02	96.09	28.79	46.1	4.3
2005	07	07	97.25	26.94	36.0	4.1
2005	07	17	94.99	21.02	-	4.6
2005	07	17	93.39	26.41	-	4.1

Year	Month	Day	Longitude (^{O}E)	Latitude (^{O}N)	Depth (km)	Magnitude (Mw)
2005	07	21	92.16	22.94	10.0	4.3
2005	08	17	93.81	22.78	47.4	4.0
2005	08	19	93.81	21.79	-	4.2
2005	08	20	88.17	31.22	54.0	4.7
2005	08	20	88.21	31.14	10.0	4.1
2005	08	28	87.42	27.64	38.8	4.5
2005	09	10	96.52	25.97	-	4.0
2005	09	12	90.20	25.72	33.0	4.1
2005	09	18	94.84	24.62	87.5	4.8
2005	10	07	88.34	31.43	10.0	4.9
2005	10	28	98.67	29.55	10.0	4.0
2005	10	29	93.96	22.60	-	4.1
2005	11	03	87.04	23.54	10.0	4.5
2005	11	10	98.61	24.68	33.0	4.5
2005	12	27	93.93	24.80	50.0	4.6
2005	12	29	96.16	24.98	33.0	4.4
2006	01	27	94.53	23.10	48.0	4.2
2006	02	01	89.09	31.93	10.0	4.5
2006	02	03	89.61	30.34	10.0	4.5
2006	02	03	98.89	30.75	-	4.1
2006	02	03	98.91	30.97	33.0	4.0
2006	02	06	90.36	31.34	33.0	4.4
2006	02	11	92.14	27.20	42.0	4.5
2006	02	12	91.61	23.90	46.0	4.1
2006	02	14	91.05	24.95	33.0	4.9
2006	02	14	88.35	27.34	33.0	4.9
2006	02	14	95.04	31.64	56.0	4.4
2006	02	14	88.94	30.37	10.0	4.4

Year	Month	Day	Longitude (°E)	Latitude (°N)	Depth (km)	Magnitude (Mw)
2006	02	16	94.28	24.26	75.0	4.2
2006	02	18	95.11	31.81	45.0	4.0
2006	02	21	95.07	31.68	33.0	4.1
2006	02	23	91.65	26.85	29.0	5.3
2006	02	23	93.08	22.93	33.0	5.2
2006	02	23	93.18	24.95	33.0	4.8
2006	02	23	91.31	26.41	10.0	4.6
2006	02	24	91.94	26.84	64.0	4.2
2006	03	02	95.49	22.29	33.0	4.8
2006	03	02	94.60	24.17	33.0	4.7
2006	03	03	87.51	30.89	33.0	4.9
2006	03	05	88.55	30.06	33.0	4.7
2006	03	05	95.20	31.77	33.0	4.5
2006	03	09	95.09	31.76	54.0	4.5
2006	03	09	95.13	31.73	60.0	4.1
2006	03	09	95.10	31.80	10.0	4.0
2006	03	21	93.94	24.70	58.0	4.5
2006	03	25	92.14	26.74	38.0	4.5
2006	03	25	95.59	21.19	33.0	4.5
2006	03	25	94.68	22.62	33.0	4.5
2006	03	25	93.85	23.17	41.0	4.4
2006	03	25	92.91	22.49	-	4.3
2006	04	02	88.30	29.91	138.4	5.0
2006	04	09	88.61	25.83	133.0	4.4
2006	04	11	87.36	28.11	10.0	4.8
2006	04	14	94.47	24.31	101.0	4.5
2006	04	19	90.33	31.50	24.0	5.3
2006	05	11	95.59	21.19	33.0	5.3

ANNEXURE II

Predominant Frequency at 141 Ambient Noise Survey Locations

Master Serial No.	Station Name	Lat (°N)	Long (°E)	Predominant Frequency	Site Geology (Basement Depth)
1	Madhavdev Nagar Maligaon	26.142	91.693	8.4	Granite-Hill
2	Sandilpur	26.169	91.669	0.2	Levee (10-150m)
3	Pandu Sadilapur	26.171	91.674	0.7	Levee
4	Signal & Telcom Trg Ctr	26.170	91.676	0.7	Levee
5	Pandu Water Terminal	26.172	91.680	1.9	Levee
6	Pandu Rly Station	26.174	91.683	1.6	Levee (around 100m)
7	Sangdham Ashram Kalipur	26.169	91.619	2.3	Granite
8	Ajra	26.106	91.616	0.7	T3 (> 200m)
9	Agyathuri	26.199	91.672	7.5	Granite
10	Bamunigaon	26.193	91.669	1.5	T3
11	Baish Para (Garigaon)	26.169	91.672	0.7	Active flood plain
12	University	26.158	91.669	1.2	T2 (> 75 m)
13	Prakrit Nagar	26.155	91.694	1.2	T2 (> 75 m)
14	Jaluk Bari	26.157	91.677	3.4	T2 (around 50 m)
15	Bansipara Maligaon	26.160	91.685	1.0	T2 (> 75 m)
16	Kamakhya Rly Station	26.155	91.695	0.8	T2 (> 75 m)
17	Dharapur West	26.140	91.628	0.7	Levee (> 250 m)
18	Dharapur	26.142	91.639	0.7	T2 (> 150 m)
19	Khanapara	26.154	91.651	0.8	T2 (around 100m)

Master Serial No.	Station Name	Lat (°N)	Long (°E)	Predominant Frequency	Site Geology (Basement Depth)
20	Forest Colony	26.148	91.666	0.8	Granite / Pediment
21	APRO	26.138	91.650	0.9	T2 (around 50 m)
22	Engineering College	26.142	91.672	2.7	T2 (> 150 m)
23	Padambari	26.146	91.679	0.4	T2 (> 100 m)
24	Gota Nagar	26.145	91.683	1.7	T3 (around 75 m)
25	Nambari	26.148	91.688	4.7	T2 (around 75 m)
26	Nambari Officer's Club	26.146	91.692	0.9	T3 (< 25 m)
27	Dharapur	26.130	91.619	0.6	T3 (> 250 m)
28	Baragaon	26.119	91.684	0.4	T2 (> 150 m)
29	Haiguthipara	26.140	91.679	0.3	
30	Devchtal	26.106	91.672	0.6	Pediment
31	Nanapara	26.135	91.623	0.5	T2 (> 225 m)
32	Teteliya	26.132	91.674	3.7	T2 (around 150 m)
33	Paschim Baragaon	26.125	91.683	2.5	T2 (> 25 m)
34	West Baragaon (Dawpara)	26.123	91.687	2.0	T2 (> 25 m)
35	Ajra	26.124	91.620	0.6	T3 (> 225 m)
36	Garchuk / Baragaon	26.119	91.694	0.4	T2 (around 100 m)
37	Pub Baragaon	26.121	91.698	9.0	T2 (around 50 m)
38	Gotsu	26.116	91.607	0.3	T2 (<100 m)
39	Gadheiu Bazar	26.115	91.616	0.7	T3 (> 225 m)
40	Remote Area	26.105	91.673	2.2	Pediment
41	Magnapara	26.104	91.676	0.9	Pediment
42	Pamachi IV	26.103	91.686	0.7	T2 (< 25 m)
43	Pama Hill	26.104	91.694	2.1	T2 (around 25 m)
44	Pamachi III	26.104	91.686	2.4	T2 (< 25 m)
45	Pamachi II	26.105	91.707	4.2	T2 (around 25 m)
46	Manakuram	26.109	91.705	1.0	T2 (< 100 m)
47	Garchuk Nagar	26.119	91.704	5.3	T2 (> 25 m)
48	Guw University	26.158	91.680	1.0	T2 (> 50 m)
49	Azra Rly Station	26.102	91.616	0.8	T3 (around 200 m)

Master Serial No.	Station Name	Lat (°N)	Long (°E)	Predominant Frequency	Site Geology (Basement Depth)
50	Khanamukh	26.140	91.635	0.9	T2 (< 200 m)
51	Kamakhya Temp (low)	26.169	91.719	1.1	Granite
52	Kalit Suba (Dalibari)	26.200	91.640	0.5	T2 (> 200 m)
53	Lachitpur	26.181	91.658	1.3	Levee (>150 m)
54	Garigaon	26.169	91.662	1.4	Levee (> 150 m)
55	Magnapara	26.103	91.682	2.0	T2 (< 25 m)
56	Napara (Dadra)	26.113	91.638	0.5	T2 (< 600 m)
57	Padmabari	26.146	91.680	0.9	T2 (> 100 m)
58	Pander Port	26.170	91.678	0.4	Levee
59	Sharmanjli	26.193	91.644	1.0	T2 (< 150 m)
60	IIT Hills Middle	26.195	91.691	1.1	T3 (> 50 m)
61	IIT hill top	26.195	91.692	0.9	T3 (> 50 m)
62	Joyguru	26.207	91.683	1.1	T2
63	Birla School	26.193	91.682	0.8	T2
64	IIT One	26.191	91.694	0.9	T3 (< 50 m)
65	IIT CRPF	26.191	91.702	1.4	T2 (> 50 m)
66	Panipara	26.183	91.666	0.9	T2 (> 150 m)
67	Silamukhti	26.194	91.669	0.7, 2.1	Granite
68	Kalibari	26.183	91.674	0.8	T2 (< 150 m)
69	Lutia Bagicha	26.189	91.696	3.2	T2 / T3
70	Mariapatti	26.180	91.682	1.1, 2.6	T2
71	IIT Low	26.190	91.692	3.4	Granite / T3
72	DPS Ahamgaon	26.108	91.721	0.9	T2 (> 150 m)
73	CID office Beltala	26.127	91.797	1.1	T2/T3 (> 100 m)
74	Bharalmukn PS	26.170	91.730	1.0	Levee (> 100 m)
75	PHE Office Betkuchi	26.110	91.724	0.8	T2 (> 150 m)
76	PWD Bamuni Moidan	26.184	91.781	1.9	T2 (< 50 m)
77	Govt. Art College Bashistha	26.097	91.789	7.5	Granite (50 m RL)
78	Swadeshi Academy Barbari	26.158	91.818	3.5	Granite/Pediment (100m RL)

Master Serial No.	Station Name	Lat (°N)	Long (°E)	Predominant Frequency	Site Geology (Basement Depth)
79	RK Mission Birubari	26.166	91.752	1.2	T2 (> 100 m)
80	S. Dev Netralaya, Beltola	26.122	91.799	2.7	T2 (around 25 m)
81	Nab Milan Sangha Bhetapara	26.120	91.787	0.9	T3 (> 75 m)
82	Assembly House, Beltola	26.144	91.788	1.5	T3 (> 50m)
83	Birubari-Rupnagar Vidyalaya	26.160	91.755	2.3	T2 (< 25m)
84	Soil Cons Office, Chidiyakhana	26.164	91.780	1.1	T2 (around 25m)
85	Irrigation Office Chandmari	26.184	91.772	1.9	T2 (> 50 m)
86	Dte of Veternary Chenkutti	26.190	91.758	2.9	
87	State Zoo Chidiyakhana	26.163	91.790	8.2	Granite
88	ASSTC Dakhingaon	26.129	91.745	4.1	Granite
89	Datalpara Phatasil	26.130	91.721	1.8	Granite
90	Housefed Dispur	26.137	91.790	1.4	T2 (> 50 m)
91	CPWD Office Fancy Bazar	26.184	91.739	1.2	Levee (around 75 m)
92	GSI Office Ganeshguri	26.155	91.785	1.7	T2 (> 50 m)
93	RRSL Gitanagar	26.172	91.796	3.8	Granite
94	Assam State Museum GNB Rd	26.185	91.752	1.1	Granite
95	K D Nursing Gopinathnagar	26.164	91.745	2.1	T2 (< 25m)
96	Kaziranga Academy Garooghuli	26.097	91.723	2.4	T3 (< 25m)
97	Ganeshpara Phatasil	26.138	91.725	1.6	T2 (around 50 m)
98	Gitanagar PS	26.173	91.781	1.2	T2 (around 75 m)
99	Guwahati Comm College	26.182	91.796	2.0	T2 (< 50 m)
100	A Ghosh Hatigaon	26.137	91.782	1.5	T2 (> 50 m)

Master Serial No.	Station Name	Lat (°N)	Long (°E)	Predominant Frequency	Site Geology (Basement Depth)
101	Veterinary Shelter Hengrabari	26.148	91.811	2.4	Pediment
102	PHE Office Hengrabari	26.152	91.793	2.4	T2 (> 50 m)
103	NJ Vidyalaya Japarigog	26.159	91.788	1.6	T2 (around 25 m)
104	Gyan Institute Jutikuchi	26.133	91.737	3.6	Granite
105	Donbosco Social Forum Jeypur	26.199	91.770	7.0	Granite
106	Jyoti Nagar	26.190	91.784	9.5	Granite
107	Veterinary Coll Khanapara	26.123	91.829	2.4	T2 (around 100 m)
108	HS School Kamakhya	26.163	91.707	3.6	Granite
109	Bodo GH Khanapara	26.118	91.815	6.6	Granite
110	DPEP Office Kahelipara	26.144	91.771	3.4	T2 (> 50 m)
111	Dept Geol & Mines Kahelipara	26.135	91.758	7.2	T2 (around 25 m)
112	Forest Beat Office Kalapahar	26.160	91.742	0.6	T2 (> 75 m)
113	Barsajai Kerakuchi	26.121	91.771	0.9	T2 (> 100 m)
114	JCFTI Kahelipara	26.146	91.768	8.2	Granite
115	4th AP Batalion Kahelipara	26.147	91.752	4.8	Granite
116	Forest Range office Kakhora	26.102	91.751	2.2	T2 (<25m)
117	Nat Pub School Lalungaon	26.113	91.738	0.9	T2 (>50m)
118	Narangi (Private Godown)	26.178	91.830	4.9	T2 (around 25m)
119	Kendriya Vidyalaya Nunmati	26.203	91.792	4.8	Granite
120	IOC Nunmati	26.182	91.814	2.4	T2 (<50m)
121	IOC High School Nunmati	26.190	91.801	4.7	Granite
122	Housfed Natbama	26.130	91.770	0.9	T2 (>50m)

Master Serial No.	Station Name	Lat (°N)	Long (°E)	Predominant Frequency	Site Geology (Basement Depth)
123	Lower Prim School Navagraha	26.191	91.767	5.9	Granite
124	IOC Nunmati	26.181	91.813	1.6	T2 (<50m)
125	SS Kalakshetra Panjabari	26.130	91.822	2.9	T2 (<25m)
126	CD Warehouse Patharquary	26.171	91.829	2.1	Granite
127	Defodil Sch Juripara Panjabari	26.137	91.818	1.0	T2 (around 75m)
128	RG Baruah College Phastasil	26.163	91.736	3.0	T2 (around 75m)
129	Patharkuchi PS	26.102	91.810	1.0	T2 (<25m)
130	DEC Training Rehaban	26.173	91.748	1.1	T2 (>100m)
131	APWD office Sawkuchi	26.122	91.749	1.5	T2 (around 25m)
132	AERC office Saramatariya	26.144	91.797	3.1	T2 (around 75m)
133	Sawkuchi Dispensary	26.111	91.769	1.0	T2 (>75m)
134	BH LTD Six mile	26.132	91.808	1.1	T2 (around 100 m)
135	Kuchpara Salgaon	26.154	91.837	1.1	T3 (>100m)
136	Noapara Mosque Satgaon	26.144	91.830	1.1	T2 (>75m)
137	Nagaland House Sachal Road	26.135	91.808	1.1	T2 (around 100m)
138	Navjyoti Elec upper Hengrabari	26.151	91.805	4.2	Granite
139	Police Camp Udayanagar	26.114	91.817	5.7	T2
140	Planetorium Ujanbazar	26.192	91.752	1.6	Granite
141	B Barooah College Ulubari	26.178	91.758	2.2	T2 (>75m)

ANNEXURE - III

Location, Depth of Ground Water Table, Date of drilling and Litho-Log of each SPT borehole (representative 5 Borehole data out of a total of 200 No presented)

Soil test borehole chart

BH No.	**: 001**	**Location**	**: Behind Building Center(AEC)**
Project	**: Microzonation**	**Date of Starting**	**: 03/01/2005**
Boring Method	**: Wash Boring**	**Date of Completion**	**: 05/01/2005**
Latitude	**: N 26.14167°**	**Ground Water table**	**: 2.10m**
Longitude	**: E 91.66125°**		

Description	Depth (m)	Strata	Sample Collected		SPT			N-Value	N_{cr}	Remarks
			D/S (m)	U/S (m)	15cm	15cm	15cm			
Filled up soil upto 1.5m	0.00									
	1.00									
Redish Clay with mix silt from 1.3 m to 3.5 m	1.50		1.50		5	9	11	20	28	
	2.00									
	3.00		3.00		3	7	10	17	22	
Greenish brown clay from 3.5 m to 4.5 m	3.50			3.50						
	4.00									
	4.50		4.50		4	9	11	20	24	
Greenish brown clay with traces of mix silt (organic material found) from 4.5 m to 9.3 m	5.00									
	6.00		6.00		3	4	6	10	11	
	7.00									
	7.50		7.50		3	4	8	12	13	
	8.00									
	9.00		9.00		3	5	10	15	15	
Clayey sand (brown colour) from 9.3 m to 10.5 m	10.00									
	10.50		10.50		8	14	18	32	23	
	11.00									
	12.00		12.00		22	28	"	refusal	31	
Fine sand from 10.5 m to 16 m	13.00									
	13.50		13.50		9	17	"	refusal	30	
	14.00									
	15.00		15.00		14	32	"	refusal	29	

Soil test borehole chart

BH No.	**: 001**	**Location**	**: Behind Building Center(AEC)**
Project	**: Microzonation**	**Date of Starting**	**: 03/01/2005**
Boring Method	**: Wash Boring**	**Date of Completion**	**: 05/01/2005**
Latitude	**: N 26.14167°**	**Ground Water table**	**: 2.10m**
Longitude	**: E 91.66125°**		

Description	Depth (m)	Strata	Sample Collected		SPT			N-Value	N_{cr}	Remarks
			D/S (m)	U/S (m)	15cm	15cm	15cm			
	16.00									
Coarse sandy clay with mix silt from 16m to 17.5m	17.00		16.50		22	28	*	refusal	28	
	18.00		18.00		29	*	*	refusal	39	
	19.00		19.50		26	*	*	refusal	37	
	20.00									
Blue sandy clay with mix silt from 17.5 m to 29.0 m	21.00		21.00		24	*	*	refusal	36	
	22.00		22.50		34	*	*	refusal	35	
	23.00									
	24.00		24.00		32	*	*	refusal	33	
	25.00		25.50		32	*	*	refusal	32	
	26.00									
	27.00		27.00		34	*	*	refusal	31	
	28.00		28.50		30	*	*	refusal	30	
	29.00									
Fine sand with mix silt										
	30.00									

Soil test borehole chart

BH No.	**: 002**	**Location**	**: Near Jalukbari.**
Project	**: Microzonation**	**Date of Starting**	**: 05/01/2005**
Boring Method	**: Wash Boring.**	**Date of Completion**	**: 07/01/2005**
Latitude	**: N 26.15736°**	**Ground Water table**	**: 0.70m**
Longitude	**: E 91.67229°**		

Description	Depth (m)	Strata	Sample Collected		SPT			N-Value	N_{cr}	Remarks
			D/S (m)	U/S (m)	15cm	15cm	15cm			
	0.00									
Filled up soil upto 2.0m	1.00									
			1.50		0	1	1	2	3	
Bluish Clay from 2m to 2.8m	2.00									
	3.00		3.00		1	2	3	5	7	
Greyish brown clay from 2.8m to 4.6m	4.00									
			4.50		3	5	6	11	14	
Redish grey clay from 4.6m to 5.0m	5.00			5.00						
	6.00		6.00		3	5	7	12	14	
	7.00									
Greyish brown clay from 5.0m to 10.0m			7.50		2	3	6	9	9	
	8.00									
	9.00		9.00		3	3	5	8	8	
	10.00			10.00						
greyish brown clay with mix silt from 10.0m to 11.8m			10.50		3	5	7	12	12	
	11.00									
	12.00		12.00		3	6	10	16	15	
Brownish silty clay from 11.8 m to 15.3 m	13.00									
			13.50		4	7	9	16	14	
	14.00									
	15.00		15.00		4	9	23	32	21	

Soil test borehole chart

BH No.	**: 002**	**Location**	**: Near Jalukbari.**
Project	**: Microzonation**	**Date of Starting**	**: 05/01/2005**
Boring Method	**: Wash Boring.**	**Date of Completion**	**: 07/01/2005**
Latitude	**: N 26.15736°**	**Ground Water table**	**: 0.70m**
Longitude	**: E 91.67229°**		

Description	Depth (m)	Strata	Sample Collected		SPT			N-Value	N_{cr}	Remarks
			D/S (m)	U/S (m)	15cm	15cm	15cm			
	16.00									
Brownish fine sand with			16.50		8	12	20	32	20	
mix silt from	17.00									
15.3m to 25.0m										
	18.00		18.00		8	12	23	35	21	
	19.00									
			19.50		9	11	22	33	20	
	20.00									
	21.00		21.00		15	25	*	refusal	26	
	22.00									
			22.50		20	28	*	refusal	25	
	23.00									
	24.00		24.00		24	*	*	refusal	24	
	25.00									
			25.50		29	*	*	refusal	24	
Brownish coarse sand with	26.00									
mix silt from 25.0m to 27.0m										
	27.00		27.00		32	*	*	refusal	23	
	28.00									
Fine sand with mix silt			28.50		30	*	*	refusal	23	
from 27.0m. To 30.0m	29.00									
	30.00									

Soil test borehole chart

BH No.	**: 003**	**Location**	**: Near Environment Science Deptt.(G.U.)**
Project	**: Microzonation**		
Boring Method	**: Wash Boring**	**Date of Starting**	**:05/01/2005**
Latitude	**: N 26.15273°**	**Date of Completion**	**:06/01/2005**
Longitude	**: E 91.65732°**	**Ground Water table**	**: 0.50m**

Description	Depth (m)	Strata	Sample Collected		SPT			N-Value	N_{cr}	Remarks
			D/S (m)	U/S (m)	15cm	15cm	15cm			
	0.00									
Bluish/ Redish silty clay	1.00									
upto 3.3m			1.50		4	6	9	15	26	
	2.00									
	3.00		3.00		2	4	6	10	17	
Bluish / redish sandy clay										
from 3.3 to 5.6 m	4.00									
			4.50		6	8	10	18	26	
	5.00									
	6.00		6.00		4	6	8	14	19	
Brownish/ bluish silty clay										
from 5.6m to 12.0m	7.00									
			7.50		4	7	8	15	19	
	8.00									
	9.00		9.00		7	12	14	26	31	
	10.00									
			10.50		8	12	13	25	28	
	11.00									
	12.00		12.00		4	8	11	19	21	
Redish and bluish clay from	13.00									
12.0m to 15.5m			13.50		5	9	13	22	23	
	14.00									
	15.00		15.00		6	9	14	23	23	

Soil test borehole chart

BH No.	**: 003**	**Location**	**: Near Environment Science Deptt.(G.U.)**
Project	**: Microzonation**		
Boring Method	**: Wash Boring**	**Date of Starting**	**:05/01/2005**
Latitude	**: N 26.15273°**	**Date of Completion**	**:06/01/2005**
Longitude	**: E 91.65732°**	**Ground Water table**	**: 0.50m**

Description	Depth (m)	Strata	Sample Collected		SPT			N-Value	N_{cr}	Remarks
			D/S (m)	U/S (m)	15cm	15cm	15cm			
	16.00									
Bluish silty clay from 15.5m			16.50		7	11	17	28	27	
to 20.0m	17.00									
	18.00		18.00		12	21	27	49	45	
	19.00									
			19.50		18	27	*	refusal	44	
	20.00									
	21.00		21.00		22	28	*	refusal	29	
	22.00									
Sand from 20.0m to 26.8 m			22.50		22	30	*	refusal	28	
	23.00									
	24.00		24.00		15	35	*	refusal	27	
	25.00									
			25.50		12	38	*	refusal	26	
	26.00									
	27.00		27.00		10	15	22	37	27	
Bluish silty clay from 26.8 m	28.00									
to 30.0 m.			28.50		10	18	23	41	29	
	29.00									
	30.00									

Soil test borehole chart

BH No.	**: 004**	**Location**	**: Near Saat Mile (Bus Stop)**
Project	**: Microzonation**	**Date of Starting**	**:07/01/2005**
Boring Method	**: Wash Boring**	**Date of Completion**	**:09/01/2005**
Latitude	**: N 26.14808°**	**Ground Water table**	**: 0.50m**
Longitude	**: E 91.64718°**		

Description	Depth (m)	Strata	Sample Collected		SPT			N-Value	N_{cr}	Remarks
			D/S (m)	U/S (m)	15cm	15cm	15cm			
Filled up soil upto 1.0m	0.00									
	1.00									
Greyish blue clay from			1.50		1	2	2	4	7	
from 1.0m to 3.15 m	2.00									
	3.00		3.00		2	8	8	16	24	
Greyish blue sandy clay										
from 3.15m to 4.65 m	4.00									
			4.50		3	1	2	3	4	
	5.00									
Bluish sandy clay with mix				5.50						
silt from 4.65m to 10.0m	6.00		6.00		0	0	0	0	0	
	7.00									
			7.50		0	1	1	2	2	
	8.00									
	9.00		9.00		2	3	4	7	7	
	10.00									
Bluish silty clay from 10.0m			10.50		3	3	5	8	8	
to 12.15 m	11.00									
	12.00		12.00		3	8	16	24	19	
Browins fine sand with mix	13.00									
silt from 12.15 to 15.30m			13.50		7	10	19	29	21	
	14.00									
	15.00		15.00		9	7	10	17	15	

Soil test borehole chart

BH No.	**: 004**	**Location**	**: Near Saat Mile (Bus Stop)**
Project	**: Microzonation**	**Date of Starting**	**:07/01/2005**
Boring Method	**: Wash Boring**	**Date of Completion**	**:09/01/2005**
Latitude	**: N 26.14808°**	**Ground Water table**	**: 0.50m**
Longitude	**: E 91.64718°**		

Description	Depth (m)	Strata	Sample Collected		SPT			N-Value	N_{cr}	Remarks
			D/S (m)	U/S (m)	15cm	15cm	15cm			
Brownish clay with mix silt from 15.3m to 17.m	16.00		16.50		6	8	10	18	15	
	17.00									
Greyish silty clay from 17.0 m to 19.20m	18.00		18.00		9	13	17	30	24	
	19.00									
Fine sand with mix silt from 19.2m to 20.3m	20.00		19.50		13	18	33+	refusal	27	
	21.00		21.00		21	27	23+	refusal	26	
	22.00									
Brown coarse sand from 20.3m to 26.0m	23.00		22.50		15	25	25+	refusal	26	
	24.00		24.00		15	28	22+	refusal	25	
	25.00									
	26.00		25.50		20	31	19+	refusal	24	
	27.00		27.00							gravel found at 26m.SPT couldnot be continued. 50 blows of DCPT at 40cm.
Gravel found from 26.0m	28.00									
			28.50							
	29.00									
	30.00									

Soil test borehole chart

BH No.	**: 005**	**Location**	**: Khanamukh (Check Gate)**
Project	**: Microzonation**	**Date of Starting**	**:07/01/2005**
Boring Method	**: Wash Boring**	**Date of Completion**	**:08/01/2005**
Latitude	**: N 26.14073°**	**Ground Water table**	**:0.50m**
Longitude	**: E 91.63915°**		

Description	Depth (m)	Strata	Sample Collected		SPT			N-Value	N_{cr}	Remarks
			D/S (m)	U/S (m)	15cm	15cm	15cm			
Bluish / Redish clay upto 5.5m	0.00									
	1.00									
			1.50		1	2	5	7	12	
	2.00									
	3.00		3.00		4	9	9	18	26	
				3.50						
	4.00									
			4.50		5	9	10	19	25	
	5.00									
	6.00		6.00		8	9	12	21	26	
Brownish silty clay from 5.5m to 9.0m	7.00									
			7.50		9	9	14	23	27	
	8.00									
	9.00		9.00		4	7	9	16	17	
	10.00									
			10.50		6	8	11	19	18	
	11.00									
Brownish clayey sand from 9.0m to 22.0m	12.00		12.00		8	10	11	21	19	
	13.00									
			13.50		8	12	14	26	21	
	14.00									
	15.00		15.00		13	26	24+	refusal	31	

Soil test borehole chart

BH No.	**: 005**	**Location**	**: Khanamukh (Check Gate)**
Project	**: Microzonation**	**Date of Starting**	**:07/01/2005**
Boring Method	**: Wash Boring**	**Date of Completion**	**:08/01/2005**
Latitude	**: N 26.14073°**	**Ground Water table**	**:0.50m**
Longitude	**: E 91.63915°**		

Description	Depth (m)	Strata	Sample Collected		SPT			N-Value	N_{cr}	Remarks
			D/S (m)	U/S (m)	15cm	15cm	15cm			
	16.00									
			16.50		15	25	25+	refusal	30	
	17.00									
	18.00		18.00		17	28	22+	refusal	29	
	19.00									
			19.50		20	31	19+	refusal	28	
	20.00									
	21.00		21.00		23	34	16+	refusal	27	
	22.00									
			22.50		25	35	15+	refusal	27	
	23.00									
Sand from 22.0m upto 27.0 m.	24.00		24.00		30	45	5+	refusal	26	
	25.00									
			25.50		32	50	*	refusal	25	
	26.00									
	27.00		27.00		38	50	*	refusal	25	
										Gravel found at 27.2m DCPT performed.
Gravel found from 27.20m	28.00									
	29.00									
	30.00		30.00							

ANNEXURE IV

Physical and Shear Parameters of Sediment as Obtained from 200 Boreholes

Bh_No.	Depth (m)	From (m)	To (m)	Bulk Den	Wet Den	Saturated Den	Dry Den	SpGr	Void R	Porosity%	LL%	PL%	PI	C Kg/cm²	ϕ
1	2.00			1.97		1.99	1.57	2.63	0.67	40.00	42.80	23.62	19.18	0.420	7.0
	3.50			1.98		1.98	1.59	2.62	0.65	39.00	44.00	22.87	21.13	0.430	6.5
	5.00			1.98		1.99	1.61	2.63	0.63	39.00	43.60	21.56	22.04	0.450	7.0
	6.50			1.97		1.98	1.58	2.63	0.66	40.00				0.420	7.5
	8.00			2.00		1.99	1.62	2.61	0.61	38.00	47.20	22.48	24.72	0.440	6.0
	10.50			2.01		2.00	1.62	2.64	0.63	39.00				0.340	11.0
	12.00			1.99		2.03	1.66	2.62	0.58	37.00	40.70	23.51	19.19	0.360	10.0
	15.00			2.00		2.00	1.62	2.62	0.62	38.00	45.90	22.63	23.27	0.450	7
Bh_No.	**Depth**	**From (m)**	**To (m)**	**Bulk Den**	**Wet Den**	**Saturated Den**	**Dry Den**	**SpGr**	**Void R**	**Porosity%**	**LL%**	**PL%**	**PI**	**C Kg/cm²**	**ϕ**
2		1.50	2.00								37.45	15.78	21.67		
		2.50	3.00	1.98				2.69	0.758					0.38	
		3.00	3.50								38.66	17.53	21.13		
		4.50	5.00								39.24	18.76	20.48		
		5.50	6.00	1.99				2.67	0.738					0.41	
		6.00	6.50								34.89	19.52	15.37		
		7.50	8.00								33.59	18.56	15.03		
		8.50	9.00	1.97				2.68	0.70					0.49	
		10.50	11.00								31.88	18.36	13.52		
		12.00	12.50								32.45	17.64	14.81		

Bh_No.	Depth	From (m)	To (m)	Bulk Den	Wet Den	Saturated Den	Dry Den	SpGr	Void R	Porosity%	LL%	PL%	PI	C Kg/cm²	ϕ
3	NO DATA	1.50	2.00												
Bh_No.	**Depth (m)**	**From (m)**	**To (m)**	**Bulk Den**	**Wet Den**	**Saturated Den**	**Dry Den**	**SpGr**	**Void R**	**Porosity%**	**LL%**	**PL%**	**PI**	**C Kg/cm²**	**ϕ**
4	NO DATA														
Bh_No.	**Depth (m)**	**From (m)**	**To (m)**	**Bulk Den**	**Wet Den**	**Saturated Den**	**Dry Den**	**SpGr**	**Void R**	**Porosity%**	**LL%**	**PL%**	**PI**	**C Kg/cm²**	**ϕ**
5		0.00	1.00	2.12			1.60	2.60	0.62		35.08	22.51	12.57	0.65	0
		1.00	3.50	2.00			1.55	2.60	0.67		34.70	21.95	12.75	0.62	0
		3.50	4.50	1.96			1.50	2.60	0.73		34.10	21.60	12.50	0.58	0
		6.00	7.00	1.91			1.50	2.63	0.75		43.10	27.19	15.91	0.25	10
		7.00	9.00	2.07			1.65	2.60	0.58		32.70	21.33	11.37	0.98	0
		13.20	13.95	2.03			1.63	2.65	0.62					0	36
Bh_No.	**Depth (m)**	**From (m)**	**To (m)**	**Bulk Den**	**Wet Den**	**Saturated Den**	**Dry Den**	**SpGr**	**Void R**	**Porosity%**	**LL%**	**PL%**	**PI**	**C Kg/cm²**	**ϕ**
6	3.5			1.87			1.45	2.60	0.793	44.00	46.30	23.75	22.55	0.20	7.5
	4.5			1.90			1.51	2.63	0.708	41.00				0.10	19.0
	6.5			1.91			1.53	2.62	0.712	41.00				0.30	11.0
	9.0			1.92			1.65	2.67	0.618	38.00				0.00	31.0
	11.0			1.96			1.59	2.60	0.635	39.00	48.80	23.67	24.63	0.48	7.0
	14.0			1.97			1.60	2.61	0.631	39.00	48.30	23.67	24.63	0.50	6.5
Bh_No.	**Depth (m)**	**From (m)**	**To (m)**	**Bulk Den**	**Wet Den**	**Saturated Den**	**Dry Den**	**SpGr**	**Void R**	**Porosity%**	**LL%**	**PL%**	**PI**	**C Kg/cm²**	**ϕ**
7	1.5			1.83		1.86	1.39	2.61	0.877	47.00	43.80	24.68	19.12	0.14	7.0
	3.0			1.85		1.88	1.43	2.62	0.832	45.00	41.50			0.13	8.5
	5.0			1.84		1.87	1.41	2.60	0.844	46.00	45.30	23.87	21.43	0.16	5.0
	8.0			1.83		1.87	1.42	2.61	0.838	45.00	48.70	22.95	25.75	0.15	6.0
	10.5			2.01		2.14	1.83	2.67	0.459	31.00				0.08	28.0
	13.5			2.03		2.05	1.71	2.60	0.520	34.00	47.60	23.22	24.3	0.48	7.0

Bh_No.	Depth (m)	From (m)	To (m)	Bulk Den	Wet Den	Saturated Den	Dry Den	SpGr	Void R	Porosity%	LL%	PL%	PI	C Kg/cm²	ϕ
8		1.00	1.45	1.842		1.973	1.562	2.650	0.696	0.410					
		1.50	1.95								42	20	22		
		2.50	2.95	1.993		2.013	1.617	2.680	0.658	0.397					
		3.00	3.45								42	20	22		
		4.00	4.45	1.997		2.025	1.634	2.680	0.640	0.390					
		4.50	4.95								42	20	22		
		5.50	5.95	2.034		2.021	1.629	2.680	0.645	0.392					
		6.00	6.45								42	20	22		
		7.00	7.45	2.006		2.028	1.640	2.680	0.634	0.388					
		7.50	7.95								46	22	24		
		8.50	8.95	2.055		2.023	1.633	2.676	0.638	0.390					
		9.00	9.45								46	22	24		
		10.00	10.45	2.039		2.020	1.628	2.676	0.643	0.392					
		10.50	10.95								46	22	24		
		11.50	11.95	2.032		2.036	1.655	2.676	0.617	0.382					
		12.00	12.45								46	22	24		

ANNEXURE V

Shear Wave Velocity Data at Different Depth

Bore Hole ID	SHEAR WAVE VELOCITY AT DEPTH m/sec (equation used)				
	0.00m-6.00m	6.00m-12.00m	12.00m-18.00m	18.00m-24.00m	24.00m-30.00m
1	312.6 (2)	308.3 (2)	315.2 (3)	372.8 (2)	355.6 (2)
2	261.0 (2)	192.3 (1)	248.9 (3)	274.4 (3)	269.3 (3)
3	312.6 (2)	266.5 (1)	293 (1)	315.2 (3)	294.8 (3)
4	269.6 (2)	265.3 (2)	248.9 (3)	284.6 (3)	274.4 (3)
5	316.9 (2)	240.0(1)	294.8 (3)	289.7 (3)	279.5 (3)
6	208.2 (1)	248.1 (2)	239.5 (2)	239.5 (2)	279.5 (3)
7	282.4 (1)	286.8 (2)	274.4 (3)	289.7 (3)	274.4 (3)
8	282.5 (2)	213.2 (3)	284.6 (3)	289.7 (3)	274.4 (3)
9	224.1 (1)	312.6 (2)	299.9 (3)	279.5 (3)	269.3 (3)
10	286.8 (2)	305.0 (3)	299.9 (3)	284.6 (3)	269.3 (3)
11	213.5 (1)	259.1 (3)	305 (3)	289.7 (3)	279.5 (3)
12	282.5 (2)	208.1 (3)	238.7 (3)	289.7 (3)	*
13	213.5 (1)	315.2 (3)	299.9 (3)	284.6 (3)	274.4 (3)
14	197.6 (1)	289.7 (3)	299.9 (3)	284.6 (3)	269.3 (3)
15	291.1 (2)	312.6 (2)	294.8 (3)	274.4 (3)	269.3 (3)
16	187.0 (1)	228.5 (3)	259.1 (3)	284.6 (3)	279.5 (3)
17	176.4 (1)	176.4 (1)	171.1 (1)	295.4 (2)	279.5 (3)
18	165.8 (1)	176.4 (1)	197.6 (1)	295.4 (2)	279.5 (3)
19	160.5 (1)	239.5 (2)	252.4 (2)	299.9 (3)	274.4 (3)

Bore Hole ID	SHEAR WAVE VELOCITY AT DEPTH m/sec (equation used)				
	0.00m-6.00m	6.00m-12.00m	12.00m-18.00m	18.00m-24.00m	24.00m-30.00m
20	181.7 (1)	176.4 (1)	187 (1)	295.4 (2)	259.1 (3)
21	155.2 (1)	181.7 (1)	187 (1)	254 (3)	278.2 (2)
22	208.2 (1)	197.6 (1)	304 (2)	294.8 (3)	279.5 (3)
23	261.0 (2)	245.3 (1)	254 (3)	274.4 (3)	274.4 (3)
24	286.8 (2)	240 (1)	277.1 (1)	294.8 (3)	284.6 (3)
25	304.0 (2)	286.8 (2)	202.9 (1)	181.7 (1)	243.8 (3)
26	229.4 (1)	229.4 (1)	289.7 (3)	284.6 (3)	269.3 (3)
27	229.4 (1)	250.6 (1)	289.7 (3)	284.6 (3)	269.3 (3)
28	181.7 (1)	208.2 (1)	299.9 (3)	284.6 (3)	274.4 (3)
29	248.1 (2)	197.6 (1)	213.5 (1)	289.7 (3)	279.5 (3)
30	252.4 (2)	213.5 (1)	351.3 (2)	289.7 (3)	274.4 (3)
31	181.7 (1)	187 (1)	213.5 (1)	218.8 (1)	274.4 (3)
32	171.1 (1)	224.1 (1)	176.4 (1)	282.5 (1)	377.1 (3)
33	293 (1)	234.7 (1)	265.3 (1)	213.5 (1)	224.1 (1)
34	218.8 (1)	181.7 (1)	218.8 (1)	208.2 (1)	271.8 (1)
35	208.2 (1)	266.5 (1)	294.8 (3)	279.5 (3)	269.3 (3)
36	250.6 (1)	266.5 (1)	321.2 (2)	208.2 (1)	310.1 (3)
37	171.1 (2)	233.6 (3)	305 (3)	294.8 (3)	279.5 (3)
38	273.9 (2)	266.5 (1)	202.9 (1)	273.9 (2)	*
39	139.3 (1)	224.1 (2)	264.2 (2)	291.1 (3)	278.2 (3)
40	149.9 (1)	187 (1)	310.1 (3)	289.7 (3)	274.4 (3)
41	171.1 (1)	165.8 (1)	245.3 (1)	334.1 (2)	284.6 (3)
42	261 (1)	250.6 (2)	265.3 (2)	279.5 (3)	254 (1)
43	202.9 (1)	265.3 (2)	284.6 (3)	284.6 (3)	274.4 (3)
44	213.5 (1)	269.3 (3)	289.7 (3)	279.5 (3)	264.2 (3)
45	171.1 (1)	176.4 (1)	265.3 (2)	208.2 (1)	240 (1)
46	202.9 (1)	294.8 (3)	284.6 (3)	274.4 (3)	264.2 (3)

Bore Hole ID	SHEAR WAVE VELOCITY AT DEPTH m/sec (equation used)				
	0.00m-6.00m	6.00m-12.00m	12.00m-18.00m	18.00m-24.00m	24.00m-30.00m
47	176.4 (1)	187 (1)	269.3 (3)	284.6 (3)	274.4 (3)
48	282.5 (2)	304 (2)	224.1 (1)	240 (1)	261.2 (1)
49	197.6 (1)	294.8 (3)	294.3 (3)	289.7 (3)	274.4 (3)
50	266.5 (1)	208.2 (1)	299.9 (3)	289.7 (3)	274.4 (3)
51	245.3 (1)	293 (1)	240 (1)	294.8 (3)	248.9 (3)
52	235.2 (2)	299.7 (2)	279.5 (3)	289.7 (3)	274.4 (3)
53	213.5 (1)	192.3 (1)	347 (2)	284.6 (3)	274.4 (3)
54	218.8 (1)	255.9 (1)	359.9 (2)	250.6 (1)	229.4 (1)
55	192.3 (1)	181.7 (1)	208.2 (1)	305 (3)	274.4 (3)
56	208.2 (1)	271.8 (1)	282.4 (1)	289.7 (3)	274.4 (3)
57	155.2 (1)	240 (1)	274.4 (3)	*	*
58	256.7 (2)	192.3 (1)	279.5 (3)	284.6 (3)	269.3 (3)
59	176.4 (1)	197.6 (1)	291.1 (2)	269.3 (3)	*
60	192.3 (1)	312.6 (2)	240 (1)	255.9 (1)	325.5 (2)
61	187 (1)	192.3 (1)	252.4 (2)	334.1 (2)	274.4 (3)
62	208.2 (1)	266.5 (1)	229.4 (1)	261.2 (1)	286.8 (2)
63	218.8 (1)	261.2 (1)	351.3 (2)	294.8 (3)	279.5 (3)
64	248.1 (2)	273.9 (2)	291.1 (2)	274.4 (3)	243.8 (3)
65	181.7 (1)	273.9 (2)	208.1 (3)	284.6 (3)	*
66	176.4 (1)	282.4 (1)	377.1 (2)	359.9 (2)	282.4 (1)
67	252.4 (2)	265.3 (1)	192.3 (1)	218.3	274.4 (3)
68	208.2 (1)	273.9 (2)	289.7 (3)	274.4 (3)	274.4 (3)
69	234.7 (1)	277.1 (1)	240 (1)	338.4 (2)	325.5 (2)
70	278.2 (2)	316.9 (3)	187 (1)	208.2	250.6
71	187 (1)	278.2 (2)	286.8	240 (2)	325.5
72	234.7 (1)	381.4 (2)	304 (2)	250.6 (1)	224.1 (1)
73	197.6(1)	186.8	269.6 (2)	269.6 (2)	284.6 (3)

Bore Hole ID	SHEAR WAVE VELOCITY AT DEPTH m/sec (equation used)				
	0.00m-6.00m	6.00m-12.00m	12.00m-18.00m	18.00m-24.00m	24.00m-30.00m
74	176.4 (1)	197.6 (1)	228.5 (3)	294.8 (3)	264.2 (3)
75	250.6 (1)	234.7 (1)	271.8 (1)	338.4 (2)	274.4 (3)
76	192.3 (1)	304 (2)	269.6 (2)	295.4	274.4 (3)
77	273.9 (2)	269.6 (2)	335.6 (3)	338.4 (2)	321.2 (2)
78	368.5 (2)	368.5 (2)	396.8 (3)	310.1 (3)	*
79	282.5 (2)	213.5 (1)	278.2 (2)	304 (1)	*
80	269.6 (2)	325.5 (2)	233.6 (3)	304 (2)	359.9 (2)
81	321.2 (1)	314.2 (1)	299.7 (1)	321.2 (2)	274.4 (3)
82	228.5 (3)	279.5 (3)	299.9 (3)	248.1 (2)	274.4 (3)
83	202.9 (1)	282.4 (1)	299.9 (3)	250.6 (1)	325.5 (2)
84	368.5 (2)	359.9 (2)	320.3 (3)	284.6 (3)	334.1 (2)
85	192.8 (3)	282.5 (2)	202.9 (1)	192.3 (2)	234.7 (1)
86	187(1)	282.5(2)	224.1(1)	274.4(3)	325.5 (2)
87	277.1 (1)	240 (1)	334.1	248.9 (2)	279.5 (3)
88	273.9 (2)	273.9 (2)	224.1 (1)	192.3 (1)	295.4 (2)
89	261 (2)	308.3 (2)	338.4 (2)	277.1 (1)	266.5 (1)
90	248.9	329.8	269.6 (2)	192.8 (3)	*
91	187 (1)	202.9 (1)	181.7 (1)	314.2 (1)	279.5 (3)
92	282.5 (2)	282.5 (2)	269.6 (2)	279.5 (3)	294.8 (3)
93	234.7 (1)	240 (1)	295.4 (2)	312.6 (2)	284.6 (3)
94	160.5 (1)	250.6 (1)	243.8 (2)	171.1 (1)	240 (1)
95	197.6 (1)	291.1 (2)	282.5 (2)	266.5 (1)	277.1 (1)
96	187 (1)	202.9 (1)	187 (1)	299.7 (2)	305 (1)
97	202.9 (1)	265.3 (2)	234.7 (1)	330.1 (1)	277.1 (1)
98	213.5 (1)	338.4 (2)	291.1 (2)	330.1 (1)	271.8 (1)
99	224.1 (1)	255.9 (1)	213.5 (1)	271.8 (1)	279.5 (3)
100	250.6 (1)	197.6 (1)	197.6 (1)	289.7 (3)	319.5 (1)

Bore Hole ID	SHEAR WAVE VELOCITY AT DEPTH m/sec (equation used)				
	0.00m-6.00m	6.00m-12.00m	12.00m-18.00m	18.00m-24.00m	24.00m-30.00m
101	347	273.9	282.5	316.9	279.5 (3)
102	255.9 (1)	312.6 (2)	291.1 (2)	224.1 (1)	269.3 (3)
103	239.5	160.5	197.6	299.9	284.6 (3)
104	265.3	295.4	187 (1)	308.3	284.6 (3)
105	261 (2)	325.5 (2)	202.9 (1)	202.9 (1)	299.9 (3)
106	197.6	282.5	256.7	261.2	279.5 (3)
107	160.5	295.4	192.3 (1)	338.4	359.9
108	224.1	303.6	264.2	295.4	279.5 (3)
109	234.7	299.7	197.9	295.4	294.8
110	208.2	181.7 (1)	213.5	308.3	*
111	287.7	255.9	269.3	316.9	312.6
112	187 (1)	274.4 (3)	299.9 (3)	284.6 (3)	269.3 (3)
113	197.6 (1)	316.9 (2)	321.2 (2)	284.6 (3)	*
114	202.9	282.4	224.1	312.6	284.6
115	218.8 (1)	269.6 (2)	278.2 (2)	197.6 (1)	264.2 (3)
116	245.3 (1)	294.8 (3)	305 (3)	384.6 (3)	279.5 (3)
117	324.8	305 (3)	192.3	310.1	279.5 (3)
118	269.6 (2)	269.6 (2)	252.4 (2)	324.8 (1)	279.5 (3)
119	187 (1)	299.7 (2)	218.8 (1)	314.2 (1)	324.8 (1)
120	269.6 (2)	312.6 (2)	286.8	187	279.5 (3)
121	252.4 (2)	192.3 (1)	271.8 (1)	192.3 (1)	308.3 (2)
122	197.6 (1)	320.3 (3)	299.9 (3)	284.6 (3)	274.4 (3)
123	239.5	286.8	291.1	282.5	305 (3)
124	252.4 (2)	291.1 (2)	265.3 (2)	284.6 (2)	334.1 (3)
125	160.5 (1)	330.5 (3)	305 (3)	284.6 (3)	274.4 (3)
126	265.3 (2)	233.6 (3)	299.9 (3)	289.7 (3)	274.4 (3)
127	269.6	282.5	229.4	269.6	304 (2)

Bore Hole ID	SHEAR WAVE VELOCITY AT DEPTH m/sec (equation used)				
	0.00m-6.00m	6.00m-12.00m	12.00m-18.00m	18.00m-24.00m	24.00m-30.00m
128	218.8 (1)	218.8 (1)	321.2 (2)	329.8 (2)	321.2 (2)
129	218.8 (1)	381.4 (2)	299.9 (3)	284.6 (3)	274.4 (3)
130	273.9 (2)	229.4 (1)	274.4 (3)	266.5 (1)	279.5 (3)
131	176.4 (1)	279.5 (3)	304 (2)	284.6 (3)	*
132	218.8 (1)	261.2 (1)	299.9 (3)	284.6 (3)	294.8 (3)
133	165.8 (1)	314.2 (1)	305 (3)	289.7 (3)	*
134	299.7 (1)	340.7 (3)	305 (3)	284.6 (3)	274.4 (3)
135	240 (1)	325.4 (3)	192.3 (1)	261.2 (1)	279.5 (3)
136	187 (1)	224.1 (1)	293 (1)	289.7 (3)	187 (1)
137	181.7 (1)	303.6 (1)	245.3 (3)	*	*
138	181.7 (1)	208.2 (1)	310.1 (3)	*	*
139	197.6 (1)	181.7 (1)	255.9 (1)	197.6 (1)	350.9 (3)
140	278.2 (2)	279.5 (3)	208.2 (1)	278.2 (2)	338.4 (2)
141	282.4 (1)	325.4 (3)	305 (3)	321.2 (2)	274.4 (3)
142	192.3 (1)	197.6 (1)	284.6 (3)	284.6 (3)	427.4 (3)
143	208.2 (1)	312.6 (2)	342.7 (2)	284.6 (3)	279.5 (3)
144	192.3 (1)	261.2 (1)	305 (3)	284.6 (3)	274.4 (3)
145	213.5 (1)	181.7 (1)	259.1 (3)	289.7 (3)	274.4 (3)
146	218.8 (1)	224.1 (1)	289.7 (3)	284.6 (3)	*
147	286.8 (2)	299.9 (3)	295.4 (2)	255.9 (1)	250.6 (1)
148	181.7 (1)	171.1 (1)	192.3 (1)	289.7 (3)	279.5 (3)
149	202.9 (1)	218.8 (1)	229.4 (1)	266.5 (1)	*
150	295.4 (2)	329.8 (2)	310.1 (3)	289.7 (3)	274.4 (3)
151	208.2 (1)	261.2 (1)	299.9 (3)	289.7 (3)	274.4 (3)
152	202.9 (1)	286.8 (2)	305 (3)	284.6 (3)	269.3 (3)
153	261.2 (1)	312.6 (2)	299.9 (3)	289.7 (3)	*
154	165.8 (1)	176.4 (1)	254 (1)	294.8 (3)	279.5 (3)

Bore Hole ID	SHEAR WAVE VELOCITY AT DEPTH m/sec (equation used)				
	0.00m-6.00m	6.00m-12.00m	12.00m-18.00m	18.00m-24.00m	24.00m-30.00m
155	208.2 (1)	202.9 (1)	266.5 (1)	284.6 (3)	223.4 (3)
156	197.6 (1)	208.2 (1)	330.5 (3)	335.6 (3)	315.2 (3)
157	187 (1)	213.5 (1)	224.1 (1)	202.9 (1)	245.3 (1)
158	208.2 (1)	278.2 (2)	259.1 (3)	299.9 (3)	*
159	213.5 (1)	218.8 (1)	287.7 (1)	294.8 (3)	279.5 (3)
160	176.4 (1)	218.8 (1)	229.4 (1)	218.8 (1)	208.2 (1)
161	229.4 (1)	273.9 (2)	181.7 (1)	213.5 (1)	299.7 (2)
162	187 (1)	229.4 (1)	213.5 (1)	289.7 (3)	279.5 (3)
163	338.4 (2)	424.4 (2)	250.6 (1)	308.3 (1)	295.4 (1)
164	245.3 (1)	286.8 (2)	304 (2)	294.8 (3)	284.6 (3)
165	229.4 (1)	197.6 (1)	255.9 (1)	284.6 (3)	274.4 (3)
166	282.5 (2)	299.7 (2)	310.1 (3)	289.7 (3)	279.5 (3)
167	208.2 (1)	261.2 (1)	315.2 (3)	289.7 (3)	279.5 (3)
168	181.7 (1)	229.4 (1)	316.9 (2)	289.7 (3)	274.4 (3)
169	176.4 (1)	197.6 (1)	238.7 (3)	*	*
170	181.7 (1)	245.3 (1)	228.5 (3)	224.1 (1)	213.5 (1)
171	240 (1)	286.8 (2)	269.6 (2)	229.4 (1)	291.1 (1)
172	213.5 (1)	187 (1)	187 (1)	277.1 (1)	*
173	202.9 (1)	213.5 (1)	261.2 (1)	213.5 (1)	325.5 (2)
174	269.6 (2)	269.6 (2)	286.8 (2)	316.9 (2)	316.9 (2)
175	197.6 (2)	278.2 (2)	299.7 (2)	224.1 (1)	284.6 (3)
176	187 (1)	250.6 (1)	234.7 (1)	213.5 (1)	243.8 (3)
177	269.6 (2)	234.7 (1)	338.4 (2)	289.7 (3)	279.5 (3)
178	187 (1)	208.2 (1)	291.1 (2)	286.8 (2)	*
179	192.3 (1)	269.3 (3)	305 (3)	284.6 (3)	274.4 (3)
180	223.4 (3)	245.3 (1)	255.9 (1)	224.1 (1)	*
181	224.1 (1)	213.5 (1)	294.8 (3)	*	*

Bore Hole ID	SHEAR WAVE VELOCITY AT DEPTH m/sec (equation used)				
	0.00m-6.00m	6.00m-12.00m	12.00m-18.00m	18.00m-24.00m	24.00m-30.00m
182	208.2 (1)	265.3 (2)	295.4 (2)	299.7 (2)	312.6 (2)
183	218.8 (1)	287.7	312.6 (2)	321.2 (2)	368.5 (2)
184	282.4 (1)	372.8 (2)	234.7 (1)	334.4 (1)	315.2 (3)
185	218.8 (1)	286.8 (2)	299.9 (3)	284.6 (3)	279.5 (3)
186	155.2 (1)	192.3 (1)	208.2 (1)	312.3 (2)	329.8 (2)
187	187 (1)	238.7 (3)	310.1 (3)	345.8 (3)	345.8 (3)
188	240 (1)	282.4 (1)	261.2 (1)	305 (3)	254 (3)
189	277.1 (1)	287.7 (1)	277.1 (1)	289.7 (3)	289.7 (3)
190	187 (1)	381.4 (2)	271.8 (1)	*	*
191	224.1 (1)	334.1 (2)	305 (3)	289.7 (3)	*
192	181.7	234.7	304 (2)	271.8	261.2
193	229.4 (1)	202.9 (1)	265.3 (2)	304 (2)	329.8 (2)
194	197.6 (1)	264.2 (3)	310.1 (3)	*	*
195	165.8 (1)	208.2 (1)	305 (3)	284.6 (3)	274.4 (3)
196	245.3 (1)	320.3 (3)	305 (3)	284.6 (3)	274.4 (3)
197	165.8 (1)	213.5 (1)	312.6 (2)	338.4 (2)	314.2 (1)
198	261.2 (1)	321.2 (2)	250.6 (1)	359.9 (2)	303.6 (1)
199	230.9	269.6 (2)	310.1 (3)	*	*
200	213.5	334.1	308.3	312.6 (2)	274.4 (3)

Equations used (after Fumal and Tinslay, 1985) :

1 - 5.3N +134 for clay and silty clay

2 - 4.3N +218 for silt loam and sandy clay

3 - 5.1N +152 for sand and gravelly sand

* Hard rock N> 50

ANNEXURE VI

Effective Shear Wave Velocity (V_s^{30}) for each Borehole

Sl. No.	Latitude (°N)	Longitude (°E)	Shear wave velocity (V_s^{30})(m/sec)
1.	26.14167	91.66125	331.13
2.	26.15736	91.67229	245.00
3.	26.15273	91.65732	295.86
4.	26.14808	91.64718	267.38
5.	26.14073	91.63915	282.19
6.	26.13753	91.62938	240.38
7.	26.12998	91.62280	280.90
8.	26.12088	91.61617	265.96
9.	26.10162	91.61213	273.22
10.	26.09853	91.60620	289.02
11.	26.09957	91.59685	264.56
12.	26.10955	91.60723	250.00
13.	26.10744	91.59333	273.22
14.	26.11728	91.59867	261.78
15.	26.13875	91.60713	287.36
16.	26.12150	91.60505	241.55
17.	26.13850	91.62132	207.47
18.	26.14743	91.63057	210.97
19.	26.15033	91.63953	234.74
20.	26.16930	91.66760	210.08

Sl. No.	Latitude (°N)	Longitude (°E)	Shear wave velocity (V_s^{30})(m/sec)
21.	26.16420	91.64974	201.61
22.	26.16909	91.68080	248.76
23.	26.14820	91.66824	261.78
24.	26.15969	91.68063	274.73
25.	26.16035	91.68913	234.74
26.	26.14802	91.67838	257.73
27.	26.13695	91.67352	263.16
28.	26.14543	91.68246	240.38
29.	26.15994	91.71165	240.38
30.	26.15052	91.68468	263.71
31.	26.17373	91.72914	210.97
32.	26.17079	91.72370	225.23
33.	26.17092	91.76926	242.72
34.	26.16844	91.72948	216.45
35.	26.15103	91.73013	260.42
36.	26.18119	91.77602	264.55
37.	26.15991	91.73655	245.10
38.	26.11085	91.78908	250.00
39.	26.17793	91.77400	222.22
40.	26.16747	91.74498	224.22
41.	26.17194	91.73618	222.22
42.	26.17378	91.77418	261.78
43.	26.17139	91.73836	257.73
44.	26.14195	91.72871	260.42
45.	26.17572	91.73512	205.76
46.	26.12717	91.72135	259.07
47.	26.18357	91.73866	228.31
48.	26.16684	91.77177	259.07
49.	26.18992	91.75242	264.55
50.	26.18618	91.74863	263.16

Sl. No.	Latitude (°N)	Longitude (°E)	Shear wave velocity (V_s^{30})(m/sec)
51.	26.16974	91.75236	261.78
52.	26.17605	91.75524	232.22
53.	26.18457	91.74117	251.26
54.	26.18155	91.77837	255.10
55.	26.18472	91.75443	223.21
56.	26.18798	91.73660	261.78
57.	26.18906	91.79023	209.79
58.	26.18773	91.74272	251.26
59.	26.18668	91.76568	223.46
60.	26.18640	91.78783	256.41
61.	26.16159	91.77460	236.97
62.	26.18573	91.76258	247.52
63.	26.18482	91.77630	274.73
64.	26.15980	91.77876	264.55
65.	26.18535	91.77317	285.71
66.	26.18437	91.76755	274.73
67.	26.16165	91.78170	235.85
68.	26.18387	91.74662	260.42
69.	26.17929	91.76470	277.78
70.	26.17230	91.77992	239.23
71.	26.16425	91.77650	253.81
72.	26.17422	91.75918	268.82
73.	26.15813	91.78677	234.74
74.	26.14147	91.79957	214.59
75.	26.16657	91.76322	270.27
76.	26.17810	91.77727	260.42
77.	26.13491	91.80510	304.88
78.	26.17299	91.76301	357.14
79.	26.14380	91.78204	264.90
80.	26.12820	91.80667	292.40

Sl. No.	Latitude (°N)	Longitude (°E)	Shear wave velocity (V_s^{30})(m/sec)
81.	26.15613	91.78868	304.88
82.	26.13284	91.78539	263.16
83.	26.12945	91.80169	264.55
84.	26.15262	91.78667	231.13
85.	26.12091	91.78821	216.45
86.	26.14098	91.78667	248.76
87.	26.15343	91.79107	271.74
88.	26.11379	91.78621	246.31
89.	26.13844	91.77660	287.36
90.	26.17570	91.77977	251.57
91.	26.12110	91.76988	222.22
92.	26.13567	91.79333	280.90
93.	26.13999	91.76104	270.27
94.	26.11780	91.77639	204.92
95.	26.12552	91.78876	257.73
96.	26.14356	91.77450	225.23
97.	26.12259	91.78823	225.10
98.	26.12951	91.79430	280.90
99.	26.14289	91.77021	246.31
100.	26.16052	91.75964	241.55
101.	26.13330	91.82640	297.62
102.	26.11461	91.79327	267.38
103.	26.15819	91.81835	214.59
104.	26.13457	91.80951	259.07
105.	26.12234	91.80431	248.76
106.	26.15590	91.82724	251.26
107.	26.16614	91.82574	243.90
108.	26.13953	91.82994	273.22
109.	26.15677	91.83789	257.73
110.	26.17557	91.83054	219.78

Sl. No.	Latitude (°N)	Longitude (°E)	Shear wave velocity (V_s^{30})(m/sec)
111.	26.13730	91.82093	285.71
112.	26.13135	91.67260	255.10
113.	26.18258	91.80232	270.27
114.	26.13245	91.81193	255.10
115.	26.12685	91.68861	241.55
116.	26.12910	91.67760	295.86
117.	26.14862	91.81223	271.74
118.	26.11473	91.74764	277.78
119.	26.11428	91.74064	256.41
120.	26.18015	91.81043	259.07
121.	26.10395	91.75164	234.74
122.	26.11338	91.72913	267.38
123.	26.178	91.80292	279.33
124.	26.11935	91.81679	282.49
125.	26.11518	91.71913	253.81
126.	26.18392	91.79392	270.27
127.	26.12281	91.82168	268.82
128.	26.12236	91.74914	271.74
129.	26.11922	91.68511	282.49
130.	26.10215	91.79817	263.16
131.	26.130	91.82118	250.00
132.	26.13719	91.6691	264.55
133.	26.13719	91.79117	251.57
134.	26.10799	91.71913	299.40
135.	26.12057	91.69611	252.53
136.	26.14931	91.67260	227.27
137.	26.11415	91.71882	232.56
138.	26.11652	91.70812	222.22
139.	26.20272	91.68222	223.21
140.	26.12770	91.81221	270.27

Sl. No.	Latitude (°N)	Longitude (°E)	Shear wave velocity (V_s^{30})(m/sec)
141.	26.11113	91.79567	299.40
142.	26.13567	91.79333	255.10
143.	26.14258	91.66810	277.78
144.	26.12057	91.71813	256.41
145.	26.19374	91.71749	236.97
146.	26.20335	91.67313	250.00
147.	26.12813	91.81169	276.24
148.	26.21956	91.73471	211.86
149.	26.22154	91.71588	227.27
150.	26.13763	91.65900	299.4
151.	26.21292	91.72890	261.78
152.	26.20357	91.71428	264.55
153.	26.22010	91.69906	289.86
154.	26.19980	91.71488	221.24
155.	26.18705	91.70547	232.56
156.	26.21166	91.70928	263.16
157.	26.18680	91.67834	212.77
158.	26.19978	91.72659	256.41
159.	26.19697	91.72600	253.81
160.	26.11761	91.82617	208.33
161.	26.22248	91.70677	232.56
162.	26.21036	91.73950	223.64
163.	26.21117	91.68965	314.47
164.	26.21898	91.72659	280.90
165.	26.20183	91.72322	243.90
166.	26.17940	91.74526	292.40
167.	26.20672	91.70496	265.96
168.	26.21031	91.71638	248.76
169.	26.18579	91.69515	199.72
170.	26.18240	91.68619	216.45

Sl. No.	Latitude (°N)	Longitude (°E)	Shear wave velocity (V_s^{30})(m/sec)
171.	26.18240	91.69445	260.42
172.	26.15342	91.69371	210.53
173.	26.18985	91.66978	235.85
174.	26.18406	91.66617	290.70
175.	26.15161	91.69443	250.00
176.	26.18217	91.67849	223.21
177.	26.18918	91.70176	277.78
178.	26.15486	91.74100	233.92
179.	26.18989	91.74735	257.73
180.	26.19969	91.69440	236.69
181.	26.16086	91.74903	240.00
182.	26.19750	91.75987	270.27
183.	26.18907	91.75780	292.40
184.	26.16324	91.76584	301.20
185.	26.18040	91.75342	270.27
186.	26.18488	91.75740	220.26
187.	26.16015	91.74101	270.27
188.	26.16733	91.75239	265.96
189.	26.17849	91.75786	284.09
190.	26.14839	91.74357	258.62
191.	26.17135	91.74653	289.69
192.	26.16959	91.77882	242.72
193.	26.14772	91.74207	257.73
194.	26.15284	91.73533	247.43
195.	26.18082	91.74796	234.74
196.	26.13603	91.73539	284.09
197.	26.137	91.74526	248.76
198.	26.12811	91.73819	294.11
199.	26.17859	91.82757	265.49
200.	26.18666	91.84341	280.9

ANNEXURE VII

Soil Density at different depth

Bore hole ID	Latitude	Longitude	DENSITY (gm/c.c)																			
			1.50	**3.00**	**4.50**	**6.00**	**7.50**	**9.00**	**10.50**	**12.00**	**13.50**	**15.00**	**16.50**	**18.00**	**19.50**	**21.00**	**22.50**	**24.00**	**25.50**	**27.00**	**28.50**	**30.00**
1	N 26.14167°	E 91.66125°	**2.04**	2.04	**2.04**	2.04	**1.85**	1.85	**1.87**	1.91	**2.20**	2.20	**2.20**	2.20	**2.20**	2.20	**2.25**	2.25	**2.25**	2.30	**2.30**	2.35
2	N 26.15736°	E 91.67229°	**1.15**	1.30	**1.97**	2.25	**2.29**	2.19	**2.25**	2.25	**2.25**	2.31	**1.99**	1.99	**1.99**	2.25	**2.25**	2.25	**2.25**	2.26	**2.26**	2.30
3	N 26.15273°	E 91.65732°	**1.50**	1.40	**1.58**	1.58	**1.58**	1.76	**1.76**	1.65	**1.70**	1.71	**1.80**	1.94	**2.20**	2.20	**2.20**	2.25	**2.25**	1.89	**1.91**	2.20
4	N 26.14808°	E 91.64718°	**1.49**	1.76	**1.72**	2.24	**2.24**	2.24	**2.24**	1.95	**2.04**	2.65	**2.00**	2.00	**2.09**	2.25	**2.25**	2.25	**2.25**	2.25	**2.25**	2.25
5	N 26.14073°	E 91.63915°	**1.71**	1.71	**1.71**	1.75	**1.75**	1.75	**1.76**	1.60	**1.69**	2.20	**2.21**	2.21	**2.22**	2.22	**2.23**	2.23	**2.23**	2.24	**2.24**	2.24
6	N 26.13753°	E 91.62938°	**1.14**	1.45	**1.78**	1.58	**1.58**	1.82	**1.82**	1.82	**1.82**	1.82	**1.82**	1.78	**1.78**	1.78	**1.79**	1.79	**1.98**	2.10	**2.20**	2.21
7	N 26.12998°	E 91.62280°	**1.86**	1.86	**1.81**	1.80	**1.81**	1.82	**1.82**	1.82	**1.60**	1.64	**1.98**	2.20	**2.20**	2.21	**2.22**	2.22	**2.24**	2.24	**2.25**	2.26
8	N 26.12088°	E 91.61617°	**1.94**	1.94	**1.94**	1.90	**1.42**	1.42	**1.50**	1.64	**1.65**	1.98	**2.20**	2.21	**2.21**	2.22	**2.22**	2.23	**2.23**	2.24	**2.25**	2.25
9	N 26.10162°	E 91.61213°	**1.80**	1.85	**1.89**	1.85	**1.90**	1.92	**1.95**	1.99	**2.20**	2.21	**2.22**	2.23	**2.23**	2.25	**2.25**	2.25	**2.26**	2.28	**2.30**	2.30
10	N 26.09853°	E 91.60620°	**1.99**	1.95	**1.95**	1.93	**1.93**	1.99	**2.00**	2.20	**2.21**	2.21	**2.22**	2.23	**2.24**	2.25	**2.25**	2.25	**2.25**	2.26	**2.28**	2.30
11	N 26.09957°	E 91.59685°	**1.71**	1.71	**1.70**	1.44	**1.51**	1.50	**1.76**	1.82	**1.98**	2.20	**2.20**	2.23	**2.23**	2.23	**2.24**	2.24	**2.25**	2.26	*****	*
12	N 26.10955°	E 91.60723°	**1.81**	1.81	**1.84**	1.84	**1.32**	1.32	**1.44**	1.46	**1.51**	1.60	**1.77**	2.20	**2.20**	2.23	**2.23**	*	*****	*	*****	*
13	N 26.10744°	E 91.59333°	**1.35**	1.60	**1.71**	1.81	**1.85**	1.90	**2.20**	2.20	**2.24**	2.24	**2.24**	2.25	**2.25**	2.25	**2.26**	2.26	**2.27**	*	*****	*
14	N 26.11728°	E 91.59867°	**1.80**	1.82	**1.85**	1.60	**1.74**	1.95	**2.10**	2.20	**2.20**	2.23	**2.23**	2.25	**2.26**	2.26	**2.26**	2.27	**2.28**	2.28	**2.30**	2.30
15	N 26.13875°	E 91.60713°	**1.82**	1.82	**1.82**	1.82	**1.82**	1.82	**1.72**	2.20	**2.21**	2.22	**2.22**	2.23	**2.23**	2.24	**2.24**	2.25	**2.26**	2.27	**2.28**	2.30
16	N 26.12150°	E 91.60505°	**1.50**	1.60	**1.60**	1.61	**1.72**	1.70	**1.70**	1.75	**1.80**	1.81	**1.90**	1.90	**1.91**	2.20	**2.20**	2.23	**2.25**	2.26	**2.26**	2.22
17	N 26.13850°	E 91.62132°	**1.32**	1.86	**1.86**	1.86	**1.76**	1.80	**1.80**	1.80	**1.81**	1.80	**1.80**	2.01	**2.01**	2.01	**2.21**	2.21	**2.23**	2.24	**2.25**	2.25
18	N 26.14743°	E 91.63057°	**1.81**	1.81	**1.79**	1.79	**1.79**	1.79	**1.79**	1.81	**1.81**	1.81	**1.82**	1.83	**1.85**	1.76	**2.21**	2.21	**2.22**	2.23	**2.23**	2.25
19	N 26.15033°	E 91.63953°	**1.93**	1.93	**1.90**	1.90	**1.90**	1.87	**1.87**	1.88	**1.88**	1.88	**1.89**	2.20	**2.23**	2.25	**2.26**	2.26	**2.27**	2.28	**2.30**	2.30
20	N 26.16930°	E 91.66760°	**2.01**	2.01	**1.75**	1.75	**1.75**	1.75	**1.75**	1.75	**1.75**	1.82	**1.82**	1.82	**1.83**	1.83	**1.76**	2.10	**2.19**	1.92	**1.92**	2.21

Bore hole ID	Latitude	Longitude	DENSITY (gm/c.c)																			
21	N 26.16420°	E 91.64974°	**1.62**	1.62	**1.66**	1.66	**1.66**	1.66	**1.66**	1.66	**1.67**	1.67	**1.67**	1.68	**1.69**	1.76	**2.21**	1.68	**1.67**	1.68	**1.69**	1.75
22	N 26.16909°	E 91.68080°	**1.10**	1.81	**1.81**	1.81	**1.81**	1.81	**1.82**	1.50	**1.20**	1.81	**1.81**	2.20	**2.20**	2.23	**2.25**	2.25	**2.26**	2.26	**2.26**	2.27
23	N 26.14820°	E 91.66824°	**1.81**	1.90	**1.91**	1.91	**1.93**	1.93	**1.93**	1.93	**1.93**	1.93	**2.21**	2.22	**2.22**	2.23	**2.23**	2.24	**2.24**	2.25	**2.25**	2.26
24	N 26.15969°	E 91.68063°	**1.44**	1.76	**1.76**	1.76	**1.71**	1.79	**1.82**	1.82	**1.78**	1.88	**1.96**	2.20	**2.19**	2.19	**2.20**	2.22	**2.22**	*	**	*
25	N 26.16035°	E 91.68913°	**1.13**	2.16	**1.81**	1.86	**1.89**	1.82	**1.83**	1.79	**1.89**	1.89	**1.81**	1.81	**1.79**	1.83	**1.84**	1.83	**1.84**	1.60	**1.96**	2.20
26	N 26.14802°	E 91.67838°	**1.45**	1.82	**1.90**	1.90	**1.90**	1.90	**1.81**	1.84	**1.90**	2.20	**2.20**	2.23	**2.23**	2.24	**2.26**	2.28	**2.29**	2.30	**2.30**	2.30
27	N 26.13695°	E 91.67352°	**1.85**	1.85	**1.85**	1.85	**1.85**	1.85	**1.89**	2.20	**2.20**	2.23	**2.24**	2.25	**2.26**	2.27	**2.27**	2.30	**2.30**	2.30	**2.31**	2.31
28	N 26.14543°	E 91.68246°	**1.85**	1.81	**1.75**	1.92	**1.84**	1.84	**1.84**	2.21	**2.21**	2.21	**2.23**	2.23	**2.24**	2.26	**2.27**	2.27	**2.28**	2.29	**2.30**	2.30
29	N 26.15994°	E 91.71165°	**1.82**	1.82	**1.84**	1.90	**1.92**	1.92	**1.83**	1.89	**1.83**	1.83	**1.83**	2.20	**2.22**	2.23	**2.25**	2.26	**2.27**	*	**	*
30	N 26.15052°	E 91.68468°	**1.10**	1.67	**1.68**	1.68	**1.68**	1.79	**1.79**	1.80	**2.20**	2.21	**2.22**	2.23	**2.24**	2.24	**2.25**	2.26	**2.26**	2.26	**2.27**	2.27
31	N 26.17373°	E 91.72914°	**1.13**	1.65	**1.76**	1.76	**1.78**	1.75	**1.81**	1.81	**1.81**	1.75	**2.00**	2.00	**2.00**	2.00	**2.00**	2.20	**2.20**	2.28	**2.25**	2.30
32	N 26.17079°	E 91.72370°	**1.12**	1.70	**1.70**	1.63	**1.63**	1.63	**1.78**	1.80	**1.80**	1.80	**1.80**	1.80	**1.70**	1.71	**1.71**	1.71	**2.20**	2.20	**	*
33	N 26.17092°	E 91.76926°	**1.97**	1.97	**1.97**	1.97	**1.97**	1.95	**1.95**	1.95	**1.95**	1.50	**1.55**	1.55	**1.57**	1.70	**1.71**	1.71	**1.70**	1.75	**1.76**	1.76
34	N 26.16844°	E 91.72948°	**1.45**	1.82	**1.85**	1.71	**1.80**	1.71	**1.71**	1.71	**1.71**	1.71	**1.71**	1.71	**1.50**	1.40	**1.51**	1.65	**2.20**	2.20	**2.20**	2.00
35	N 26.15103°	E 91.73013°	**1.93**	1.93	**1.86**	1.86	**1.86**	1.86	**2.20**	2.20	**2.20**	2.25	**2.26**	2.27	**2.27**	2.28	**2.30**	2.30	**2.30**	2.30	**	*
36	N 26.18119°	E 91.77602°	**1.10**	1.60	**1.60**	1.84	**1.92**	1.96	**2.19**	1.92	**1.96**	2.20	**1.92**	1.95	**1.92**	1.86	**1.92**	2.10	**2.14**	*	**	*
37	N 26.15991°	E 91.73655°	**1.20**	1.45	**1.50**	1.50	**1.50**	1.50	**1.79**	1.85	**1.80**	2.20	**2.20**	2.20	**2.25**	2.25	**2.25**	2.25	**2.26**	2.28	**2.30**	2.30
38	N 26.11085°	E 91.78908°	**1.12**	1.44	**1.46**	2.02	**2.02**	1.85	**1.92**	1.91	**1.75**	1.75	**1.75**	1.75	**1.76**	1.78	**1.46**	1.48	**	*	**	*
39	N 26.17793°	E 91.77400°	**1.98**	1.98	**1.98**	1.98	**1.98**	1.98	**2.10**	2.10	**2.10**	2.20	**2.20**	1.80	**1.80**	1.70	**1.91**	1.72	**1.71**	1.72	**1.73**	1.73
40	N 26.16747°	E 91.74498°	**1.10**	1.10	**1.76**	1.76	**1.78**	1.78	**1.78**	1.79	**2.20**	2.20	**2.20**	2.20	**2.23**	2.25	**2.26**	2.27	**2.27**	2.28	**2.28**	2.30
41	N 26.17194°	E 91.73618°	**1.62**	1.62	**1.73**	1.73	**1.65**	1.65	**1.65**	1.65	**1.65**	1.65	**1.65**	1.65	**1.65**	2.20	**2.20**	2.23	**2.23**	2.25	**2.26**	2.26
42	N 26.17378°	E 91.77418°	**1.82**	1.88	**1.88**	1.88	**1.88**	1.89	**1.87**	1.97	**1.87**	1.85	**1.86**	1.85	**1.88**	2.20	**2.20**	2.24	**2.25**	1.81	**1.82**	1.82
43	N 26.17139°	E 91.73836°	**1.88**	1.90	**1.90**	1.90	**1.90**	1.90	**1.88**	1.88	**1.88**	2.20	**2.20**	2.23	**2.23**	2.23	**2.25**	2.25	**2.26**	2.26	**2.27**	2.27
44	N 26.14195°	E 91.72871°	**1.98**	1.98	**1.98**	1.98	**1.72**	1.78	**2.21**	2.21	**2.22**	2.23	**2.24**	2.24	**2.25**	2.26	**2.26**	2.27	**2.27**	2.27	**2.28**	2.28

Bore hole ID	Latitude	Longitude	DENSITY (gm/c.c)																			
45	N 26.17572°	E 91.73512°	**1.70**	1.70	**1.70**	1.70	**1.45**	1.45	**1.45**	1.45	**1.51**	1.51	**1.45**	1.53	**1.55**	1.53	**1.52**	1.53	**1.56**	1.61	**1.76**	1.78
46	N 26.12717°	E 91.72135°	**1.93**	1.93	**1.95**	1.95	**1.77**	2.20	**2.20**	2.20	**2.20**	2.24	**2.24**	2.25	**2.25**	2.25	**2.26**	2.27	**2.28**	2.28	**2.30**	2.30
47	N 26.18357°	E 91.73866°	**1.88**	1.86	**1.88**	1.89	**1.96**	1.96	**1.93**	1.93	**1.95**	2.20	**2.21**	2..21	**2.21**	2.21	**2.21**	2.23	**2.23**	2.24	**2.25**	2.25
48	N 26.16684°	E 91.77177°	**1.82**	1.82	**1.83**	1.83	**1.84**	1.83	**1.92**	1.92	**1.92**	1.92	**1.92**	1.92	**1.92**	1.92	**1.95**	1.98	**2.20**	2.20	**2.22**	2.22
49	N 26.18992°	E 91.75242°	**1.15**	1.84	**1.84**	1.84	**1.84**	1.86	**1.86**	1.60	**1.61**	1.65	**2.20**	2.20	**2.22**	2.23	**2.23**	2.23	**2.24**	2.24	**2.25**	2.25
50	N 26.18618°	E 91.74863°	**1.77**	1.77	**1.77**	1.78	**1.78**	1.78	**1.78**	1.78	**1.60**	1.95	**2.20**	2.20	**2.20**	2.22	**2.22**	2.23	**2.24**	2.24	**2.24**	2.25
51	N 26.16974°	E 91.75236°	**1.44**	1.55	**1.60**	1.75	**1.75**	1.73	**1.76**	1.73	**1.73**	1.81	**1.81**	1.81	**1.73**	2.20	**2.20**	2.23	**2.25**	1.80	**1.81**	1.89
52	N 26.17605°	E 91.75524°	**1.12**	1.90	**1.90**	1.90	**1.90**	1.90	**1.86**	1.86	**1.86**	1.81	**1.81**	1.91	**2.20**	2.20	**2.20**	2.20	**2.25**	2.25	**2.25**	2.30
53	N 26.18457°	E 91.74117°	**1.81**	1.81	**1.81**	1.81	**1.77**	1.77	**1.77**	1.85	**2.20**	2.20	**2.20**	2.20	**2.20**	2.25	**2.25**	2.25	**2.25**	2.20	*	*
54	N 26.18155°	E 91.77837°	**1.97**	1.97	**1.97**	1.97	**1.97**	1.97	**1.95**	1.95	**1.99.**	2.20	**2.20**	1.85	**1.80**	1.80	**1.80**	1.85	**1.58**	1.80	**1.85**	1.88
55	N 26.18472°	E 91.75443°	**1.44**	1.78	**1.78**	1.71	**1.71**	1.71	**1.71**	1.74	**1.79**	1.79	**1.80**	1.81	**2.20**	2.20	**2.20**	2.25	**2.25**	2.25	**2.25**	2.32
56	N 26.18798°	E 91.73660°	**1.40**	1.88	**1.88**	1.88	**1.88**	1.79	**1.79**	1.75	**0.50**	1.91	**2.20**	2.20	**2.20**	2.20	**2.20**	2.25	**2.25**	2.25	**2.30**	2.30
57	N 26.18906°	E 91.79023°	**1.12**	1.12	**1.59**	1.59	**1.59**	1.65	**1.65**	2.20	**2.20**	2.20	**2.25**	*	*	*	*	*	*	*	*	*
58	N 26.18773°	E 91.74272°	**1.41**	1.70	**1.70**	1.70	**1.70**	1.70	**2.27**	2.27	**2.27**	2.27	**2.27**	2.27	**2.27**	2.25	**2.30**	2.30	**2.30**	2.30	**2.35**	2.35
59	N 26.18668°	E 91.76568°	**1.12**	1.75	**1.75**	1.70	**1.98**	2.27	**2.27**	1.71	**1.71**	1.91	**1.91**	1.75	**2.20**	2.20	**2.20**	2.25	*	*	*	*
60	N 26.18640°	E 91.78783°	**1.13**	1.92	**1.92**	1.94	**1.94**	1.94	**1.94**	1.94	**2.20**	1.85	**1.85**	1.71	**1.71**	1.71	**1.71**	1.85	**2.20**	2.20	**2.20**	*
61	N 26.16159°	E 91.77460°	**1.44**	2.08	**2.08**	2.08	**2.08**	1.85	**1.85**	1.83	**1.85**	1.81	**1.79**	1.79	**1.78**	2.20	**2.20**	2.20	**2.25**	2.25	**2.25**	2.30
62	N 26.18573°	E 91.76258°	**1.40**	1.71	**1.71**	1.94	**1.93**	1.93	**1.93**	2.00	**2.03**	2.03	**2.03**	2.03	**2.03**	2.09	**2.09**	2.12	**2.00**	1.81	**2.03**	2.20
63	N 26.18482°	E 91.77630°	**1.89**	1.89	**1.91**	1.90	**1.90**	2.00	**2.00**	2.05	**2.20**	2.20	**2.21**	2.21	**2.21**	2.21	**2.25**	2.25	**2.25**	2.30	**2.30**	2.35
64	N 26.15980°	E 91.77876°	**1.88**	1.88	**1.89**	1.87	**1.87**	1.87	**1.88**	1.70	**1.77**	1.85	**1.70**	1.73	**1.84**	2.20	**2.20**	1.81	**1.81**	1.82	**1.81**	1.81
65	N 26.18535°	E 91.77317°	**1.50**	1.70	**1.68**	1.65	**1.69**	1.76	**1.76**	1.76	**1.76**	1.75	**1.76**	1.77	**1.91**	1.92	**2.20**	2.20	*	*	*	*
66	N 26.18437°	E 91.76755°	**1.85**	2.05	**1.60**	2.07	**2.07**	2.07	**2.07**	2.20	**2.20**	2.25	**2.25**	1.68	**1.70**	2.20	**2.20**	2.20	**2.20**	2.20	**2.20**	2.25
67	N 26.16165°	E 91.78170°	**1.75**	1.77	**1.76**	1.89	**1.89**	1.85	**1.89**	1.89	**1.89**	1.85	**1.85**	1.85	**1.92**	1.89	**2.20**	2.20	**2.20**	2.20	**2.25**	2.25
68	N 26.18387°	E 91.74662°	**1.88**	1.88	**1.88**	1.88	**1.84**	1.84	**1.85**	1.89	**2.20**	2.20	**2.20**	2.20	**2.20**	2.25	**2.25**	2.25	**2.30**	2.32	**2.33**	2.35

Bore hole ID	Latitude	Longitude	DENSITY (gm/c.c)																			
69	N 26.17929°	E 91.76470°	**1.12**	1.19	**1.60**	2.07	**2.08**	2.08	**1.91**	1.74	**1.79**	1.79	**1.72**	2.20	**2.12**	2.11	**2.20**	2.20	**2.20**	2.21	**2.22**	2.22
70	N 26.17230°	E 91.77992°	**1.40**	1.92	**1.92**	1.92	**1.87**	1.87	**1.87**	1.89	**1.75**	1.87	**1.87**	1.87	**1.83**	1.83	**1.81**	1.83	**1.83**	2.20	**1.87**	1.91
71	N 26.16425°	E 91.77650°	**1.15**	1.15	**1.90**	1.90	**1.90**	1.90	**1.84**	1.88	**1.88**	1.88	**1.87**	1.87	**1.86**	1.60	**1.97**	2.20	**2.27**	2.27	**2.28**	2.28
72	N 26.17422°	E 91.75918°	**1.91**	1.91	**1.91**	1.91	**1.91**	2.20	**2.21**	2.20	**2.21**	1.92	**2.12**	1.92	**1.95**	1.96	**1.95**	2.20	**2.21**	1.94	**1.92**	1.94
73	N 26.15813°	E 91.78677°	**1.80**	1.80	**1.80**	1.79	**1.65**	1.66	**1.61**	1.59	**1.67**	1.65	**1.65**	1.57	**1.65**	1.65	**1.65**	2.20	**2.20**	2.24	**2.26**	2.26
74	N 26.14147°	E 91.79957°	**1.13**	1.75	**1.81**	1.81	**1.81**	1.93	**1.93**	1.55	**2.17**	2.17	**1.45**	1.44	**2.20**	2.22	**2.23**	2.23	**2.24**	1.81	**1.98**	2.21
75	N 26.16657°	E 91.76322°	**1.89**	1.95	**1.94**	1.93	**1.92**	1.92	**1.92**	1.91	**1.91**	1.92	**1.91**	1.91	**1.92**	2.20	**2.20**	2.20	**2.21**	2.21	**2.23**	2.25
76	N 26.17810°	E 91.77727°	**1.99**	1.80	**1.80**	1.79	**2.01**	2.10	**2.10**	2.10	**1.88**	1.68	**1.68**	1.68	**1.68**	1.68	**1.68**	1.68	**1.92**	2.20	**2.20**	2.20
77	N 26.13491°	E 91.80510°	**1.68**	1.98	**1.98**	1.98	**1.97**	1.99	**2.09**	1.93	**1.84**	2.20	**2.20**	2.00	**2.07**	2.07	**2.20**	2.20	**2.20**	2.25	**1.92**	2.20
78	N 26.17299°	E 91.76301°	**1.12**	1.12	**1.93**	1.44	**1.92**	1.56	**1.57**	1.57	**2.20**	2.20	**2.20**	2.20	**2.25**	2.25	**2.25**	2.30	*	*	*	*
79	N 26.14380°	E 91.78204°	**1.70**	1.90	**1.90**	1.85	**1.84**	1.84	**1.84**	1.84	**1.93**	1.93	**1.93**	1.98	**1.98**	2.00	*	*	*	*	*	*
80	N 26.12820°	E 91.80667°	**1.44**	1.90	**1.90**	1.89	**1.92**	1.97	**1.90**	1.97	**1.94**	1.97	**1.79**	1.80	**1.77**	1.79	**2.20**	2.20	**1.96**	1.95	**1.90**	1.91
81	N 26.15613°	E 91.78868°	**1.80**	2.03	**2.03**	2.03	**2.09**	2.09	**2.20**	2.07	**2.03**	1.97	**1.91**	1.95	**1.77**	2.10	**2.19**	2.20	**2.20**	2.21	**2.22**	2.23
82	N 26.13284°	E 91.78539°	**1.58**	1.80	**1.99**	1.88	**1.89**	1.89	**2.21**	2.21	**2.21**	2.21	**2.23**	2.23	**1.82**	1.80	**2.07**	1.82	**1.82**	2.20	**2.22**	2.23
83	N 26.12945°	E 91.80169°	**1.69**	1.71	**1.71**	1.92	**1.92**	1.92	**1.92**	1.92	**1.92**	2.20	**2.21**	1.81	**1.83**	1.83	**1.84**	2.20	**2.21**	2.21	**2.22**	2.23
84	N 26.15262°	E 91.78667°	**1.12**	1.82	**1.92**	1.95	**2.15**	1.92	**1.81**	2.20	**2.21**	2.20	**2.18**	2.19	**2.20**	2.20	**2.21**	2.21	**2.17**	1.85	**1.82**	1.80
85	N 26.12091°	E 91.78821°	**1.80**	1.81	**1.80**	1.12	**1.51**	1.51	**1.57**	1.65	**1.65**	1.65	**1.92**	1.92	**1.92**	1.80	**1.81**	1.81	**1.81**	1.81	**2.20**	2.21
86	N 26.14098°	E 91.78667°	**1.10**	1.68	**1.86**	1.91	**1.91**	1.71	**1.71**	1.71	**1.80**	1.68	**2.20**	1.71	**1.71**	2.20	**2.20**	2.21	**2.21**	1.89	*	*
87	N 26.15343°	E 91.79107°	**1.68**	1.98	**1.98**	2.07	**1.92**	1.97	**2.10**	2.09	**1.91**	2.04	**2.07**	1.91	**1.88**	1.92	**1.81**	1.82	**2.20**	2.20	**2.21**	2.25
88	N 26.11379°	E 91.78621°	**1.45**	1.68	**1.70**	1.72	**1.72**	1.70	**1.70**	1.72	**1.98**	1.76	**1.71**	1.72	**1.72**	1.72	**1.72**	1.72	**1.71**	1.72	**2.20**	2.21
89	N 26.13844°	E 91.77660°	**1.44**	1.80	**1.86**	1.86	**1.86**	1.86	**1.89**	1.98	**2.20**	2.12	**1.89**	1.88	**2.20**	2.23	**2.24**	2.25	**1.99**	*	*	*
90	N 26.17570°	E 91.77977°	**1.76**	2.05	**1.91**	2.05	**2.10**	2.05	**2.05**	2.11	**2.12**	2.04	**2.04**	2.04	**2.04**	2.04	*	*	*	*	*	*
91	N 26.12110°	E 91.76988°	**1.44**	1.71	**1.82**	1.69	**1.70**	1.75	**1.75**	1.75	**1.81**	1.88	**1.88**	1.88	**2.20**	2.22	**2.23**	2.25	**2.25**	2.26	**2.28**	2.30
92	N 26.13567°	E 91.79333°	**2.33**	2.33	**2.33**	2.20	**2.02**	2.02	**2.02**	1.94	**1.94**	1.94	**1.94**	1.96	**1.95**	2.20	**2.20**	2.20	**2.25**	2.25	**2.25**	2.35

Bore hole ID	Latitude	Longitude	DENSITY (gm/c.c)																		
93	N 26.13999°	E 91.76104°	**1.65**	1.70	**1.78**	1.78	**1.78**	1.78	**1.94**	1.94	**1.69**	1.69	**1.69**	1.69	**1.79**	1.70	**1.80**	1.85	**2.20**	2.20	**2.20**	2.20
94	N 26.11780°	E 91.77639°	**1.85**	1.96	**1.96**	1.15	**2.20**	2.20	**1.76**	1.75	**1.75**	1.76	**1.71**	1.75	**1.70**	1.75	**1.76**	1.85	**1.86**	1.89	**2.20**	2.20
95	N 26.12552°	E 91.78876°	**1.54**	1.90	**1.80**	1.80	**1.78**	1.91	**1.92**	1.85	**1.85**	1.80	**1.75**	1.87	**2.20**	2.20	**2.20**	2.20	**2.20**	2.25	**2.25**	2.29
96	N 26.14356°	E 91.77450°	**1.44**	1.85	**1.84**	1.76	**1.90**	2.08	**2.08**	1.85	**1.84**	1.85	**1.80**	1.79	**1.79**	1.78	**1.78**	1.78	**1.96**	2.25	*	*
97	N 26.12259°	E 91.78823°	**1.75**	1.97	**1.97**	1.96	**1.96**	1.96	**1.96**	1.96	**1.96**	1.98	**1.98**	2.20	**2.20**	1.78	**1.78**	1.76	**1.78**	1.76	**2.20**	2.25
98	N 26.12951°	E 91.79430°	**1.20**	1.20	**1.86**	1.86	**1.86**	1.87	**1.90**	1.87	**1.87**	1.85	**1.76**	1.78	**1.81**	2.17	**2.17**	2.18	**1.94**	2.20	**2.20**	2.21
99	N 26.14289°	E 91.77021°	**1.45**	1.77	**1.90**	1.80	**1.81**	2.10	**2.10**	2.10	**1.82**	1.68	**1.82**	1.82	**1.82**	1.89	**2.20**	2.21	**2.20**	2.23	**2.25**	2.25
100	N 26.16052°	E 91.75964°	**1.83**	1.83	**1.83**	1.83	**1.78**	1.78	**1.78**	1.79	**1.79**	1.79	**1.71**	1.73	**1.70**	1.70	**2.20**	2.20	**1.79**	1.79	**1.79**	1.79
101	N 26.13330°	E 91.82640°	**1.76**	1.92	**2.20**	2.20	**1.67**	1.92	**1.90**	1.92	**1.95**	1.92	**1.77**	1.76	**1.76**	1.76	**2.20**	2.21	**2.23**	*	*	*
102	N 26.11461°	E 91.79327°	**1.41**	1.73	**1.73**	2.10	**1.92**	2.21	**2.21**	1.92	**1.90**	1.92	**1.92**	2.20	**2.22**	1.92	**2.03**	1.92	**2.21**	2.22	**2.24**	2.24
103	N 26.15819°	E 91.81835°	**1.68**	1.68	**1.67**	1.67	**1.67**	1.62	**1.62**	1.44	**1.44**	1.44	**1.71**	1.71	**2.20**	2.21	**2.22**	2.22	**2.24**	2.26	**2.26**	2.30
104	N 26.13457°	E 91.80951°	**1.12**	1.65	**1.65**	1.77	**1.89**	1.80	**1.92**	1.77	**1.77**	1.89	**1.66**	1.67	**1.77**	1.95	**2.21**	2.24	**2.25**	2.26	**2.28**	2.30
105	N 26.12234°	E 91.80431°	**1.65**	1.70	**1.77**	1.76	**2.21**	2.22	**1.95**	1.89	**1.89**	1.04	**1.52**	1.92	**1.78**	1.78	**1.93**	1.92	**2.19**	2.21	**2.22**	2.23
106	N 26.15590°	E 91.82724°	**1.65**	1.65	**1.76**	1.77	**1.97**	1.97	**1.97**	1.97	**1.97**	1.97	**1.71**	1.71	**1.90**	1.96	**2.21**	2.21	**2.23**	2.23	**2.24**	2.26
107	N 26.16614°	E 91.82574°	**1.61**	1.61	**1.78**	1.69	**1.69**	1.77	**1.92**	1.93	**1.76**	1.76	**1.71**	1.71	**1.97**	2.19	**2.19**	2.26	**2.26**	2.10	**2.24**	2.26
108	N 26.13953°	E 91.82994°	**1.62**	1.76	**1.80**	1.92	**1.92**	1.95	**1.76**	2.20	**2.20**	1.80	**1.76**	1.76	**1.96**	2.20	**2.21**	2.22	**2.19**	2.20	**2.20**	2.20
109	N 26.15677°	E 91.83789°	**1.92**	2.02	**2.02**	1.92	**1.92**	1.88	**2.19**	1.44	**1.44**	1.75	**1.76**	1.47	**1.47**	1.47	**1.92**	1.95	**1.95**	1.95	**2.20**	2.22
110	N 26.17557°	E 91.83054°	**1.10**	1.10	**1.52**	1.69	**1.81**	1.62	**1.62**	1.69	**1.69**	1.91	**1.93**	1.82	**1.79**	2.21	**2.22**	*	*	*	*	*
111	N 26.13730°	E 91.82093°	**1.44**	1.76	**1.79**	1.80	**1.75**	1.89	**1.89**	1.89	**2.20**	2.20	**1.74**	1.74	**1.92**	1.92	**1.92**	1.92	**1.92**	1.92	**1.92**	1.93
112	N 26.13135°	E 91.67260°	**1.79**	1.79	**1.79**	1.79	**1.52**	1.60	**2.09**	2.20	**2.20**	2.20	**2.25**	2.25	**2.27**	2.28	**2.30**	2.31	**2.32**	2.32	**2.34**	2.35
113	N 26.18258°	E 91.80232°	**1.60**	1.79	**1.73**	1.73	**1.73**	1.78	**1.80**	2.20	**2.20**	1.86	**1.85**	1.87	**1.90**	2.20	**2.20**	2.20	*	*	*	*
114	N 26.13245°	E 91.81193°	**1.65**	1.92	**1.92**	1.68	**1.85**	1.85	**1.85**	1.77	**1.78**	1.58	**1.87**	1.87	**1.88**	1.88	**1.88**	1.89	**2.20**	2.20	**2.20**	2.25
115	N 26.12685°	E 91.68861°	**1.83**	1.83	**1.83**	1.83	**1.76**	1.76	**1.76**	1.80	**1.83**	1.83	**1.83**	1.90	**1.90**	1.76	**1.76**	1.78	**1.78**	2.20	**2.20**	2.20
116	N 26.12910°	E 91.67760°	**1.71**	1.17	**1.74**	1.80	**1.80**	1.93	**2.20**	2.20	**2.20**	2.20	**2.20**	2.25	**2.25**	2.25	**2.25**	2.25	**2.25**	1.91	**1.93**	*

Bore hole ID	Latitude	Longitude	DENSITY (gm/c.c)																			
117	N 26.14862°	E 91.81223°	**1.86**	1.19	**1.19**	2.20	**2.20**	1.97	**1.80**	1.84	**1.80**	1.68	**1.68**	1.87	**1.87**	2.10	**1.98**	2.20	**2.20**	2.25	**2.17**	2.17
118	N 26.11473°	E 91.74764°	**1.51**	1.45	**1.45**	2.02	**2.02**	2.01	**2.01**	2.01	**2.01**	1.76	**1.80**	1.80	**1.80**	2.20	**2.20**	2.20	**2.25**	2.25	**2.20**	2.30
119	N 26.11428°	E 91.74064°	**1.45**	1.19	**1.88**	1.30	**1.30**	1.88	**1.90**	2.20	**2.20**	1.86	**1.86**	1.86	**1.86**	1.92	**2.20**	2.20	**2.20**	2.23	**2.23**	2.24
120	N 26.18015°	E 91.81043°	**1.95**	1.60	**1.75**	1.85	**1.80**	1.95	**1.85**	1.85	**1.85**	1.85	**1.85**	1.82	**1.82**	1.82	**1.82**	1.82	**1.43**	2.20	**2.20**	2.25
121	N 26.10395°	E 91.75164°	**1.62**	1.76	**1.65**	1.94	**1.76**	1.77	**1.80**	1.80	**1.95**	1.96	**2.19**	2.19	**1.81**	1.81	**1.81**	1.92	**1.93**	1.93	**2.18**	2.19
122	N 26.11338°	E 91.72913°	**1.21**	1.76	**1.68**	1.68	**2.21**	2.22	**2.22**	2.24	**2.25**	2.26	**2.28**	2.30	**2.30**	2.21	**2.23**	2.25	**2.25**	2.25	**2.22**	2.22
123	N 26.17800°	E 91.80292°	**1.67**	1.01	**1.67**	1.76	**1.80**	1.80	**1.92**	1.92	**1.93**	1.93	**1.84**	1.84	**1.92**	1.92	**1.95**	1.94	**1.92**	2.22	**2.24**	2.25
124	N 26.11935°	E 91.81679°	**1.60**	1.60	**1.95**	1.80	**1.80**	1.92	**1.93**	1.92	**1.93**	1.92	**1.75**	1.75	**1.75**	1.75	**2.20**	1.44	**1.80**	1.80	**2.21**	2.22
125	N 26.11518°	E 91.71913°	**1.12**	1.60	**1.60**	1.61	**2.20**	2.20	**2.21**	2.22	**2.23**	2.24	**2.26**	2.27	**2.27**	2.28	**2.30**	2.30	**2.31**	2.32	**2.32**	2.32
126	N 26.18392°	E 91.79392°	**1.60**	1.76	**1.76**	1.76	**1.68**	1.92	**1.94**	1.93	**2.21**	1.99	**2.21**	2.21	**2.18**	2.19	**2.19**	2.20	**2.20**	2.21	**2.22**	2.24
127	N 26.12281°	E 91.82168°	**1.69**	1.75	**1.80**	1.84	**1.80**	1.84	**1.94**	1.95	**1.92**	1.84	**1.84**	1.84	**1.84**	1.84	**1.94**	1.92	**2.00**	*	*	*
128	N 26.12236°	E 91.74914°	**1.76**	1.81	**1.81**	2.21	**1.81**	1.84	**1.76**	1.97	**1.82**	2.00	**2.20**	2.21	**2.21**	2.23	**2.23**	2.25	**2.22**	2.22	**2.23**	2.26
129	N 26.11922°	E 91.68511°	**1.83**	1.83	**1.61**	1.80	**1.99**	1.99	**2.21**	2.22	**2.22**	2.22	**2.23**	2.23	**2.23**	2.24	**2.24**	2.25	**2.25**	2.26	**2.28**	*
130	N 26.10215°	E 91.79817°	**1.80**	1.82	**1.76**	1.76	**1.98**	1.93	**1.93**	1.78	**1.78**	2.19	**2.20**	2.21	**2.21**	1.82	**2.15**	2.17	**2.19**	2.20	**2.20**	2.20
131	N 26.13000°	E 91.82118°	**1.95**	1.95	**1.80**	1.76	**1.80**	1.97	**2.19**	2.21	**1.97**	1.93	**1.66**	2.20	**2.22**	2.25	**2.27**	2.30	**2.30**	*	*	*
132	N 26.13719°	E 91.66910°	**1.84**	1.92	**1.44**	1.44	**1.39**	1.80	**2.20**	2.20	**2.20**	2.23	**2.23**	2.25	**2.26**	2.28	**2.30**	2.23	**2.24**	2.25	**2.27**	2.30
133	N 26.13719°	E 91.79117°	**1.31**	1.68	**1.68**	1.68	**1.60**	1.60	**2.17**	2.17	**2.17**	2.17	**2.20**	2.20	**2.25**	2.25	**2.25**	2.25	*	*	*	*
134	N 26.10799°	E 91.71913°	**1.44**	1.44	**1.89**	1.93	**2.07**	2.20	**2.21**	2.23	**2.25**	2.25	**2.25**	2.25	**2.27**	2.27	**2.28**	2.30	**2.31**	2.31	**2.33**	2.35
135	N 26.12057°	E 91.69611°	**1.61**	1.85	**1.65**	1.75	**2.17**	2.20	**2.20**	2.20	**1.61**	1.61	**1.61**	1.61	**1.61**	1.61	**2.20**	2.20	**2.25**	2.25	**2.25**	2.30
136	N 26.14931°	E 91.67260°	**1.35**	1.75	**1.61**	1.61	**1.80**	1.80	**1.92**	1.99	**2.01**	1.97	**2.20**	2.23	**2.25**	2.25	**2.27**	2.30	**1.47**	1.52	**1.52**	1.52
137	N 26.11415°	E91.71882°	**1.15**	1.85	**1.85**	1.85	**1.85**	1.78	**2.20**	2.21	**1.80**	1.99	**1.97**	*	*	*	*	*	*	*	*	*
138	N 26.11652°	E 91.70812°	**1.70**	1.70	**1.77**	1.75	**1.76**	1.79	**1.80**	1.85	**2.20**	2.20	**2.20**	*	*	*	*	*	*	*	*	*
139	N 26.20272°	E 91.68222°	**1.13**	1.74	**1.74**	1.68	**1.76**	1.80	**1.90**	1.80	**1.82**	1.92	**1.82**	1.95	**1.92**	1.80	**1.92**	1.82	**2.20**	*	*	*
140	N 26.12770°	E 91.81221°	**1.14**	1.85	**1.85**	1.85	**1.85**	2.20	**2.20**	1.82	**1.82**	1.82	**1.85**	1.85	**1.87**	1.87	**1.85**	1.89	**1.89**	1.91	**2.20**	2.20

Bore hole ID	Latitude	Longitude	DENSITY (gm/c.c)																			
141	N 26.11113°	E 91.79567°	**1.93**	1.93	**1.93**	2.18	**2.18**	2.20	**2.20**	2.20	**2.25**	2.25	**2.25**	1.85	**1.85**	1.95	**2.20**	2.20	**2.20**	2.25	**2.25**	2.30
142	N 26.13567°	E 91.79333°	**1.83**	1.83	**1.83**	1.84	**1.84**	1.84	**1.84**	1.84	**1.89**	1.89	**2.20**	2.20	**2.20**	2.25	**2.25**	2.30	**2.30**	2.30	**2.35**	2.35
143	N 26.14258°	E 91.66810°	**1.85**	1.72	**1.72**	1.65	**1.89**	1.91	**1.91**	2.20	**2.20**	2.25	**2.25**	2.25	**2.25**	2.27	**2.27**	2.27	**2.30**	*	*	*
144	N 26.12057°	E 91.71813°	**1.44**	1.99	**1.99**	1.99	**1.99**	1.85	**1.81**	1.93	**2.20**	2.20	**2.21**	2.21	**2.23**	2.23	**2.25**	2.30	**2.30**	2.30	*	*
145	N 26.19374°	E 91.71749°	**1.87**	1.87	**1.87**	1.87	**1.87**	1.87	**1.78**	1.78	**1.78**	1.78	**2.20**	2.20	**2.20**	2.25	**2.25**	2.25	**2.30**	2.30	**2.30**	2.35
146	N 26.20335°	E 91.67313°	**1.75**	1.80	**1.95**	1.84	**1.80**	1.98	**1.80**	1.95	**1.97**	2.19	**2.20**	2.23	**2.23**	2.25	**2.27**	2.30	*	*	*	*
147	N 26.12813°	E 91.81169°	**1.41**	1.94	**1.94**	1.93	**1.93**	2.20	**2.20**	1.90	**1.90**	1.91	**1.90**	1.97	**1.99**	1.96	**2.10**	1.89	**1.91**	1.91	**1.91**	*
148	N 26.21956°	E 91.73471°	**2.25**	2.25	**2.25**	2.26	**2.26**	1.49	**1.68**	1.68	**1.80**	1.91	**1.91**	2.20	**2.22**	2.24	**2.25**	2.25	**2.27**	2.28	**2.30**	*
149	N 26.22154°	E 91.71588°	**1.77**	1.77	**1.77**	1.80	**1.79**	1.79	**1.92**	1.92	**1.90**	1.92	**1.93**	2.04	**2.04**	2.04	**2.07**	2.20	*	*	*	*
150	N 26.13763°	E 91.65009°	**1.80**	1.80	**1.80**	1.20	**1.20**	1.65	**1.75**	2.20	**2.20**	2.20	**2.25**	2.28	**2.30**	2.30	**2.30**	2.32	**2.35**	2.35	**2.36**	*
151	N 26.21292°	E 91.72890°	**1.79**	1.79	**1.79**	1.79	**1.80**	1.80	**1.80**	1.81	**2.21**	2.22	**2.24**	2.24	**2.26**	2.26	**2.27**	2.28	**2.30**	2.30	*	*
152	N 26.20357°	E 91.71428°	**1.51**	1.84	**1.85**	1.83	**1.84**	1.82	**1.89**	1.91	**2.20**	2.21	**2.22**	2.23	**2.25**	2.27	**2.27**	2.28	**2.30**	2.31	**2.31**	*
153	N 26.22010°	E 91.69906°	**1.80**	1.86	**1.86**	1.99	**1.95**	1.90	**1.91**	2.20	**2.20**	2.20	**2.23**	2.25	**2.25**	2.25	*	*	*	*	*	*
154	N 26.19980°	E 91.71488°	**1.68**	1.68	**1.11**	1.11	**1.53**	1.53	**1.53**	1.53	**1.80**	2.20	**2.21**	2.22	**2.24**	2.25	**2.26**	2.28	**2.28**	2.30	**2.30**	2.31
155	N 26.18705°	E 91.70547°	**1.79**	1.79	**1.92**	1.84	**1.83**	1.84	**1.86**	1.80	**1.86**	2.20	**2.21**	2.22	**2.23**	2.25	**2.27**	2.28	**2.28**	2.30	**2.32**	2.35
156	N 26.21166°	E 91.70928°	**1.79**	1.78	**1.87**	1.87	**1.87**	1.87	**1.87**	1.88	**1.90**	2.20	**2.20**	2.23	**2.23**	2.25	**2.26**	2.27	**2.28**	2.30	**2.18**	2.20
157	N 26.18680°	E 91.67834°	**1.40**	1.40	**1.49**	1.49	**1.49**	1.49	**1.89**	1.89	**1.61**	1.61	**1.61**	1.95	**1.82**	1.84	**1.96**	1.96	**1.99**	2.01	**2.01**	1.99
158	N 26.19978°	E 91.72659°	**1.68**	1.58	**1.58**	1.76	**1.80**	1.82	**1.92**	1.44	**1.52**	1.72	**2.20**	2.21	**2.25**	2.27	*	*	*	*	*	*
159	N 26.19697°	E 91.72006°	**1.76**	1.82	**1.77**	1.77	**1.70**	1.70	**1.70**	1.72	**1.75**	2.20	**2.22**	2.24	**2.24**	2.25	**2.26**	2.27	**2.30**	*	*	*
160	N 26.11761°	E 91.82617°	**1.65**	1.68	**1.99**	1.99	**1.99**	1.99	**1.97**	1.99	**1.97**	1.99	**1.92**	1.97	**1.99**	1.97	**1.95**	1.95	**1.97**	1.92	**1.97**	1.99
161	N 26.22248°	E 91.70677°	**1.78**	1.78	**1.78**	1.80	**1.82**	1.80	**1.92**	1.91	**1.76**	1.76	**1.80**	1.92	**1.93**	1.92	**1.95**	1.99	**2.01**	2.03	**2.05**	2.05
162	N 26.21036°	E 91.73950°	**1.68**	1.78	**1.78**	1.44	**1.52**	1.60	**1.95**	1.30	**1.68**	1.76	**1.78**	1.80	**1.60**	1.76	**2.21**	2.22	**2.22**	2.23	**2.24**	2.25
163	N 26.21117°	E 91.68965°	**1.73**	1.73	**1.73**	1.97	**2.12**	2.15	**2.13**	2.19	**2.17**	1.95	**2.02**	2.00	**1.99**	2.20	**1.97**	1.65	**1.65**	2.00	**2.02**	*
164	N 26.21898°	E 91.72659°	**1.73**	1.73	**1.92**	1.95	**1.58**	1.52	**1.52**	1.58	**1.68**	1.68	**1.75**	1.76	**2.20**	2.21	**2.22**	2.24	**2.27**	*	*	*

Bore hole ID	Latitude	Longitude	DENSITY (gm/c.c)																			
165	N 26.20183°	E 91.72322°	**1.82**	1.92	**1.86**	1.81	**1.81**	1.81	**1.81**	1.83	**1.83**	1.85	**2.21**	2.21	**2.22**	2.23	**2.24**	2.25	**2.26**	2.26	**2.28**	2.30
166	N 26.17940°	E 91.74526°	**1.08**	1.11	**1.81**	1.81	**1.81**	1.52	**1.67**	2.19	**2.20**	2.21	**2.20**	2.21	**2.21**	2.22	**2.23**	2.24	**2.25**	2.27	*	*
167	N 26.20672°	E 91.70496°	**1.39**	1.44	**1.34**	1.34	**1.58**	1.52	**1.58**	1.87	**2.21**	2.21	**2.22**	2.22	**2.23**	2.24	**2.25**	2.26	**2.26**	2.27	**2.28**	2.30
168	N 26.21031°	E 91.71638°	**1.60**	1.60	**1.60**	1.60	**1.60**	1.58	**1.58**	1.58	**1.58**	1.65	**2.21**	2.21	**2.22**	2.23	**2.24**	2.25	**2.26**	2.27	**2.28**	2.30
169	N 26.18579°	E 91.69515°	**1.12**	1.12	**1.43**	1.43	**1.72**	1.72	**1.80**	1.86	**1.90**	*	*	*	*	*	*	*	*	*	*	*
170	N 26.18240°	E 91.68619°	**1.68**	1.68	**1.68**	1.83	**1.41**	1.41	**1.97**	1.95	**1.99**	1.80	**1.92**	1.92	**1.92**	1.95	**1.97**	1.99	**1.82**	1.97	**1.99**	2.01
171	N 26.18240°	E 91.69445°	**1.68**	1.66	**2.09**	2.09	**2.09**	1.60	**1.60**	1.52	**1.52**	1.46	**1.44**	1.54	**1.99**	1.95	**1.97**	1.99	**1.70**	1.76	**1.70**	1.84
172	N 26.15342°	E 91.69371°	**1.65**	1.85	**1.85**	1.81	**1.85**	1.85	**1.85**	1.85	**1.31**	1.31	**1.82**	1.80	**1.80**	1.89	**2.20**	*	*	*	*	*
173	N 26.18985°	E 91.66978°	**1.68**	1.80	**1.76**	1.90	**1.84**	1.88	**1.92**	1.93	**1.65**	1.65	**1.99**	1.97	**2.01**	2.04	**2.04**	2.20	**2.21**	2.22	**2.25**	2.25
174	N 26.18406°	E 91.66617°	**1.10**	1.19	**1.50**	1.50	**1.44**	1.44	**1.46**	1.44	**1.64**	1.52	**1.50**	1.50	**1.68**	2.10	**1.87**	1.76	**1.76**	1.97	**1.98**	2.03
175	N 26.15161°	E 91.69443°	**1.10**	1.68	**1.67**	1.70	**1.70**	1.70	**1.70**	1.50	**1.90**	1.92	**1.68**	1.68	**1.65**	2.18	**2.19**	2.20	**2.20**	2.20	**2.21**	2.22
176	N 26.18217°	E 91.67849°	**1.20**	1.53	**1.53**	1.53	**1.53**	1.55	**1.55**	1.55	**1.56**	1.76	**1.86**	1.92	**1.80**	1.65	**1.55**	1.55	**1.68**	*	*	*
177	N 26.18918°	E 91.70176°	**1.32**	1.68	**1.82**	1.52	**1.12**	1.12	**1.69**	1.60	**1.68**	2.21	**2.21**	2.22	**2.23**	2.24	**2.25**	2.25	**2.27**	2.28	**2.30**	*
178	N 26.15486°	E 91.70041°	**1.68**	1.70	**1.80**	1.80	**1.80**	1.48	**1.78**	1.99	**1.93**	1.93	**1.94**	1.55	**1.59**	1.60	**1.77**	*	*	*	*	*
179	N 26.18989°	E 91.74735°	**1.20**	1.20	**1.48**	1.48	**1.48**	1.61	**1.67**	2.21	**2.21**	2.22	**2.23**	2.23	**2.25**	2.26	**2.26**	2.27	**2.28**	2.28	**2.30**	2.31
180	N 26.19969°	E 91.69440°	**1.54**	1.54	**1.54**	1.92	**1.92**	1.54	**1.92**	1.92	**1.97**	1.99	**2.04**	1.95	**1.92**	1.76	**1.92**	2.21	*	*	*	*
181	N 26.16086°	E 91.74903°	**1.85**	2.05	**2.05**	2.05	**2.05**	1.95	**1.80**	1.95	**2.20**	2.21	**2.22**	*	*	*	*	*	*	*	*	*
182	N 26.19750°	E 91.75987°	**1.56**	1.56	**1.56**	1.56	**1.44**	1.44	**1.50**	1.32	**1.52**	1.60	**1.60**	1.58	**1.58**	1.60	**1.76**	1.76	**1.82**	1.85	**1.98**	1.87
183	N 26.18907°	E 91.75780°	**1.72**	1.72	**1.92**	1.80	**1.76**	2.05	**2.01**	2.00	**2.01**	1.92	**2.05**	2.04	**1.92**	2.01	**2.21**	2.21	*	*	*	*
184	N 26.16324°	E 91.76584°	**1.70**	1.85	**1.85**	1.97	**1.97**	2.12	**2.17**	1.82	**1.82**	1.82	**1.82**	1.60	**2.19**	2.20	**2.20**	2.21	**2.22**	2.24	**2.12**	*
185	N 26.18040°	E 91.75342°	**1.65**	1.82	**1.80**	1.80	**1.80**	1.80	**1.80**	1.97	**2.12**	2.19	**2.19**	2.20	**2.20**	2.21	**2.22**	2.24	**2.24**	2.26	*	*
186	N 26.18488°	E 91.75740 °	**1.37**	1.37	**1.68**	1.55	**1.68**	1.68	**1.80**	1.92	**1.92**	1.92	**1.85**	1.88	**1.90**	1.90	**2.20**	2.21	**2.21**	2.23	**2.24**	*
187	N 26.16015°	E 91.74101°	**1.10**	1.12	**1.92**	1.92	**1.92**	1.80	**1.97**	2.12	**2.17**	2.20	**2.21**	2.22	**2.24**	*	*	*	*	*	*	*
188	N 26.16733°	E 91.75239°	**1.60**	1.77	**1.73**	1.73	**1.73**	1.73	**1.73**	2.19	**2.20**	1.92	**1.95**	2.20	**2.20**	1.99	**2.19**	2.19	**2.20**	1.67	**1.77**	1.70

Bore hole ID	Latitude	Longitude	DENSITY (gm/c.c)																			
189	N 26.17849°	E 91.75786°	**1.10**	1.30	**1.87**	1.87	**1.87**	1.87	**1.93**	1.93	**1.93**	1.93	**2.19**	2.20	**2.20**	2.21	**2.21**	2.23	*	*	*	*
190	N 26.14839°	E 91.74357°	**1.75**	1.77	**1.77**	1.77	**1.85**	1.99	**1.99**	2.02	**2.02**	2.03	*	*	*	*	*	*	*	*	*	*
191	N 26.17135°	E 91.74653°	**1.10**	1.85	**1.80**	1.80	**1.92**	1.68	**2.19**	2.20	**2.21**	2.21	**2.21**	2.22	**2.22**	2.24	**2.25**	*	*	*	*	*
192	N 26.16959°	E 91.77882°	**1.10**	1.10	**1.12**	1.77	**1.77**	1.85	**1.90**	1.60	**1.60**	1.60	**1.73**	1.73	**1.95**	1.95	**2.02**	2.20	**2.20**	1.98	**1.98**	1.98
193	N 26.14772°	E 91.74207°	**1.68**	1.85	**2.11**	2.11	**2.11**	1.92	**1.80**	1.85	**1.85**	1.50	**1.44**	1.49	**1.85**	1.60	**2.19**	2.20	**2.20**	2.20	*	*
194	N 26.15284°	E 91.73533°	**1.10**	1.68	**1.83**	1.76	**1.92**	2.18	**2.19**	2.19	**2.20**	2.20	*	*	*	*	*	*	*	*	*	*
195	N 26.18082°	E 91.74796°	**1.68**	1.81	**1.81**	1.68	**1.68**	1.80	**1.80**	2.09	**2.19**	2.19	**2.20**	2.20	**2.21**	2.21	**2.23**	2.23	**2.24**	2.25	**2.25**	2.26
196	N 26.13603°	E 91.73539°	**1.60**	1.45	**1.45**	2.18	**1.92**	2.19	**2.20**	2.21	**2.21**	2.22	**2.23**	2.25	**2.25**	2.26	**2.27**	2.27	**2.28**	2.28	**2.30**	2.30
197	N 26.13700°	E 91.74526°	**1.01**	1.65	**1.75**	1.75	**1.60**	1.80	**1.97**	1.85	**1.87**	1.95	**2.02**	2.19	**2.20**	2.20	**2.20**	2.24	*	*	*	*
198	N 26.12811°	E 91.73819°	**1.12**	1.92	**1.92**	1.97	**1.97**	1.92	**1.99**	1.95	**1.89**	1.89	**2.20**	2.20	**2.24**	2.25	**2.26**	2.27	**2.30**	2.17	**2.15**	2.17
199	N 26.17859°	E 91.82757°	**1.08**	1.40	**1.40**	1.40	**1.65**	1.65	**1.80**	1.68	**2.20**	2.20	**2.20**	2.21	*	*	*	*	*	*	*	*
200	N 26.18666°	E 91.84341°	**1.80**	1.40	**1.40**	2.02	**2.05**	1.99	**1.98**	2.00	**2.01**	2.17	**1.94**	1.60	**1.60**	2.19	**2.19**	2.20	**2.20**	2.21	**2.22**	2.25

ANNEXURE VIII

Factor of Safety at 200 Borehole locations

Sl. No.	Lat (°N)	Long (°E)	Factor of Safety
1	26.14167	91.66125	0.79
2	26.18139	91.66905	0.61
3	26.15273	91.65732	2.00
4	26.14808	91.64718	2.00
5	26.14073	91.63915	0.16
6	26.13753	91.62938	2.00
7	26.12998	91.6228	0.38
8	26.12088	91.61617	0.13
9	26.10162	91.61213	0.22
10	26.09853	91.6062	2.00
11	26.09957	91.59685	0.23
12	26.10955	91.60723	0.15
13	26.10744	91.59333	2.00
14	26.11728	91.59867	0.32
15	26.13875	91.60713	2.00
16	26.1215	91.60505	0.25
17	26.1385	91.62132	2.00
18	26.14374	91.6313	2.00
19	26.14869	91.64002	2.00

Sl. No.	Lat (°N)	Long (°E)	Factor of Safety
20	26.16634	91.66854	0.33
21	26.16104	91.65187	0.32
22	26.16871	91.68077	0.18
23	26.1482	91.66824	2.00
24	26.15969	91.68063	0.98
25	26.16035	91.68913	0.35
26	26.14802	91.67838	1.14
27	26.13695	91.67352	2.00
28	26.14543	91.68246	2.00
29	26.15994	91.71165	2.00
30	26.15052	91.68468	2.00
31	26.17373	91.72914	1.22
32	26.17079	91.7237	2.00
33	26.17092	91.76926	2.00
34	26.16844	91.72948	2.00
35	26.15111	91.73592	2.00
36	26.18119	91.77602	2.00
37	26.15861	91.73801	0.28
38	26.11085	91.78908	2.00
39	26.17793	91.774	2.00
40	26.16747	91.74498	0.36
41	26.17194	91.73618	0.64
42	26.18146	91.74272	2.00
43	26.17139	91.73836	2.00
44	26.14177	91.73309	2.00
45	26.17572	91.73512	2.00
46	26.12674	91.72171	2.00

Sl. No.	Lat (°N)	Long (°E)	Factor of Safety
47	26.17742	91.74059	2.00
48	26.16684	91.77177	2.00
49	26.18647	91.75336	2.00
50	26.18618	91.74863	0.54
51	26.16974	91.75236	2.00
52	26.17605	91.75524	2.00
53	26.18308	91.74365	2.00
54	26.18155	91.77837	2.00
55	26.18472	91.75443	2.00
56	26.202	91.76137	2.00
57	26.18906	91.79023	2.00
58	26.1849	91.75906	2.00
59	26.18495	91.76629	2.00
60	26.1864	91.78783	2.00
61	26.16159	91.7746	2.00
62	26.18573	91.76258	2.00
63	26.18482	91.7763	2.00
64	26.1598	91.77876	2.00
65	26.18535	91.77317	2.00
66	26.18437	91.76755	2.00
67	26.16165	91.7817	2.00
68	26.18387	91.74662	0.31
69	26.17929	91.7647	2.00
70	26.1723	91.77992	2.00
71	26.16425	91.7765	2.00
72	26.17422	91.75918	2.00
73	26.15813	91.78677	2.00

Sl. No.	Lat (°N)	Long (°E)	Factor of Safety
74	26.14147	91.79957	0.77
75	26.16657	91.76322	2.00
76	26.1781	91.77727	2.00
77	26.13491	91.8051	2.00
78	26.17299	91.76301	2.00
79	26.1438	91.78204	2.00
80	26.1282	91.80667	2.00
81	26.15613	91.78868	2.00
82	26.13284	91.78539	0.24
83	26.12945	91.80169	2.00
84	26.15262	91.78667	2.00
85	26.12091	91.78821	2.00
86	26.14098	91.78667	2.00
87	26.15343	91.79107	2.00
88	26.11379	91.78621	2.00
89	26.13844	91.7766	2.00
90	26.1757	91.77977	2.00
91	26.1211	91.76988	2.00
92	26.13567	91.79333	2.00
93	26.13999	91.76104	2.00
94	26.1178	91.77639	2.00
95	26.12552	91.78876	2.00
96	26.14356	91.7745	2.00
97	26.12259	91.78823	2.00
98	26.12951	91.7943	2.00
99	26.14289	91.77021	2.00
100	26.16052	91.75964	2.00

Sl. No.	Lat (°N)	Long (°E)	Factor of Safety
101	26.1333	91.8264	2.00
102	26.11461	91.79327	2.00
103	26.15819	91.81835	2.00
104	26.13457	91.80951	2.00
105	26.12234	91.80431	2.00
106	26.1559	91.82724	2.00
107	26.16614	91.82574	2.00
108	26.13953	91.82994	2.00
109	26.15677	91.83789	2.00
110	26.17557	91.83054	2.00
111	26.1373	91.82093	2.00
112	26.13135	91.6726	0.43
113	26.18258	91.80232	2.00
114	26.13245	91.81193	2.00
115	26.12411	91.68858	2.00
116	26.1291	91.6776	0.37
117	26.14862	91.81223	0.35
118	26.11473	91.74764	2.00
119	26.11428	91.74064	2.00
120	26.18015	91.81043	2.00
121	26.10395	91.75164	2.00
122	26.11338	91.72913	2.00
123	26.178	91.80292	2.00
124	26.11935	91.81679	0.93
125	26.11518	91.71913	2.00
126	26.18392	91.79392	2.00
127	26.12281	91.82168	2.00

Sl. No.	Lat (°N)	Long (°E)	Factor of Safety
128	26.12236	91.74914	2.00
129	26.11922	91.68511	2.00
130	26.10215	91.79817	2.00
131	26.13	91.82118	1.32
132	26.2009	91.75969	2.00
133	26.13719	91.79117	2.00
134	26.10799	91.71913	2.00
135	26.12057	91.69611	2.00
136	26.14931	91.6726	2.00
137	26.11415	91.71882	2.00
138	26.11652	91.70812	2.00
139	26.20272	91.68222	2.00
140	26.1277	91.81221	2.00
141	26.11113	91.79567	2.00
142	26.13567	91.79333	2.00
143	26.14258	91.6681	2.00
144	26.1171	91.71469	2.00
145	26.19374	91.71749	2.00
146	26.20141	91.6794	2.00
147	26.12813	91.81169	2.00
148	26.21956	91.73471	2.00
149	26.22154	91.71588	2.00
150	26.13763	91.65009	0.14
151	26.21292	91.7289	2.00
152	26.20357	91.71428	2.00
153	26.22502	91.70291	2.00
154	26.1998	91.71488	2.00

Sl. No.	Lat (°N)	Long (°E)	Factor of Safety
155	26.18705	91.70547	2.00
156	26.21166	91.70928	2.00
157	26.1868	91.67834	2.00
158	26.19978	91.72659	0.99
159	26.19697	91.72006	2.00
160	26.11761	91.82617	2.00
161	26.22248	91.70677	2.00
162	26.21036	91.7395	2.00
163	26.20227	91.62142	2.00
164	26.21898	91.72659	2.00
165	26.20183	91.72322	2.00
166	26.1794	91.74526	2.00
167	26.20672	91.70496	2.00
168	26.21031	91.71638	2.00
169	26.18579	91.69515	2.00
170	26.1824	91.68619	2.00
171	26.1824	91.69445	2.00
172	26.15342	91.69371	2.00
173	26.18985	91.66978	2.00
174	26.18406	91.66617	2.00
175	26.15161	91.69443	2.00
176	26.18217	91.67849	2.00
177	26.18918	91.70176	2.00
178	26.15486	91.70041	2.00
179	26.18365	91.74958	0.61
180	26.19969	91.6944	2.00
181	26.16086	91.74903	2.00

Sl. No.	Lat (°N)	Long (°E)	Factor of Safety
182	26.20292	91.7625	2.00
183	26.17972	91.75775	2.00
184	26.16324	91.76584	2.00
185	26.1804	91.75342	1.36
186	26.18488	91.7574	2.00
187	26.16015	91.74101	2.00
188	26.16733	91.75239	2.00
189	26.17849	91.75786	2.00
190	26.14839	91.74357	2.00
191	26.17135	91.74653	2.00
192	26.16959	91.77882	2.00
193	26.14772	91.74207	2.00
194	26.15284	91.73533	0.40
195	26.18082	91.74796	1.03
196	26.13603	91.73539	1.12
197	26.137	91.74526	2.00
198	26.12811	91.73819	2.00
199	26.17859	91.82757	2.00
200	26.18666	91.84341	2.00

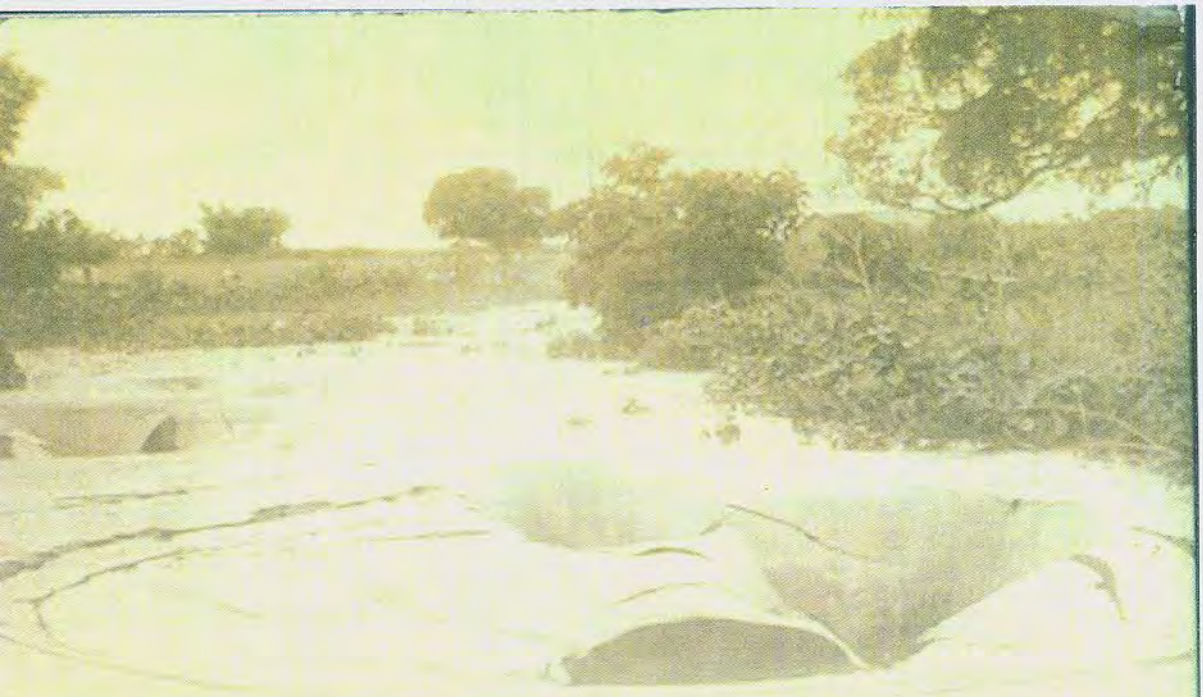

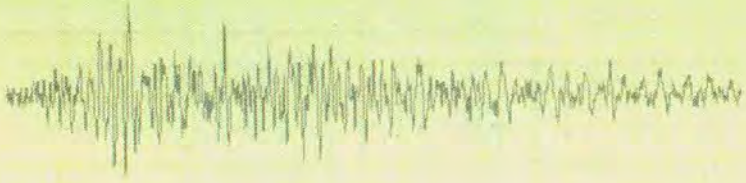

For further information contact:

Brijesh K Bansal
Director and In-charge (Seismology)
Department of Science & Technology
Technology Bhavan
New Mehrauli Road, New Delhi - 110 016
E-mail: bansalbk@nic.in
Telefax: +91-11-26519954